

1-1-2001

# Synthesis and characterization of highly functionalized carbon-chain polymers.

Lawino C. Kagumba  
*University of Massachusetts Amherst*

Follow this and additional works at: [https://scholarworks.umass.edu/dissertations\\_1](https://scholarworks.umass.edu/dissertations_1)

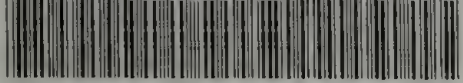
---

## Recommended Citation

Kagumba, Lawino C., "Synthesis and characterization of highly functionalized carbon-chain polymers." (2001). *Doctoral Dissertations 1896 - February 2014*. 1020.  
[https://scholarworks.umass.edu/dissertations\\_1/1020](https://scholarworks.umass.edu/dissertations_1/1020)

This Open Access Dissertation is brought to you for free and open access by ScholarWorks@UMass Amherst. It has been accepted for inclusion in Doctoral Dissertations 1896 - February 2014 by an authorized administrator of ScholarWorks@UMass Amherst. For more information, please contact [scholarworks@library.umass.edu](mailto:scholarworks@library.umass.edu).





312066 0275 8515 9



SYNTHESIS AND CHARACTERIZATION OF HIGHLY FUNCTIONALIZED  
CARBON-CHAIN POLYMERS

A Dissertation Presented

By

LAWINO C. KAGUMBA

Submitted to the Graduate School of the  
University of Massachusetts Amherst in partial fulfillment  
of the requirements for the degree of

DOCTOR OF PHILOSOPHY

September 2001

Polymer Science and Engineering

© Copyright by Lawino C. Kagumba 2001

All rights reserved



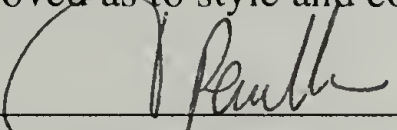
SYNTHESIS AND CHARACTERIZATION OF HIGHLY FUNCTIONALIZED  
CARBON-CHAIN POLYMERS

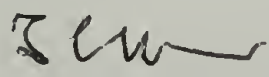
A Dissertation Presented

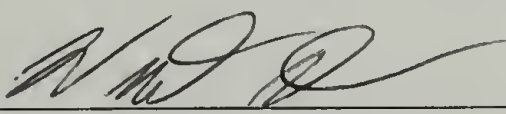
By


LAWINO C. KAGUMBA

Approved as to style and content by:

  
\_\_\_\_\_  
Jacques Penelle, Chair

  
\_\_\_\_\_  
Thomas J. McCarthy, Member

  
\_\_\_\_\_  
Vincent Rotello, Member

  
\_\_\_\_\_  
Thomas J. McCarthy, Department Head  
Polymer Science and Engineering

To my parents, Helga and Mboya



## ACKNOWLEDGMENTS

My graduate school experience was a challenging but fruitful experience, and my success can be attributed to many people. I would like to thank my primary advisor Dr. Penelle, from whom I was able learn a lot and grow tremendously in my knowledge of polymer science. I thank him for his patience, advice and willingness to go the extra mile when I needed it. I would also like to thank Dr. McCarthy and Dr. Rotello for serving as members of my committee. I am grateful to have worked with Dr. Atkins and Dr. Waddon on the crystallography project, and to Dr. Dickinson for his help with the NMR. I thank Dr. Russell, Dr. Vogl and Dr. Hsu for their encouragement and concern for my well-being during my stay at PSE. I am also grateful to my group members, Joel Schall, Xie Tao, Robyn McKiernan, Gabi Menges, Jim Goldbach, Javid Rzaev, Kanad Das and Sterling Alfred for all their help, and to our staff members Eileen Besse and Sophia Hsu who were invaluable in the whole process.

Outside of the PSE department, I am grateful to so many of my friends who each gave so much to me in many different ways over the years: Naomi Gonsalves, Robyn Hall, Cheryl Brandt, April Robinson, Funmilayo Osode, Angela Assè, Krissy Haberman, Kanad Das, Melissa Myambo, Mutuhi Mugo, Sunita Rajouria, Maria Silva, Sylvia Heredia, Tanya Karrakashan, Sarah Bolton, Yvonne Akpalu, Maura Aguirre, Tommy Alessi, Desiree Josias and family, Chip and Ruby Mitchell, Jessica Miller, Olive Munene, and to all my brothers and sisters in the Springfield Church of Christ. Lastly a special thanks to my mum and dad, sisters - Ada and Jenny, and brother Phillip. Your love and support through the years provided me with encouragement words cannot express.

## ABSTRACT

### SYNTHESIS AND CHARACTERIZATION OF HIGHLY FUNCTIONALIZED CARBON-CHAIN POLYMERS

SEPTEMBER 2001

LAWINO C. KAGUMBA

B.A., SMITH COLLEGE

Ph.D., UNIVERSITY OF MASSACHUSETTS AMHERST

Directed by: Professor Jacques Penelle

This project involves the design, synthesis and characterization of a new class of carbon-chain polymers with substituents on every *third* and every *fourth* carbon along the backbone. 1,1-Dicyanocyclopropane **1**, alkyl 1-cyanocyclopropanecarboxylates **2a-d** and 1-phenylcyclopropanecarbonitrile **4** undergo ring-opening polymerization in the presence of thiophenolate anions at 60 °C, yielding highly functionalized carbon-chain polymers of general structure  $(\text{CH}_2\text{CH}_2\text{C}(\text{XY}))_n$ . Monomer **1** is highly reactive, while **2a-d** show intermediate reactivity between **1** and **4**. GPC analysis indicated poly(**2a-d**) had narrow molecular weight distributions ( $\overline{M}_w/\overline{M}_n < 1.17$ ). Due to the poor solubility of poly(**1**) and poly(**4**), their molecular weights could not be measured. Thermogravimetric analysis (TGA) shows that poly(**1**) is highly stable up to 360 °C, while poly(**2a-d**) and poly(**4**) are stable up to 200 °C. X-ray analysis indicated that the polymers are all semi-crystalline, with melting temperatures above their decomposition temperatures. A detailed study of the crystal structure of poly(diethyl-1,1-cyclopropanecarboxylate) poly(**3b**) indicated that the conformation of the backbone is close to a  $TG\overline{G}TG\overline{G}$  structure.



Similar attempts to ring-open polymerize dialkyl-1,1-cyclobutanedicarboxylates **5a-c** and ethyl 1-cyanocyclobutanecarboxylate **6** using thiophenolate anions at temperatures ranging from 140 to 180 °C were unsuccessful. For these reactions, the thiophenolate preferentially attacks the carbon on the ester substituent (Krapcho reaction) and not the ring-carbons. 1,1-Dicyanocyclobutane **8** ring-opens in the presence of potassium or sodium thiophenolate at 140 °C, but only oligomers ( $\overline{Xn} < 5$ ) were obtained after long reaction times. An alternative synthetic strategy to synthesize the desired poly(1,1-difunctionalized tetramethylene)s ( $\text{CH}_2\text{CH}_2\text{CH}_2\text{C}(\text{XY})_n$ ) was attempted via the anionic polymerization of ethyl 2-cyano-2,4-pentadienoate **9** and diethyl 2-propenylidene malonate **10**. NMR and IR analysis of samples (initiated with piperidine in benzene at 25 °C) indicated that the microstructure of poly(**9**) consisted only of 1,4-addition units, but for poly(**10**), a mixture of 3,4- (66%), 1,4- (17%) and 1,2 (17%) units are obtained. Subsequent hydrogenation of a sample of poly(**9**) with only a 1,4-microstructure using diimide as a hydrogenation agent. The results indicated up to 80% hydrogenation was achieved. This strategy, although not direct, provides a feasible method to achieving our target carbon-chain polymers with substituents on every *fourth* carbon.

# TABLE OF CONTENTS

	Page
ACKNOWLEDGMENTS .....	v
ABSTRACT .....	vi
LIST OF TABLES .....	xiv
LIST OF FIGURES .....	xvi
LIST OF SCHEMES .....	xxi
CHAPTER	
1. CONTROL OF MACROMOLECULAR ARCHITECTURES .....	1
1.1 Overview.....	1
1.2 Role of Substituents .....	1
1.3 Substituent Location in Carbon-Chain Polymers .....	4
1.4 Goals and Objectives .....	9
1.5 Summary of Each Chapter .....	13
1.6 References .....	14
2. RING-OPENING POLYMERIZATION OF CYCLOPROPANES .....	17
2.1 Introduction .....	17
2.2 Background: The Chemistry of Cyclopropanes .....	18
2.2.1 Structure and Bonding .....	18
2.2.2 Reactivity .....	20
2.2.3 Ring-Opening Reactions .....	22
2.2.4 Reactivity of Three-membered Heterocycles .....	25
2.2.5 Polymerizability of Cyclopropanes.....	26
2.2.5.1 Thermodynamics of Polymerization .....	26
2.2.5.2 Kinetics of Polymerization .....	28
2.2.6 Ring-Opening Polymerization of Cyclopropanes: Literature Survey .....	30
2.2.6.1 Cationic Polymerization .....	30
2.2.6.2 Coordination Polymerization.....	32



2.2.6.3	Radical Polymerization .....	32
2.2.6.4	Anionic Polymerization .....	33
2.2.7	Summary .....	35
2.3	Ring-Opening Polymerization of 1,1-Disubstituted Cyclopropanes: Overview.....	36
2.3.1	Ring-Opening Polymerization of 1,1- Dicyanocyclopropane <b>1</b> .....	37
2.3.1.1	Introduction.....	37
2.3.1.2	Experimental .....	40
2.3.1.3	Results and Discussion .....	42
	2.3.1.3.1 Monomer synthesis .....	42
	2.3.1.3.2 Anionic Polymerization of <b>1</b> .....	43
	2.3.1.3.3 Solid state polymerization.....	48
2.3.1.4	Characterization of Poly( <b>1</b> ) .....	49
	2.3.1.4.1 Structural Analysis .....	49
	2.3.1.4.2 Molecular Weight determination .....	51
	2.3.1.4.3 Thermal Analysis .....	52
	2.3.1.4.4 Crystallinity .....	53
2.3.1.5	Conclusions .....	54
2.3.2	Ring-Opening Polymerization of Alkyl 1-Cyanocyclopropane carboxylates <b>2a-d</b> .....	55
2.3.2.1	Introduction .....	55
2.3.2.2	Experimental .....	55
2.3.2.3	Results and Discussion .....	59
	2.3.2.3.1 Synthesis of monomers <b>2a-d</b> .....	59
	2.3.2.3.2 Anionic ring-opening polymerization of <b>2a-d</b> .....	60
	2.3.2.3.3 Quasi-Living Characteristics of the polymerization of <b>2a</b> .....	72
	2.3.2.3.4 Adhesion testing of Poly( <b>2a-d</b> ) .....	79

2.3.2.4	Characterization of Poly( <b>2a-d</b> ) .....	81
2.3.2.4.1	Physical Properties .....	81
2.3.2.4.2	Structural Characterization .....	81
2.3.2.4.3	Thermal Analysis .....	84
2.3.2.5	Comparison of Properties of Poly( <b>2a-d</b> ) with Poly( $\alpha$ - cyanoacrylates .....	85
2.3.2.5.1	Thermal Properties.....	85
2.3.2.5.2	Crystalline Properties.....	85
2.3.2.5.3	Solubility.....	87
2.3.2.6	Conclusions .....	87
2.3.3	Ring-Opening Polymerization of Phenyl 1-Cyclopropane carbonitrile <b>4</b> .....	89
2.3.3.1	Introduction.....	89
2.3.3.2	Experimental .....	89
2.3.3.3	Results and Discussion .....	90
2.3.3.3.1	Anionic Polymerization of <b>4</b> .....	90
2.3.3.4	Characterization of Poly( <b>4</b> ) .....	91
2.3.3.4.1	Structural characterization.....	91
2.3.3.4.2	Molecular Weight determination.....	93
2.3.3.4.3	Thermal Analysis.....	93
2.3.3.4.4	Crystallinity .....	94
2.3.3.5	Conclusions.....	95
2.3.4	Influence of Substituents on the Reactivity of 1,1-Disubstituted Cyclopropanes .....	96
2.3.4.1	Introduction.....	96
2.3.4.2	Results and Discussion .....	96
2.3.4.3	Conclusions.....	102
2.4	References .....	103



3.	STEREOCHEMISTRY OF POLYMERIZATION OF ALKYL 1-CYANO CYCLOPROPANE CARBOXYLATES .....	111
3.1	Introduction.....	111
3.2	Background .....	112
3.2.1	Tacticity .....	112
3.2.2	Stereochemical Control .....	115
3.2.3	Analytical Tools.....	116
3.3	Experimental .....	117
3.4	Results and Discussion .....	119
3.4.1	Polymer Synthesis and Characterization .....	119
3.4.2	Analysis of model compound (i).....	121
3.4.3	Analysis of the NMR spectra of (i) via simulation .....	123
3.4.4	Analysis of the polymer microstructures .....	129
3.4.5	<sup>13</sup> C-NMR Analysis .....	131
3.4.6	Analysis of the stereochemistry of polymerization .....	139
3.5	Conclusions.....	142
3.6	References .....	142
4.	RING-OPENING POLYMERIZATION OF CYCLOBUTANES .....	145
4.1	Introduction.....	145
4.2	Background: The Chemistry of Cyclobutanes .....	147
4.2.1	Structure and Bonding .....	147
4.2.2	Reactivity in Ring-Opening Reactions: Comparison with Cyclopropanes.....	149
4.2.3	Comparison of Three- and Four-membered Heterocycles.....	151
4.2.4	Polymerizability of Cyclobutanes.....	153
4.2.4.1	Thermodynamics of Polymerization .....	153
4.2.4.2	Kinetics of Polymerization .....	153
4.2.5	Ring-Opening Polymerization of Cyclobutanes: Literature Survey .....	154
4.2.5.1	Anionic Polymerization .....	154
4.2.5.2	Cationic Polymerization .....	156

4.2.5.3	Coordination Polymerization.....	156
4.2.5.4	Polymerization of Three- and Four-membered Heterocycles.....	157
4.3	Ring-Opening Polymerization of 1,1-Disubstituted Cyclobutanes .....	159
4.3.1	Experimental .....	159
4.3.2	Results and Discussion .....	162
4.3.2.1	Monomer synthesis .....	162
4.3.2.2	Anionic Polymerization .....	166
4.4	Conclusions.....	172
4.5	References.....	172
5.	ANIONIC POLYMERIZATION OF 1,1-DIFUNCTIONALIZED BUTADIENES .....	176
5.1	Introduction.....	176
5.2	Background .....	177
5.2.1	Butadiene Polymerization.....	177
5.2.2	Stereochemistry of Butadiene Polymerization.....	179
5.2.3	Hydrogenation of Polybutadienes.....	179
5.3	Experimental .....	181
5.4	Results and Discussion .....	184
5.4.1	Monomer synthesis .....	184
5.4.2	Anionic polymerization .....	188
5.4.3	Radical Polymerization.....	190
5.4.4	Structural Analysis of Poly(9) and Poly(10).....	190
5.4.5	Hydrogenation Results.....	197
5.5	Conclusions .....	198
5.6	References .....	198

6.	ANALYSIS OF THE CRYSTAL STRUCTURE OF POLY(1,1-DISUBSTITUTED TRIMETHYLENE)S .....	202
6.1	Introduction.....	202
6.2	Background.....	203
6.2.1	Crystallinity in Polymers .....	203
6.2.2	Factors determining crystal structure.....	205
6.2.3	Crystal structure determination.....	207
6.3	Experimental .....	210
6.4	Structure and Morphology of Poly(diethyl-1,1-cyclopropane- Dicarboxylate).....	213
6.4.1	Results.....	213
6.4.1.1	Electron Microscopy .....	213
6.4.1.2	Electron Diffraction .....	215
6.4.1.3	X-ray Diffraction .....	218
6.4.2	Discussion .....	223
6.4.2.1	Backbone Conformation .....	223
6.4.2.2	Consideration of Side Group Geometry .....	230
6.4.2.3	Chain Packing and Crystal Structure Refinement .....	232
6.4.2.4	Nature of Lamellar-like Crystals .....	238
6.4.2.5	General Considerations Relating to Decorated Alkanes .....	243
6.5	Structure of Poly(1), Poly(2a-d) and Poly(4) .....	244
6.5.1	Results and Discussion .....	244
6.5.1.1	Wide Angle X-ray Scattering.....	244
6.6	Conclusions.....	248
6.7	Acknowledgements.....	250
6.8	References.....	250
	FINAL CONCLUSIONS.....	253
	APPENDIX.....	255
	BIBIOGRAPHY .....	257



# LIST OF TABLES

Table		Page
2.1	Strain Energies ( $\text{kJ}\cdot\text{mol}^{-1}$ ), Bond Angles and Bond Lengths of Three-Membered Cyclics .....	21
2.2	Semi-empirical Heats and Entropies of Polymerization at 25 °C.....	28
2.3	Polymerizability of Various Cyclics.....	29
2.4	Data on the Ring-Opening Polymerization of <b>1</b> with Various Nucleophiles.....	44
2.5	Nucleophilicities of some Common Reagents.....	46
2.6	Anionic Polymerization of Monomers <b>1</b> and <b>vii</b> .....	48
2.7	Yields, Boiling Points and $^1\text{H}$ -NMR Data for Cyclopropanes <b>2a-d</b> .....	60
2.8	$^{13}\text{C}$ -NMR Data of monomers <b>2a-d</b> .....	60
2.9	Ring-Opening Polymerization of <b>2a</b> at 60 °C.....	62
2.10	Ring-Opening Polymerization of <b>2a</b> with various initiators at 60 °C.....	65
2.11	Polymerization of <b>2a</b> at 60, 100 and 120 °C.....	72
2.12	Equilibrium Acidities of Various Acids in DMSO at 25 °C.....	74
2.13	Yields(%) and $\overline{Mn}$ values of Poly( <b>2a</b> ) .....	76
2.14	Adhesion Testing of <b>2a-d</b> .....	80
2.15	$^1\text{H}$ -NMR Data of Poly( <b>2a-d</b> ) .....	82
2.16	$^{13}\text{C}$ -NMR Data of Poly( <b>2a-d</b> ) .....	83
2.17	Glass Transition Temperatures ( $T_g$ , °C) of Poly(Alkyl Cyanoacrylate)s .....	86
2.18	Ring-Opening Polymerization of <b>4</b> at 60 °C.....	90
3.1	NMR Parameters for <i>meso</i> and <i>dl</i> structures ( <b>ii</b> and <b>ii'</b> ), Expressed in Hz .....	125
3.2	Input Data for the Simulation of the $^1\text{H}$ -NMR Spectra of the $-\text{CH}_2\text{CH}_2-$ region of <i>meso</i> and <i>dl</i> diastereomers of ( <b>i</b> ) .....	126

4.1	Strain Energies ( $\text{kcal}\cdot\text{mol}^{-1}$ ), Bond Angles and Bond Lengths of Three and Four Membered Cycles.....	151
4.2	Nucleophilic fission of strained saturated heterocycles.....	152
4.3	Reaction Conditions for <b>5a-d</b> , <b>6</b> and <b>8</b> with Sodium (Na) and Potassium(K) Thiophenolates in DMSO .....	167
5.1	Polymerization of <b>9</b> and <b>10</b> .....	189
6.1	Comparison of Observed and Calculated Diffraction Spacings (nm) and Relative Intensities: Electron Diffraction Data ( $hk0$ ) from Individual Poly( <b>3b</b> ) Lamellar Crystals.....	218
6.2	X-ray Diffraction Data from Oriented, Sedimented Poly( <b>3b</b> ) Lamellar- like Crystals .....	222
6.3	Torsional Rotation Angles for the Backbone and Side Group Bonds in Refined Poly( <b>3b</b> ) Crystal Structure .....	232
6.4	Measured d-spacings from WAXS Patterns .....	247

## LIST OF FIGURES

Figure	Page
1.1 Structure of Side Chain Liquid Crystals .....	3
1.2 Typical Substitution Patterns for Carbon-Chain Polymers .....	5
1.3 Segments of Poly(vinylidene cyanide) $[\text{CH}_2-(\text{CN})_2]_4$ .....	6
1.4 Various Substitution Patterns for Carbon-Chain Polymers .....	9
1.5 All-Trans Conformation of the Main-Chain of a Polymer with Two Substituents on Every Third Carbon.....	11
1.6 Theoretical Conformational Analysis of n-butane (a) and 2,2,5,5 tetramethylhexane (b) .....	12
2.1 Coulson-Moffit Model of Cyclopropane .....	19
2.2 Walsh Model of Cyclopropane. ....	20
2.3 Examples of Various Cyclopropanes that undergo Nucleophilic Ring-Opening Reactions. ....	24
2.3 Free Energy of Polymerization of Cycloalkanes as a Function of the Number of Atoms in the Ring (x) A. unsubstituted; B. methyl substituted; C. 1,1-dimethyl-substituted.....	27
2.5 Structures of 2-Vinyl and 2-Phenyl-1,1-Disubstituted Cyclopropanes .....	33
2.6 Space-Filling Model Comparing Segments of Poly(vinylidene cyanide) $[\text{CH}_2-\text{C}(\text{CN})_2]_4$ (a) and Poly(1,1-dicyanocyclopropane) $[-\text{CH}_2-\text{CH}_2\text{C}(\text{CN})_2]_4$ (b) .....	38
2.7 Solid-State $^{13}\text{C}$ -NMR CP-MAS Spectrum of Poly(1) after the application of a TOSS pulse sequence.....	50
2.8 Solid-State $^{13}\text{C}$ -NMR CP-MAS Spectrum of Poly(1) in a gated decoupling TOSS experiment.....	51
2.9 Thermogravimetry Curve of Poly(1) obtained at a Heating Rate of $10^\circ\text{C}\cdot\text{min}^{-1}$ under $\text{N}_2$ .....	52
2.10 WAXS Pattern of a Powder Sample of Poly(1).....	53



2.11	GPC Spectrogram of a sample of Poly( <b>2a</b> ) displaying the Bimodal distribution .....	63
2.12	Comparison of $\overline{Mn}$ values obtained from NMR vs. GPC.....	64
2.13	Dependence of the conversion (%) with Time for the Polymerization of <b>2a</b> with Thiophenolate Initiators.....	67
2.14	Evolution of the Number Average Molecular Weight ( $\overline{Mn}$ ) with Time for the Polymerization of <b>2a</b> with Thiophenolate Initiators .....	68
2.15	Evolution of the Degree of Polymerization ( $\overline{Xn}$ ) with % Conversion for the Polymerization of <b>2a</b> using Thiophenolate Initiators .....	71
2.16	IR Spectrum obtained during the polymerization of <b>2a</b> .....	75
2.17	IR Spectrum of Poly( <b>2a</b> ) after Termination .....	76
2.18	Structures of Tetrabutylammonium Salts of CH-Acidic Carbonyl Compounds .....	78
2.19	$^1\text{H}$ -NMR Spectrum of Poly( <b>2a-d</b> ) .....	82
2.20	$^{13}\text{C}$ -NMR Spectrum of Poly( <b>2a-d</b> ).....	83
2.21	TGA spectrogram of Poly( <b>1</b> ) Poly( <b>2a-d</b> ).....	84
2.22	Trend in Evolution of Conversion with Time for the Polymerization of <b>4</b> .....	91
2.23	$^1\text{H}$ -NMR Spectrum of Poly( <b>4</b> ) in $\text{d}_6$ -DMSO at 125 °C .....	92
2.24	$^{13}\text{C}$ -NMR Spectrum of Poly( <b>4</b> ) in $\text{d}_6$ -DMSO at 125 °C .....	93
2.25	TGA Spectrum of Poly( <b>4</b> ).....	94
2.26	WAXS pattern of Poly( <b>4</b> ) .....	94
2.27	Comparison of the Reactivity of Cyclopropane monomers <b>1,2, 4</b> .....	98
2.28	Structures of cyclo-isopropylidenecyclopropane-1,1-dicarboxylate <b>xii</b> and spiro[cyclopropane-1,9'-fluorene] <b>xiii</b> .....	101
2.29	Strucures of 2-Vinyl-1,1-Disubstituted Monomers .....	102

3.1	Stereoregular carbon-chain polymers with substituents on every second carbon.....	113
3.2	Stereoregular carbon-chain polymers with substituents on every third carbon .....	113
3.3	1-phenylbenzosuberyl methacrylate .....	116
3.4	<sup>1</sup> H-NMR Spectrum of Poly( <b>2a</b> ) showing the Expanded –CH <sub>2</sub> CH <sub>2</sub> - Region .....	120
3.5	<sup>1</sup> H-NMR spectrum of the Model Compound (i) .....	122
3.6	<sup>1</sup> H-NMR Spectrum of the –CH <sub>2</sub> -CH <sub>2</sub> - Region of the Model Compound (i) .....	122
3.7	Structures of <i>meso</i> and <i>dl</i> Diastereomers of (i).....	123
3.8	<i>Meso</i> and <i>dl</i> Diastereomers of Diphenyl-Substituted Adiponitriles (ii) .....	124
3.9	Conformations and equivalence relationships between the hydrogen atoms of -CH <sub>2</sub> -CH <sub>2</sub> - groups, for <i>meso</i> and <i>dl</i> conformations .....	127
3.10	<sup>1</sup> H-NMR Spectrum of the –CH <sub>2</sub> CH <sub>2</sub> - Region of the <i>meso</i> and <i>dl</i> Diastereomers obtained from the Simulation .....	128
3.11	Theoretical and Experimental Spectra of a 50:50 Diastereomeric Mix of the model compound (i).....	129
3.12	A Comparison of the Theoretical and Experimental Spectra of the –CH <sub>2</sub> CH <sub>2</sub> - Region of Poly( <b>2a</b> ) .....	130
3.13	Quantitative <sup>13</sup> C-NMR Spectrum of Poly( <b>2a</b> ) .....	132
3.14	<sup>13</sup> C-NMR Spectrum showing the Main Chain Ethylene and Side Chain Methylene Carbons of Poly( <b>2a</b> ) (500 MHz NMR).....	133
3.15	<sup>13</sup> C-NMR Spectrum showing the Ethylene Carbons (33 ppm) of the Model Compound (i).....	134
3.16	DEPT Spectrum of an atactic PECA sample .....	137
3.17	Comparison of the diad and tetrad levels of PECA and Poly( <b>2a</b> ) .....	138
3.18	Triad level sensitivity of the side chain carbons of PECA and Poly( <b>2a</b> ).....	139
3.19	Proposed 12-membered cyclic intermediate formed during the polymerization of <b>2a</b> .....	141

4.1	Conformations of cyclobutane .....	148
4.2	“Bent” orbitals of the cyclobutane ring .....	149
4.3	<sup>1</sup> H-NMR spectrum of reaction of <b>5b</b> with PhSK (Expt. 4) in (CD <sub>3</sub> ) <sub>2</sub> SO.....	168
4.4	Activated Cyclopropanes and Cyclobutane Derivatives.....	171
5.1	Polybutadiene microstructures.....	177
5.2	Polymer microstructures arising from 1,2- and 3,4- additions to 1-methyl butadiene .....	178
5.3	<sup>1</sup> H-NMR Spectrum of <b>9</b> (CDCl <sub>3</sub> ).....	187
5.4	Isomers of <b>9</b> .....	187
5.5	<sup>13</sup> C-NMR Spectrum of <b>9</b> (CDCl <sub>3</sub> ).....	188
5.6	<sup>1</sup> H-NMR Spectrum of Poly( <b>9</b> ) in CDCl <sub>3</sub> .....	191
5.7	Theoretical Chemical Shifts (ppm) of vinylic protons for 1,2-; 1,4- and 3,4- Units as calculated from NMR tables .....	192
5.8	<sup>13</sup> C-NMR spectrum of Poly( <b>9</b> ) in CDCl <sub>3</sub> .....	193
5.9	IR spectrum of Poly( <b>9</b> ) .....	194
5.10	IR Analysis of out-of-plane C-H Bending for 1,2; 1,4 and 3,4 units .....	194
5.11	Proposed Tetrahedral Intermediates <b>i</b> and <b>ii</b> .....	196
6.1	Transmission electron micrographs of the Poly( <b>3b</b> ) lamellar-like crystals isothermally crystallized from benzene .....	213
6.2	Selected area <i>hk0</i> electron diffraction patterns .....	216
6.3	Wide-angle X-ray diffraction patterns of Poly( <b>3b</b> ) .....	219
6.4	Two orthogonal views (perpendicular to the c-axis) of the basic backbone ( <i>TG</i> $\overline{GTG}$ $\overline{G}$ ) conformation of Poly( <b>3b</b> ).....	225
6.5	Calculated potential energy profiles for the various bond torsional angles of the backbone of Poly( <b>3b</b> ) .....	228



6.6	Two orthogonal views, parallel and perpendicular to the c-axis showing the carbon and oxygen atoms for the pair of $-\text{COOCH}_2\text{CH}_3$ side groups .....	230
6.7	Computer simulated X-ray diffraction pattern from refined model (top) compared with the experimental X-ray pattern (bottom) .....	233
6.8	Views of the refined structure of the Poly( <b>3b</b> ) crystal in stick mode.....	235
6.9	Space filling model of the lamellar-like crystal structure of Poly( <b>3b</b> ) .....	239
6.10	Structures of Poly(1,1-disubstituted trimethylene)s .....	244
6.11	WAXS patterns of Poly(1,1-disubstituted trimethylene)s .....	245

## LIST OF SCHEMES

Scheme	Page
2.1 Cationic polymerization of 3 methyl-1-butene .....	17
2.2 Retrosynthetic Analysis of the Ring-Opening Polymerization of Activated Cyclopropanes.....	18
2.3 Comparison of Addition Reactions in Alkenes and Cyclopropanes.....	22
2.4 Homologous (1,5) Version of the Classical Michael Addition.....	23
2.5 Nucleophilic Addition Reactions to Vinyl Cyclopropanes.....	24
2.6 Ring-Opening of Vinyl Cyclopropanes via Radical Mechanisms.....	25
2.7 Cationic Polymerization of Vinyl Cyclopropane.....	31
2.8 Structure of Dialkyl Cyclopropane-1,1-Dicarboxylates .....	34
2.9 Ring-Opening Polymerization of 1,1-Dicyanocyclopropane .....	37
2.10 Synthesis of 1,1-Dicyanocyclopropane .....	43
2.11 Ring-Opening Polymerization of Alkyl 1-Cyanocyclopropane carboxylates .....	55
2.12 Synthesis of Alkyl 1-Cyanocyclopanecarboxylates .....	59
2.13 Comparison of the structure of the Propagating Anions during the Polymerization of $\alpha$ -Cyanoacrylates and <b>2a-d</b> .....	73
2.14 Possible Side Reactions During the Polymerization of <b>2a-d</b> .....	74
3.1 Iso-, syndio- and heterotactic Diads.....	114
3.2 Synthesis of Poly(alkyl 1-cyanocyclopanecarboxylate)s .....	119
3.3 Synthesis of diethyl 2,5-dicyanoadipate .....	121
4.1 Carbon-chain polymers with substituents on every third and every fourth carbon atom.....	146

4.2	Ring-Opening Polymerization of Functionalized Cyclobutane .....	147
4.3	Spontaneous reaction of TCNE and EVE to yield 1,1,2,2-tetracyano-3-ethoxycyclobutane .....	155
4.4	Ring-Opening Polymerization of Cyclobutanes .....	155
4.5	Ring-Opening Polymerization of <b>iii</b> .....	156
4.6	Ring-Opening Polymerization of methylene cyclobutane ( <b>iv</b> ) .....	157
4.7	Synthesis of 1,1-disubstituted cyclobutanes .....	162
4.8	Cyclization of diethyl ( $\omega$ -bromoalkyl) malonates .....	163
4.9	Cyclization of 3, 4, 6 and 11-membered rings.....	165
4.10	Synthesis of Cyclobutane-1,1-Dicarbonitrile <b>8</b> .....	165
4.11	Competitive Krapcho reaction .....	169
5.1	Synthesis of Poly(1,1-difunctionalized tetramethylene)s .....	176
5.2	General Synthesis of 1,1-difunctionalized-1,3-butadienes .....	185
5.3	Synthesis of diethyl-propenylidene malonate <b>10</b> .....	186
5.4	Mechanisms for 1,2-; 1,4-; and 3,4-; additions .....	195

# SYNTHETIC CONTROL OF MACROMOLECULAR ARCHITECTURES

## 1.1 Overview

The design of polymers with specific structures has developed over many years. With a better understanding of polymer chemistry, control of molecular weight, end-groups, and polymer tacticity has been achieved. Control of polymeric structures is important because the properties of the polymers are directly linked to their macromolecular structures. For example, Ziegler-Natta catalysts used in coordination polymerization of various monomers<sup>1-5</sup> have been used to synthesize highly tactic polymers with distinct properties from their atactic counterparts.<sup>6</sup> Much work has been done to understand these structure-property relationships by studying the properties of polymers with a variety of well characterized structures and architectures. In addition to the choice of the backbone structure, the nature of the substituents placed along the polymer backbone also plays a crucial role in determining the overall properties of the polymer. This role is discussed in the next section. This role is discussed in the next section.

## 1.2 Role of Substituents

Among the important characteristics of the polymer backbone are its flexibility and the stability of the skeletal bonds to chemical reagents and elevated temperatures.<sup>5</sup> The flexibility of the chains depends on the ease of torsion of the backbone bonds, which is crucial for applications involving mechanical stress or thermal treatment. The side



groups attached to the backbone also have a significant effect on polymer properties such as solubility, crystallinity, and surface properties, and can protect the backbone against chain cleavage reactions.

The low polarity of the carbon-hydrogen bonds along the backbone of polyethylene explains its hydrophobicity. The small size of the hydrogen atoms enables the ordered packing of the chains in a zigzag conformation favoring crystallinity in the polymer. Changing the side groups attached on every second carbon from hydrogen to phenyl groups increases the  $T_g$  by almost 200 °C compared to polyethylene. Phenyl groups are stiff and relatively bulky, increasing the barrier to torsion of the backbone bonds. The attachment of fluorine atoms on every second carbon imparts properties such as thermal and oxidative stability, and solvent, oil and fuel resistance due to the strong carbon-fluorine (C-F) bonds.<sup>7</sup> Polar hydrophilic groups such as cyano or hydroxyl groups increase the solubility of the polymers in polar solvents; poly(acrylamide) is an example of a polymer that is highly soluble in water. Steric and polar interactions between side groups on the same chains or different chains also influences the glass transition and melting temperatures.<sup>8</sup>

The placement of specific substituents along the carbon backbone has been used to produce polymers for certain target applications. Side-chain liquid crystalline polymers (LCP's) are such an example. The mesogenic side groups, usually attached to the backbone with flexible spacers,<sup>9</sup> form ordered arrays in the melt or in solution.<sup>10</sup> The structure of side-chain liquid crystalline polymers are shown in Figure 1.1.

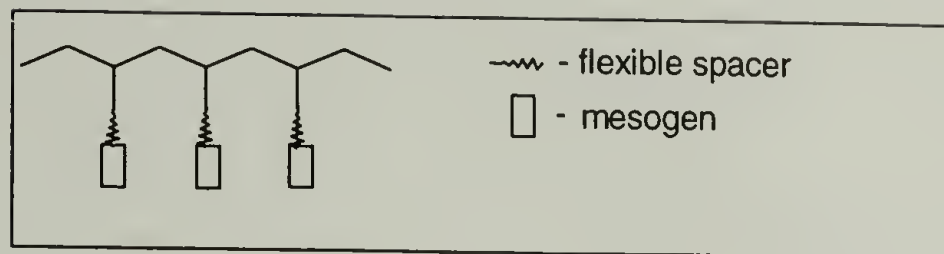


Figure 1.1 Structure of Side Chain Liquid Crystals.

The mesogenic side chains in LCP melts can be oriented in an electric field, producing transparent films which can be imprinted by using laser beam technology. This imprinted information can be indefinitely stored at temperatures below the  $T_g$  of the polymer.<sup>11,12</sup>

The backbone of carbon-chain polymers normally contains pendant functional groups distributed on every *second* carbon atom. These polymers are synthesized by chain polymerizations of vinyl monomers and contribute to a large volume of synthetic polymers produced in industry today.<sup>13</sup> A few examples include polystyrene, polypropylene, poly(vinyl chloride), poly(acrylonitrile), and poly(vinyl alcohol)- with phenyl, methyl, chloro, cyano, and hydroxyl groups on every second carbon atom respectively. From the wide variety of distinct applications of these polymers, it is apparent that the nature of the substituents on the backbone chain influences the structure and properties of the final polymers. For example, the average glass transition temperature ( $T_g$ ) of atactic polypropylene (PP) consisting of chains of saturated hydrocarbons with methyl groups on every second carbon atom is  $-13\text{ }^{\circ}\text{C}$ ,<sup>14</sup> whereas the  $T_g$  of polyethylene with hydrogen “substituents” on the backbone chain is  $-80\text{ }^{\circ}\text{C}$ .<sup>15-17</sup>

The methyl group along the backbone of PP is also sufficiently bulky that the tacticity (hence crystallinity) of the polymer largely influences its overall properties.

Isotactic PP has applications ranging from automatic interior trim parts to biaxially oriented moisture barrier packaging materials and high performance fabrics for athletic wear. On the other hand, atactic PP is a soft, soluble, and often-tacky semi-solid, and is used in adhesives, sealants and as a bitumen modifier.<sup>6</sup>

### 1.3 Substituent Location on Carbon-Chain Polymers

The influence of the nature of the substituent on the polymer structure and general properties has been widely studied.<sup>8</sup> However, the effect of varying the density of substitution remains relatively unexplored. The size and nature of the substituents that can be placed on every *second* carbon is limited due to the unfavorable steric and electronic repulsive interactions between adjacent side groups. A high density of substitution on the backbone is important because the final properties of the polymer will often depend on the number of moieties per unit volume. Examples of the major substitution patterns for aliphatic carbon-chain polymers are shown in Figure 1.2, where X represents all possible substituents excluding hydrogen.

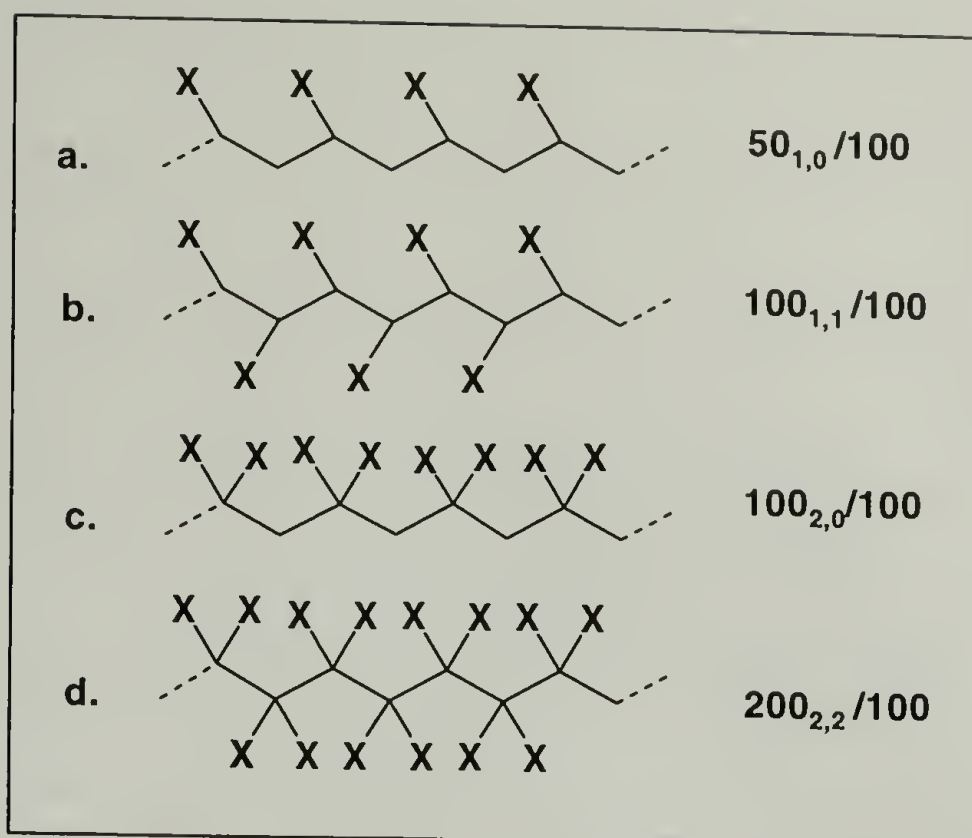


Figure 1.2. Typical Substitution Patterns for Carbon-Chain Polymers.

$X_{a,b}/100$ : X refers to the total number of functional groups per 100 carbon atoms, and a, b refer to the number substituents on each carbon in the repeat unit.

The nomenclature used in Figure 1.2 was created to distinguish between polymers having the same total number of substituents per 100 carbons, but having a different substitution pattern in the repeat unit. The substitution pattern in example **a** depicts carbon-chain polymers with single substituents on every second carbon, with a total of 50 substituents per 100 carbon atoms. The variety of substituents that can be placed on every second carbon arises from the relative ease of synthesis from the respective vinyl monomers.

The versatility of vinylic polymerizations lies in the choice of the method of initiation. Depending on the type of substituent(s) on the monomer, the polymerization mechanism can either be cationic, anionic, radical, or via coordination with various metal complexes.<sup>1-5,8</sup> Typical examples of the pattern **a** include polymers synthesized from mono-substituted alkenes such as styrene, vinyl chloride and acrylonitrile.



In examples **b** and **c**, the density of substitution is 100 functional groups per 100 carbon atoms. In example **b**, steric crowding due to the presence of substituents on adjacent carbons limits the size of the substituents that can be placed at such close intervals. The radical polymerization of various dialkyl fumarates yields polymers with one ester substituent on every carbon atom in the polymer backbone.<sup>18</sup> In comparison to polymers with two ester substituents on every carbon atom along the backbone (example **c**), these polymers display complete loss of chain flexibility.<sup>19</sup>

Polymers with the density distribution in example **c** include poly(vinylidene cyanide) (PVCN) and poly(vinylidene fluoride/chloride). A space-filling model for segments of poly(vinylidene cyanide) in an all-trans conformation (Figure 1.3a), shows that the carbon and nitrogen atoms of the cyano groups are at Van der Waal distances. As a result, strong 1,3 non-bonded repulsive interactions occur due to the close proximity of adjacent substituents (Figure 1.3b).



Figure 1.3a

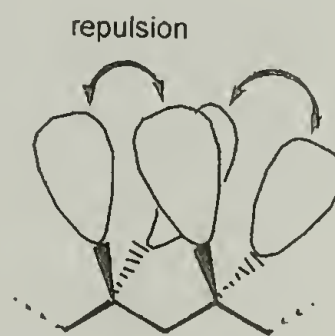


Figure 1.3b

Figure 1.3a. Space-Filling Model of Segments of Poly(vinylidene cyanide)  $[\text{CH}_2-(\text{CN})_2]_4$ .

Figure 1.3b. 1,3 Non-Bonded Repulsive Interactions arising from the presence of Substituents on Every Second Carbon Atom on an Aliphatic Chain.

Polymer chains attempt to minimize the repulsive interactions associated with the close proximity of adjacent substituents by adopting conformations other than the all-trans conformation. However, for poly(vinylidene cyanide) and other 1,1-disubstituted systems

in general, highly unfavorable repulsive interactions are present regardless of the conformation. In the case of poly(vinylidene fluoride) PVDF, four different crystalline forms with different conformations are known.<sup>20</sup> The two main conformations are the  $\alpha$ -form and the  $\beta$ -form. The  $\alpha$ -form (Type II) has a trans-gauche-trans-gauche conformation and the  $\beta$ -form (Type II) has an all-trans (planar zigzag) conformation. The  $\alpha$ -form is the most thermodynamically stable conformation, placing the hydrogen and fluorine atoms alternately on each side of the chain, minimizing the repulsion between the gem-fluorine atoms. The all-trans ( $\beta$ -form) is obtained by mechanical deformation of melt extruded or compression-molded specimen<sup>21</sup> and exhibits high piezo- and pyroelectric activity.<sup>22</sup> This is due to the strong net dipole moment normal to the chain direction arising from the alignment of all the fluorine atoms on one side of the backbone chain.

Polytetrafluoroethylene (PTFE) is an example of a polymer with a density of substitution of 200 substituents per 100 carbon atoms as shown in **d**. The fluorine atoms are significantly larger than hydrogen atoms and steric crowding does not favor an all-trans structure such as in polyethylene. Therefore, during crystallization, the polymer chains minimize the unfavorable repulsive interactions between the pendant groups by adopting helical conformations (a 13/6 helix below 19°C and a 15/7 at higher temperatures).<sup>23,24</sup> On the contrary, poly(vinyl fluoride) which contains 25% of the fluorine atoms found in PTFE, is able to incorporate the fluorine atoms in an all-trans zigzag conformation similar to polyethylene.

PTFE is chemically inert, and heat and solvent resistant due to the shielding of the carbon backbone by the fluorine atoms and the stronger carbon-fluorine bonds.<sup>25</sup> The fluorine atoms form a regular uniform sheath that provides protection to the carbon

backbone. PTFE also has excellent insulation properties and a low coefficient of friction for a wide variety of temperatures. This is due to the reduced surface energy resulting from the high density of fluorine atoms along the chain. In poly(vinyl fluoride), 75% of the strong carbon-fluorine bonds are replaced by weaker carbon-hydrogen bonds. Consequently, the polymer is less resistant to solvents and less thermally stable than the highly fluorinated PTFE, but more stable than the corresponding non-fluorinated polymers.<sup>26</sup> Yet, neither polymer displays the unique pyro- and piezoelectric activity exhibited by poly(vinylidene fluoride) due to its strong net dipole moment.

Modifications of the density of substitution along the backbone also have an effect on the polymer properties. For example, the random replacement of fluorine groups in PTFE with perfluoromethyl groups lowers the degree of crystallinity from 98% to 70% and enables the conventional melt processing of the copolymer due to the lowering of the melt viscosity.<sup>27</sup> With a minor change in the overall density of substitution of fluorine groups directly attached to the backbone, the material properties were enhanced to obtain processable polymers, while maintaining the desirable mechanical properties of the PTFE homopolymer. While the nature of the backbone is important in determining certain “default” properties of the polymer such as its strength and stability, it is evident that the density and precise location of the substituents along the backbone chain exert a strong influence over the final properties of the polymer.



## 1.4 Goals and Objectives

The main goal of this project was to design and synthesize highly functionalized carbon-chain polymers with well-controlled architectures and to study the effect of the density of substitution on the properties of the polymer. Instead of the conventional placement of substituents on every *second* carbon or at random positions along the backbone of carbon-chain polymers, substituents can also be placed on every third carbon, every fourth carbon, or every fortieth carbon. Some of the possible architectures obtained by placing substituents on every third carbon (e,f) and every fourth carbon (g, h) are described in Figure 1.4.

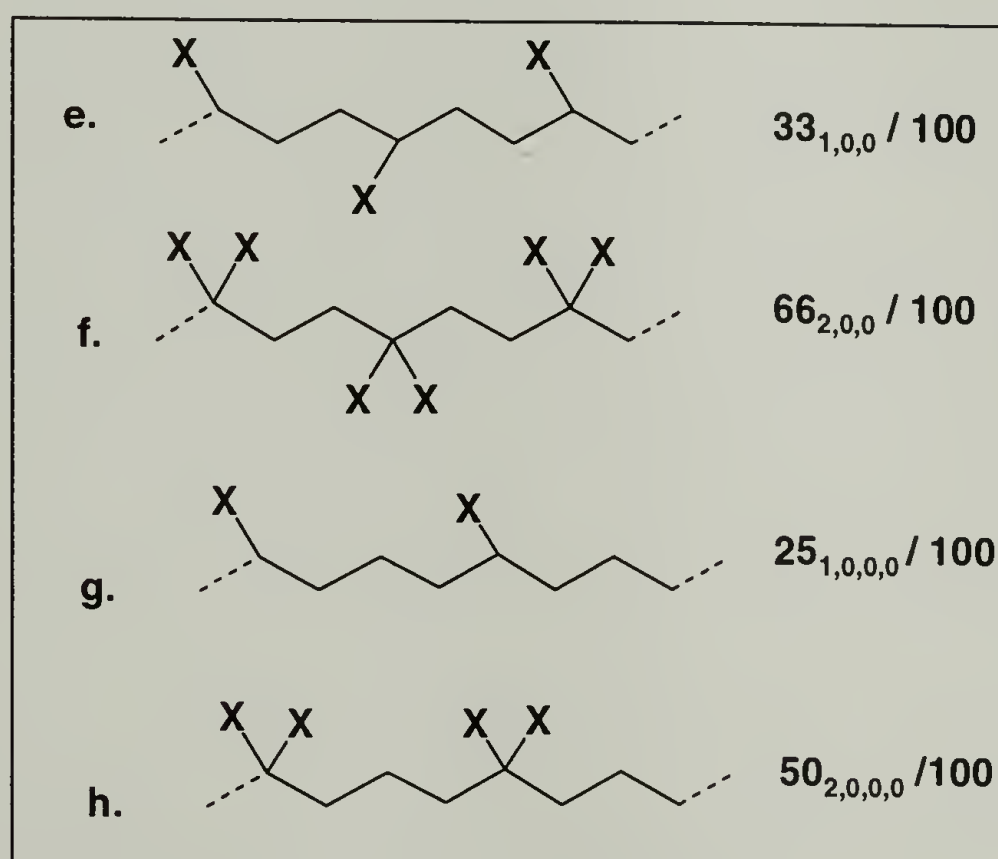


Figure 1.4. Various Substitution Patterns for Carbon-Chain Polymers.

$X_{a,b,c,d} / 100$ : X refers to the total # of functional groups per 100 carbon atoms, and a,b,c,d refer to the # substituents on each carbon in the repeat unit.



In this project, the synthesis of carbon-chain polymers with highly polar (geminal) nitrile and/or larger ester groups on every *third* carbon and every *fourth* carbon was pursued with two main objectives in mind. First, It was proposed that the strong repulsive interactions between adjacent substituents on every second carbon will be significantly minimized by increasing the distance between the quaternary centers. This in turn would allow large and/or highly polar substituents that could not be easily accommodated on classical vinyl polymers to be placed along the polymer backbone.

Secondly, to understand the influence of changing the density of substitution on the overall properties of the polymer such as thermal stability, local conformation of the polymer backbone and crystallinity. Ultimately, we hoped to tailor the unique polymer structure to applications such as pyro- and piezoelectricity, second order non-linear optical properties, or for the vectorial transport of ions or electrons along the backbone chain, which not only require a high density of substitution, but in addition, the specific alignment of the moieties along the backbone in order to utilize the collective intermolecular interactions.

At the onset of this project, several synthetic routes were investigated in order to determine the most efficient synthetic route to achieving polymers with nitrile/and or ester substituents, arranged in the patterns shown in **f** and **h** (Figure 1.4). The highly polar nitrile groups along the backbone are of interest for piezoelectric polymers, while the ester groups are versatile groups for further functionalization of the backbone.

The architectures displayed in examples **f** and **h** exhibit potential for the placement of large (ester) and/or highly polar (cyano) substituents along the backbone. Conformational analysis of a short chain of carbon with substituents on every third

carbon (example **f**) indicated that the main chain is easily able to adopt an all-trans conformation with a distance of 7.6 Å between pendant groups on either side (Figure 1.5).<sup>28</sup> Each rectangle depicts a pendant substituent.

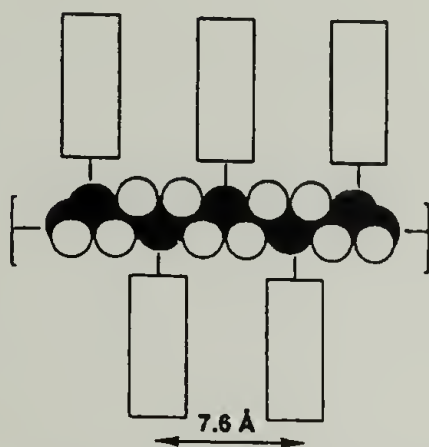


Figure 1.5. All-Trans Conformation of the Main-Chain of a Polymer with Two Substituents on Every Third Carbon.

A distance of 7.6 Å is adequate for the accommodation of large and/or polar substituents such as ester or cyano groups. The density of substitution in examples **e** and **g** is low, and will not be studied in this project. However, the influence of a lower density of substitution on the polymer properties remains an interesting topic for future investigation.

An example of a polymer with the substitution pattern shown in example **f** was synthesized via the cationic polymerization of 3-methyl-1-butene, yielding a polymer with two dimethyl substituents on every third carbon.<sup>29</sup> Compared to poly(isobutylene), which has two methyl substituents on every second carbon, the glass transition temperature of the former increased by at least 60 °C due to increased stiffness of the backbone chain.<sup>14</sup> The rotational barriers along the central carbon-carbon bond for *n*-butane and 2,2,5,5 tetramethylhexane (Figure 1.6) were compared using molecular mechanics calculations (MM2 force field).<sup>28</sup>

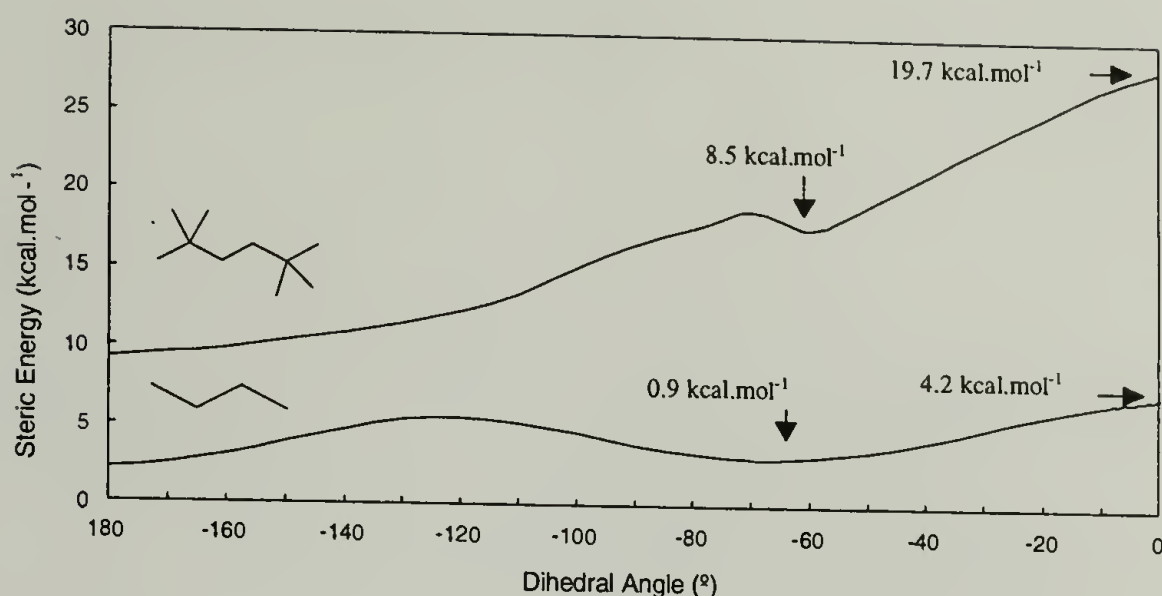


Figure 1.6. Theoretical Conformational Analysis of n-butane (a) and 2,2,5,5-tetramethylhexane (b).

The results demonstrated that the full rotation along the central carbon-carbon bond in tetramethylhexane is very difficult, indicating that the placement of side groups on a short “chain” of carbons has a marked effect on the rotational flexibility of the molecule. Conformational studies of the polymers (in solution and solid state) with gem-diester substituents on every third carbon atom along the polymer backbone by Raman spectroscopy indicated increased stiffness in the backbone. Fine-tuning the nature, density and location of the substituents along the main chain, rather than the nature of the backbone will provide possible control over the stiffness of the polymer backbone.

## 1.5 Summary of Each Chapter

**Chapter 2.** A discussion of the reactivity and polymerizability of cyclopropanes is presented, with comparisons to 1,1-disubstituted cyclopropanes, three membered heterocycles, and vinylcyclopropanes. The synthesis and ring-opening polymerization of 1,1-dicyanocyclopropane **1**, alkyl 1-cyanocyclopropane carboxylates **2a-d**, and phenyl 1-cyclopropanecarbonitrile **4** was achieved under various reaction conditions. The resulting polymer structures were characterized and provide evidence for the ring-opened structures. A comparison of their properties to the homologues with substituents on every second carbon is made.

**Chapter 3.** A detailed analysis of the stereochemistry of poly(alkyl 1-cyanocyclopropanecarboxylates) is provided in this chapter. The influence of reaction conditions on the resulting tacticity was examined and hypotheses on the mechanism of the reaction are presented.

**Chapter 4.** The reactivity of cyclobutanes towards ring-opening is examined and compared to cyclopropanes. In order to obtain carbon-chain polymers with substituents on every fourth carbon, the anionic ring-opening polymerization of dialkyl cyclobutane-1,1-dicarboxylates **5a-c**, ethyl 1-cyanocyclobutanecarboxylate **6**, and 1,1-dicyanocyclobutane **8** under anionic conditions was attempted. The failure to achieve the poly(tetramethylenes) via ring-opening of the activated cyclobutanes is discussed in this chapter.



**Chapter 5.** An alternative route to achieving the desired poly(1,1-di-functionalized tetramethylene)s via the synthesis and polymerization of 1,1-disubstituted butadienes (ethyl 2-cyano-2,4-pentadienoate **9** and diethyl 2-propenylidene malonate **10**) is presented in this chapter. Characterization of the polymer microstructures by  $^1\text{H}$ - and  $^{13}\text{C}$ -NMR spectroscopy is provided. Initial studies on the hydrogenation of the resulting butadiene polymers are presented.

**Chapter 6.** This chapter provides a detailed analysis of the crystalline structure of poly(diethyl cyclopropane-1,1-dicarboxylate) poly(**3b**) using X-ray and electron diffraction analysis. Wide Angle X-ray Scattering (WAXS) data on poly(1,1-dicyanocyclopropane) poly(**1**), poly(alkyl 1-cyanocyclopropanecarboxylate)s (poly **2a**), and poly(phenyl 1-cyclopropanedicarbonitrile) poly(**4**) are also provided.

## 1.6 References

- (1) Natta, G.; Pino, P.; Corradini, P.; Danusso, F.; Mantica, E.; Mazzanti, G.; Moraglio, G. *J. Am. Chem. Soc.* **1955**, 77, 1708.
- (2) Natta, G.; Pasquon, I.; Zambelli, A.; Gatti, G. *J. Polym. Sci.* **1961**, 51, 387.
- (3) Natta, G.; Danuso, F.; Sianesi, D. *Makromol. Chem.* **1959**, 30, 238.
- (4) Natta, G.; Danuso, F.; Sianesi, D. *Makromol. Chem.* **1958**, 28, 253.
- (5) Natta, G. *J. Polym. Sci* **1955**, 16, 143.
- (6) Levowitz, I. In *Modern Plastics Encyclopedia*, **1998**; Vol. 75, p B3.
- (7) Allcock, H. R.; Lampe, F. W. In *Contemporary Polymer Chemistry*; Prentice Hall: New Jersey, 1990; p 546.
- (8) Allcock, H. R.; Lampe, F. W. In *Contemporary Polymer Chemistry*; Prentice-Hall: New Jersey, 1990; p 542.

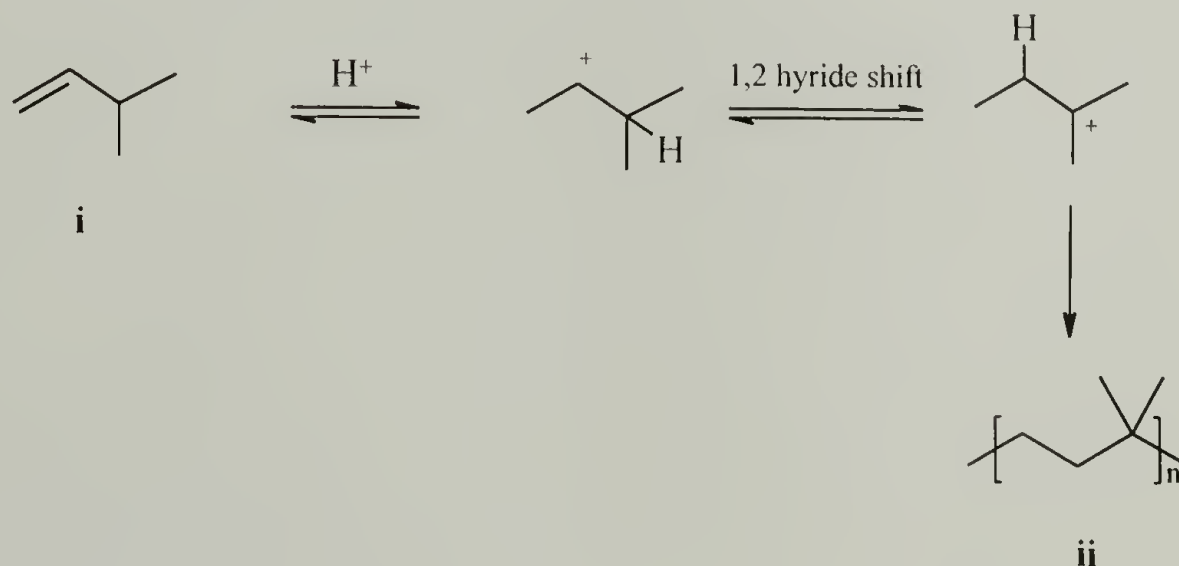
- (9) Finkelmann, H.; Rehage, G.; Gordon, M. In *Liquid Crystal Polymers II/III, Advances in Polymer Science Series*; Springer-Verlag: New York, 1984; Vol. 60/61, p 99.
- (10) Allcock, H. R.; Lampe, F. W. In *Contemporary Polymer Chemistry*; Prentice-Hall: New Jersey, 1990; p 146.
- (11) Coles, H. J.; Simon, R.; Chapoy, L. L. In *Recent Advances in Crystalline Polymers*; Elsevier Applied Science Publishers: Barking, UK, 1984; p 324.
- (12) Shibaev, V. P.; Kostromin, S. G.; Plate, N. A.; Ivanov, S. A.; Vetrov, V. Y.; Yakolev, I. A. *Polymer Commun.* **1983**, 24, 364.
- (13) Odian, G. In *Encyclopedia of Polymer Science and Engineering*; Mark, H., Bikales, N. M., Overberger, C. G., Menges, G., Kroschwitz, J. I., Eds.; Wiley-Interscience: New York, 1985; Vol. 3, p 274.
- (14) Andrews, R. J.; Grulke, E. A. In *Polymer Handbook*; Brandrup, J., Immergut, E. H., Grulke, E. A., Eds.; Wiley-Interscience: New York, 1999; Vol. VI, p 207.
- (15) Illers, K. H.; *Kolloid-Z. Polym.* **1974**, 252, 1.
- (16) Illers, K. H.; *Kolloid-Z. Polym.* **1973**, 251, 394.
- (17) Illers, K. H.; *Kolloid-Z. Polym.* **1969**, 231, 62.
- (18) Otsu, T.; Matsumoto, A.; Shiraishi, K.; Amaya, N.; Koinuma, Y. *J. Polym. Sci., Part A: Polym. Chem.* **1992**, 30, 1559 and references therein.
- (19) Choi, S. B.; Takahara, A.; Amaya, N.; Murata, Y.; Kajiyama, T. *Polym. J.* **1989**, 21, 215.
- (20) Lovinger, A. J. In *Developments in Crystalline Polymers-1*; Bassett, D. C., Ed.; Applied Science Publishers: London, 1982, Chapt. 5.
- (21) Richardson, A.; Hope, P. S.; Ward, I. M. *J. Polym. Sci., Part B: Polym. Phys.* **1983**, 21, 2525.
- (22) Dohany, E. J.; Humphrey, J. S. In *Encyclopedia of Polymer Science and Engineering*; Mark, H., Bikales, N. M., Overberger, C. G., Menges, G., Kroschwitz, J. I., Eds.; Wiley-Interscience: New York, 1985; Vol. 17, pp 536-538.
- (23) Bunn, C. W. *J. Polym. Sci.* **1955**, 16, 322.

- (24) Young, R. J.; Lovell, P. In *Introduction to Polymers*; Chapman & Hall: New York, 1991; p 251.
- (25) Gangal, S. V. In *Encyclopedia of Polymer Science and Engineering*; Mark, H., Bikales, N. M., Overberger, C. G., Menges, G., Kroschwitz, J. I., Eds.; Wiley-Interscience: New York, 1985; Vol. 16, pp 577-613.
- (26) Brasure, D.; Ebnesajjad, S. In *Encyclopedia of Polymer Science and Engineering*; Mark, H., Bikales, N. M., Overberger, C. G., Menges, G., Kroschwitz, J. I., Eds.; Wiley-Interscience: New York, 1985; Vol. 17, p 476.
- (27) Miller, W. T.; U.S. Patent 2, 283, May 27, 1952.
- (28) Penelle, J., unpublished results (molecular mechanics conformational analysis results obtained using the Cambridge Soft Chem3D version 3.5 software and the MM2 force field.).
- (29) Kennedy, J. P.; Thomas, R. M. *Makromol. Chem.* **1962**, 53, 28.

## RING-OPENING POLYMERIZATION OF CYCLOPROPANES

## 2.1 Introduction

Access to polymers with a variety of functional groups on every *second* carbon can be achieved by chain polymerization of mono- and 1,1-disubstituted vinyl monomers. In this chapter, the synthesis of carbon-chain polymers with two geminal substituents on every *third* carbon is discussed. An example of a polymer with two methyl substituents on every third carbon was synthesized by the “phantom” cationic polymerization of 3-methyl-1-butene (i) (Scheme 2.1).<sup>1,2</sup> This polymerization proceeds via a 1,2 hydride shift to the more stable tertiary carbocation. Since the rate of the 1,2-hydride shift is faster than the propagation, the isomerized repeat unit (ii) is obtained.<sup>3</sup>

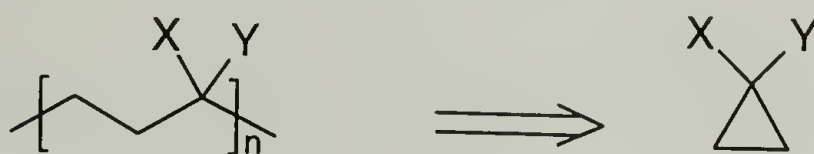


Scheme 2.1. Cationic polymerization of 3-methyl-1-butene (i)

From a retrosynthetic viewpoint, a more direct way to achieve polymers with two substituents on every third carbon is via the ring-opening polymerization of substituted



cyclopropane rings (Scheme 2.2). In order to determine the feasibility of cyclopropanes towards ring-opening polymerization, the chemistry, thermodynamics and kinetics of polymerization of the rings was examined. A discussion is provided in the following section.



Scheme 2.2. Retrosynthetic Analysis of the Ring-Opening Polymerization of Activated Cyclopropanes.

## 2.2 Background: The Chemistry of Cyclopropanes

### 2.2.1 Structure and bonding

The bonding in cyclopropane has been described by two models: the Coulson-Moffitt model<sup>4</sup> and the Walsh model.<sup>5</sup> There is much evidence that the bonding orbitals of the carbon atoms in cyclopropanes are not the same as for a normal carbon atom in a saturated alkane, which has one *s* and three *p* orbitals hybridized to give four  $sp^3$  orbitals. Instead, the carbon atoms in the cyclopropane ring have four non-equivalent orbitals. The two orbitals involved in ring bonding have more *p* character, while the two orbitals directed to the outside bonds have more *s* character. These carbon-carbon bonding orbitals have also been referred to as  $sp^5$  orbitals because of their greater “p-like” character.<sup>6,7</sup>

The Moffitt model constructs the cyclopropane ring from three  $sp^3$ -hybridized orbitals, which are approximately 22° outward as depicted in Figure 2.1. In normal carbon-carbon bonds, the  $sp^3$  orbitals overlap such that the straight line connecting the

nuclei becomes an axis around which the electron density is symmetrical. In cyclopropane rings, the electron density is directed away from the ring and the bonds are intermediate in character between  $\sigma$  and  $\pi$ . These bonds are also referred to as “bent”.<sup>4,8,9</sup> Consequently, in many aspects, the chemistry of the cyclopropane ring is similar to that of the carbon-carbon double bond.

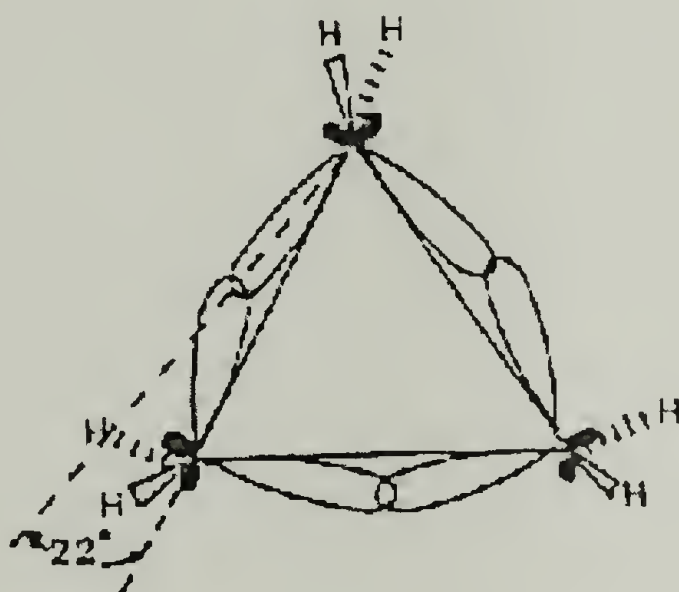


Figure 2.1. Coulson-Moffitt Model of Cyclopropane

The Walsh model constructs the cyclopropane ring from three  $sp^2$ -hybridized orbitals that are radially oriented towards the center of the ring. The molecular orbital diagram of this basis set is depicted in Figure 2.2. The overlap of the orbitals comprising  $\psi_2$  is viewed as a distorted  $\pi$ -bond, which gives reason for the resemblance of the chemistry of the cyclopropane ring to that of the carbon-carbon double bond.

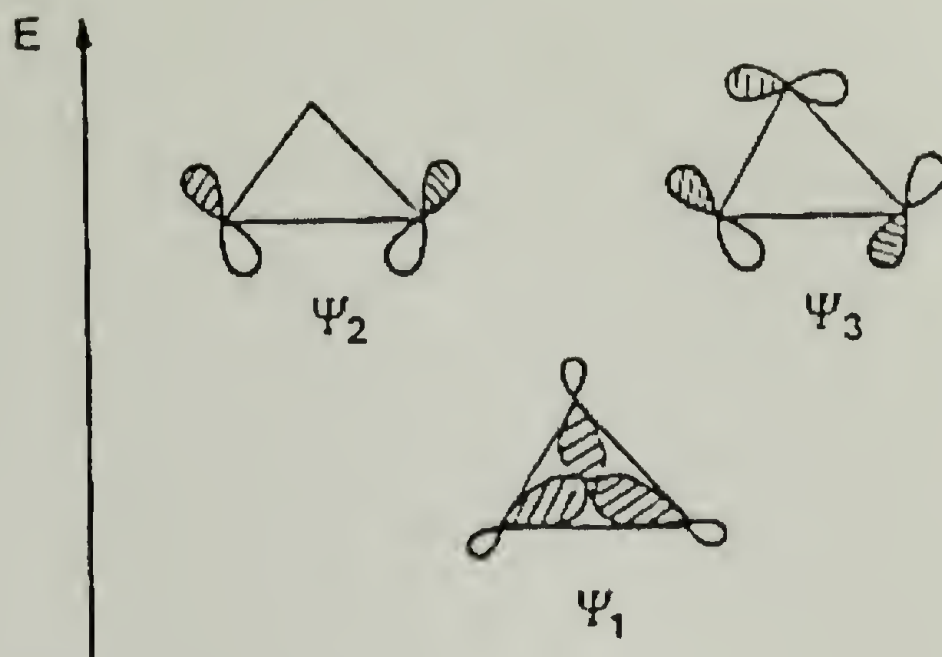


Figure 2.2. Walsh Model of Cyclopropane

### 2.2.2 Reactivity

The unique reactivity of cyclopropanes is associated with the relief of its ring strain and the similarity of the chemistry of its carbon-carbon bond to that of a carbon-carbon double bond. Three-membered alkane rings are highly strained because the  $60^\circ$  carbon-carbon-carbon angles are considerably less than the ideal  $109.5^\circ$  for  $sp^3$ -hybridized orbitals.<sup>10,11</sup> The cyclopropane ring is also known to suffer from additional torsional strain due to the coplanar arrangement of the carbon atoms forcing the carbon-hydrogen bonds to be eclipsed.<sup>12</sup>

Cyclopropane rings containing heteroatoms differ in bond angles, bond lengths and bond strengths depending on the nature of the heteroatom.<sup>13</sup> The strain energies, bond angles and bond lengths of some three-membered rings are shown in Table 2.1.<sup>14,15</sup> The replacement of one of the carbon atoms with an oxygen or nitrogen does not

significantly change the geometry and the resulting ring strain. However, for the sulfur heterocycle, longer bond lengths and lower ring strain-energy are measured.

Table 2.1. Strain Energies ( $\text{kJ} \cdot \text{mol}^{-1}$ ), Bond Angles and Bond Lengths of Three Membered Cyclics<sup>13</sup>



	Cyclopropane X= CH <sub>2</sub>	Oxirane X=O	Thiirane X=S	Aziridine X=N-H
Ring Strain ( $\text{kJ} \cdot \text{mol}^{-1}$ ) <sup>a</sup>	115	114	83	113
Bond lengths (Å)				
X-C	1.51	1.436	1.819	1.488
C-C	1.51	1.472	1.492	1.483
C-H		1.082	1.078	
Bond Angles, (degrees)				
C-X-C	60	61.4	48.4	59.6
X-C-C	60	59.3	65.8	60.2
H-C-H		116.57	116.0	

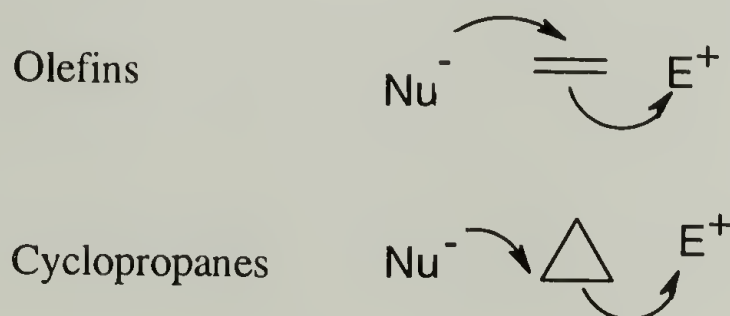
<sup>a</sup>  $1 \text{ kcal} \cdot \text{mol}^{-1} = 4.189 \text{ kJ} \cdot \text{mol}^{-1}$

A detailed review of the use of cyclopropanes in chemical synthesis describes the reactivity of cyclopropanes and its derivatives towards various electrophiles, nucleophiles and in free radical reactions.<sup>12</sup> A discussion of their reactivity towards ring-opening is outlined in the next section, with comparisons made to ethylene oxide (oxirane) and thiirane.



### 2.2.3 Ring-Opening Reactions

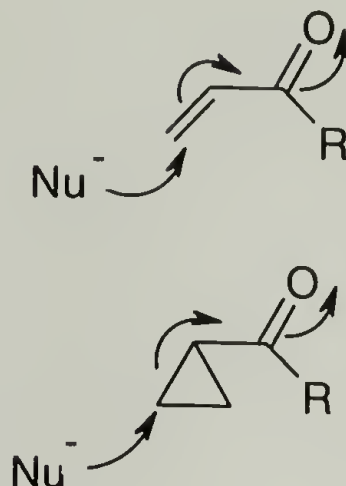
The cleavage of cyclopropane rings can be achieved by thermal, oxidative, reductive, electrophilic, nucleophilic and other methods.<sup>12</sup> The ring-opening of cyclopropanes via radical mechanisms with less reactive radicals such as  $I\cdot$  and  $Br\cdot$  have been reported.<sup>16-21</sup> For extremely reactive radicals such as  $Cl\cdot$  or  $t-BuO\cdot$ , hydrogen abstraction is observed.<sup>22</sup> No example of cleavage by a carbon-centered radical has ever been discovered despite many attempts. Simple heterolytic fragmentation of cyclopropane rings is possible when the ring is substituted with functional groups that enhance the unidirectional flow of electrons.<sup>23,24</sup> Addition reactions of cyclopropanes can be compared to alkene additions (Scheme 2.3) and depend on the nature of the substituent (electron-donating or electron accepting) attached to the ring.



Scheme 2.3. Comparison of Addition Reactions in Alkenes and Cyclopropanes

The opening of cyclopropane rings resulting from addition reactions with various electrophiles has been reported.<sup>25,26</sup> Substituted cyclopropanes such as 1,1,2-trimethylcyclopropane undergo electrophilic additions ( $SbF_5-HSO_3F$ ,  $-50\text{ }^{\circ}C$ ), following Markovnikov's rule.<sup>27</sup> The earliest reported example of the nucleophilic ring-opening reaction of substituted cyclopropanes was by Bone and Perkin in 1895.<sup>28</sup>

The sodium salt of diethyl malonate was used to ring-open diethyl 1,1-cyclopropanedicarboxylate. This reaction is the homologous (or 1,5) version of the classical Michael addition (Scheme 2.4).<sup>29</sup>



Scheme 2.4. Homologous (1,5) Version of the Classical Michael Addition.

Other examples of nucleophiles that have been used to ring-open activated cyclopropanes include: various amines, mercaptans and thiophenol,<sup>30,31</sup> and soft nucleophiles such as thiophenolates, azides, or organocuprates.<sup>29,32</sup> In these examples, the cyclopropanes have two geminal electron-withdrawing substituents such as nitriles, amides and ester groups. For dialkyl 1,1-cyclopropanedicarboxylates (**3**), hard nucleophiles like Grignard reagents, or butyl lithium, preferentially attack the carbonyl on the ester group and cannot be used to ring-open these cyclopropanes.<sup>33</sup> The ring-opening reactions of 1,1-bis(phenylsulfonyl)cyclopropane (**iii**),<sup>34</sup> and cyclopropanes with two electron-donating alkoxy groups and one electron-withdrawing ester group on the adjacent carbon (**iv**) have also been reported (Figure 2.3).<sup>35</sup>

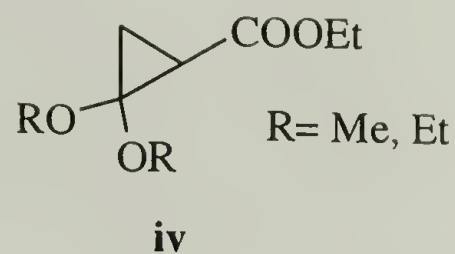
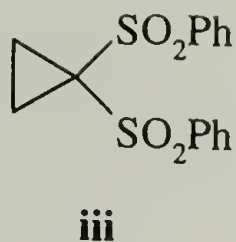
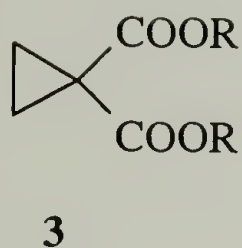
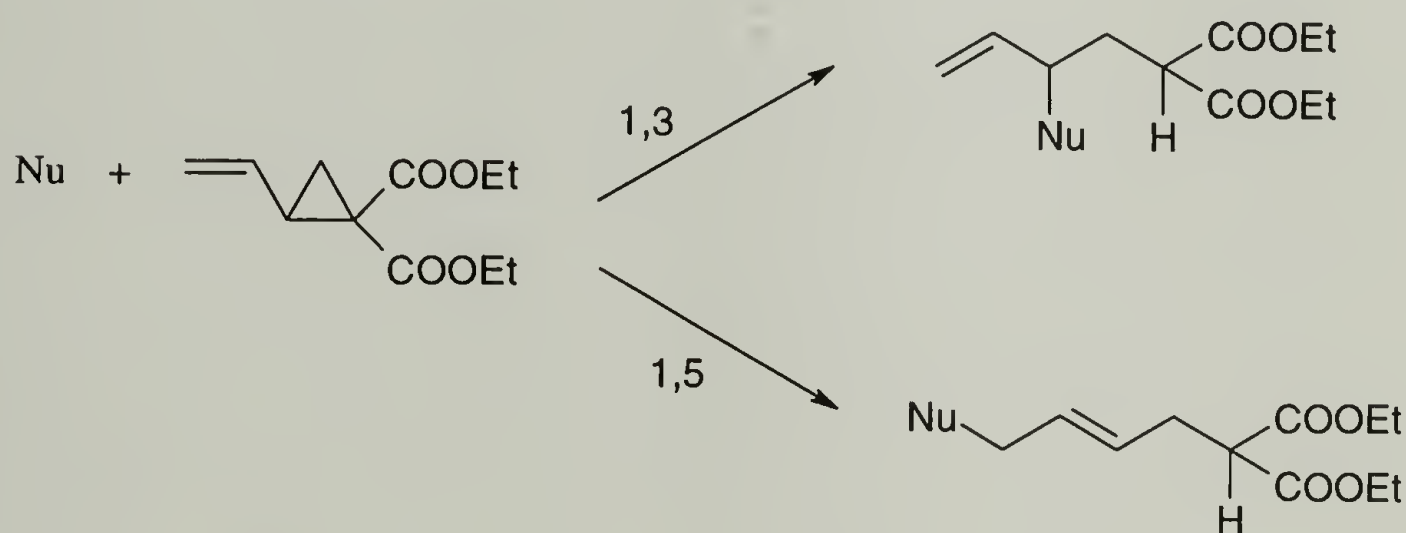


Figure 2.3. Examples of Various Cyclopropanes that undergo Nucleophilic Ring-Opening Reactions.

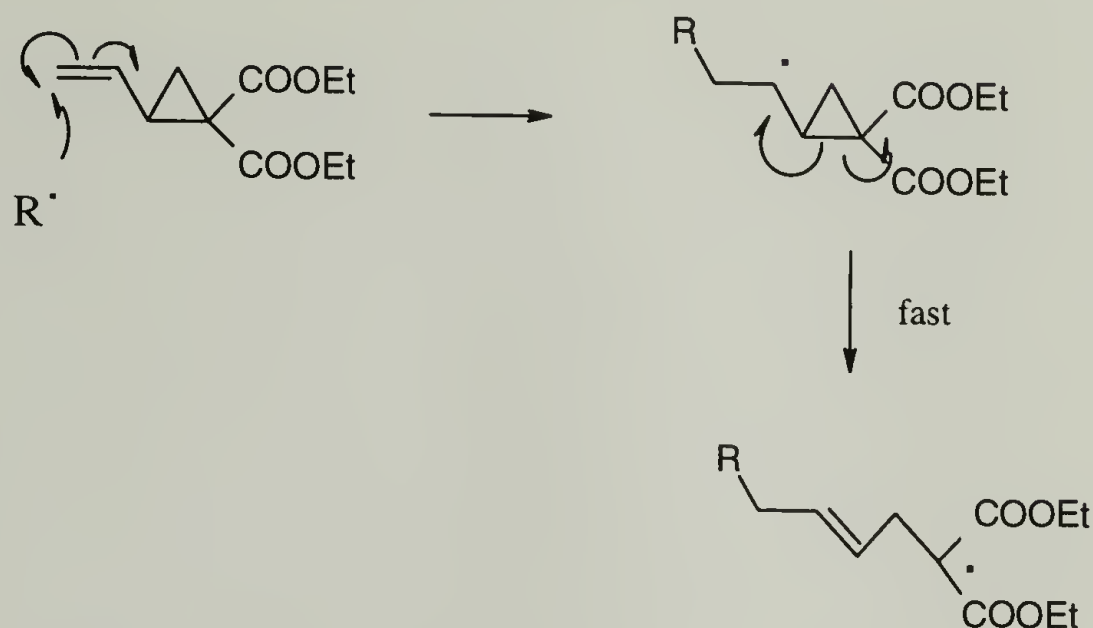
Vinyl cyclopropanes also undergo nucleophilic ring-opening additions when substituted with two gem electron-withdrawing groups.<sup>36,37</sup> Danishefsky et al. showed that some of these nucleophilic additions occur via an  $S_N2$  pathway (complete inversion of configuration is observed) in a predominantly 1,3 mode (Scheme 2.5).



Scheme 2.5. Nucleophilic Addition Reactions to Vinyl Cyclopropanes.  
[Nu = nucleophile]

In addition, vinyl cyclopropanes primarily rearrange via biradical intermediates to yield cyclopentene when heated.<sup>38-43</sup> Radical initiated ring-opening reactions yielding 1,5 products (including dimers) were reported.<sup>36,44</sup>

The mechanism is believed to occur via addition to the double bond and subsequent rearrangement by opening of the cyclopropyl ring (Scheme 2.6). No direct attack on the carbon-carbon bond of the ring has ever been observed.



Scheme 2.6. Ring-Opening of Vinyl Cyclopropanes via Radical Mechanisms.

#### 2.2.4 Reactivity of three-membered heterocycles

The reactivity of various three-membered heterocyclics towards nucleophilic ring-opening generally increases with an increase in the electronegativity of the heteroatom.<sup>13</sup> Oxiranes and thiiranes display much higher reactivity than cyclopropane towards ring-opening. For example, ethylene oxide is a highly reactive compound, undergoing ring-opening by reaction with amines in aqueous solutions at ambient temperature without any significant base catalysis.<sup>45,46</sup> The mechanism occurs by attack of the nucleophile on one of the epoxide carbon atoms breaking the highly polar carbon-oxygen bond and relieving the ring strain. Thiirane (sulfur derivative) has a much lower ring strain-energy in comparison to oxirane or aziridine (Table 2.1). However, it is reported that sulfur containing heterocycles are highly reactive due to the stronger and easier polarization of the sulfur-carbon bond, and for anionic reactions, the higher nucleophilicity of the



thiolate compared to the alcoholate anion. A comparison of the reactivity of three and four-membered heterocycles is provided in chapter 4.

### 2.2.5 Polymerizability of Cyclopropanes

It is well known that for a chemical reaction to occur the equilibrium between the reactants and products must favor the products (thermodynamics) and there must be a mechanism allowing the reaction to occur (kinetics).<sup>47</sup> Therefore, the feasibility of the ring-opening polymerization of cycloalkanes and their derivatives will depend on the favorability of both thermodynamic and kinetic factors.

#### 2.2.5.1 Thermodynamics of Polymerization

Polymerizations are generally associated with considerable loss in translational energy. As a result, the ring-opening polymerization of cycloalkanes to form linear macromolecules occurs only if the monomer concentration  $[M]$  is above the equilibrium monomer concentration  $[M]_c$  at a given temperature; or if at a given monomer concentration, the temperature  $T$  is less than the ceiling temperature  $T_c$ , where  $T_c$  is defined as the critical temperature above which polymerization does not occur.  $[M]_c$  and  $T_c$  are related to the free energy of polymerization ( $\Delta G$ ,  $\Delta G = \Delta H - T\Delta S$ ) and can be experimentally determined.<sup>48</sup> The free energy of polymerization ( $\Delta G_{lc}$ ) must be negative for the polymerization to be thermodynamically favorable.

The values of  $\Delta G_{lc}$  for the polymerization of non-substituted cycloalkanes can be estimated from thermodynamic data provided from the reagents and products (polyethylene). These values are plotted against the ring size in Figure 2.4.<sup>47,49</sup> With the

exception of cyclohexanes and substituted cyclopentanes, the  $\Delta G_{lc}$  values for the ring-opening polymerization of cycloalkanes (ring size 3-8) are negative. For both unsubstituted and substituted cyclopropanes, the  $\Delta G_{lc}$  values are largely negative. The values for the semi-empirical heats and entropies of polymerization at 25 °C for ethylene and various cycloalkanes are shown in Table 2.2. The data shows that the free energy of polymerization of cyclopropane and cyclobutane rings considerably more negative than for ethylene.

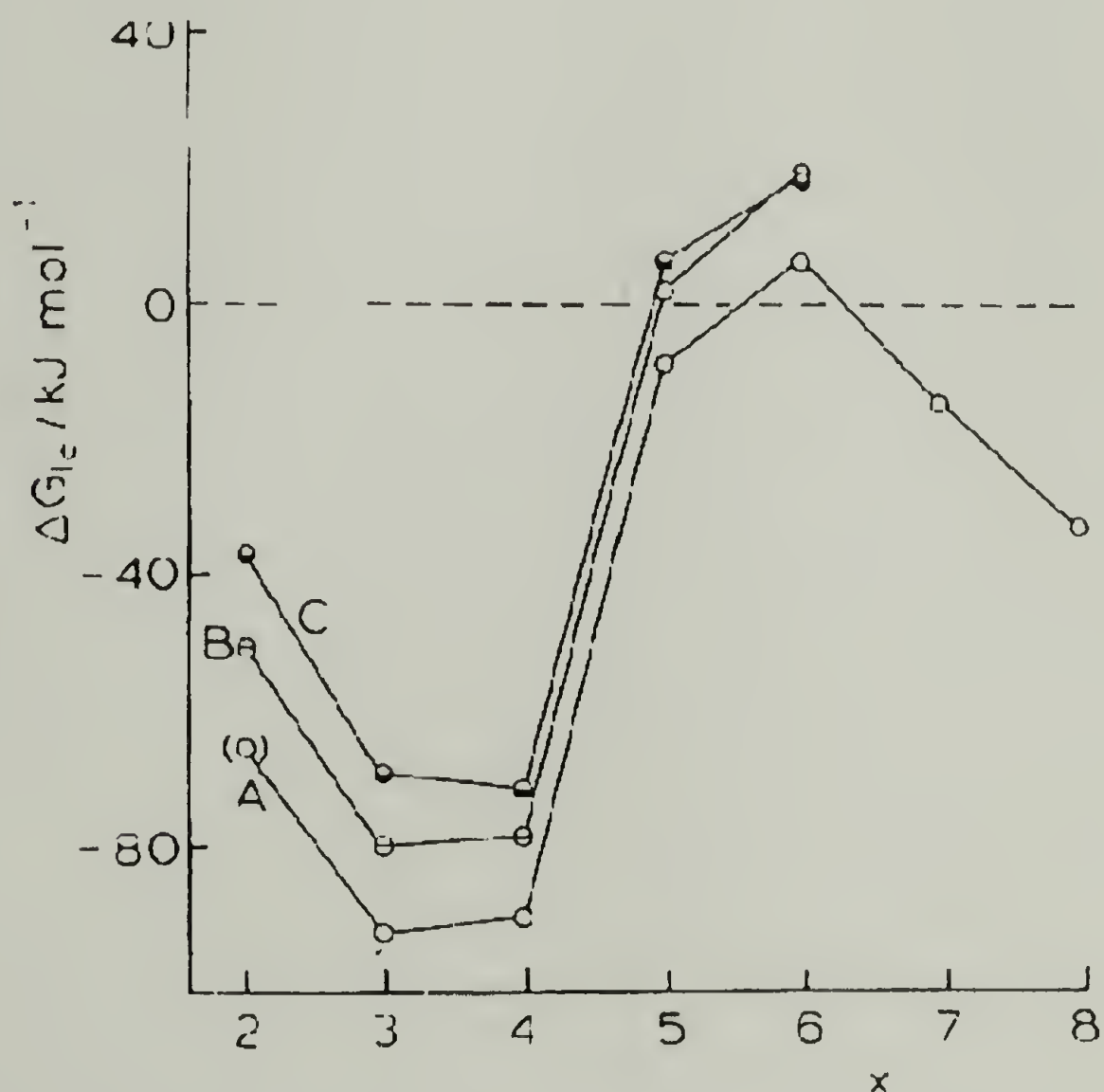


Figure 2.4. Free Energy of Polymerization of Cycloalkanes as a Function of the Number of Atoms in the Ring (x) A. unsubstituted; B. methyl substituted; C. 1,1-dimethylsubstituted.<sup>49</sup>

Table 2.2. Semi-Empirical Heats and Entropies of Polymerization at 25 °C.<sup>50,51</sup>

Monomer	$-\Delta H_x^\circ$	$-\Delta S_x^\circ$	$-\Delta G_x^\circ$
gg value: ethylene	22.35	34.0	12.2
lc values: cycloalkanes			
[CH <sub>2</sub> ] <sub>x</sub> ; x = 3	27.0	16.5	22.1
x = 4	25.1	13.2	21.2
x = 5	5.2	10.2	2.2
x = 6	-0.7	2.5	-1.4
x = 7	5.1	0.7	4.9
x = 8	8.3	-8.9	11.0

g = gas, l = liquid, c = condensed amorphous polymer

All values are in kcal·mol<sup>-1</sup>

#### 2.2.5.2. Kinetics of Polymerization

The ability of a cycloalkane to polymerize by ring-opening also depends on the availability of a reaction pathway. Unsubstituted cyclopropanes do not easily ring-open because of the absence of polarization in the carbon-carbon bonds and cleavage of the carbon-carbon  $\sigma$ -bond is associated with a high energy of activation.<sup>52</sup> Therefore, the overall polymerizability of cyclopropanes is poor.

As previously discussed, placing electron-withdrawing substituents on the cyclopropane ring is known to dramatically increase their reactivity towards nucleophilic ring-opening additions. The kinetics of polymerization can be also improved by placing activating electron donating and/or electron withdrawing substituents on the ring. For example, by placing electron-withdrawing groups on the ring, the less electrophilic carbon becomes an acceptable nucleofuge and a stable propagating center can be generated upon reaction with a nucleophile. This electronic effect within the monomer makes it susceptible to nucleophilic attack, but also stabilizes the active sites that are generated. This is evident in the case of cyclic monomers with heteroatoms, such as



ethylene oxide. This monomer readily undergoes anionic ring-open polymerization because cleavage of the carbon-oxygen bond is favored by the transfer of electrons to the more electronegative oxygen atom. The kinetic polymerizability of heterocyclics will depend on the nature of the heteroatom and its electronegativity.<sup>13</sup> The kinetic factor is evident when the overall polymerizability of cycloalkanes are compared to cycloalkenes and heterocyclics. Despite the thermodynamic favorability, the unavailability of a reaction mechanism prevents the cycloalkane monomers from polymerizing. (Table 2.3).

Table 2.3. Polymerizability of Various Cyclics<sup>49</sup>

Cyclic compound	$\Delta G_{lc}$	Mechanism available	Examples of polymerization
cycloalkanes			
[CH <sub>2</sub> ] <sub>x</sub> ;			
x = 3	Large negative	+	few
x = 4	Large negative	r	very few
x = 5	Small negative	No	none
x = 6	Small positive	No	none
x = 7	Small negative	No	none
cycloalkenes			
[CH <sub>2</sub> ] <sub>x</sub> ;			
x = 4	Large negative	c	many
x = 5	Small negative	c	many
x = 6	Small positive	c	few
x = 7	Small negative	c	many
heterocyclics			
[OCH <sub>2</sub> ] <sub>x</sub> ;			
x = 2	Large negative	-/ +/ c	many
x = 3	Large negative	-/+	many

- (anionic); + (cationic); c (coordination); r (radical)



## 2.2.6 Ring Opening Polymerization of Cyclopropanes: Literature Survey

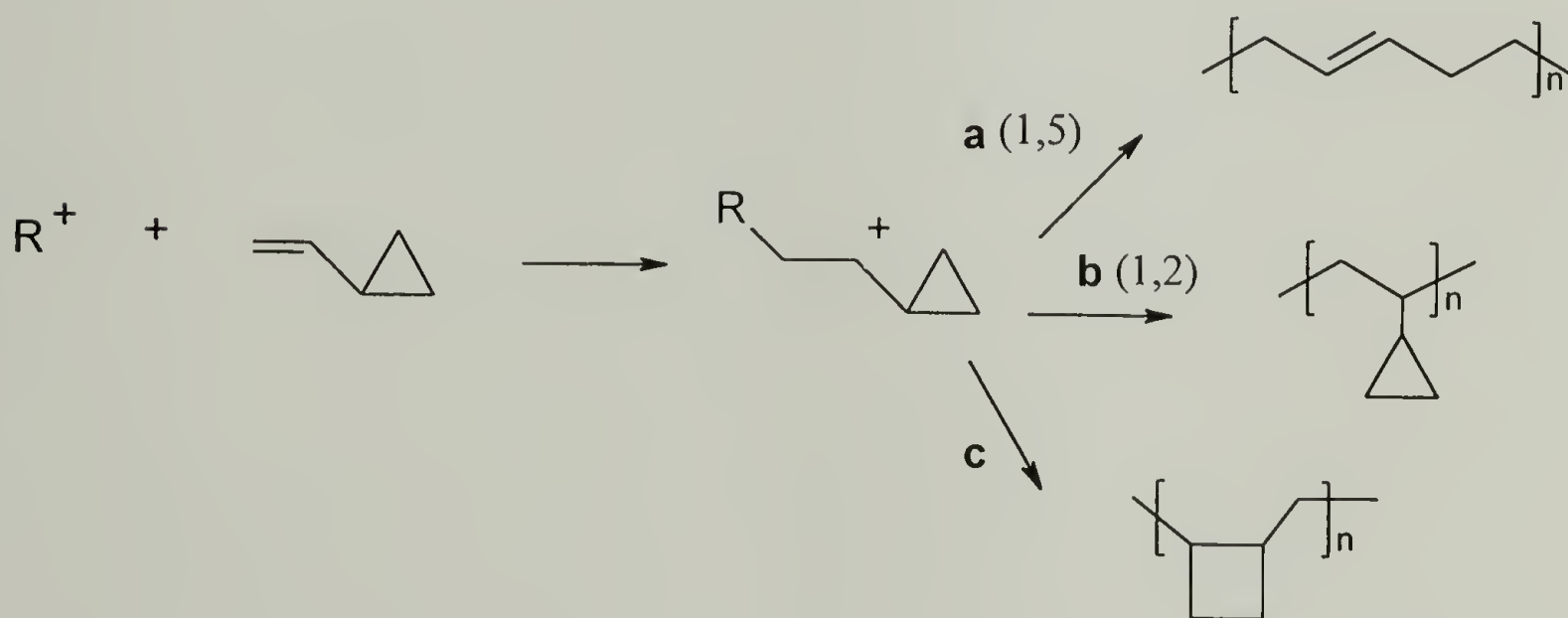
Unsubstituted cyclopropanes are difficult to polymerize for reasons highlighted in the previous section.<sup>48</sup> It is clear that the relief of the large ring strain provides a strong thermodynamic driving force.<sup>53</sup> However, despite this favorable thermodynamic driving force, no example of the efficient ring-opening polymerization of unsubstituted cyclopropane has been reported. On the other hand, various examples of ring-opening polymerization (oligomerization) of activated cyclopropanes by cationic, anionic, radical and coordination mechanisms are available in the literature, and an overview is given in the following section.

### 2.2.6.1 Cationic Polymerization

The polymerization of cyclopropane by aluminium tribromide (with hydrobromic acid as a cocatalyst) was reported by Tipper and Walker.<sup>54</sup> Substituted cyclopropanes such as 1,1-dimethylcyclopropane, 1,2-dimethylcyclopropane, ethylcyclopropane, and n-propylcyclopropane were also polymerized with various aluminium halides by Pine and coworkers in 1953.<sup>55</sup> Characterization of these polymers was minimal, but the available data suggested a cationic chain mechanism. The work by Aoki et al. on the effect of different catalysts on the cationic polymerization of 1,1-dimethylcyclopropane and phenylcyclopropane showed that  $\text{AlBr}_3$  was the only effective catalyst of those studied ( $\text{AlCl}_3$ ,  $\text{SnCl}_4$ ,  $\text{TiCl}_4$  and  $\text{BF}_3\cdot\text{OEt}_2$ ).<sup>56</sup> The cationic polymerization of various cyclopropanes substituted with alkyl, chlorine or phenyl substituents was also studied, but in all these examples the molecular weights obtained were low ( $\overline{M}_n \sim 1000$ ), typical of oligomers.<sup>57,58</sup> Oxiranes also polymerize under cationic conditions, but a mixture of

low molecular weight ( $\overline{Mn} < 1000$ ) linear oligomers, and greater than 90% cyclic oligomers (predominantly dimers) are obtained.<sup>59,60</sup>

Vinyl cyclopropane has also been polymerized under cationic conditions (Scheme 2.7). The resulting polymers contained pendant cyclopropane units, indicating the polymerization primarily occurred via the double bonds (1,2 polymerization) **b**. The cyclopropyl group is known to stabilize adjacent carbenium ion.<sup>61,62</sup> The polymer structures also contain a small amount of 1,5 units **a** (as a result of rearrangement of the primary carbenium ion) and of cyclobutane units **c**. A variety of substituted 1,1-disubstituted 2-vinyl cyclopropane monomers (with methyl, halides and phenyl groups) have been polymerized cationically. Only low to moderate molecular weights in moderate conversion were obtained.<sup>63-68</sup>



Scheme 2.7. Cationic Polymerization of Vinyl Cyclopropane.

#### 2.2.6.2 Coordination Polymerization

The polymerization of some substituted cyclopropanes with Ziegler-Natta catalysts has been reported, although evidence for the polymerization mechanism (cationic or coordination) is lacking. For example, 1,1-dimethylcyclopropane and phenylcyclopropane were polymerized with  $\text{C}_2\text{H}_5\text{AlCl}_2/\text{TiCl}_3$  to yield polymers with molecular weights ( $\overline{Mn}$ )  $< 1500$ .<sup>56</sup> Other work by Pinazzi and coworkers on the polymerization of 1,1-dimethyl-2,2-dichlorocyclopropane using  $\text{Et}_3\text{Al}/\text{TiCl}_4$  and  $\text{Et}_2\text{AlCl}/\text{TiCl}_4$  yielded polymers with higher molecular weights ( $\overline{Mn} \sim 3000\text{-}5000$ ).<sup>69-74</sup> Vinyl cyclopropane polymerizes mainly via 1,2 addition on the double bond under transition metal catalysis, forming moderate to high molecular weight polymers.<sup>65,75,76</sup>

#### 2.2.6.3 Radical Polymerization

A claim on the radical polymerization of cyclopropane was made by Harris and coworkers in 1936.<sup>77</sup> Later work by Ivin showed that the oligomerization of cyclopropane under the same conditions occurs via the formation of a bialllyl radical intermediate, similar to that obtained from propene.<sup>78</sup> Early work on the radical ring-opening polymerization of vinyl cyclopropanes yielded low molecular weight polymers with low conversions.<sup>63-66</sup> Some of these vinyl cyclopropane monomers contained additional activating substituents such as methyl groups on the double bond, or chloride(s) on the cyclopropane ring. Lishanskii and coworkers reported the first high molecular weight polymers obtained from the radical polymerization of vinyl cyclopropanes.<sup>79,80</sup> The vinylcyclopropane monomer contained an additional ester group on the adjacent carbon. Vinylcyclopropane monomers with two electron-withdrawing groups (esters and nitriles)

on the adjacent carbon were polymerized by Cho and coworkers.<sup>81</sup> The polymerizations are favored because of the resonance stabilization of the propagating radical. The diphenyl analogue is believed to have failed to polymerize because the resonance stabilization was too high. High molecular weights and high conversions were obtained using AIBN at 55 °C after 16-20 hours. Characterization of these polymers by NMR and IR indicated that the 1,5 structure was predominant, suggesting that the radical addition occurs via the double bond and then rearranges as described in Scheme 2.6.

#### 2.2.6.4 Anionic Polymerization

Unlike epoxides, the anionic ring-opening polymerization of cyclopropane does not occur due to the absence of polarization in the potentially cleavable bonds. However, the anionic ring-opening polymerization of cyclopropanes substituted with strong electron-withdrawing groups (**v**, **vi**) was reported by Cho et al. in 1979 (Figure 2.5).<sup>82,83</sup>



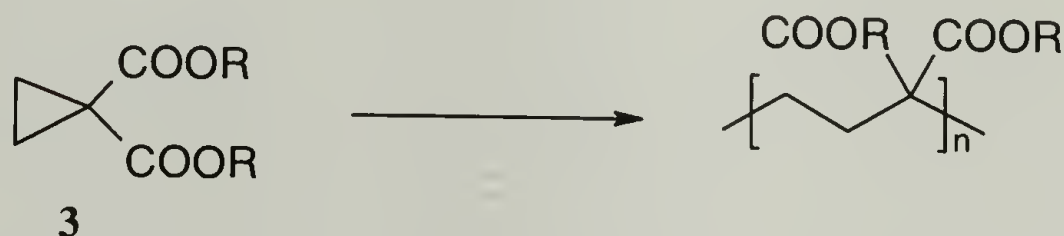
Figure 2.5. Structures of 2-Vinyl and 2-Phenyl-1,1-Disubstituted Cyclopropanes

Both the diester and the diphenyl vinyl analogues in this series failed to polymerize under the given polymerization conditions (NaCN, 0-25 °C, DMF). Characterization of the polymers was minimal but proved that the polymerization involved the opening of the



cyclopropane ring and not addition to the double bond for the vinyl monomers. These experiments indicated that the successful anionic ring-opening polymerization of cyclopropanes required at least one strong electron-withdrawing group such as a nitrile group, and an additional activating phenyl or vinyl group on the adjacent carbon.

Later work in our group (Xie T., Gorissen, P.) on the anionic ring-opening polymerization of dialkyl cyclopropane-1,1-dicarboxylates (**3**) proved that the electron-donating group (in the 2 position) was not essential for the polymerization of these cyclopropanes to high molecular weight (Scheme 2.8).<sup>84-86</sup>



R= Me (**a**), Et (**b**), n-Pr (**c**), n-Hex (**d**), i-Pr (**e**), t-Bu(**f**)

Scheme 2.8. Structure of Dialkyl Cyclopropane-1,1-Dicarboxylates

Furthermore, controlled living polymerization of some of the monomers was demonstrated, yielding polymers with narrow molecular weight distributions and controlled molecular weights.<sup>87</sup> The ester substituents along the backbone offered versatility to further functionalization of the main chain. For example, the hydrolysis of poly(di n-propyl-cyclopropane-1,1-carboxylate) provided a polyelectrolyte containing two carboxylate anions (COO<sup>-</sup>) on every third carbon.<sup>88</sup>

### 2.2.7 Summary

Despite the high ring-strain of cyclopropanes, their overall polymerizability largely depends on the activating substituents placed on the ring. The most desirable method to achieve our target polymer structure (Scheme 2.1) was via the anionic ring-opening polymerization of cyclopropanes with two activating geminal electron-withdrawing groups. The synthesis and polymerization of several 1,1-disubstituted cyclopropanes is described in the following section (2.3). Based on previous work (by Xie Tao in our group) on the ring-opening polymerization of various dialkyl 1,1-cyclopropanedicarboxylates **3**, it is evident that the anionic mechanism provides a feasible method to achieve well controlled polymerizations. The absence of side reactions, the living characteristic of the polymerizations (for some monomers), high molecular weights and narrow molecular weight distributions are desirable features of this method.

### 2.3 Ring-Opening Polymerization of 1,1-Disubstituted Cyclopropanes: Overview

As mentioned in the previous section, the anionic ring-opening polymerization of cyclopropanes geminally substituted by two ester groups was achieved in our group.<sup>84,85,89</sup> The resulting trimethylene polymers  $(\text{CH}_2\text{CH}_2\text{C}(\text{COOR})_2)_n$  have two ester substituents on every third carbon atom along the backbone. The two electron-withdrawing ester substituents on the ring stabilize the propagating anion upon ring-opening, providing the driving force for the nucleophilic cleavage of the otherwise inert carbon-carbon bond. This reaction is analogous to the carbon-oxygen cleavage obtained during the ring-opening polymerization of epoxides discussed in Section 2.2.4.2.

Although oligomers of other cyclopropanes had already been obtained, these reports constituted the first example of a well-controlled polymerization yielding polymers of defined structures, composition, and molecular weights. In particular, experimental conditions were identified under which the polymerization was living even at high temperatures.<sup>87</sup> Due to the failure of the ring-opening polymerization of monosubstituted cyclopropanes, it is evident that the activation of cyclopropane rings by two electron-withdrawing groups is necessary for the ring-opening polymerization to occur under anionic conditions.

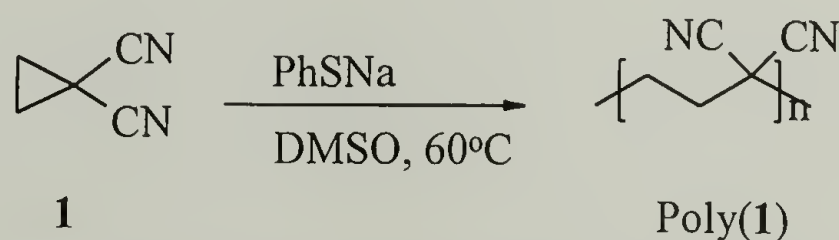
Organic chemistry predicts that side substituents that are more electron-withdrawing than an ester should provide even further activation of cyclopropane towards anionic ring-opening polymerization. Therefore, the polymerization of cyclopropane monomers with strong electron-withdrawing nitrile substituents; 1,1-dicyanocyclopropane **1** (section 2.3.1), alkyl 1-cyanocyclopropanecarboxylates **2a-d**

(section 2.3.2) and phenyl 1-cyclopropanecarbonitrile **4** (section 2.3.3) was studied. A comparison of the influence of the substituents on the reactivity of all the monomers is included in section 2.3.4. The resulting polymers were characterized, and comparisons drawn on the influence of the nature of the substituent on the thermal stability, solubility, and crystallinity.

### 2.3.1 Ring-Opening Polymerization of 1,1-Dicyanocyclopropane

#### 2.3.1.1 Introduction

In this section, the anionic ring-opening polymerization of cyclopropanes activated by two gem-nitrile groups is discussed (Scheme 2.9). The nitrile group is a strong electron-withdrawing group that provides the necessary activation for the carbon-carbon bond cleavage by stabilization of the resulting carbanion. The resulting polymer provides a novel structure with two nitrile groups on every third carbon atom along the backbone.



Scheme 2.9. Ring-Opening Polymerization of 1,1-Dicyanocyclopropane.

With this new architecture, the 1,3 non-bonded repulsive interactions between adjacent nitriles (mainly dipole-dipole interactions) are minimized due to the increased distance between the groups on the backbone. This is evident in the space-filling models comparing segments of polymer chains with two nitrile substituents on every *second*



the segments of poly(vinylidene cyanide) (A), the carbon and nitrogen atoms of the nitrile groups are at van der Waal distances from each other. Polymer chains will attempt to minimize the repulsive interactions associated with the close proximity of adjacent substituents by adopting conformations other than the all-trans conformation. However, for poly(vinylidene cyanide), some fraction of the repulsive dipole-dipole interactions are present regardless of the conformation. As a result the polymer is thermally and hydrolytically unstable, undergoing chain scission at room temperature that is further catalyzed by atmospheric moisture.<sup>90</sup>



Figure 2.6. Space-Filling Model Comparing Segments of Poly(vinylidene cyanide)  $[\text{CH}_2\text{-C(CN)}_2]_4$  (A) and Poly(1,1-dicyanocyclopropane)  $[-\text{CH}_2\text{-CH}_2\text{C(CN)}_2]_4$  (B).

It is well known that polymers that display piezoelectric activity have large dipole moments.<sup>91,92</sup> The orientation of dipoles in polymer thin films with a zero net polarization can be achieved by applying strong electric fields.<sup>93,94</sup> If the orientation is maintained after removal of the external field, then such thin films often display piezoelectric behavior. This orientation of the dipoles under a strong electric field is referred to as poling. For example, the copolymer of vinylidene cyanide and vinyl acetate is an example of an amorphous polymer that displays high piezoelectric activity.<sup>95</sup> A study of the poling time dependence of the absorbance band due to  $-\text{C-CN}$  stretching indicated that the origin of the marked piezoelectric behavior is due to the rotation of the  $-\text{C-CN}$  group, which has a strong dipole moment of 4.0 debye. The alternating structure of this

copolymer places the two gem-nitrile groups on every *fourth* carbon. This spaces out the nitrile groups and allows them to align in an electric field and maintain that alignment after the driving force provided by the external electric field is removed.

The spacer group between the dipoles largely affects the properties of the material. This is evident in the negligible piezoelectric activity observed in some copolymers of vinylidene cyanide (VCDN) with methyl methacrylate<sup>96</sup> or with styrene (St)<sup>97</sup> even after drawing and poling/annealing treatments. These copolymers have the same side-chain nitrile groups with highly alternating and stereochemically atactic sequences.<sup>97,98</sup> In order to obtain high piezoelectric activity, the  $C(CN)_2$  dipoles of the VCDN copolymers must be forced to align in the film thickness direction by drawing, poling and annealing under a high direct current electric field at high temperature just below the glass transition temperature.<sup>92,96</sup> Recent studies related the piezoelectric activity of VCDN copolymers to the flexibility of the main-chain.<sup>99-105</sup> Conformational analysis of P(VDCN/St) by NMR indicated that the copolymer has a predominantly trans conformation (80%) about the methylene-methine bond and one of the three conformers (gauche-) is significantly suppressed.<sup>106</sup> It was suggested that the suppression of one or more conformers limits the chain flexibility, consequently reducing the extent of alignment of the dipoles.<sup>107</sup>

The highly polar nitrile groups along the backbone of poly(vinylidene cyanide) offer potential for a large net polarization in the polymer, but its instability even at ambient temperature limits its use.<sup>90</sup> The effect of placing gem-nitrile groups on every *third* carbon instead of every *second* carbon on the properties of the polymer is discussed in this section. The thermal stability, solubility and crystalline/amorphous behavior of the

resulting polymer is also presented. The effect of placing a methylene spacer between the nitrile groups on the conformation and flexibility of the main-chain was of particular interest in relation to studying its potential as a piezoelectric polymer. However, the intractability of the resulting polymer limited this study.

#### 2.3.1.2 Experimental

##### Measurements

Solution  $^1\text{H}$ - and  $^{13}\text{C}$ -NMR spectra were recorded on a Bruker DPX 300 spectrometer. Solid-state  $^{13}\text{C}$  CP-MAS NMR spectra were obtained with a Bruker DSX 300 spectrometer. IR data was obtained on a BIORad FTS 175C FT-IR spectrometer. Thermogravimetric (TGA) and differential scanning calorimetry (DSC) experiments were carried out on a Perkin–Elmer TAC 7/DX instrument at a heating rate of  $10\text{ }^\circ\text{C}\cdot\text{min}^{-1}$  under nitrogen. Elemental Analysis was performed at the Microanalysis Laboratory of the University of Massachusetts, Amherst.

##### Materials

All chemicals were purchased from Aldrich, with the exception of potassium carbonate (anhydrous, p.a) obtained from Acros. Malononitrile and 1,2-dibromoethane, 18-crown-6 (1,4,7,10,13,16,-hexaoxacyclooctadecane), 4,7,13,16,21,24-hexaoxa-1,10-diazabicyclo[8.8.8]hexacosane, and sodium cyanide were used without further purification. The amines used as initiators were distilled over  $\text{CaH}_2$  prior to use.



DMSO used for the polymerization reactions was purified by distillation under vacuum (40 °C/ 2 mm Hg) and dried over 4Å molecular sieves.

**Synthesis of 1,1-dicyanocyclopropane 1.** Malononitrile (9.0g, 0.14 mol), 1,2-dibromoethane (57.0g, 0.3 mol), anhydrous potassium carbonate (70.0g, 0.5 mol) and DMSO (250 mL) were introduced into a 500 mL 2-neck round bottom flask. The mixture was vigorously stirred for 48 hours at room temperature using a mechanical stirrer. Water (2.5 L) was added and the product extracted with diethyl ether (6 x 500 mL) and concentrated. The residue was washed with water (4 x 200 mL), dried over magnesium sulfate, and distilled under reduced pressure (94-97 °C / 14 mm Hg). Yield: 3.2 g (25 %).  $^1\text{H}$ -NMR ( $\delta$  (ppm),  $\text{CDCl}_3$ ): 1.8 (s, 4H).  $^{13}\text{C}$ -NMR ( $\delta$ (ppm),  $\text{CDCl}_3$ ): 18.3 ( $\text{CH}_2$ ), 29.0 ( $\text{C}(\text{CN})_2$ ), 115.1 (CN). IR (liquid film):  $2256\text{ cm}^{-1}$  (CN). Anal. Calc. for  $\text{C}_5\text{H}_4\text{N}_2$  (92.09): C, 65.21; H, 4.39; N, 30.41. Found: C, 65.22; H, 4.35; N, 30.43.

**Synthesis of thiophenolate initiators.** Distilled thiophenol (10.70g, 97 mmol) was added dropwise to a mixture of freshly scrapped metallic sodium (or potassium) (87 mmol) in 250 mL dry ether. The mixture was stirred for 24 hours and the resulting solid was filtered and washed with dry ether (5 x 200 mL). The product was dried in vacuo for 24 hours at room temperature. Yield: 11.92g (92%).  $^1\text{H}$  NMR ( $\text{DMSO-d}_6$ , 200 MHz):  $\delta$  (ppm) = 7.0 (d), 6.6 (d), 6.4 (m). Anal. Calc. for  $\text{C}_6\text{H}_5\text{SNa} \cdot (\text{H}_2\text{O})_{0.5}$  (141.12): C, 51.05; H, 4.28; S, 22.71. Found: C, 51.05; H, 4.24; S, 20.86.

**Polymerization procedure.** 1,1-Dicyanocyclopropane **1** (1.103g, 12 mmol) was added to a solution of the initiator (0.453 mmol) dissolved in 2 mL DMSO under nitrogen. The polymerization tube was placed in an oil bath at 30 or 60 °C. The



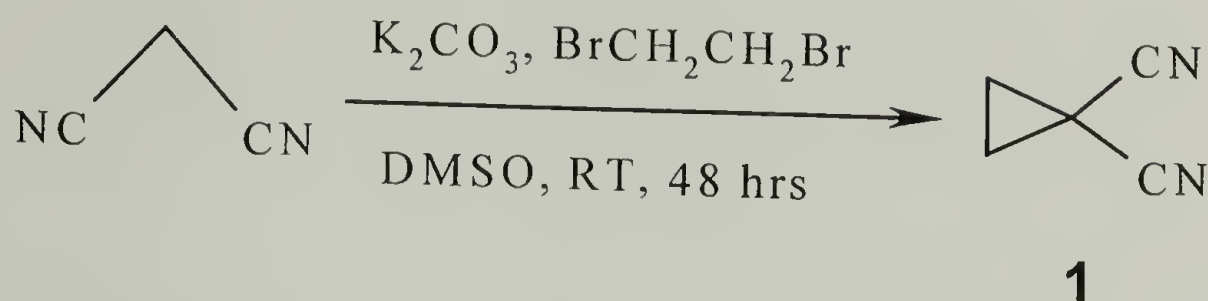
precipitate formed during polymerization was filtered, washed with  $1 \text{ mol} \cdot \text{L}^{-1}$  aqueous sulfuric acid, acetone and diethyl ether. Poly (**1**) was dried for 24 h at  $60^{\circ}\text{C}$  in a high-vacuum oven.

### 2.3.1.3 Results and Discussion

2.3.1.3.1 Monomer Synthesis. The synthesis of monomer **1** via the condensation of malononitrile with a 1,2-dihalogenoethane in the presence of a base has been previously reported.<sup>108</sup> However, low yields were obtained with poor purity. The monomer was also synthesized by Zefirov et al. using a similar procedure (using  $\text{K}_2\text{CO}_3$  as the base, and DMSO solvent) that affords decent yields (50 %) of monomer **1**.<sup>109</sup> Previous synthesis of **1** in our group using Zefirov's procedure, showed that the final product contained a low amount ( $<1\%$ ) of some unknown impurity and some residual DMSO (2%) when analyzed by gas chromatography.

In this work, monomer **1** was synthesized by slight modification of Zefirov's procedure (Scheme 2.10). The use of a mild base such as potassium carbonate is sufficient, due to the high acidity of the malononitrile ( $\text{pK}_a(\text{H}_2\text{O}) = \text{pK}_a(\text{DMSO}) = 11.0$ ). Vigorous stirring was necessary in order to ensure the fine dispersion of the base in the heterogeneous reaction. The crude product was purified via distillation under vacuum to remove the residual 1,2-dibromoethane and DMSO. During distillation an insoluble residue was observed, possibly formed from the polymerization of the highly reactive cyclopropane monomer by nucleophilic impurities. The yields improved when the organic layer was washed several times with water and dried prior to distillation. Monomer **1** is colorless and GC analysis confirmed the high purity of the monomer (99.9%). The high purity of the monomer is crucial for anionic polymerization, since

residual impurities such as 1,2-dibromoethane will react with the propagating carbanion and terminate the polymerization. NMR spectroscopy was used to confirm the structure of the monomer.



Scheme 2.10. Synthesis of 1,1-Dicyanocyclopropane **1**.

2.3.1.3.2 Anionic Polymerization of **1**. Monomer **1** readily polymerizes at room temperature when thiophenolate salts (PhSK, PhSNa) are used as the initiator. Previous studies had demonstrated that thiophenolate anions are efficient initiators for the ring-opening polymerization of dialkyl cyclopropane-1,1-dicarboxylates.<sup>84,87</sup> They were used in this study to offer a basis for comparison of the reactivities of the two monomers. At 60 °C (3.8 mol-% PhSNa, 0.227 mol·mL<sup>-1</sup> (DMSO)), the polymerization reaches completion in under 20 minutes. The rapid formation of a white precipitate was observed during each polymerization. Attempts to re-dissolve this solid in organic solvents such as chlorinated solvents (CHCl<sub>3</sub>), or highly polar solvents (DMSO, DMF) were unsuccessful. The use of “exotic” solvents such as tetramethylene sulfone or tetramethylurea, which are known to dissolve poly(vinylidene cyanide), also proved unsuccessful.<sup>110,111</sup> The difficulty of dissolving similar nitrile containing polymers such as poly(2-vinylcyclopropane-1,1-dicarbonitrile) has been previously described.<sup>82</sup> Evidence for the

expected ring-opened structure was provided by solid state  $^{13}\text{C}$ -NMR analysis and will be detailed later (Figure 2.7).

The anionic ring-opening polymerization of **1** was also achieved using a variety of nucleophilic initiators. A summary of the data obtained is provided in Table 2.4.

**Table 2.4.** Data on the Ring-Opening Polymerization of **1** with Various Nucleophiles.

Initiator <sup>a</sup>	Temp. (° C)	Time (min.)	Yield (%) <sup>c</sup>
PhSK <sup>b</sup>	30	120	76
PhSNa <sup>b</sup>	30	120	44
PhSK	30	12	21
PhSK <sup>d</sup> (crown ether)	30	12	26
PhSK <sup>e</sup> (cryptofix)	30	12	27
PhSNa <sup>b</sup>	60	60	100
NaCN <sup>b</sup>	60	60	50
PhSNa <sup>b</sup>	60	15	90
CH <sub>3</sub> C(Na)(COOEt) <sub>2</sub> <sup>b</sup>	60	15	98
Et <sub>3</sub> N	60	15	14
pyridine	60	15	3
Et <sub>2</sub> NH	60	15	- <sup>f</sup>
pyrrolidine	60	15	14
n-methyl pyrrolidine	60	15	32
Et <sub>2</sub> NH	60	135	2

(a) [M]/[I] 27/1 (b) Dissolved 0.227 mol . L<sup>-1</sup> DMSO solvent (c) Yields determined by gravimetry (d) PhSNa: 18 crown-6 (1:1) (e) PhSK: 4,7,13,16,21-24 hexaoxa-1,10-diazabicyclo[8.8.8]hexacosane (cryptofix)(1:1) (f) No polymer was isolated by precipitation.

Molecular weight determination of poly(**1**) could not be achieved due to its complete insolubility. Therefore, a comparison of the reactivities of the various initiators could only be based on the polymer yields obtained. The thiophenolate salts of sodium and potassium are by far the most reactive nucleophilic initiators, showing increased rates of polymerization with increased temperature. The influence of the counterion is provided in

the following section. The high efficiency of the thiophenolate initiators is evident as they provide quantitative yields with the ring-opened polymer structure ( $^{13}\text{C}$ -NMR analysis) as the only product. Comparable reactivities were also observed with the sodium salt of diethyl methylmalonate.

A correlation can be made between the increasing nucleophilic strength of the initiators and their increased reactivity towards ring-opening polymerization. An early attempt to quantify the nucleophilicity of a given group was provided by Swain-Scott (Equation 1), where  $n$  is the nucleophilicity of a given group,  $s$  is the sensitivity of a substrate  $s$  to nucleophilic attack ( $s = 1.0$  for  $\text{CH}_3\text{I}$ ),  $k_0$  is the rate for  $\text{H}_2\text{O}$  (the standard  $n=0$ ).<sup>112</sup>

$$\log \frac{k}{k_0} = s n \quad (\text{Eq. 1})$$

The values of  $n$  for some nucleophiles are shown in Table 2.5.<sup>113</sup> The same order of nucleophilicities was obtained by Edwards and Pearson for  $\text{S}_{\text{N}}2$  mechanisms in protic solvents. It was recognized that the nucleophilicity of a compound largely depends on solvation effects. However, Swain-Scott parameters do not account for this solvation effect. In polar aprotic solvents, anions are solvated by ion-dipole interactions and not by hydrogen bonding. Other attempts to correlate nucleophilic activities have also been reported.<sup>114-116</sup>



Table 2.5. Nucleophilicities of some Common Reagents<sup>113</sup>

Nucleophile	<i>n</i>	Nucleophile	<i>n</i>
SH <sup>-</sup>	5.1	Br <sup>-</sup>	3.5
CN <sup>-</sup>	5.1	PhO <sup>-</sup>	3.5
I <sup>-</sup>	5.0	AcO <sup>-</sup>	2.7
PhNH <sub>2</sub>	4.5	Cl <sup>-</sup>	2.7
OH <sup>-</sup>	4.2	F <sup>-</sup>	2.0
N <sub>3</sub> <sup>-</sup>	4.0	NO <sub>3</sub> <sup>-</sup>	1.0
Pyridine	3.6	H <sub>2</sub> O	0.0

In this study, the lower reactivity observed for the polymerization of **1** with sodium cyanide over sodium thiophenolate can be explained by the decrease in its nucleophilicity resulting from the increased solvation of the cyanide ion due to strong dipole interactions with the solvent. As expected, lower yields were obtained with the weak amine nucleophiles in comparison to the strong thiophenolate nucleophiles. Polymerization with diethylamine and pyrrolidine initiators was unsuccessful, probably due to chain termination by transfer of the acidic proton on the nitrogen, which is further activated as an ammonium ion after initiation has occurred.

**Influence of the Counterion.** The propagation rate constant and the polymerization rate for anionic mechanisms are dramatically influenced by the nature of the counterion. An almost two-fold increase in reactivity was observed when potassium was used as the counterion instead of sodium. The effect of complexing the potassium ion with a crown ether or cryptand was also studied. However, no further increase in the reactivity of **1** was observed. These results contrast the data previously reported in our group for the ring-opening polymerization of diisopropyl 1,1-cyclopropanedicarboxylate

**3c** using the same initiators. In this case, the rate of polymerization of increased by approximately one order of magnitude when the potassium ion was complexed with a crown ether or cryptand.<sup>87</sup>

The above results suggest, as is often the case in anionic polymerizations, the presence of two or more propagating species (tightly bound, solvent separated or highly solvated free-ions) that co-exist in equilibrium. Each species has different reactivity and their relative concentrations have a dramatic effect on the polymerization rate. The concentration of each species depends on the nature of the counterion and the physical conditions of the reaction (solvent and temperature). For the polymerization of **1**, the increased reactivity observed with the  $K^+$  counterion over  $Na^+$  can be attributed to the formation of a loosely bound ion-pair with the propagating  $Na^+$  counterion. The lack of change in reactivity when the  $K^+$  was complexed with a crown ether or cryptand provides evidence that the propagating species (prior to complexation) is comparable to a free-ionic species. In the case of the diester monomer **3c**, due to the dramatic increase in the rate of polymerization when the  $K^+$  was complexed with a crown ether or cryptand, it is evident that the  $K^+$  is more tightly bound to the propagating carbanion prior to complexation. Based on kinetic data, it was determined that the increase in the rate of reaction upon complexation was of about the same order of magnitude as the reactivity of the free carbanion.<sup>87</sup>

**Comparison of the reactivity of 1 with 2-vinyl-1,1-dicyanocyclopropane.** The polymerization of **1** under anionic conditions was compared to 2-vinyl-1,1-dicyanocyclopropane (**vii**) reported by Cho et al.<sup>82</sup> A comparison of the reactivity of **1**

with other 1,1-disubstituted cyclopropanes is provided in section 2.3.4. In order to provide a basis for comparison of the reactivity of the two monomers, **1** was polymerized under identical conditions (NaCN (1.2 mol-%) in DMF at 7 °C). Under these conditions, a 6% yield was obtained for monomer **1** compared to the 83% obtained for the vinyl cyclopropane monomer **vii**. (Table 2.6). It is evident that the activating electron-donating group (in the 2-position) increases the reactivity of the monomer towards ring-opening. However, this activating substituent is not essential for the rapid polymerization **1**. As demonstrated in the previous section (Table 2.4), increasing the temperature, or using stronger nucleophiles can dramatically increase the rate of the initiation and thus the overall rate of polymerization.

Table 2.6. Anionic Polymerization of Monomers **1** and **vii**

Monomer <sup>a</sup>	Temp. (°C)	Time (h)	Yield (%) <sup>b</sup>
<b>viii</b>	7	24	83
<b>1</b>	7	24	6
<b>1</b>	60	1	50

<sup>a</sup> 1.2 mole % NaCN, 0.11 g. mL<sup>-1</sup> DMF

<sup>b</sup> Yields determined by gravimetry

2.3.1.3.3 Solid State Polymerization. An interesting aspect of the polymerization of monomer **1** was notable. Due to its poor solubility, precipitation of the polymer was observed at low conversion (<10 %) for each of the reactions. Some of the reactions were carried out in a minimum amount of DMSO, enough to dissolve the solid initiators. In these cases, complete solidification of the mixture was observed at 25%



conversion. However, this did not hinder further propagation of the carbanionic species, and quantitative conversions were achieved. Precipitation during polymerization is known to cause chain termination due to the physical inaccessibility of the unreacted monomer to the growing chain end.

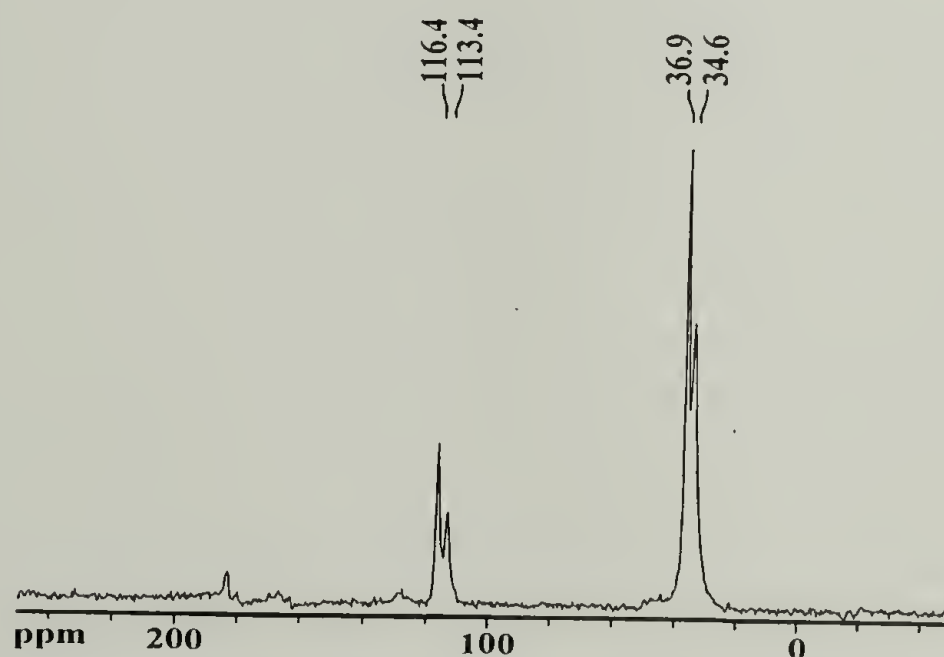
This behavior is especially unique considering the precipitated polymer is highly crystalline (WAXS data, p.245). This high degree of crystallinity was observed for powder samples directly obtained from the polymerization. It is proposed that as the polymer precipitates from the reaction mixture, the interactions between the strong dipole moment of the nitrile groups along the backbone force the chains to align into ordered structures. The solid-state polymerization of crystalline monomers has been reported, but the lattice structure of these monomers is considerably disrupted upon polymerization and amorphous polymers are produced.<sup>117</sup> In addition, diffusion of the monomer into the crystal structure is highly limited. Therefore, in this case, it is suggested that the polymerization occurs at the interphase between the crystalline and amorphous regions where the chain ends are located. As the polymerization proceeds, additional units of the chain are then added into the crystalline region.

#### 2.3.1.4. Characterization of Poly(1)

2.3.1.4.1 Structural Analysis. A sample of poly(1) was obtained from the polymerization of **1** at 60°C for 15 min, using PhSNa initiator (0.227 mol·L<sup>-1</sup> DMSO) (Table 2.4) As no suitable solvent for poly(1) could be found, solid-state <sup>13</sup>C-NMR experiments were performed to determine the structure. The <sup>13</sup>C spectrum of poly(1) obtained is shown in Figure 2.7 using Cross Polarization-Magic Angle Spinning (CP-



MAS) experiments. This method is performed on  $^{13}\text{C}$  with cross polarization from  $^1\text{H}$ , and provides high-resolution NMR spectra in the solid state. Spinning side-bands resulting from the chemical-shift anisotropy of the signals and the spinning rate are typically observed in the CP-MAS experiment. A method to suppress these spinning side-bands known as the Total Suppression of Sidebands (TOSS) pulse sequence was applied. Four peaks are observed at 34.6, 36.9, 113.4 and 116.4 ppm. The peaks at 34.6 and 36.9 ppm can be assigned to the backbone carbons, while the peaks at 113.4 and 116.4 can be assigned to the carbon of the nitrile ( $\text{C}\equiv\text{N}$ ) groups. Asymmetrical peak splitting of this carbon is due to residual dipolar coupling to the quadrupolar  $^{14}\text{N}$  nuclei, typically observed when a carbon atom is directly bonded to nitrogen-14 ( $I=1$ ). The small peak at 180 ppm is a residual side band and not part of the structure.



**Figure 2.7.** Solid-State  $^{13}\text{C}$ -NMR CP-MAS Spectrum of Poly(1) after the application of a TOSS pulse sequence.

Figure 2.8 shows the CP-MAS spectrum obtained in a gated decoupling TOSS experiment. This was performed to selectively observe unprotonated  $^{13}\text{C}$  atoms. The peak at 34.6 ppm disappeared and could be assigned to the ethylene carbons (1), while the peak at 37 ppm was assigned to the quaternary carbon (2). The spectra provide evidence that confirms the expected ring-opened structure of poly (1).

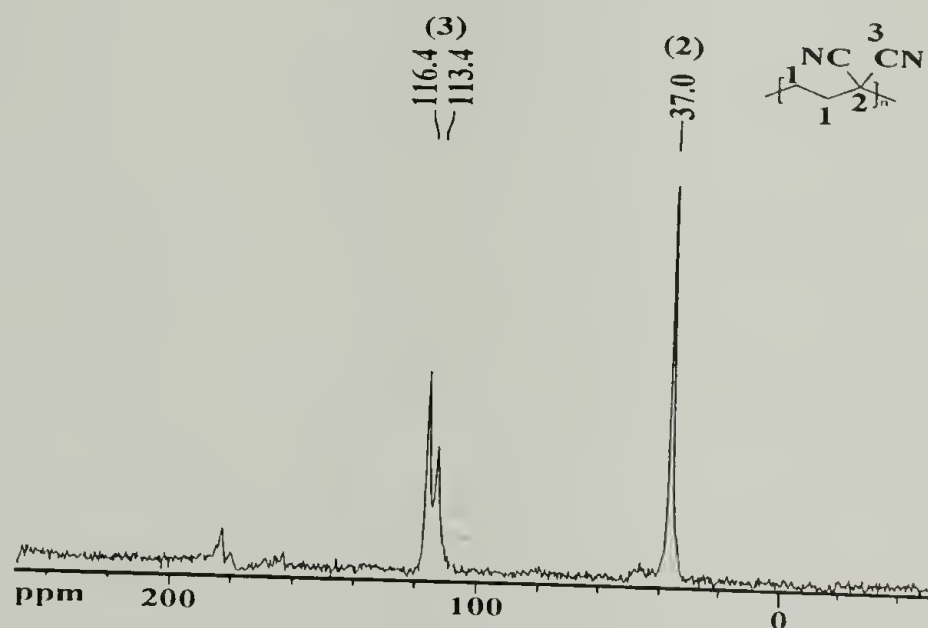


Figure 2.8. Solid-State  $^{13}\text{C}$ -NMR CP-MAS Spectrum of Poly(1) in a gated decoupling TOSS experiment.

IR analysis of the polymer revealed complete disappearance of the absorptions characteristic of **1**, such as the peak at  $1256\text{ cm}^{-1}$  due to the carbon-carbon ring-stretching vibrations. In addition, the presence of the band at  $751\text{ cm}^{-1}$  characteristic of the rocking mode for a  $\text{XC}-(\text{CH}_2)_2\text{-CX}$  subunit provides further evidence that supports the structure of poly(**1**).

2.3.1.4.2 Molecular weight determination. Due to the limitations associated with the insolubility of poly(**1**), the molecular weight determination by any method requiring dissolution of the polymer could not be performed.

The absence of the signal due to the end-group in the solid-state NMR (Figure 2.7) indicates high conversion ( $\overline{Mn} \sim 4000$ ).

2.3.1.4.3 Thermal Analysis. The thermal decomposition of poly(1) was analyzed using TGA (Figure 2.9). The polymer is stable at room temperature. The onset of decomposition occurs at 366 °C, with 5% weight loss recorded at 410 °C. The polymer degrades to form a black insoluble char, with a char yield of 18% at 1000 °C.

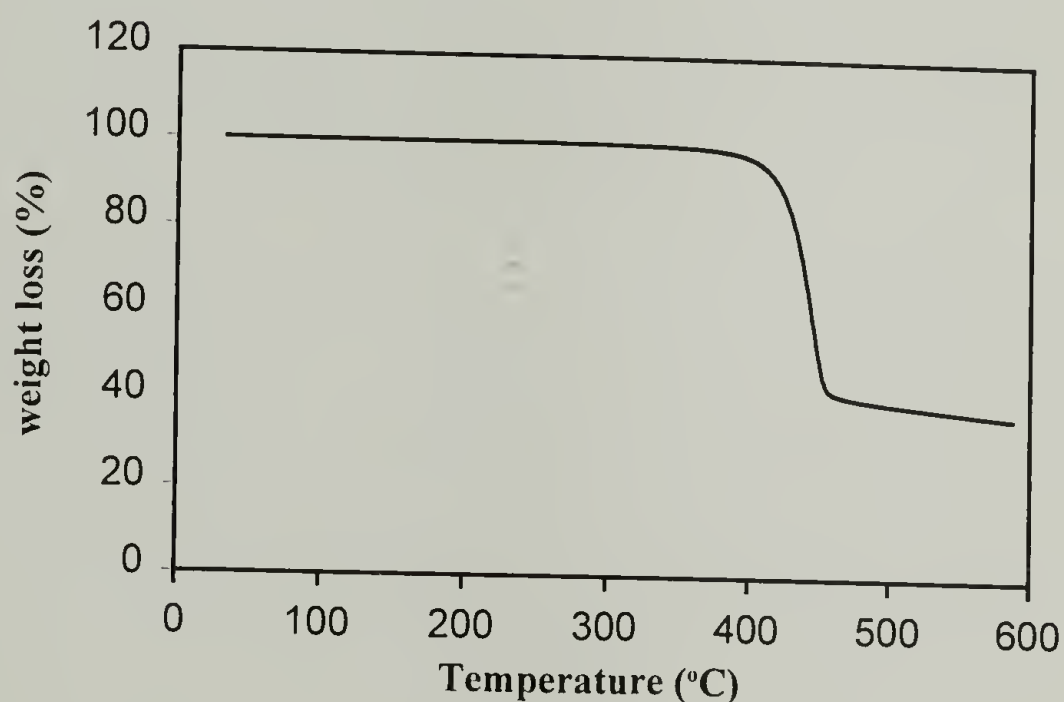


Figure 2.10. Thermogravimetry Curve of Poly(1) obtained at a Heating Rate of  $10\text{ }^{\circ}\text{C} \cdot \text{min}^{-1}$  under  $\text{N}_2$

Poly(1) shows a dramatic increase in thermal stability in comparison to its lower homologue- poly(vinylidene cyanide), which has geminal nitrile substituents on every second carbon. Poly(vinylidene cyanide) is unstable at room temperature undergoing rapid chain scission when exposed to atmospheric moisture.<sup>90</sup> The polymer depolymerizes to vinylidene cyanide and malononitrile at temperatures above 160 °C.

Poly(1) does not degrade by depolymerization due to unfavorable thermodynamic and kinetic factors associated with the formation of a three-membered ring. Instead, degradation occurs at temperatures above 350 °C with probable loss of hydrogen cyanide (HCN) to form unsaturated units in the backbone, with a relatively high char yield of 18-30% at 1000 °C. Further analysis of the pyrolysis product was not performed.

2.3.1.4.4 Crystallinity. WAXS patterns were obtained for powder samples of poly(1) (Figure 2.10). The polymers are semi-crystalline, and details of the analysis of the crystalline structure are provided in Chapter 6. Increasing the distance between the highly polar nitrile groups on the backbone minimizes the 1,3 non-bonded interactions and enables backbone chains to adapt stable conformations that result into a well-defined crystalline structure. Preliminary evidence suggests that the backbone is all-trans, however further studies of the crystal structure was limited due to the inability to obtain oriented samples either in the melt or via sedimented mats. In comparison, x-ray diffraction patterns of poly(vinylidene cyanide) show little evidence of crystallinity. In this case, regardless of the conformation of the polymer chains, the strong repulsive interactions between the adjacent nitrile substituents on the backbone are present.

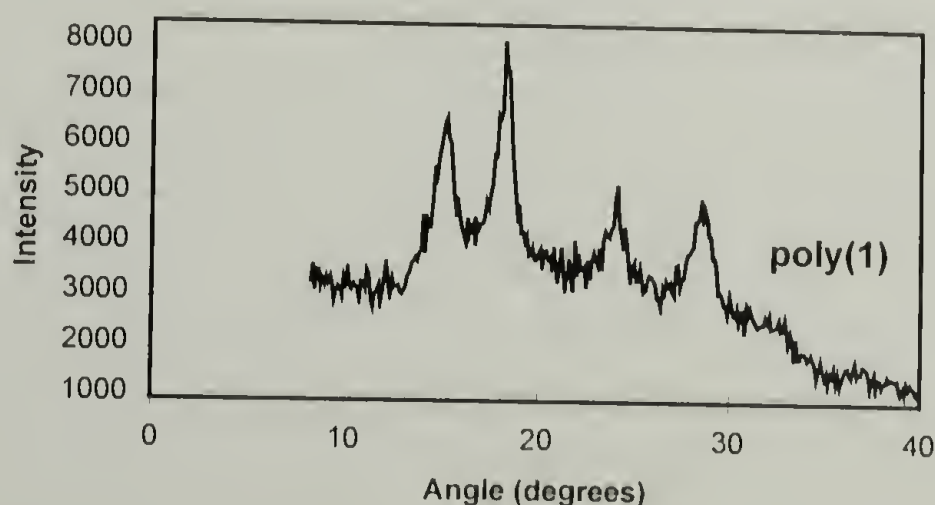


Figure 2.10. WAXS Pattern of Powder Sample of Poly(1)



DSC analysis of poly(**1**) revealed no melting transitions below the decomposition temperature, suggesting that decomposition of the polymer occurs before melting ( $T_m > 366\text{ }^{\circ}\text{C}$ ). Consequently, processability of the polymer is highly limited as it decomposes before melting. In addition, the strong dipole-dipole interactions between the polymer chains, coupled with its high degree of crystallinity render the polymer completely insoluble. The overall intractability of poly(**1**) limited the study of its piezoelectric behavior.

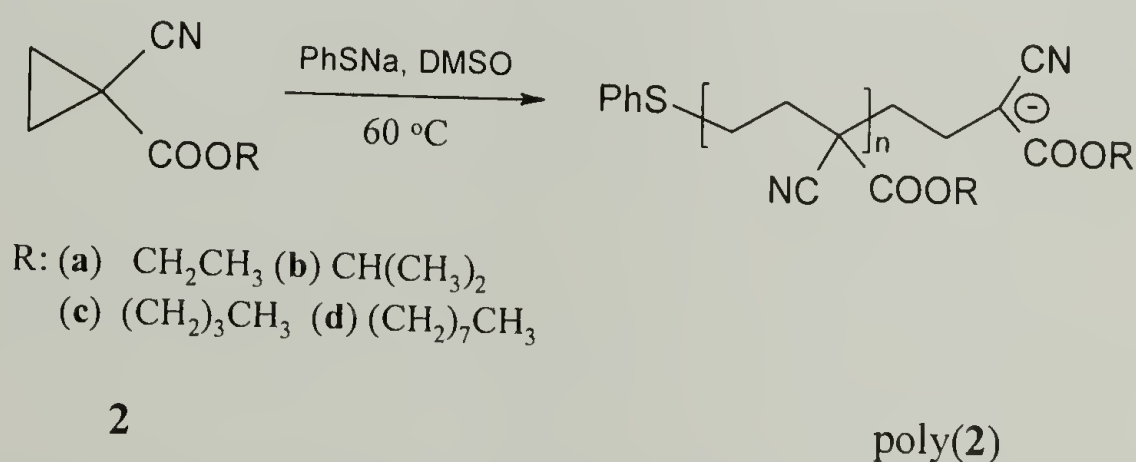
#### 2.3.1.5 Conclusions

The rapid and efficient ring-opening polymerization of 1,1-dicyanocyclopropane **1** was achieved using potassium or sodium thiophenolate as the initiator at  $60\text{ }^{\circ}\text{C}$ . Structural analysis of the resulting polymer provided evidence for the ring-opened structure only, yielding a carbon-chain polymer containing two geminally-substituted nitriles on every third atom along the backbone. A significant increase in the reactivity of the dinitrile monomer **1** in comparison to dialkyl cyclopropane-1,1-dicarboxylates **3** was observed, due to the increased stabilizing effects of the propagating carbanion provided by the strong electron-withdrawing nitrile groups. The placement of two nitrile groups on every third instead of every second carbon has a marked effect on the properties of the resulting polymers. Dramatic improvements in the thermal and chemical stability were observed due to the minimization of the strong repulsive interactions between adjacent nitrile substituents. In addition, while poly(vinylidene cyanide) is an amorphous polymer, poly(**1**) is highly crystalline, with preliminary results suggesting that the chains are able to maintain an-all trans conformation.

## 2.3.2 Synthesis and Characterization of Poly(Alkyl 1-Cyanocyclopropanecarboxylate)s

### 2.3.2.1 Introduction

The anionic ring-opening polymerization of alkyl 1-cyanocyclopropanecarboxylates **2a-d** is presented in this section (Scheme 2.11). As the polymerization of **2a-d** yields polymers with chiral centers on every third carbon, the issue of tacticity for polymers of this type is introduced for the first time. The stereochemistry of the resulting polymers was analyzed using  $^1\text{H}$ -NMR spectroscopy, with most of the experimental results being reported in chapter 3. Comparisons of poly(**2a-c**) were also made with their respective homologues, poly( $\alpha$ -cyanoacrylates) (commonly known as “superglue”), which have geminal ester and nitrile substituents on every second carbon.



Scheme 2.11. Ring-Opening Polymerization of Alkyl 1-Cyanocyclopropanecarboxylates.

### 2.3.2.2 Experimental

#### Measurements

The  $^1\text{H}$ - and  $^{13}\text{C}$ -NMR spectra for the monomers were recorded on a Bruker DPX 300 spectrometer in  $\text{CDCl}_3$  (at room temperature) and on a Bruker AMX-2 500 spectrometer in  $(\text{CD}_3)_2\text{SO}$  at  $115^\circ\text{C}$  for the polymers. IR spectra were recorded on a

BioRad FTS 175C FT-IR spectrometer. Elemental analysis was performed at the Micro Analysis Laboratory of University of Massachusetts, Amherst. Thermogravimetric analysis (TGA) and Differential Scanning Calorimetry (DSC) experiments were performed on a Perkin-Elmer TAC 7/DX instrument at a heating rate of 10 °C/min. Gel Permeation Chromatography (GPC) analysis was obtained using a Polymer Laboratory PL-GPC ultra high temperature chromatograph with a Hewlett-Packard 1100 series isocratic pump and two PLgel 5  $\mu$ m MIXED-D columns. Dimethylformamide (DMF) was used as the eluent, at a flow rate of 1 mL $\cdot$ min.<sup>-1</sup>. The samples were run at 100 °C, and calibrated using polystyrene standards.

### Materials

Ethyl (99+%), butyl (95%), and octyl (99%) cyanoacetates, and 1,2-dibromoethane (99%) were purchased from Aldrich and used without further purification. Isopropyl cyanoacetate was obtained from Fluka and anhydrous potassium carbonate from Acros. DMSO used for the polymerization was purified by distillation under vacuum (40 °C/ 2mm Hg), discarding the first and last 25% and drying over 4Å molecular sieves. All other solvents were reagent grade and used without further purification. Tetrabutylammonium thiophenolate was purchased from Fluka and used as received.

**Synthesis of alkyl 1-cyano cyclopropanecarboxylates 2a-d.** Alkyl cyanoacetate (0,1 mol equivalent), 1,2-dibromoethane (28g, 0.15 mol), potassium carbonate (40g, 0.29 mol) and 80 mL DMSO were added into a round bottom flask. The heterogeneous mixture was stirred vigorously for 24 hours using a mechanical stirrer. Water (250 mL) was added to the reaction mixture and the product extracted with



3 x 150 mL portions of diethyl ether. The ether layers were combined and concentrated by evaporation. The residue was washed with water (30 mL) and dried overnight under  $\text{MgSO}_4$ . The crude products were distilled under vacuum to yield the corresponding cyclopropane monomers. Yields, boiling points and NMR spectroscopic data are provided in Table 2.7 and 2.8. Anal. Calc. for  $\text{C}_7\text{H}_9\text{NO}_2$  (139.16) **2a**: C, 60.41; H, 10.06; N, 6.53. Found: C, 60.16; H, 10.00; N, 6.60. Calc. for  $\text{C}_8\text{H}_{11}\text{NO}_2$  (153.19) **2b**: C, 62.72; H, 9.14; N, 7.14. Found: C, 62.50; H, 9.04; N, 7.32. Calc. for  $\text{C}_9\text{H}_{13}\text{NO}_2$  (167.23) **2c**: C, 64.64; H, 8.38; N, 7.85. Found: C, 64.50; H, 8.36; N, 8.02. Calc. for  $\text{C}_{13}\text{H}_{21}\text{NO}_2$  (223.34) **2d**: C, 69.91; H, 9.50; N, 6.27. Found: C, 69.85; H, 9.64; N, 6.29.

IR (liquid film,  $\text{cm}^{-1}$ ) **2a**: 3115, 2986, 2941, 2250, 1737, 1371, 1312, 1279, 1190, 1025, 972, 859, 747. **2b**: 3121, 2986, 2940, 2248, 1736, 1361, 1309, 1281, 1190, 1106, 977, 933, 899, 749. **2c**: 3115, 2962, 2934, 2879, 2249, 1740, 1466, 1311, 1184, 1059, 936, 747. **2d**: 3120, 2960, 2928, 2857, 2249, 1740, 1468, 1312, 1176, 944, 747.

**Synthesis of thiophenolate initiators.** Potassium and sodium thiophenolate initiators were synthesized according to a reported procedure.<sup>84</sup> Tetrabutylammonium thiophenolate was purchased from Fluka Chemicals and used as received. Lithium thiophenolate was synthesized following a slightly modified procedure<sup>118</sup> described as follows: diphenyldisulfide (1.2 g, 0.005 mol) was dissolved in 30 mL dry hexane and  $n\text{-BuLi}$  (4.2 mL) of a 1.3M solution in cyclohexane was slowly added at room temperature. The white precipitate formed was washed several times with hexane and then dried in vacuo at 50 °C (0.9 mmHg). The final product was stored under argon. Yield. 1.05g (88%). Anal. Calc. for  $\text{C}_6\text{H}_5\text{SLi}(\text{H}_2\text{O})_{0.2}$  (119.65): C, 60.20; H, 4.55; S, 26.78; Li, 5.80. Found: C, 60.56; H, 4.94; S, 24.60; Li, 5.90.

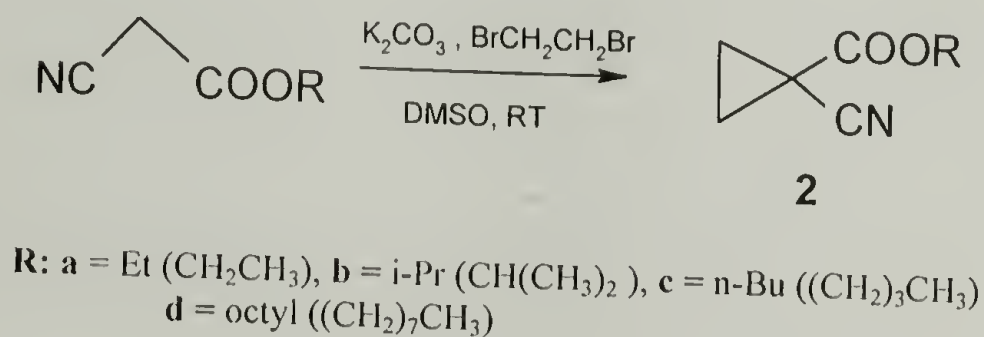


**Polymerization procedure.** Potassium and sodium thiophenolate initiators were dried just before use at 200 °C for 2 hours under vacuum (1 mmHg) using a Büchi Kugelrohr apparatus. The initiator (0.21 mmol equivalent) was dissolved in 0.3 mL DMSO (for bulk polymerizations) or in 5.0 mL DMSO (for solution polymerizations). The cyclopropane monomer (5.34 mmol equivalent) was added and the solution bubbled under nitrogen for 10 minutes. The tube was sealed and placed in an oil bath at 60 °C for a given time. For bulk polymerizations, the solid polymer product was washed with a 1 mol·L<sup>-1</sup> aqueous H<sub>2</sub>SO<sub>4</sub> solution, and then with water, acetone, and diethyl ether. For the polymerizations in solution, the reaction was terminated by adding a few drops of 1 mol·L<sup>-1</sup> aqueous H<sub>2</sub>SO<sub>4</sub> solution. The polymer was precipitated in methanol, filtered and washed several times with water and acetone. The polymers were dried in vacuo at 60 °C for 24 hours.

**Adhesive testing.** Preliminary lab shear tests using grit-blasted mild steel laps with no gaps on a 0.5" joint were performed. Test samples of poly(**2a-d**) were prepared by spreading the monomers between two steel laps, and then curing for two hours at 100 °C. The laps were clamped in place using metal clamps. The adhesive strength of the polymers was measured using the standard ASTM-D1002 test. Each experiment is the average value of the shear strengths obtained from five different experiments.

### 2.3.2.3 Results and Discussion

2.3.2.3.1 Synthesis of monomers **2a-d**. Zefirov's procedure<sup>109</sup> was slightly modified in order to obtain 1,1-disubstituted cyclopropane monomers of high purity. The analytical purity of the final product is crucial for anionic polymerizations, because residual impurities such as dibromoethane can react with the propagating carbanion and terminate the polymerization. In this project, the procedure was extended to include the synthesis of alkyl 1-cyanocyclopropanecarboxylate monomers with isopropyl, n-butyl and n-octyl groups on the ester substituent (Scheme 2.12).



**Scheme 2.12.** Synthesis of Alkyl 1-Cyanocyclopropanecarboxylates

Vigorous mixing of the heterogeneous mixture was employed by mechanical stirring, in order to finely disperse the potassium carbonate into the solution. The absence of residual alkyl cyanoacetate or dibromoethane in the final product was confirmed by <sup>1</sup>H-NMR. Elemental analysis indicated that the purity of the monomers was greater than 99.7%. All the monomers are colorless liquids and are stable at room temperature. The yields, boiling points and spectroscopic data are summarized in Tables 2.7 and 2.8. Literature values are provided where available.

Table 2.7. Yields, Boiling Points and  $^1\text{H}$ -NMR<sup>a</sup> Data for Cyclopropanes **2a-d**

No.	Yield (%)	b.p. in °C / mm Hg)	$^1\text{H}$ NMR data ( $\delta$ in ppm, J in Hz )	
			ring $\text{CH}_2$	ester substituent
			$\delta_{1,2}$	$\delta$
<b>2a</b>	69	45 / 0.4	1.59-1.72	1.34 (t); 4.27 (q)
	92	56-58 / 1.5 <sup>b</sup>		
<b>2b</b>	54	45 / 0.3	1.58-1.71	1.31(d); 5.1(m)
<b>2c</b>	51	60 / 0.3	1.58-1.74	0.95 (t); 1.42(m); 4.20 (t)
<b>2d</b>	31	98 / 0.6	1.57-1.75	0.89 (t); 1.24 -1.44 (broad); 4.19(t)

<sup>a</sup> TMS reference,  $\text{CDCl}_3$   
<sup>b</sup> Literature <sup>109</sup>

Table 2.8.  $^{13}\text{C}$ -NMR Data of monomers **2a-d**

No.	$\text{CH}_2\text{CH}_2$ (ring)	CN	$\text{C} -$ (CN, COOR)	Ester substituent	
				COO	( R )
<b>2a</b>	13.3	118.7	19.0	167.7	14.1; 63.0
<b>2b</b>	13.5	118.8	19.1	167.2	21.6; 71.0
<b>2c</b>	13.3	118.7	19.0	167.8	13.6; 15.3; 30.4; 67.0
<b>2d</b>	13.3	118.7	19.0	167.8	14.0; 15.3; 22.6; 25.7 28.4; 29.1; 31.7; 66.7

2.3.2.3.2 Anionic Polymerization of **2a-d**. Freshly synthesized sodium thiophenolate is known to initiate the ring-opening polymerization of 1,1-dicyanocyclopropane (**1**) (section 2.3.2) and diethyl cyclopropane-1,1-carboxylate **3b**.<sup>84</sup> Due to the high efficiency of sodium thiophenolate in the ring-opening of these

monomers, it was also used to initiate the ring-opening polymerization of alkyl 1-cyanocyclopropane-carboxylates **2a-d**. In addition, sodium and potassium thiophenolates are thermally stable and easy to dry. As previously discussed, the carbon-carbon bond of the cyclopropane ring reacts like a double bond (Section 2.2.1-2.2.2). The ring-opening reaction is analogous to the attack of a nucleophile on the carbon-carbon double bond of an  $\alpha,\beta$ -unsaturated ketone. Therefore, the use of a soft base increases the selectivity of the nucleophilic attack on the cyclopropane ring and not at the carbonyl carbon on the ester. Indeed, this side reaction was not observed for the ring-opening reaction of dialkyl cyclopropane-1,1-dicarboxylates.<sup>84,87</sup> Some of the typical anionic initiators such as organolithium compounds are hard bases and preferentially attack the carbonyl site on the ester.

Results for the polymerization **2a** initiated with PhSK at 60 °C are listed in Table 2.9. Yields refer to isolated yields of poly(**2a**) obtained by gravimetry. In these experiments, a minimum amount of DMSO (0.3 mL) was used to dissolve the initiator. The reaction mixture was initially homogenous, but precipitation of the polymer was observed after 15 minutes. However, despite this precipitation from the reaction mixture, increasing molecular weights were recorded with time, and quantitative conversions were achieved. In addition, the polymers obtained had narrow molecular weight distributions. A more detailed discussion of the influence of the initiator, the counterion and reaction conditions on the polymerization of **2a-d** will be presented after the next section on the characterization of the molecular weight of the resulting polymers.



Table 2.9. Ring-Opening Polymerization of **2a** at 60 °C <sup>a</sup>.

Reaction time (min.)	Yield (%)	M <sub>n</sub> (NMR)	M <sub>n</sub> (GPC) <sup>b</sup>	M <sub>w</sub> /M <sub>n</sub> (GPC)
15	39	2090	6,540	1.07
25	52	2340	8,060	1.04
60	84	4730	12,400	1.05
180	100	5250	14,700	1.05

<sup>a</sup> 3.59 mmol of **2a** in 0.3 mL DMSO, 3.8 mol-% PhSK

<sup>b</sup> Samples were calibrated with polystyrene standards. See section 2.3.3.3 for a discussion on the discrepancy between GPC and NMR values.

**Molecular weight determination.** Before further discussion of the characteristics of the polymerization of these monomers is presented, a section on the determination of the molecular weight of these samples is included. This is essential in order to present the corrected molecular weight values obtained after calibration of the GPC data using NMR spectroscopy. Poly(**2a-c**) are only soluble in highly polar solvents like DMSO or DMF with heating above 100 °C. Therefore, the molecular weights of poly(**2a-d**) were determined by high temperature GPC (100 °C in DMF) and calibrated relative to polystyrene standards. GPC curves of the polymers showed single and in some cases, bimodal distributions (peaks **A** and **B**), without clear trends between the type of distribution and the polymerization conditions. An example of a GPC trace of a sample of poly(**2a**) with a bimodal distribution is shown in Figure 2.11. Peak **A** corresponds to a lower molecular weight fraction ( $\overline{Mn} = 18,000$ ), while peak **B** corresponded to a higher molecular weight fraction with  $\overline{Mn} = 260,000$ . For samples with a bimodal distribution,

the area under the peak **B** was typically 3-5% of the area under the main peak **A**. Among other hypotheses, it was suspected that the high molecular weight fraction was due to aggregation of unterminated polymer chains (living carbanions). To check this hypothesis, the samples were redissolved in DMF and terminated using trifluoroacetic acid. Further runs through the GPC columns showed the area of peak **B** diminished (to less than 1%) in relation to peak **A**. This provided strong evidence that our hypothesis was correct. Therefore, the molecular weight data presented throughout this section was based only on evaluation of the main peak **A**.

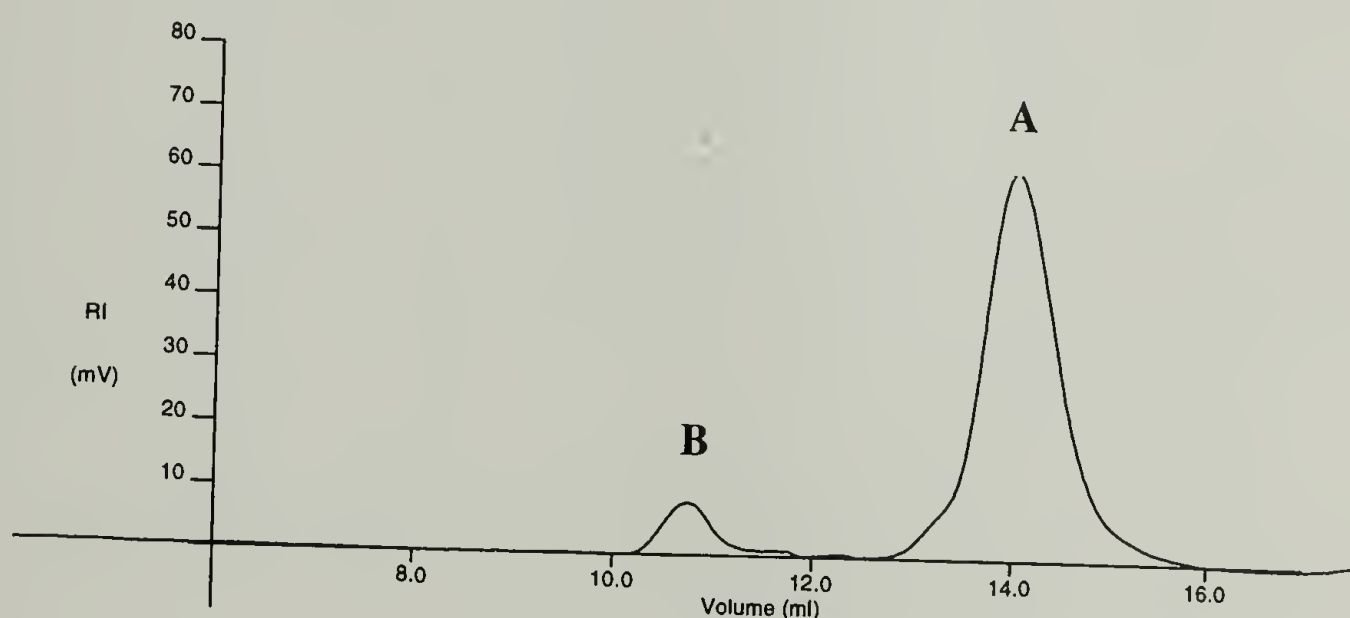


Figure 2.11. GPC Spectrogram of a sample of Poly(**2a**) displaying the Bimodal distribution.

The true nature of separation of GPC is based on the hydrodynamic volume and not molecular weight. Therefore, it is expected that there will be a distinct difference in the hydrodynamic volume of the poly(alkyl 1-cyanocyclopropanecarboxylate)s in comparison to the polystyrene standards used for the calibration, due to the differences in

the structure and polarity of the moieties attached to the backbone. Therefore, as a means of comparison, molecular weight analysis of the polymers was also performed using end-group analysis via  $^1\text{H}$ -NMR spectroscopy. The peak area of the signal due to the aromatic protons of the PhS-end-group (7.2 ppm) was compared to the methylene protons ( $\text{OCH}_2$ , 4.2 ppm) of the ester group on the polymer (Figure 2.18). The absolute degree of polymerization using this method was compared to the apparent degree of polymerization obtained by GPC. The  $\overline{Mn}$  values obtained from NMR analysis were used to determine the error associated with the use of polystyrene standards as calibrants for these polymers. A graph of the  $\overline{Mn}$  values obtained by NMR for poly(2a) (data provided in Table 2.9) was plotted against those obtained by GPC is shown in Figure 2.12. From the slope of the graph it is clear that the GPC values overestimate the actual molecular weights by a factor of 3.

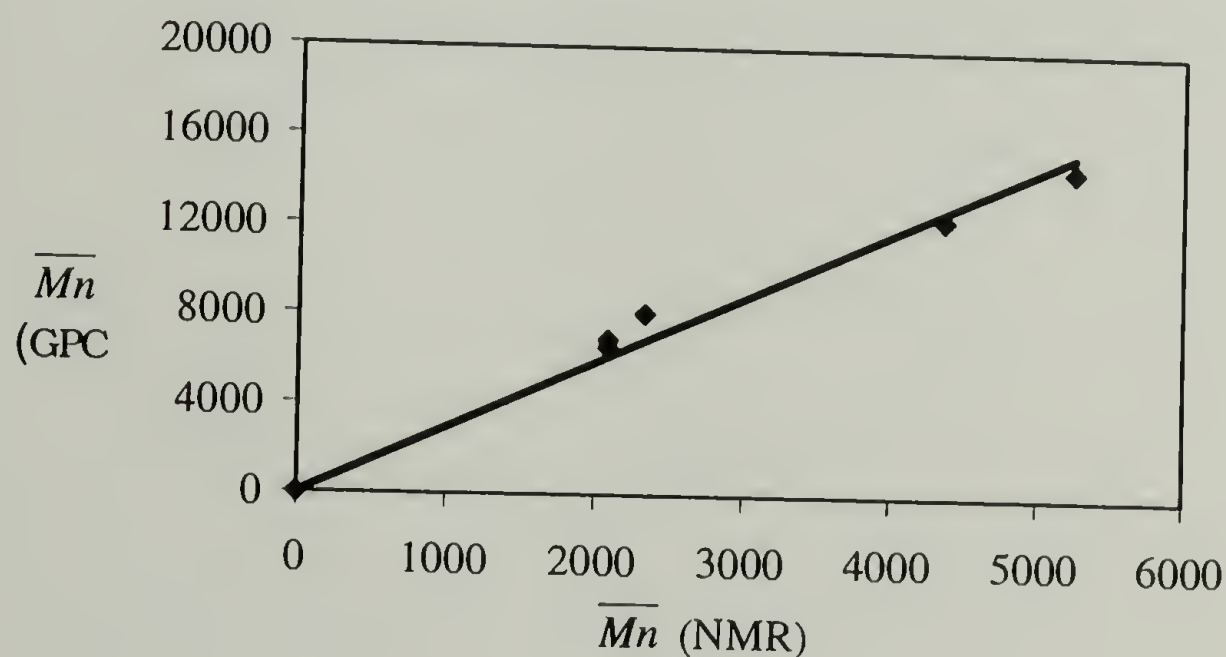


Figure 2.12. Comparison of  $\overline{Mn}$  values obtained from NMR vs. GPC (data provided in Table 2.9).

**Influence of Initiators.** A study of the reactivity of various nucleophilic initiators towards the ring-opening polymerization of ethyl 1-cyanocyclopropane carboxylate **2a** was performed. Thiophenolate salts (with  $K^+$ ,  $Na^+$ ,  $Li^+$  and  $Bu_4N^+$  counterions), aliphatic and aromatic amines such as triethylamine( $Et_3N$ ), pyridine, N-methyl pyrrolidine (NMP) and 1,8-diazabicyclo-[5.4.0]undec-7-ene (DBU) were tested as initiators. For the thiophenolate salts, the influence of the counterion was also studied and the results are provided in a separate discussion in following. Except for  $PhSLi$ , the polymerizations of **2a** at 60 °C initiated with thiophenolate anions reached quantitative conversion after three hours. Lower yields and  $\overline{Mn}$  were obtained for the polymerizations initiated with amine initiators. The results are summarized in Table 2.10. No polymers were isolated after 1 hour at 60 °C using  $Et_3N$  and pyridine initiators. However, an increase in conversion was observed for all the amine initiators with an increase in reaction time, except for pyridine, which did not yield any polymer even after 24 hours. Analysis of the pyridine/monomer reaction mixture by  $^1H$ -NMR showed no change in the relative concentrations of the reagents.

Table 2.10. Ring-Opening Polymerization of **2a** with various initiators at 60 °C<sup>a</sup>.

Initiator	Yield (%)	$M_n$ (corrected)	$M_w/M_n$ (GPC)
PhSK	84	4130	1.05
DBU	43	2940	1.16
NMP	59	2940	1.20
$Et_3N$	b	-	-
pyridine	b	-	-

(a) 3.59 mmol of **2a** in 0.3 mL DMSO, 3.8 mol-% initiator,  $t = 1$  h

(b) No polymer was isolated by precipitation



Analysis of the data in Table 2.10 showed the general trend of increasing reactivity towards polymerization with an increase in nucleophilic strength of the initiator. This is based on the  $\overline{Mn}$  and assumes that the initiation is quantitative. The thiophenolate salts are the strongest nucleophiles and display the highest reactivity as expected. DBU and NMP are less reactive, while pyridine did not initiate the ring-opening polymerization of **2a** under these conditions. Evidence for the decrease in the efficiency of the initiation of the amines was provided by the increase in the PDIs of the polymers ( $1.12 < \text{PDI} < 1.20$ ) in comparison with  $\text{PhS(K/Na/N(Bu)}_4)$  ( $\text{PDI} < 1.07$ ).

**Influence of the Counterion.** The reactivity of thiophenolate salts with potassium, sodium, lithium and tetrabutylammonium counterions was examined in order to determine the influence of the counterion on the rate of polymerization. With the exception of  $\text{Li}^+$ , very little difference (if any) in the kinetic features between  $\text{K}^+$ ,  $\text{Na}^+$ , and  $\text{Bu}_4\text{N}^+$  counterions was observed for the polymerization of **2a** (Figure 2.13-2.15). In these figures, each data point corresponds to a separate experiment. These results contrast with the dicyano **1** (section 2.3.2) and diester **3** monomers, where the influence of the counterion is very significant.<sup>87</sup> In both cases, polymerizations initiated by potassium thiophenolate proceeded about twice as fast as those initiated by sodium.

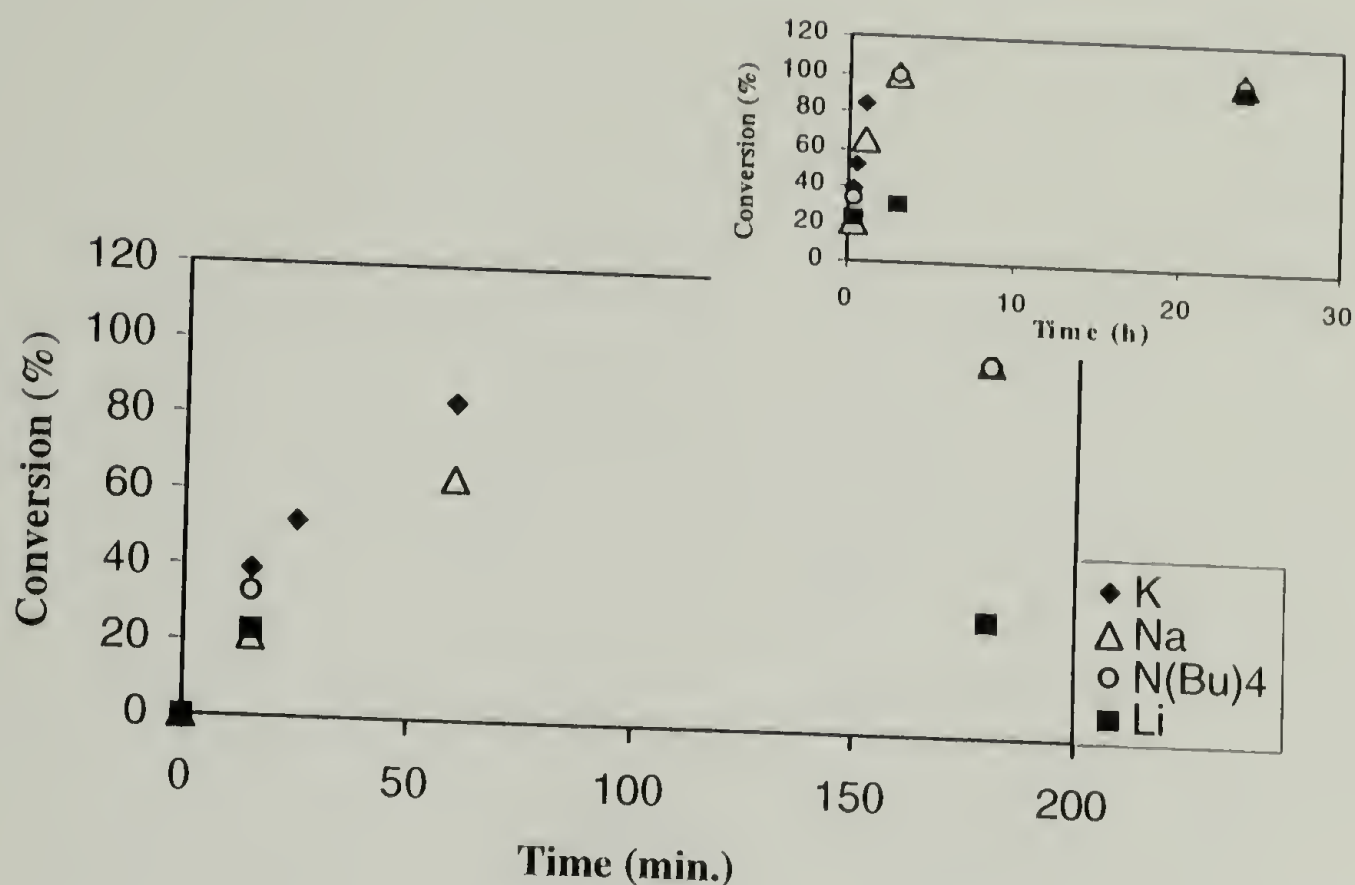


Figure 2.13. Dependence of the conversion (%) with Time for the Polymerization of **2a** with Thiophenolate Initiators -  $\text{PhS}^-\text{X}^+$  ( $\text{X} = \text{K}, \text{Na}, \text{Li}, (\text{NBu})_4$ ); ( $60^\circ\text{C}$ , 3.8 mol-% initiator, 3.59 mmol **2a** in 0.3 mL DMSO).

With the exception of polymers initiated by  $\text{PhSLi}$ , the yields were quantitative after three hours. For  $\text{PhSLi}$ -initiated polymerizations, the yields were much lower after 3 hours (30%), although quantitative conversion was achieved after long reaction times of more than 24 hours. The  $\overline{Mn}$  of the polymers initiated with  $\text{PhS}(\text{K}^+, \text{Na}^+, \text{and } \text{Bu}_4\text{N}^+)$  reached a plateau between 4,000 and 5,000 (Figure 2.14). The maximum theoretical  $\overline{Mn}$  at quantitative conversion is 4,000. This theoretical limit was calculated from the  $[\text{M}]_0/[\text{I}]_0$  ratio multiplied by the mass of the repeating unit, assuming the initiation is quantitative. For initiation with  $\text{PhSLi}$ , despite the low conversion after 3 hours,  $\overline{Mn}$  values close to 5000 were obtained. At 100% conversion, the polymers had narrow

polydispersity indexes ( $PDI = 1.06$ ), providing evidence for a single initiation species. It is believed that decrease in the efficiency of the PhSLi initiator is most probably related to the presence of inactive impurities. Analysis of the Li:S ratio by elemental analysis, indicated that the most probable impurity is LiOH, a byproduct obtained during synthesis of the initiator.

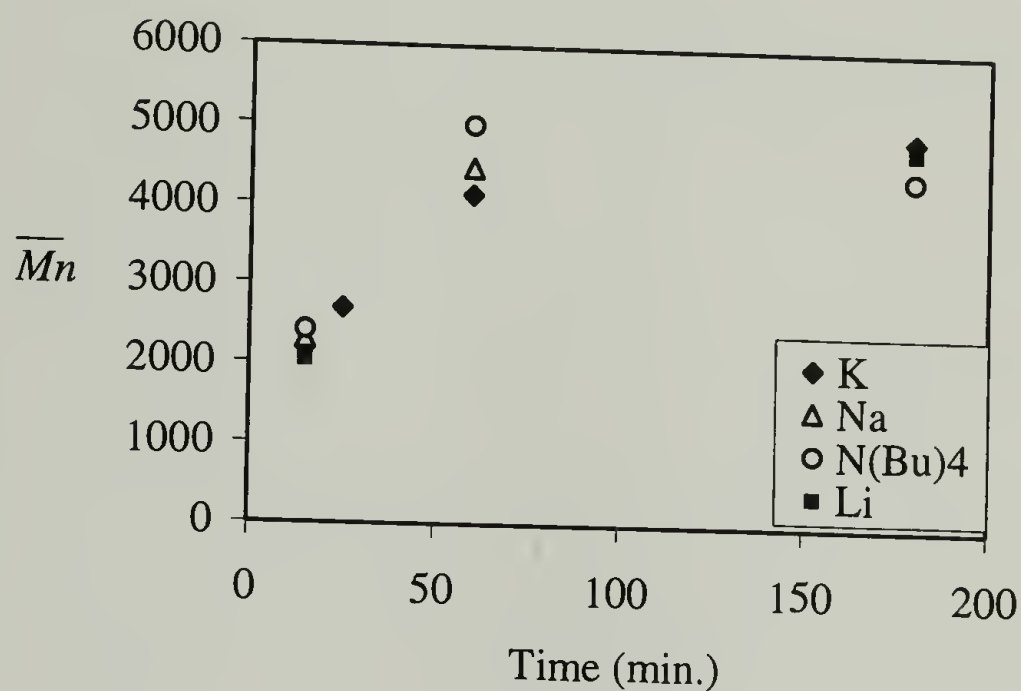


Figure 2.14. Evolution of the Number Average Molecular Weight ( $\overline{M}_n$ ) with Time for the Polymerization of **2a** with Thiophenolate Initiators -  $\text{PhS}^-\text{X}^+$  ( $\text{X} = \text{K}, \text{Na}, \text{Li}, (\text{NBu})_4$ ); ( $60^\circ\text{C}$ , 3.8 mol-% initiator, 3.59 mmol **2a**) in 0.3 mL DMSO).

In the case of the nitrile-ester monomer **2a**, it is apparent that relative concentrations of probable propagating species do not significantly change with a change in the counterion. This suggests that neither of the counterions are preferentially coordinated to the propagating carbanion. In the example of the polymerization of diisopropyl cyclopropane-1,1-dicarboxylate **3e**, dramatic changes in the rate of polymerization were observed when  $\text{K}^+$  was used as the counterion instead of  $\text{Na}^+$ . Dramatic changes in the rate of polymerization with a change in the counterion provide



strong evidence for the existence of at least two species in equilibrium. In this case, the results suggest that the  $\text{Na}^+$  counterion is more tightly bound to the propagating carbanion than the larger  $\text{K}^+$  counterion. Similar results of this counterion effect were reported for the alkylation of dimethyl ethyl malonate carbanion with methyl iodide in DMSO at 25 °C.<sup>119-121</sup> This study provided evidence for strong ion-pairing by  $\text{Li}^+$  and  $\text{Na}^+$  cations that transforms the reactive species into unreactive ones. It was determined that there was a linear correlation between the degree of dissociation of the ion-pairs and the rate constants.

The counterion effect can also be further understood by examining the interaction between the counterion and the carbanionic species in solution. Considerable effort has been made to study the structural properties of carbon-based anionic species formed from many different types of organolithium reagents including alkyl lithiums, and deprotonated forms of carbonyl compounds (enolates), nitriles, nitroalkanes, sulfoxides, sulfones and other CH-acidic precursors.<sup>122</sup> Despite the fact that it has long been determined that the anionic part of these species is intimately involved with lithium by the way of Li-O, Li-N, or Li-C bonds, the term "carbanion" is still being loosely used to describe these species.<sup>123-125</sup> It has been demonstrated that these species exist as dimers, tetramers, or higher aggregates. On the contrary, until recently, tetrabutylammonium salts of CH-acidic esters, ketones, nitriles, nitroalkanes and sulfones were believed to be "naked" ions and therefore true carbanions. Reetz and coworkers determined the structure of several tetrabutylammonium salts using X-ray scattering on single crystals prepared from various CH-acidic carbonyl compounds.<sup>126</sup> The results indicated that both the ethyl diethyl malonate and cyanoacetate carbanions are dimeric in solid state and in DMSO



solution. In spite of the well-known ability of DMSO to break up hydrogen bonds, the dimeric nature of the anion was still retained. This dimeric state of the carbanions is due to C-H $\cdots$ O hydrogen bonds originating from  $\alpha$ -methylene units of the tetrabutylammonium counterions. However, for the cyanoacetate carbanion, only one terminal oxygen atom is available to hydrogen-bond to the tetrabutylammonium counterion. These results demonstrated that these carbanions are not truly "naked" as previously believed. With regard to the polymerization of **2a**, it is suggested that due to the weaker coordination between the N<sup>+</sup>(Bu)<sub>4</sub> counterion and the cyanoester carbanion, dramatic differences in the reactivity are not observed (in comparison to K<sup>+</sup> and Na<sup>+</sup>).

Changes in the average degree of polymerization DP ( $\overline{Xn}$ ) with conversion are shown in Figure 2.15. The DP increases with conversion for all polymerizations, but only distinctly linearly with the PhSK initiator. This linear increase in  $\overline{Xn}$  with conversion, provides evidence for the absence of any competitive chain-transfer reactions. It should be noted that despite the precipitation of the polymer from the reaction mixture after about 15% conversion, physical termination of the chains does not occur. In fact, for all polymers, narrow molecular weight distributions are observed.

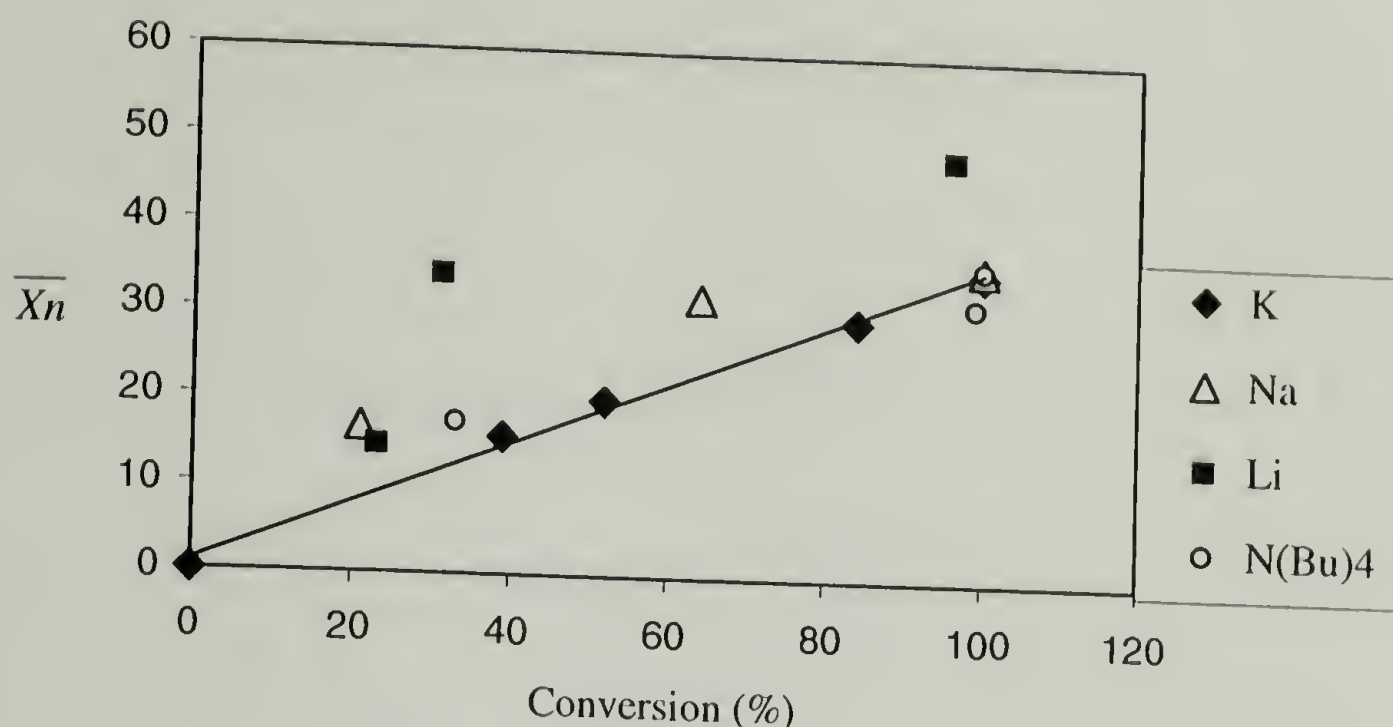


Figure 2.15. Evolution of the Degree of Polymerization ( $\overline{Xn}$ ) with % Conversion for the Polymerization of **2a** using Thiophenolate initiators [ $\text{PhS}^- \text{X}^+$  ( $\text{X} = \text{K}, \text{Na}, \text{Li}, \text{N}(\text{Bu})_4$ )] (3.59 mmol monomer in 0.3mL DMSO, 3.8 mol-% initiator;  $[\text{M.}]/[\text{I}] = 27/1$ , 60 °C)

**Note:** Based on 100% yields obtained for these polymers, at long reaction times- the conversion and the yield are assumed to be equivalent.

**Influence of Temperature.** Solution polymerization of **2a-d** was performed at 60, 100 and 120 °C in DMSO. At 60 °C, the polymer precipitated from solution even at low conversions (~15%) due to the poor solubility of the polymer below 100 °C. At 100 and 120 °C, the polymerizations were homogeneous throughout the entire polymerization, and a significant increase in the viscosity was observed. At 60 °C, no polymer was isolated by precipitation after 15 minutes. NMR analysis of the reaction mixture indicated the formation of dimers ( $\overline{Xn} = 2$ ). These results clearly show that the rate of polymerization increased with an increase in temperature, but further experiments were not performed.

Table 2.11. Polymerization of **2a** at 60, 100 and 120 °C <sup>a</sup>.

Temp. (°C)	Yield (%)	$\overline{X}_n$ (NMR/GPC)	PDI (GPC)
60	- <sup>b</sup>	2	-
100	12	20	1.08
120	72	43	1.07

<sup>a</sup> 3.59 mmol **2a** in 5 mL DMSO, 3.8 mol-% PhSNa, time = 15 minutes

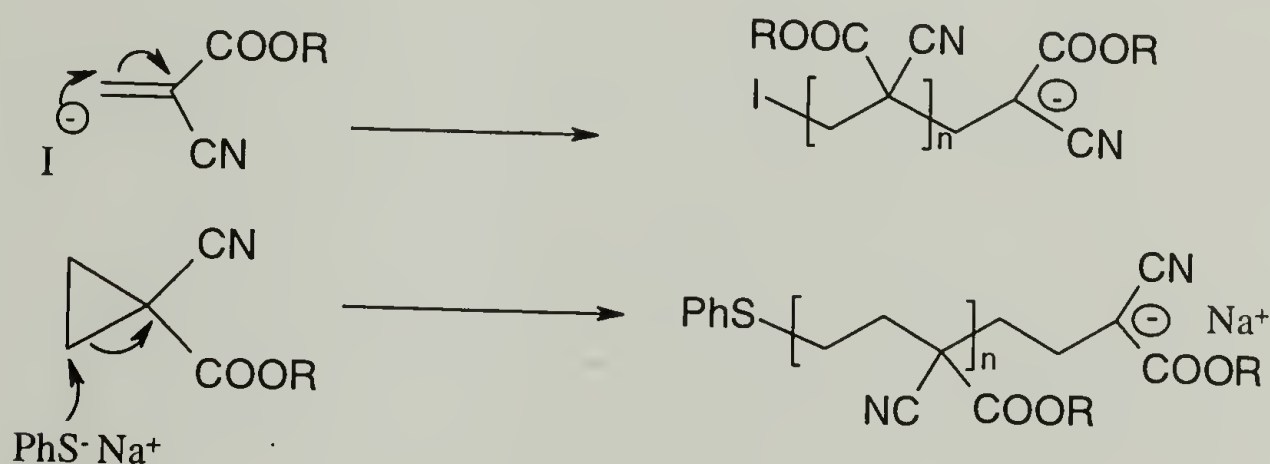
<sup>b</sup> no polymer was isolated

#### 2.3.2.3.3. Quasi-Living characteristics of the polymerization of **2a**.

**Kinetics.** The polymerization of **2a** initiated with PhSK showed a linear increase in molecular weight with conversion reaching the theoretical limit of 4,000 ( $\overline{M}_n$ ) at full conversion (within experimental error in determining  $\overline{M}_n$ ) (Figure 2.14). This provides evidence for the absence of any competitive side reactions resulting in chain-transfer reaction(s). In addition, polymers obtained from initiation with thiophenolate anions had narrow polydispersity indexes (PDI's) ranging from 1.02-1.07 over the entire range of the polymerization. These results provide partial evidence for living polymerizations. Additional features of the living aspects of the polymerization of **2a** are provided in the next sections.

**Lack of chain termination reactions.** The propagating carbanions during the polymerization of **2a-d** are the same as that obtained during the anionic polymerization of  $\alpha$ -cyanoacrylates (Scheme 2.13). Classical propagating carbanions such as those of polystyrene, or poly(methyl methacrylate) must be carefully protected against terminating agents such as water, oxygen, alcohols, and carbon dioxide. On the contrary, cyanoacetate carbanions are highly stabilized by two electron-withdrawing groups and

are weak bases ( $pK_a = 16.4$  (in DMSO)). The polymerizations of  $\alpha$ -cyanoacrylates are unaffected by oxygen, water ( $pK_a$  ( $H_2O$ ) in DMSO = 32), or carbon dioxide.<sup>127</sup> The propagating anions are terminated only after the addition of strong acids such as HCl. These polymerizations also proceed in the presence of large excesses of halogenated compounds such as chloroform or ethylene dichloride. They can even be carried out in open beakers!



Scheme 2.13. Comparison of the Propagating Anions during the Polymerization of  $\alpha$ -Cyanoacrylates and **2a-d**.

The remarkable stability of (poly)cyanoacrylate anions was demonstrated in a study of the termination of the polymerization of  $\alpha$ -cyanoacrylates using a variety of acids, whose  $pK_a$ 's are shown in Table 2.12.<sup>128</sup> The study showed that weak acids such as acetic acid and mono- or dichloroacetic acid only retard the polymerization. The rapid termination of fully initiated chains by acid was observed only when strong acids such p-toluenesulfonic acid, trichloroacetic acid and picric acid were used.

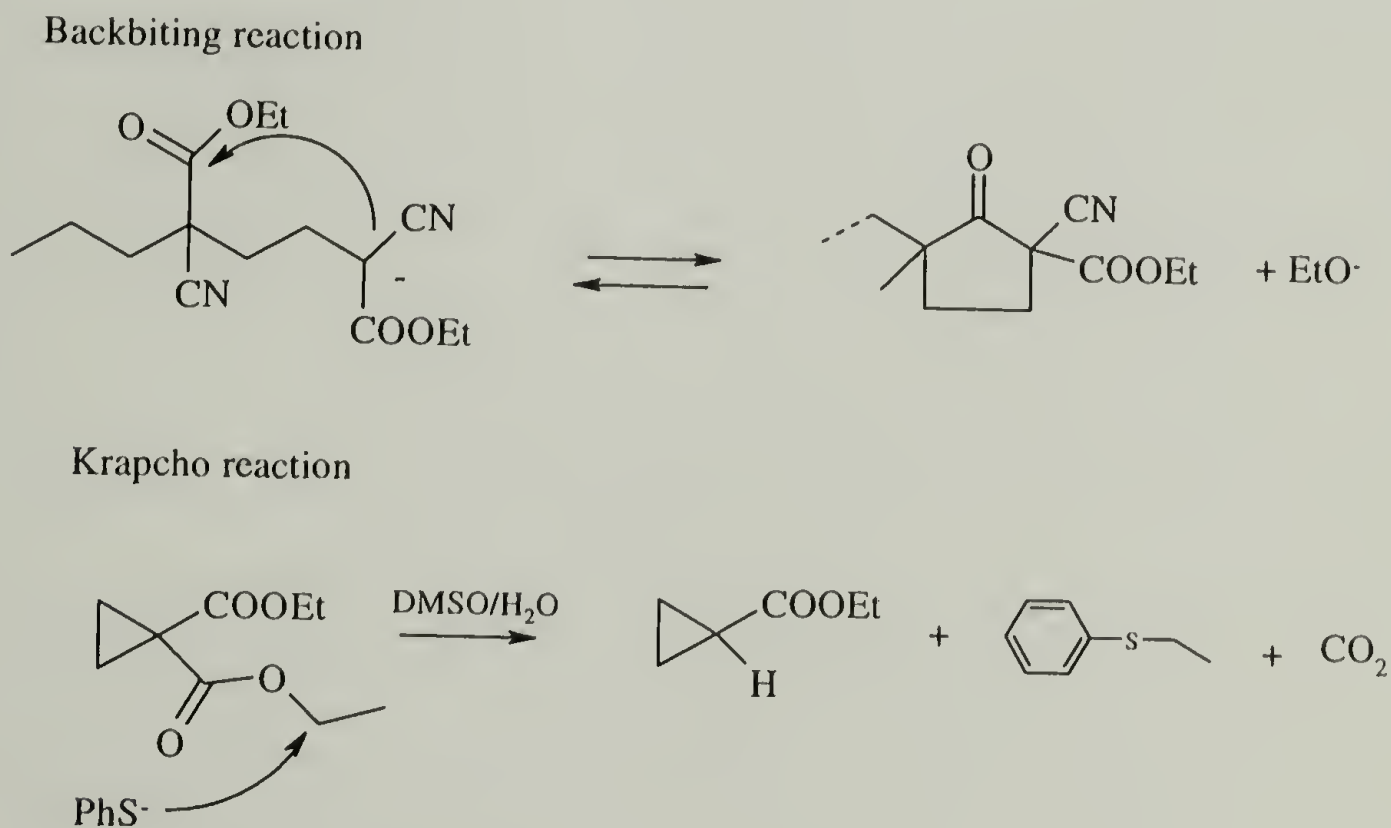


Table 2.12. Equilibrium Acidities of Various Acids in DMSO at 25 °C.<sup>129</sup>

Acid	pK <sub>a</sub>
Acetic acid	12.3
Dichloroacetic acid	6.4
Trifluoroacetic acid	3.45
Methylsulfonic acid	1.6
HCl	1.8
Picric acid	~0 <sup>a</sup>

Note: pK<sub>a</sub>(H<sub>2</sub>O) in DMSO = 32

In addition, NMR spectroscopy of the polymers initiated with the thiophenolate initiators supported clean initiation and propagation steps, with no evidence for the presence of side reactions such as the Krapcho reaction, or backbiting reactions (Scheme 2.14).



Scheme 2.14. Possible Side Reactions During the Polymerization of **2a-d**

The stability of the propagating carbanion of **2a** was also demonstrated using IR spectroscopy. The IR spectrum of the tetrabutylammonium salt of ethyl cyanoacetate was previously reported and shows an absorption at  $2140\text{ cm}^{-1}$  characteristic of the  $\text{C}^-$ -CN moiety.<sup>126</sup> IR spectra of the poly(**2a**) prior to termination with a strong acid is shown in Figure 2.16. The band at  $2137\text{ cm}^{-1}$  (indicated with an arrow) is characteristic of the  $\text{C}^-$ -CN stretching. This band only disappeared upon termination with a strong acid (Figure 2.17). This  $\text{C}^-$ -CN stretching band was also visible for a sample of **2a** polymerized under exposure to atmospheric oxygen, carbon dioxide and moisture.

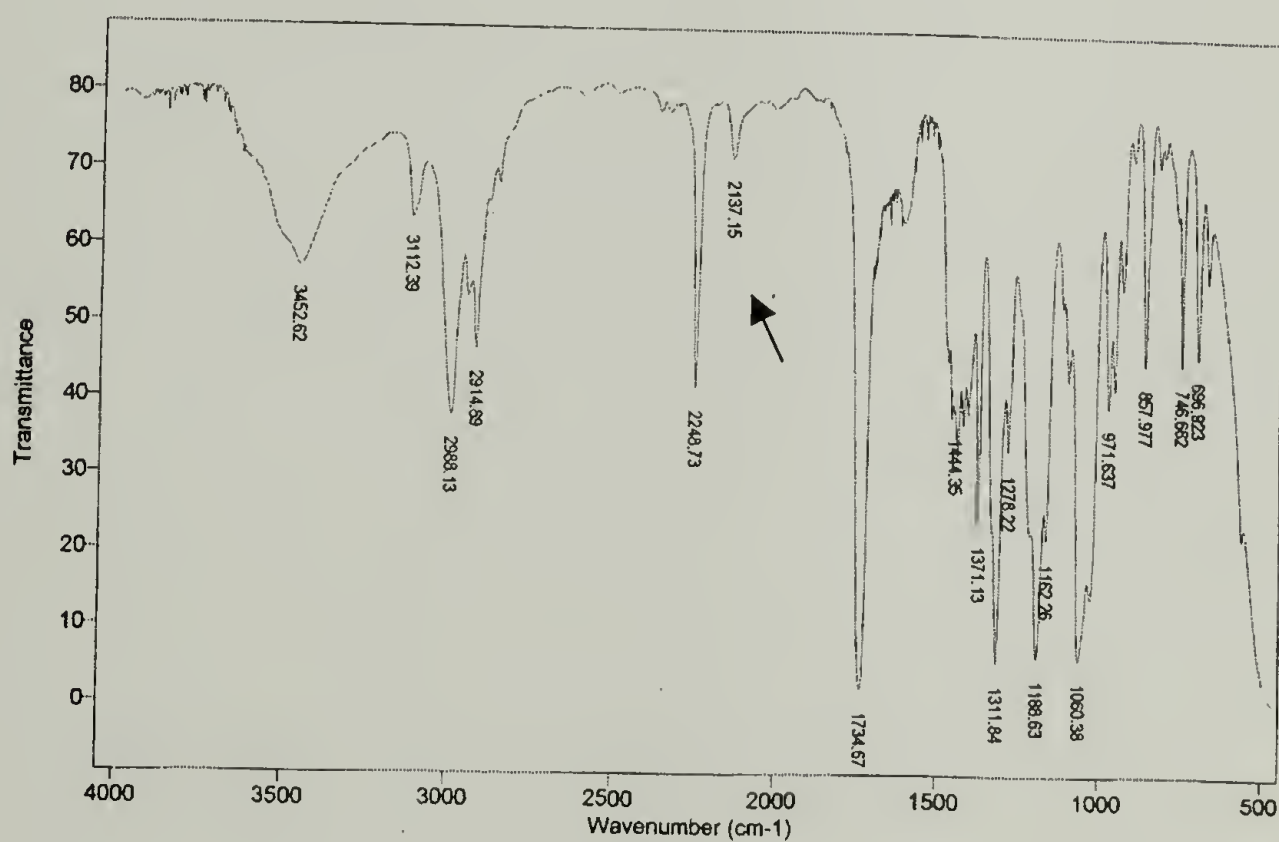


Figure 2.16. IR Spectrum obtained during the Polymerization of **2a**

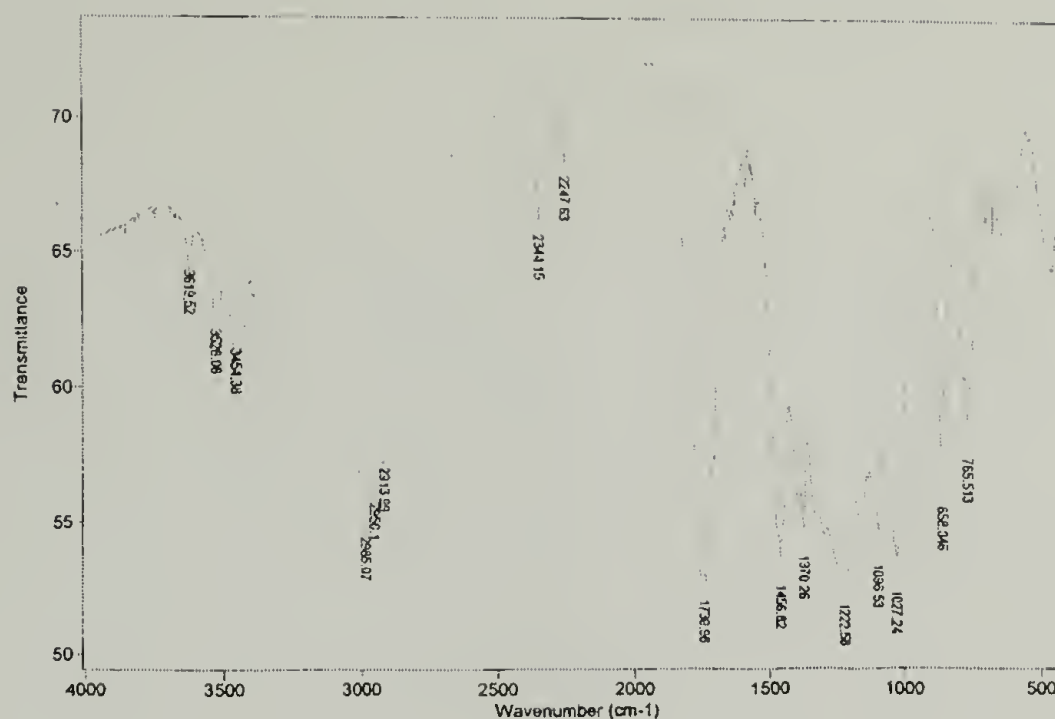


Figure 2.17. IR Spectrum of Poly(**2a**) after Termination

**Re-initiation.** The subsequent addition of **2a** to a sample of the same monomer that was polymerized to quantitative conversion, was monitored using molecular weight analysis. Before the addition of the second aliquot, the polymer had completely solidified due to precipitation of the polymer from solution at 60 °C (Sample #1, Table 2.13). An increase in the degree of polymerization with time was observed (Sample #2), although not all of the monomer was consumed after 24 h.

Table 2.13. Yields(%), and  $\overline{Mn}$  values of Poly(**2a**)

Sample	Time	$\overline{Mn}$	PDI
#1 <sup>a</sup>	3 h	13,200	1.07
#2 <sup>b</sup>	24 h	17,300	1.13

<sup>a</sup> 3.59 mmol /0.3 mL DMSO, 3.8 mol-% PhSNa

<sup>b</sup> added 7 mmol **2a**

The data provided evidence that the propagating carbanions remain active during the entire polymerization. The remarkable stability of the carbanions was demonstrated by IR (Figure 2.16). In addition, precipitation of the polymer from the reaction mixture did not physically terminate the polymerization. Access of the monomer to the propagating chain ends is typically limited by precipitation, but in this case, it is apparent that the monomer can diffuse into the solid and continue to propagate. However, this physical limitation slows down the rate of polymerization significantly. After 24 h, only 50% of the monomer is consumed, whereas complete conversion of the first aliquot was observed after 3 hours.

**Block copolymer synthesis.** The use of tetrabutylammonium salts of ethyl dialkyl malonates **viii**, methyl malononitrile **ix**, and cyanoacetates **x** and nitroalkanes as initiators for the polymerization of acrylates and (methyl) methacrylates has been reported in the literature (Figure 2.18).<sup>126,130,131</sup> Depending on the solvent used, the resulting polymers had molecular weights  $\overline{Mn}$  ranging from 1360 to 20,000, with polydispersity indices ranging within 1.14 to 2.71. Based on the similarity in structure of the propagating anion in poly(**2a**)(**xi**), it was possible that the polymerization of methyl methacrylate could also be initiated with the propagating carbanion resulting from the ring-opening polymerization of **2a-d**(**xi**), and that a block cyclopropane-PMMA copolymer could be obtained using this strategy.



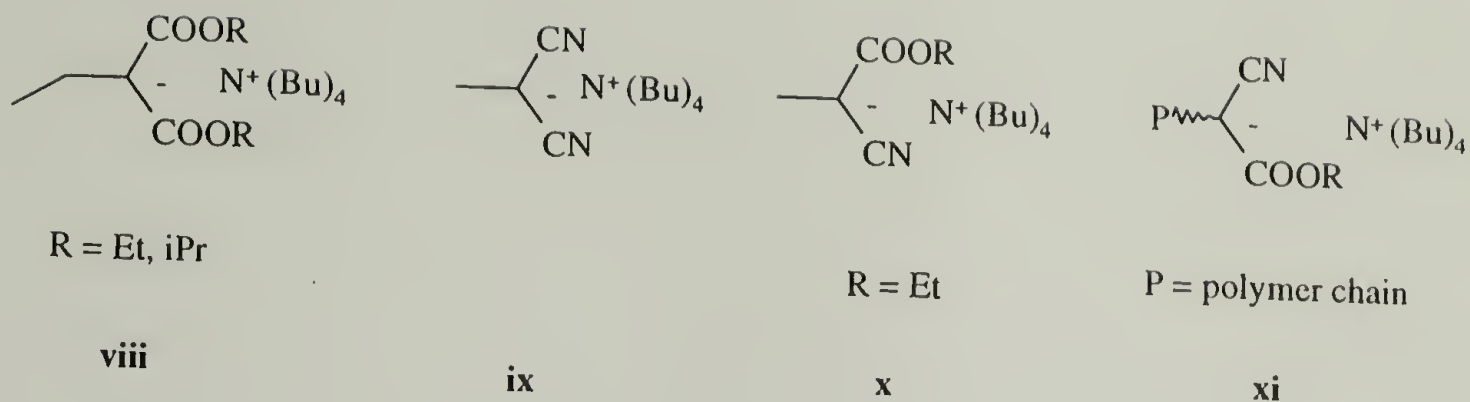


Figure 2.18. Structures of Tetrabutylammonium Salts of CH-Acidic Carbonyl Compounds.

In the previous section, it was demonstrated that the chains remain active towards polymerization and continue to propagate when additional monomer is added. Therefore, attempts were made to grow a second block of MMA from the polymeric carbanion (xi) under conditions similar to those used for the polymerization of MMA using tetrabutylammonium salts reported in the literature.<sup>126,131</sup> The polymerizations of MMA were typically carried out at ambient temperature in THF. Therefore, in these experiment the polymerization of **2d** was first carried out to quantitative conversion using  $\text{PhSN}(\text{Bu})_4$  (3.8 mol-%) at 60 °C in THF. Monomer **2d** was selected over **2a-c** because of the solubility of poly(**2d**) in THF over the entire polymerization at 60 °C. After the monomer was completely consumed, the solution was cooled down to ambient temperature and MMA was added. Analysis of the polymer before and after the addition of MMA was performed by NMR and GPC. NMR data showed no evidence of the peaks expected of poly(methylmethacrylate) and the GPC data also showed no changes in the degree of polymerization after the addition of MMA. Under these conditions, it is believed that the limitation of this reaction was due to the physical inaccessibility of the MMA monomer to the propagating chains, as a result of the precipitation of poly(**2d**) from solution at ambient temperature. Poly(**2a-d**) require moderate to high temperatures (60 to over

100 °C) to dissolve. However, the polymerization of MMA at such high temperatures is unfavorable since side reactions such as backbiting reactions leading to cyclic products become favored.

2.3.2.3.4 Adhesion Testing of Poly(**2a-d**). As previously mentioned, the propagating carbanion resulting from the ring-opening polymerization of **2a-d** under anionic conditions is stabilized by the ester and nitrile electron-withdrawing groups. This carbanion is chemically equivalent to the propagating carbanion obtained during the anionic polymerization of  $\alpha$ -cyanoacrylates (Scheme 2.13). Poly( $\alpha$ -cyanoacrylates) are more commonly known as “superglues” with instantly curable adhesive properties.<sup>132</sup>

$\alpha$ -Cyanoacrylate monomers are generally low viscosity liquids with excellent wetting properties. In combination with the polar effects of the cyano and carboxylate groups, these materials exhibit excellent adhesion to a variety of substrates and are commercially available products.<sup>133</sup> Due to the electron-withdrawing properties of the adjacent nitrile and carboxylate groups on carbon, these vinyl monomers undergo extremely rapid anionic polymerization on contact with weak catalytic amounts of anionic and certain covalent bases such as amines and phosphines.<sup>127,134</sup> Cyanoacrylates also polymerize under radical conditions, but relatively slowly in comparison to the anionic polymerization. The monomers are among the most reactive known, and must be stabilized by both anionic and radical inhibitors.

In contrast, alkyl cyanocyclopropanecarboxylates **2a-d** polymerize slowly in the presence of strong nucleophiles like thiophenolate salts (at ambient temperature) and weaker nucleophiles such as triethylamine (at 60 °C). The monomers **2a-d** are low viscosity liquids and are easy to synthesize and handle in comparison to the cyanoacrylates. The poor solubility of poly(**2a-c**) in chlorinated, aromatic or even highly polar solvents at ambient temperature is a desirable quality of these polymers, because the solvent resistance of materials used in adhesive joints is an important factor in a variety of applications. Therefore, adhesive strength of monomers **2a-d** was tested under conditions similar to those used in the testing of cyanoacrylate monomers. The results are summarized in Table 2.14.

Table 2.14. Adhesion Testing of **2a-d**

Monomer	Max.shear strength (PSI)	S.D (%)	Failure mode	comments
<b>2a</b> <sup>a</sup>	266	16	Adhesive	Run off
<b>2a</b> <sup>b</sup>	313	18	Adhesive	
<b>2a</b> <sup>c</sup>	427	19	Adhesive	
<b>2b</b> <sup>a</sup>	248	23	Adhesive	Run off
<b>2c</b> <sup>a</sup>	336	13	Adhesive	Run off
<b>2d</b> <sup>a</sup>	342	15	Cohesive	Run off
ECA <sup>d</sup>	719	-	Mix	-

Polymerizations of **2a-d** were carried out using PhSN(BU)<sub>4</sub> as the initiator dissolved in the monomer [M]/[I] (a) = 30/1 (b) 60/1 (c) 120/1 (d) ECA = ethyl cyanoacrylate, cured at ambient temperature for 24 hours.

Preliminary tests of the monomers indicated that the primary mode of failure for **2a-c** was adhesive. Run-off refers to the material that flows out of the joint region during curing. This reduces the effective material under the joint, lowering the adhesive strength.



Although the data obtained indicate that the cyclopropane monomers **2a-d** are less effective than ethyl cyanoacrylate (ECA), it must be noted that these set of experiments are preliminary and do not represent optimized conditions. For example, the curing conditions are crucial in determining the adhesive strength of a material. ECA cured for an additional 2 hours at 120 °C (after a 24 hour room temperature cure) displays an increase in shear strength from 719 to 3400 Psi. Therefore, further testing of **2a** under a variety of cure conditions is necessary, in order to determine the feasibility of the use of these monomers as adhesives.

#### 2.3.2.4 Characterization of Poly(**2a-d**)

2.3.2.4.1 Physical properties. Poly(**2a-d**) are all white solids. Poly(**2a-c**) are soluble only in highly polar solvents such as DMSO and DMF at temperatures above 100 °C. Poly(**2d**) has a longer alkyl (n-octyl) side chain and shows a dramatic improvement in its solubility, dissolving in toluene, THF and chlorinated solvents at room temperature. However, higher molecular weight samples of poly(**2d**) (>3000) required moderate heating (30-60 °C) to dissolve. If solutions of each sample of poly(**2a-d**) in DMSO at 100 °C are cooled to ambient temperature, the polymers do not precipitate out of solution, but form a clear homogeneous gel.

2.3.2.4.2 Structural Characterization. The polymers were analyzed by high temperature <sup>1</sup>H- and <sup>13</sup>C-NMR and IR spectroscopy. <sup>1</sup>H- and <sup>13</sup>C-NMR of poly(**2a**) [(CD<sub>3</sub>)<sub>2</sub>SO, 100 °C] are provided in Figure 2.19 and 2.20 respectively. The peaks are consistent with the polymer structure expected of the ring-opened product. A summary of



the  $^1\text{H}$  and  $^{13}\text{C}$ -NMR data of poly(**2a-d**) is shown in Table 2.15 and 2.16 respectively. A complete analysis of the tacticity of these polymers is provided in chapter 3.

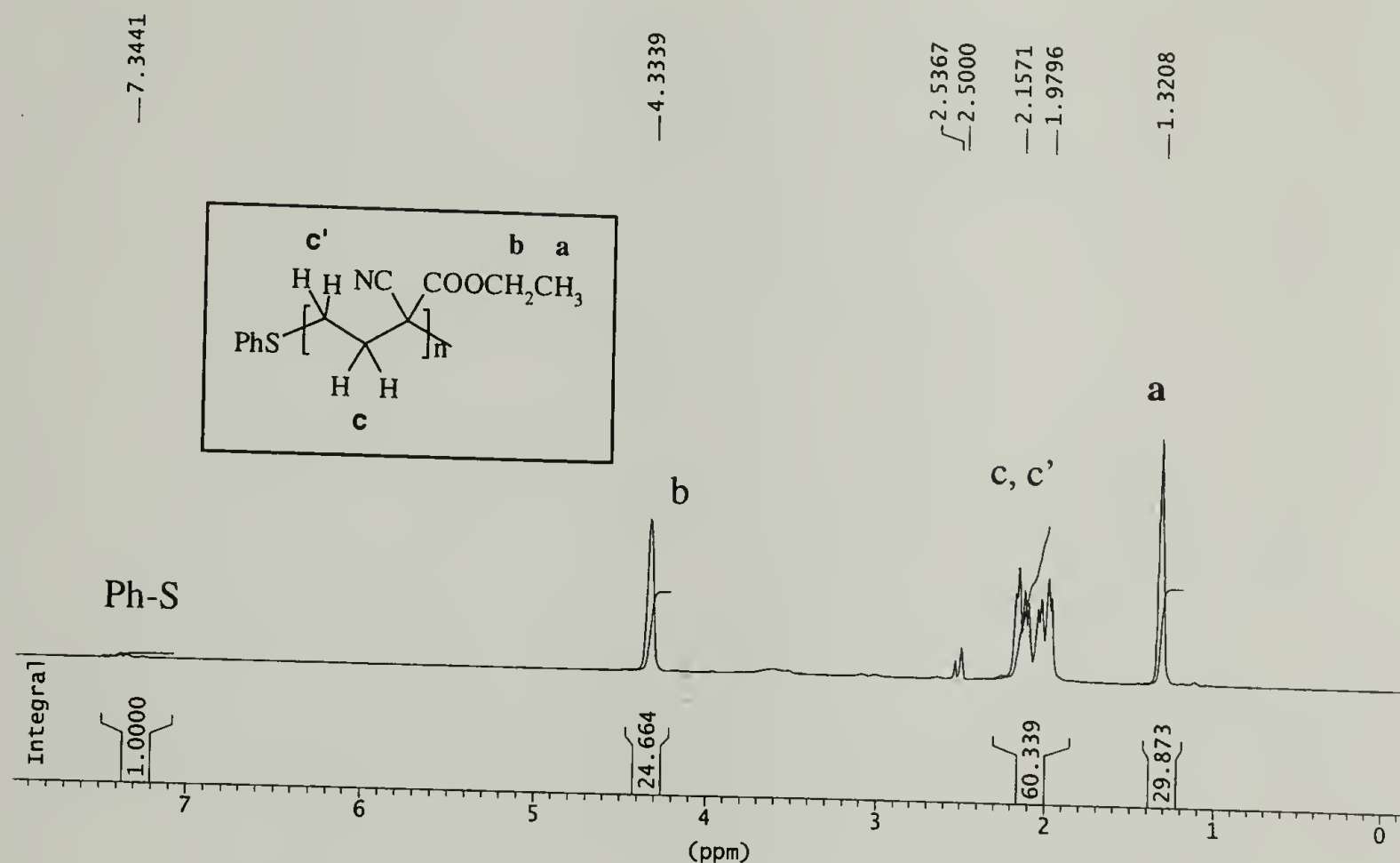


Figure 2.19.  $^1\text{H}$ -NMR Spectrum of Poly(**2a**)

Table 2.15.  $^1\text{H}$ -NMR Data of Poly(**2a-d**)

Polymer	$^1\text{H}$ NMR data ( $\delta$ in ppm)	
	backbone $\text{CH}_2$ $\text{CH}_2$	ester substituent
	$\delta$	$\delta$
<b>2a</b>	1.59-1.72	1.34 (t); 4.27 (q)
<b>2b</b>	1.58-1.71	1.31(d); 5.1(m)
<b>2c</b>	1.58-1.74	0.95 (t);1.42(m); 4.20 (t)
<b>2d</b>	1.57-1.75	0.89 (t); 1.24 -1.44 (broad); 4.19(t)

<sup>a</sup> TMS reference,  $\text{CDCl}_3$

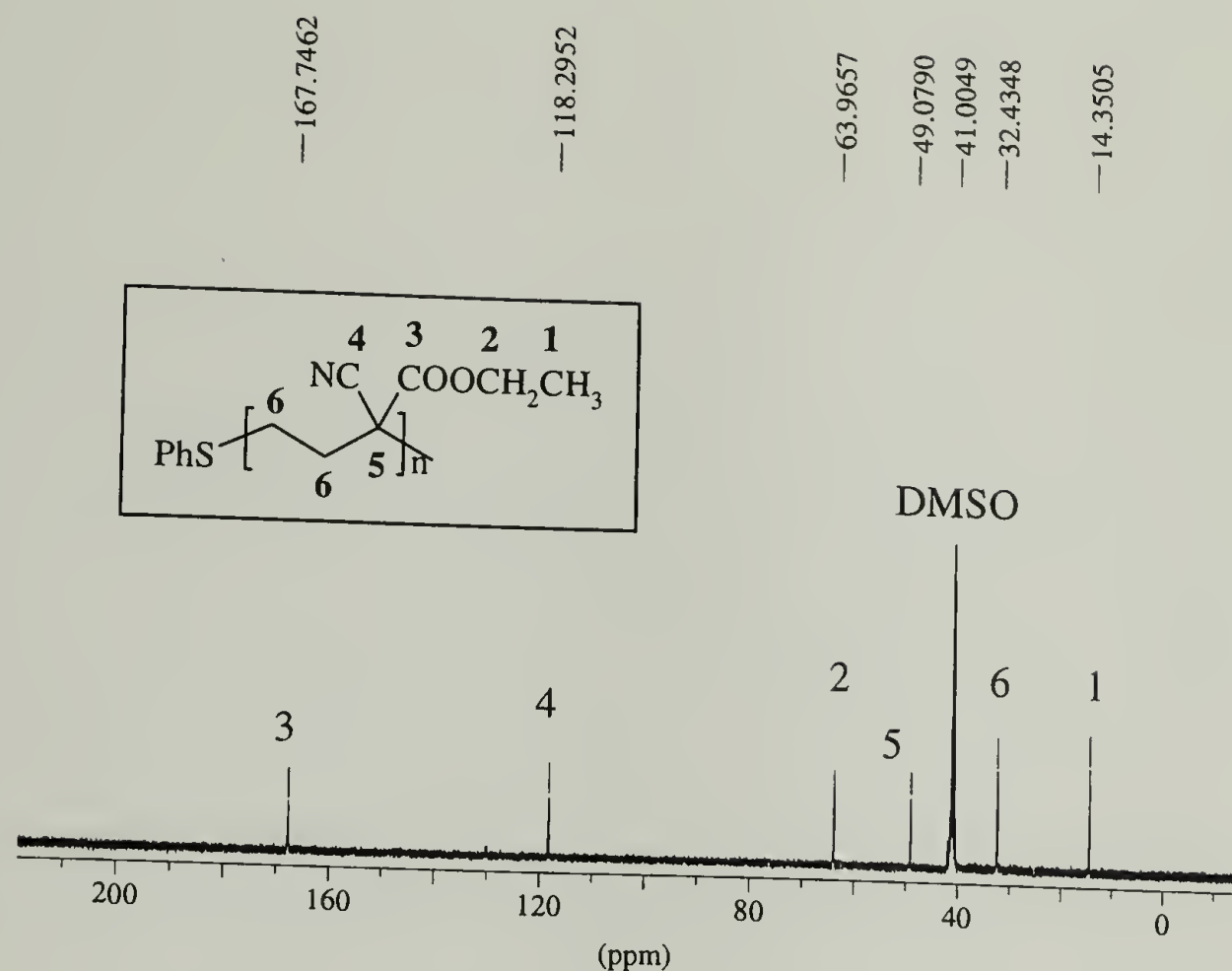


Figure 2.20.  $^{13}\text{C}$ -NMR Spectrum of Poly(2a)

Table 2.16.  $^{13}\text{C}$ -NMR Data of Poly(2a-d)

No.	$\text{CH}_2\text{CH}_2$ (backbone)	CN	$\underline{\text{C}}_{(\text{quart.})}$	Ester substituent	
				COO	( R )
2a	32.4	118.3	49.0	167.7	14.1; 63.0
2b	32.0	118.8	49.0	167.2	21.6; 71.0
2c	32.3	118.7	49.1	167.8	13.6; 15.3; 30.4; 67.0
2d	32.2	118.7	49.1	167.8	14.0; 15.3; 22.6; 25.7 28.4; 29.1; 31.7; 66.7

The main IR bands of the polymers include CN stretching at  $2249\text{cm}^{-1}$ , C=O stretching at  $1740\text{cm}^{-1}$ , C-O stretching at  $1222\text{cm}^{-1}$  (Figure 2.17). The strong peak at  $1190\text{cm}^{-1}$  due to the C-C stretching of the cyclopropane ring completely disappears.

2.3.2.4.3 Thermal Analysis. The thermal decomposition of poly(**2a-d**) was monitored using thermogravimetric analysis from ambient temperature to 600 °C (Figure 2.21). The onset of decomposition for all the polymers is above 210 °C. The polymers are less stable than poly(1,1-dicyanocyclopropane), which does not decompose below 350 °C. The onset of decomposition for the diethyl-ester poly(**3b**) at 280 °C<sup>1</sup> indicates that poly(**3b**) is more stable than poly(**2a**). Although the polymers are semi-crystalline (see chapter 6 for details), DSC analysis of the polymers revealed no melting transitions below the decomposition temperature, and no distinct glass transition temperatures were observed for any of the polymers.

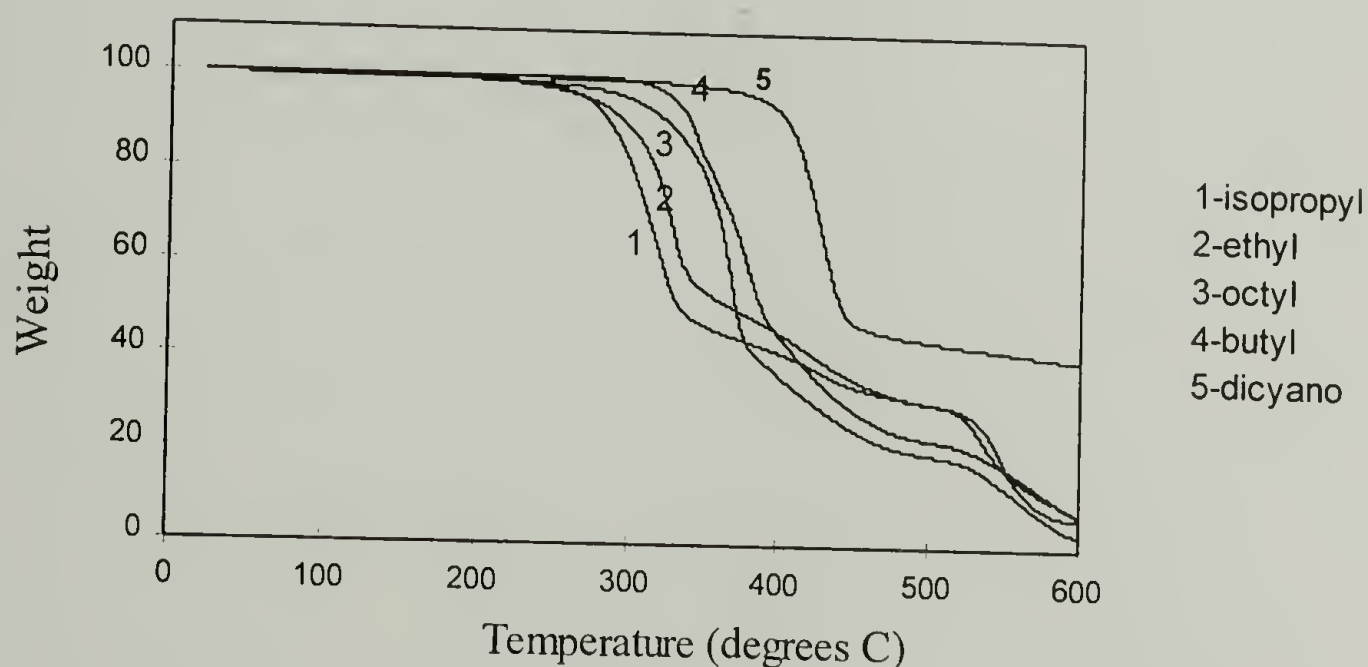


Figure 2.21. TGA spectrogram of Poly(**1**) and Poly(**2a-d**)

### 2.3.2.5 Comparison of the properties of Poly(**2a-d**) with Poly( $\alpha$ -cyanoacrylates).

2.3.2.5.1 Thermal properties. Poly( $\alpha$ -cyanoacrylates) are the analogues of poly(**2a-d**) with geminal ester and nitrile substituents on every second carbon, instead of every third carbon atom. Poly( $\alpha$ -cyanoacrylates) are brittle, colorless thermoplastics of little flexibility. The polymers undergo a clean retropolymerization reaction at 140-180 °C and are susceptible of hydrolysis even at neutral pH and begin degrading at temperatures above 70 °C.<sup>135,136</sup> In comparison, poly(**2a-d**) are stable up to 210 °C, probably undergoing initial decomposition via decarboxylation of the ester group. Unlike poly( $\alpha$ -cyanoacrylates), these polymers do not decompose via depolymerization to the monomer due to unfavorable thermodynamics associated with the formation of a three membered ring, as well as the absence of a suitable mechanism for that reaction.

2.3.2.5.2 Crystalline properties. WAXS studies of poly(**2a-d**) (Chapter 6) indicated that the polymers are all semi-crystalline. However, DSC analysis of the polymers revealed neither melting transitions, nor distinct glass transition temperatures for any of the polymers below their decomposition temperatures. On the contrary, poly( $\alpha$ -cyanoacrylates) do not show any peaks in X-ray scattering, and are all amorphous. They also do not show any recrystallization upon storage.<sup>132</sup> Glass transition temperatures have been determined by DSC, dynamic mechanical analysis (DMA), and dilatometry.<sup>137-139</sup> The results for some poly( $\alpha$ -cyanoacrylates) are shown in Table 2.17.



Table 2.17. Glass Transition Temperatures ( $T_g$ , °C) of Several Poly(Alkyl-Cyanoacrylate)s <sup>137-139</sup>

Alkyl group on the ester	DMA	DSC	Dilatometry
Methyl	96	136	100
Ethyl	116	140	115
Isopropyl	-	-	66
n-butyl	128	-	56
Isobutyl	-	130	51

It is evident that the additional methylene unit in the backbone of the poly(alkyl cyanocyclopropanes) largely affects the ability of these polymers to crystallize. WAXS data provide preliminary evidence that the polymer chains (of poly(**2a-d**)) adopt an all-trans conformation (chapter 6). This means that the theoretical distance between the ester and nitrile substituents on the same side of the backbone increases three-fold. This distribution pattern provides adequate space for the highly polar and larger ester groups to arrange into an ordered lattice, effectively minimizing the unfavorable non-bonded interactions between adjacent substituents on the backbone. On the contrary, for poly(alkyl cyanoacrylate)s, an all-trans backbone is unfavorable due to the close distance between the adjacent substituents. As mentioned before, no evidence of crystallinity has ever been reported for these polymers.

2.3.2.5.3 Solubility. Poly( $\alpha$ -cyanoacrylates) are soluble in a range of solvents at 20 °C.<sup>140</sup> Poly(ethyl and n-butyl cyanoacrylate)s dissolve in THF, dichloromethane, acetone, acetonitrile, and DMF. In comparison, poly(ethyl and butyl cyanocyclopropanecarboxylate)s poly(**2a,c**) are only soluble in highly polar solvents when heated above 100 °C. This decrease in solubility can be associated with the high degree of crystallinity of the polycyclopropanes compared to their amorphous counterparts.

#### 2.3.2.6 Conclusions

The synthesis of highly crystalline poly(alkyl 1-cyanocyclopropanecarboxylates) was achieved using anionic ring-opening polymerization of the corresponding monomers with nucleophilic initiators. Studies on the polymerization of **2a** using thiophenolate salts with various counterions indicated very little difference in the kinetic behavior. However, polymerization with PhSK displayed some characteristics typical of living systems. IR spectroscopy provided evidence for the lack of termination of the poly(**2a**) carbanion under conditions typically observed for anionic polymerizations. The stabilization of the carbanion upon ring-opening is provided by the two geminal electron-withdrawing groups. Attempts to grow a second block of methyl methacrylate from the propagating carbanion of **2d** was unsuccessful, primarily believed to be due to the physical inaccessibility of the monomer to the active chain ends.

This new substitution pattern has a direct influence on the resulting polymer properties, such as improvement in the thermal (by 50-80 °C) and chemical stabilities, and resistance to solvents when compared to their analogues with substituents on every second carbon. The polymers also show very high tendencies to crystallize, in contrast to

their completely amorphous counterparts. It is evident that increasing the distance between neighbouring substituents on the backbone allows the very bulky side groups and highly polar nitrile groups to orient themselves along the chains promoting the high degree of crystallinity observed by WAXS scattering.

### 2.3.3 Ring-Opening Polymerization of 1-Phenyl Cyclopropanecarbonitrile

#### 2.3.3.1 Introduction

In continuation of our study of the anionic ring-opening polymerization of a series of 1,1-disubstituted cyclopropanes, the polymerization of 1-phenyl cyclopropanecarbonitrile **4** under similar conditions is reported in this section. In the previous sections (2.3.1-2.3.2), it was demonstrated that substitution with two strong electron-withdrawing groups on the cyclopropane ring provides sufficient stabilization of the propagating carbanion to favor the ring-opening. No example can be found in the literature of the anionic ring-opening reaction (or polymerization) of cyclopropanes with only one strong electron-withdrawing group. Therefore, an additional (geminally-substituted) group on the ring seems to be essential for the ring-opening (polymerization). During the polymerization of monomer **4**, the anion-stabilizing effect of the phenyl group is mainly via delocalization on the aromatic ring.

#### 2.3.3.2 Experimental

##### Measurements, Materials and Procedures

Refer to Section 2.4.2 for details on the measurements and procedures for the polymerization. 1-Phenyl cyclopropanecarbonitrile **4** was purchased from Aldrich and distilled before use. B.p 133-137 °C/ 30 mm Hg. Anal. Calc. C<sub>10</sub>H<sub>9</sub>N (143.19): C, 83.87; H, 6.35; N, 9.78. Found: C, 83.77; H, 6.44; N, 9.70.



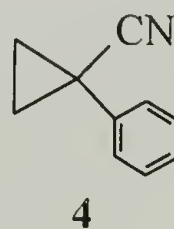
### 2.3.3.3 Results and Discussion

2.3.3.3.1 Anionic Polymerization of **4**. The ring-opening polymerization of phenyl 1-cyclopropanecarbonitrile **4** was achieved using PhSNa (3.8 mol-%) at 60 °C in DMSO (Table 2.18). A black solid precipitate was observed after two hours of polymerization. The final polymer was isolated as a pale yellow powder, and was soluble in nitrobenzene with gentle heating (30 °C), but required high temperatures (>115 °C) to dissolve in polar solvents such as DMF and DMSO. High temperature <sup>1</sup>H- and <sup>13</sup>C-NMR spectroscopy (Figure 2.22-2.23) provided evidence for the expected structure of the ring-opened product. However, attempts to characterize the molecular weight of the polymers using GPC even at high temperature failed due to their poor solubility (in DMF).

Table 2.18. Ring-Opening Polymerization of **4** at 60 °C <sup>a</sup>.

#	Reaction time (h)	Yield <sup>b</sup> (%)
1	3	26
2	27	37

<sup>a</sup> 3.59 mmol of **2e** in 0.3 mL DMSO, 3.8 mol-% PhSNa  
<sup>b</sup> determined by gravimetry



The data provided in Table 2.18 provides evidence that the anionic ring-opening polymerization of **4** occurs at 60 °C, but low yields were obtained even after long reaction times. Figure 2.22 was added to help visualize the trend in the evolution of conversion with time, and has no theoretical meaning. The arrow indicates the theoretical conversion (93%) assuming first-order kinetics. Further calculation assume that the polymerization is living ( $\overline{Xn} = [M]_0/[I]_0$ ), and that the yield after 3 hours is equal to the

conversion. Assuming these conditions, the degree of polymerization  $\overline{X}_n$  is 10, compared to the expected value of 24 (at quantitative conversion). This result indicated that the initiation and/or propagation step are not efficient. Evidence of chain termination resulting from side reactions (formation of a dark precipitate) is possible. Spectral evidence of the final product indicated the ring-opened structure was the only product. It is suggested that probable termination results from the precipitation of the polymer (physical "death") from the reaction mixture. The influence of the phenyl substituent on the ring and the relative reactivity of 1,1-disubstituted cyclopropanes is discussed in following (section 2.3.4).

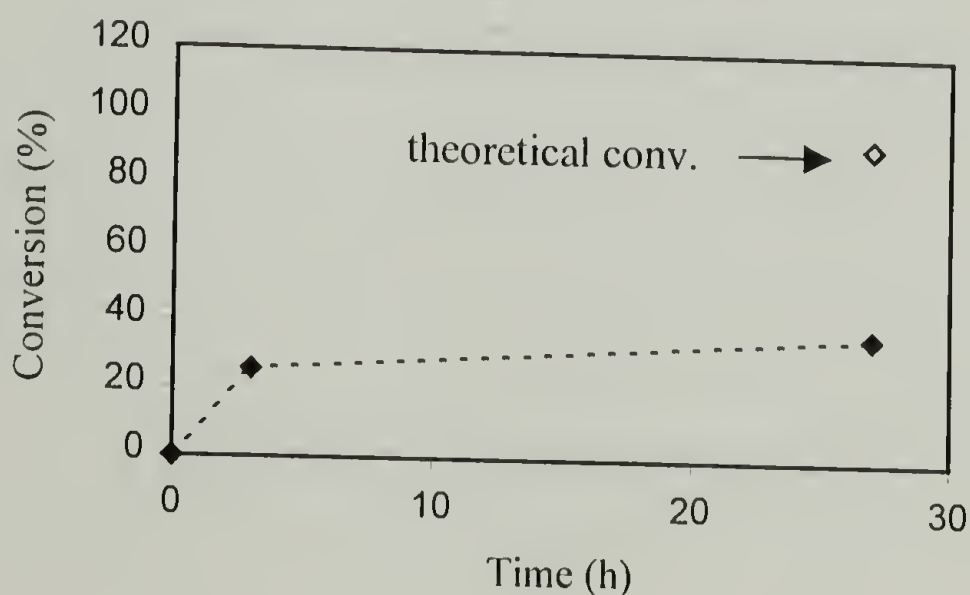


Figure 2.22. Trend in Evolution of Conversion with Time for the Polymerization of **4** [3.59 mmol of **4** in 0.3 mL DMSO, 3.8 mol-% PhSNa, 60 °C]

#### 2.3.3.4 Characterization of Poly(**4**)

2.3.3.4.1. Structural characterization. Poly(**4**) dissolves in highly polar solvents DMF, DMSO with heating above 115 °C, and in nitrobenzene with gentle heating (30 °C). It is insoluble in THF, chlorinated solvents (CH<sub>2</sub>Cl<sub>2</sub>, CH<sub>3</sub>Cl), and aromatics

(benzene, di/trichlorobenzenes). The structure of poly(4) (sample #2, Table 2.18) was confirmed by high temperature  $^1\text{H}$ - and  $^{13}\text{C}$ -NMR spectroscopy in  $(\text{CD}_3)_2\text{SO}$ , 125  $^\circ\text{C}$  (Figure 2.23 and 2.24 respectively). In the  $^1\text{H}$ -NMR spectrum, peaks due to the monomer are masked by signals from the polymer, however the  $^{13}\text{C}$ -NMR spectrum confirms the absence of the carbon peaks of the cyclopropane ring. Attempts to analyze the microstructure of the resulting polymer by  $^1\text{H}$ -NMR were unsuccessful due to the poor resolution observed for ethylene protons of the backbone. The IR spectrum of poly(4) provided evidence for the disappearance of the peak at  $1190\text{ cm}^{-1}$  due to C-C ring-stretching and the peaks are consistent with the ring opened structure.

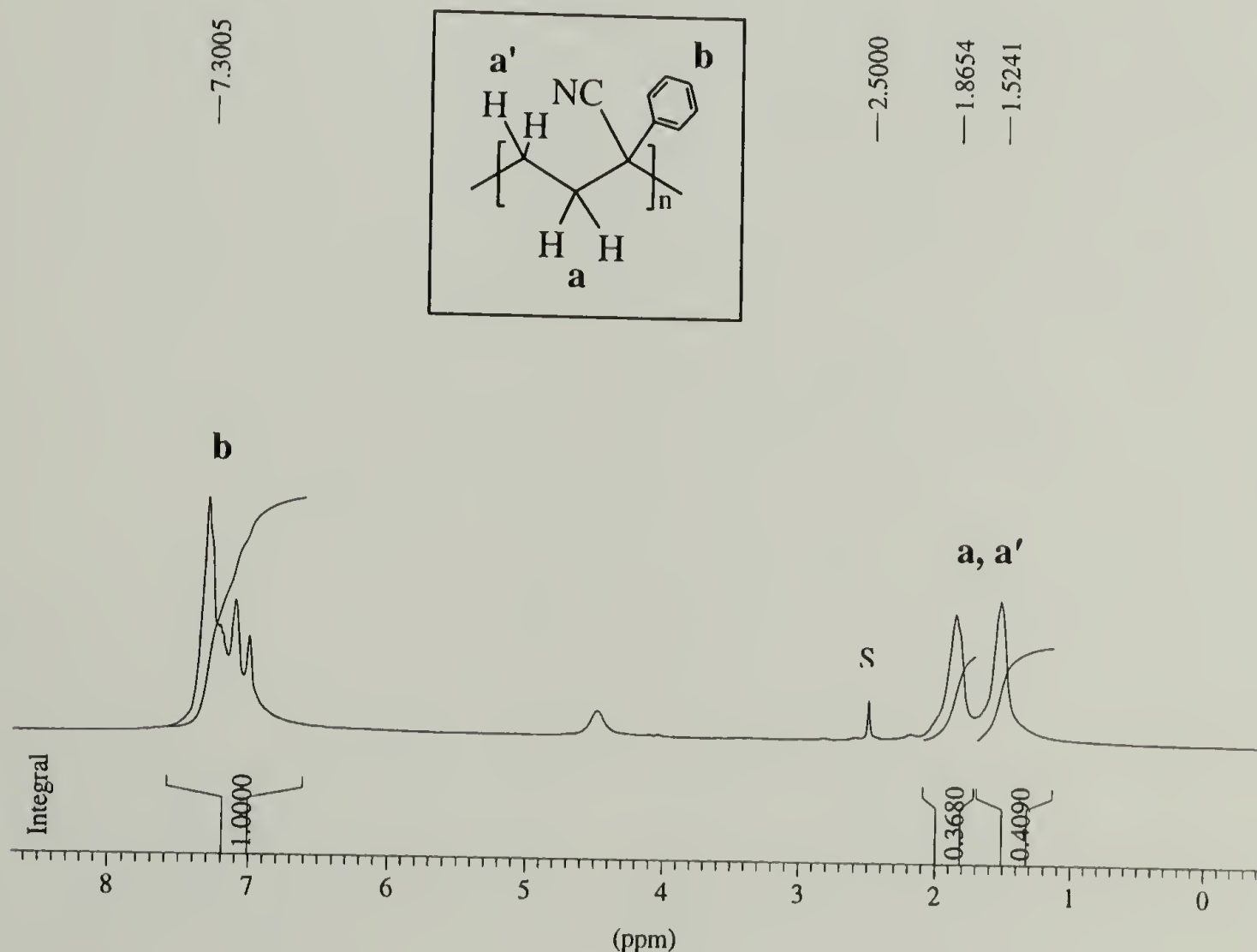


Figure 2.23.  $^1\text{H}$ -NMR Spectrum of Poly(4) in  $\text{d}_6$ -DMSO at 125  $^\circ\text{C}$   
(S = solvent peak)

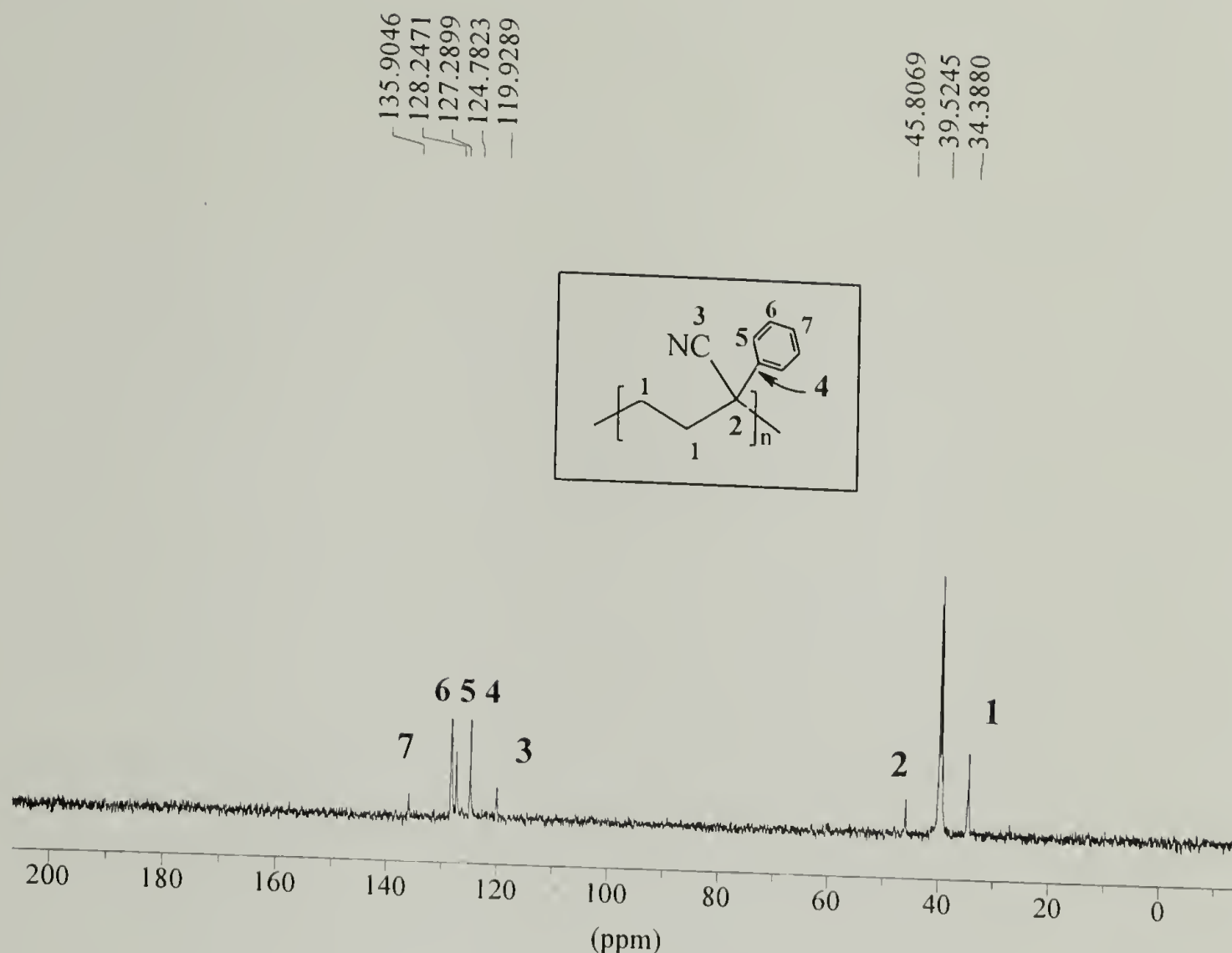


Figure 2.24.  $^{13}\text{C}$ -NMR Spectrum of Poly(4) in  $\text{d}_6$ -DMSO at 125 °C.

2.3.3.4.2 Molecular weight determination. Analysis of the  $\overline{Mn}$  was attempted by GPC, but the polymers were insoluble under the experimental conditions even at higher temperatures. Endgroup analysis via  $^1\text{H}$ -NMR spectroscopy was limited since the polymer peaks due to the phenyl ring mask the endgroup (PhS-). The peak due to the H- at the other chain end was not observed at the expected chemical shift.

2.3.3.4.3 Thermal Analysis. TGA analysis indicated that the onset of decomposition occurred at 200 °C (Figure 2.25), probably via the initial loss of HCN. The polymer is much less stable than the dicyano-substituted poly(1) which starts to



decompose at 350 °C. Poly(**2a-d**) (cyano-ester-substituted) start to decompose at similar temperatures (210 °C) compared to Poly(**4**).

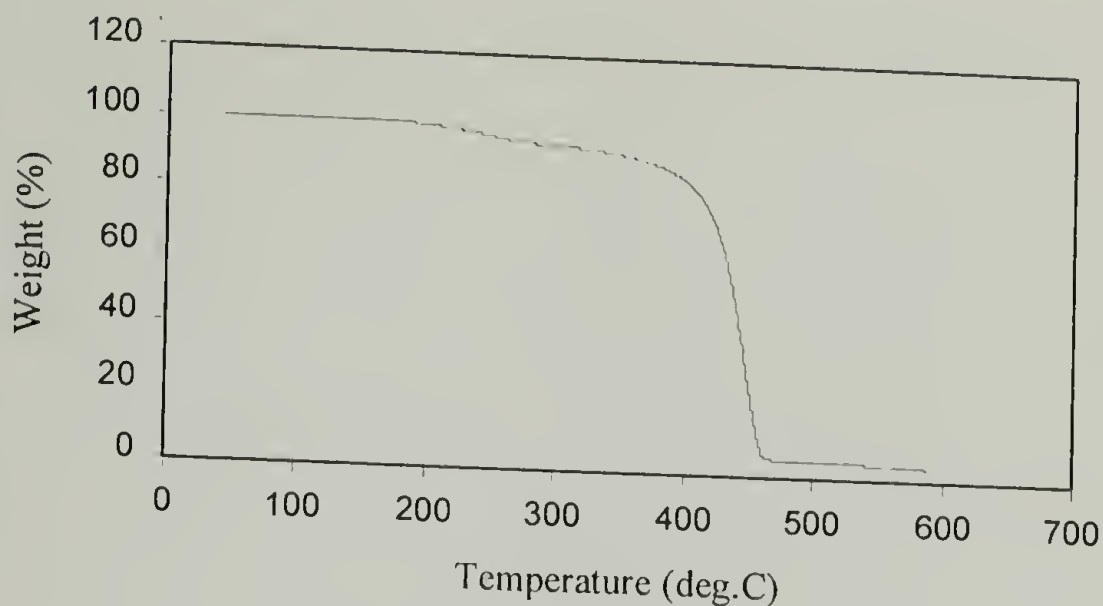


Figure 2.25. TGA Spectrum of Poly(**4**)

2.3.3.4.4 Crystallinity. WAXS data of a powder sample of poly(**4**) provided evidence that the polymer is semi-crystalline (Figure 2.26). Further analysis and comparisons of the crystalline structure with the other poly(trimethylene)s is provided in chapter 6.

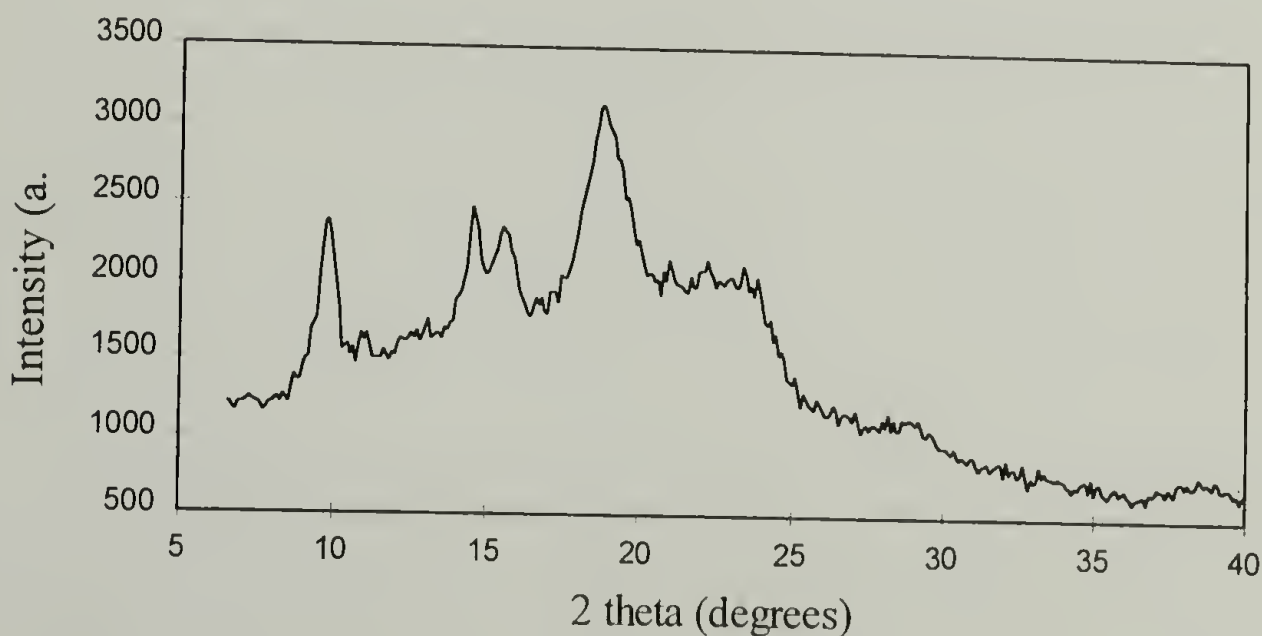


Figure 2.26. WAXS pattern of Poly(**4**)

#### 2.3.3.5 Conclusions

This study demonstrated that the anionic ring-opening polymerization of 1-phenyl cyanocyclopropane **4** can be initiated with sodium thiophenolate (3.8 mol-%) at 60 °C. Since no examples of the anionic polymerization of monosubstituted cyclopropanes (such as 1-cyanocyclopropane) have been reported, it is evident that the phenyl substituent on the ring provides the necessary additional stabilization to the carbanion generated upon ring-opening. However, low yields obtained after long reaction times indicated that the reaction is less efficient than observed for the 1,1-disubstituted cyclopropane monomers with dinitrile **1**, nitrile/ester **2**, or diester **3** groups, possibly due to chain termination resulting from precipitation of the chains from the reaction mixture. The resulting polymer structure poly(**4**) is thermally stable up to 200 °C, and the polymer is semi-crystalline.

### 2.3.4 Influence of substituents on the reactivity of 1,1-disubstituted cyclopropanes.

#### 2.3.4.1 Introduction

Based on thermodynamic and kinetic considerations (previously discussed in section 2.2), it is evident that the efficient anionic ring-opening polymerization of cyclopropanes can only be achieved if a highly stabilized carbanion is generated upon ring-opening. Several examples of the ring-opening polymerization of 1,1-disubstituted cyclopropanes under anionic conditions were presented in sections 2.3.2-2.3.4,<sup>141,142</sup> and others have been reported in the literature.<sup>84,85,87,141,142</sup> In this section, the influence of the ring-substituents on the anionic polymerization was investigated by comparing the reactivity of 1,1-dicyanocyclopropane **1**, ethyl 1-cyanocyclopropanecarboxylate **2a**, diethyl cyclopropane-1,1-dicarboxylate **3b**, and phenyl cyclopropanecarbonitrile **4** under similar conditions. It is believed that the reactivity of these monomers is related to the stabilizing effects of the propagating carbanion by the substituents on the ring, which were evaluated using the pK<sub>a</sub> values of the corresponding C-H acids.

#### 2.3.4.2 Results and Discussion

Previous work on the anionic ring-opening polymerization of **3b** provided evidence that the polymerization can be achieved using sodium thiophenolate (PhSNa, 4.5 mol-%, **3b**/DMSO (5/2: v/v)) at 80 °C, but after a long induction period of 30 hours.<sup>84</sup> For decently rapid polymerization, heating at or above 140 °C is generally required. However, quantitative conversions were limited due to chain termination resulting from precipitation of the polymer. No polymerization was observed below 80 °C. In contrast, the increased reactivity of **1** (over the diethyl-ester monomer **3b**) is evident in its ability

to polymerize at temperatures well below 80 °C. The dinitrile monomer **1** polymerizes moderately at 30 °C, and rapidly at 60 °C in the presence of PhSNa initiator. Quantitative conversions were achieved at 60 °C (3.8 mol-% PhSNa) in under 20 minutes. The experiments detailed in Table 2.4 provided further evidence of the high reactivity of **1**, which polymerizes in the presence of weak nucleophiles (such as triethylamine) at 60 °C.

Due to the insolubility of poly(**1**), a more complete study of the polymerization kinetics of **1** was limited, and a general comparison of its reactivity with the other monomers (**2a**, **3b**, and **4**) could only be made based on polymer yields. In this comparison, some assumptions are made. First, that the initiation is quantitative in all cases (no side reactions). Second, the initiation step is much faster than propagation step and therefore, the rate of polymerization depends only on the propagation reaction. While **3b** does not react appreciably below 80 °C, **1**, **2a**, and **4** readily polymerize at this temperature (3.8 mol-% PhSNa, 3.59 mmol monomer in 0.3 mL DMSO). Ethyl 1-cyanocyclopropane **2a** polymerizes fairly rapidly under these conditions, reaching quantitative conversion in less than three hours. The nitrile-phenyl monomer **4** is much less reactive than **2a**, achieving low conversions (<40%) even after long reaction times (24 h). Based on this polymerization data, the order of reactivity from the most reactive monomer is **1** > **2a** > **4** > **3b**. A summary of the polymerization data of **1**, **2a** and **4** is shown in Figure 2.27.



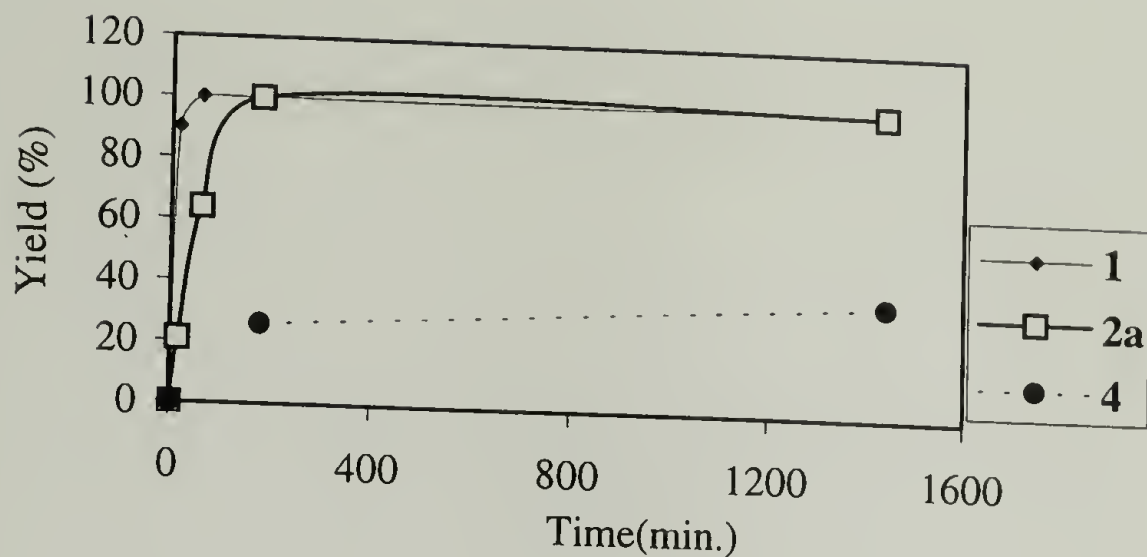


Figure 2.27. Comparison of Reactivity of Cyclopropane Monomers **1**, **2a**, **4** (3.8 mol-% PhSNa, 3.59 mmol in 0.3 mL DMSO at 60 °C, yields determined by gravimetry. Note: Monomer **3b** does not react under these conditions).

At the onset of this project, the expected order of reactivity for the 1,1-disubstituted cyclopropanes was rationalized based on the ability of the substituents to stabilize the carbanion upon ring-opening, in analogy to the ring-opening polymerization of oxirane or thiirane. The less electronegative carbon of the cyclopropyl ring is transformed into an acceptable nucleofuge and a stable propagating end-group by activation with two electron-withdrawing substituents. Despite the similar ring strain energies of oxirane (114 kJ/mol) and unsubstituted cyclopropanes (115 kJ/mol), the latter do not polymerize due to the absence of polarization in the potentially cleavable bonds. On the contrary, oxirane is highly reactive, undergoing ring-opening polymerization by sodium hydroxide at ambient temperature.<sup>143,144</sup>

The stabilization of the propagating anion of the heterocycles (oxirane and thiirane) was quantified using the  $pK_a$  scale as a measure of anion stability. The  $pK_a$  values of the aliphatic alcoholates or thiolates are  $(CH_3O-H) = 29.0$  (in DMSO) or 15.5 (in  $H_2O$ ), and  $(RS-H) = 17.0$  (in DMSO for  $R = (CH_2)_4$ ) or 10-11 in  $H_2O$ ). From these

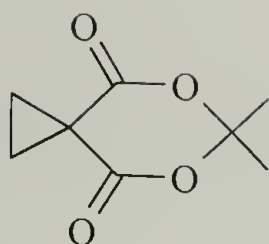
values, it was evident that the carbanion must be stabilized by at least two electron-withdrawing groups in order to match the stabilities of aliphatic alcoholates or thiolates. The  $pK_a$  values in DMSO at 25 °C of the equivalent CH-acids are  $((NC)_2CH-H) = 11.0$ ,  $((CN,COOEt)CH-H) = 13.1$ ,  $((EtOOC)_2CH-H) = 16.4$  and  $((NC,C_6H_5)CH-H) = 22.0$ .<sup>129</sup> Following this basic reasoning, the greatest stabilization of the carbanion would be provided by the CH-acid with lowest  $pK_a$  value. The stabilization effects of the substituents on the transition state determine the polymerizability of the cyclic monomers via ring-opening. In this case, the predicted order of reactivity towards anionic ring-opening from the most reactive monomer would be **1** > **2a** > **3b** > **4**. The polymerization results indicate that this reasoning is partly correct. Monomer **1** is much more reactive than the nitrile-ester **2a** or diester monomers **3b**. However, **4** displayed intermediate reactivity between **2a** and **3b**, and is not the least reactive as predicted.

The acidifying effect of the phenyl group in carbon acids has been well studied.<sup>145</sup> For example, by replacing one of the hydrogen atoms in  $CH_3CN$  by a phenyl group,  $(C_6H_5,CN)CH-H$ , the  $pK_a$  of the C-H acid decreases from 31.3 to 21.9 in DMSO at 25 °C. It was demonstrated that the phenyl group has a relatively small polar effect, and the large acidifying effect is primarily due to the stabilization of the charge via delocalization. The ratio of the resonance to polar contribution for the anion-stabilizing effect of the phenyl group is much larger than for any of the strong electron-withdrawing groups. This acidifying effect is attenuated by steric factors, since steric crowding will prevent the overlap between the p orbital of the carbanion and the  $\pi$  system of the phenyl group. Based on the  $pK_a$  scale as a measure for the stability (and thus reactivity) of the cyclopropane monomers, it is evident that other factor(s) play a role in the enhancement

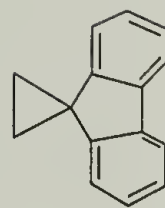
of the polymerization of **4**. Substituents on the ring can have dramatic effects on the geometries and stabilities of strained organic molecules.<sup>146</sup> The geometry of several cyclopropane rings with electron-acceptor and electron-donor substituents have been analyzed using molecular orbital calculations and the results obtained are consistent with structural data provided from X-ray crystallography.<sup>147</sup> From these studies, it was determined that electron-withdrawing substituents (such as nitrile and ester groups) shorten the distal ring-bond relative to the individual mean C-C (ring) distance. The effect of phenyl substituents is complex, since they appear to both accept and donate electron density to the ring. However, a mean distal bond shortening similar to nitrile substituents was obtained. We believe that the unexpected increase in reactivity of **4** may be attributed the increased destabilization of the ring due to steric interactions and donation of electron density from the phenyl to the cyclopropane orbitals.

The ring-opening polymerization of other 1,1-disubstituted cyclopropanes such as cyclo-isopropylidenecyclopropane-1,1-dicarboxylate **xii**<sup>148</sup> and spiro[cyclopropane-1,9'-fluorene] **xiii**<sup>149</sup> have also been reported (Figure 2.28). The **xii** monomer polymerizes at room temperature ( $I = \text{PhSNa}$ ,  $[M]_0/[I]_0 = 5.4/1$ , 0.5 mL DMSO) yielding a polymer precipitate after 2.5 hours. The increased reactivity of this monomer in comparison to the diester monomer **3b** was not unexpected considering the pKa of Meldrum's acid (the equivalent C-H acid) is 7.3 vs. 16.4 for diethyl malonate (in DMSO).<sup>129</sup>





**xii**



**xiii**

Figure 2.28. Structures of cyclo-isopropylidenecyclopropane-1,1-dicarboxylate **xii** and spiro[cyclopropane-1,9'-fluorene] **xiii**

The ring-opening polymerization of the cyclopropane monomer **xiii** was also achieved using fluorenyllithium at temperatures higher than 100 °C. The poor solubility of the resulting polymer limited the molecular weight due to chain termination resulting from precipitation. In this example, the pKa of the fluorenyl group (22.6) is close to (C<sub>6</sub>H<sub>5</sub>,CN)CH-H (21.9) (in DMSO at 25 °C).<sup>129</sup> In this case, it is suspected that the constrained geometry of the fluorenyl- cyclopropane ring also plays an important role in the polymerizability of the monomer.

The anionic ring-opening polymerization of several 1,1-disubstituted 2-vinyl cyclopropanes (1.2 mol-%NaCN, 0.11g M/mL DMF, 7 °C) have also been reported.<sup>82</sup> Under these conditions, 1,1-dicyano-2-vinylcyclopropane (**xiv**) and ethyl 1-cyano-2-vinylcyclopropane carboxylate (**xv**) polymerize very slowly, reaching quantitative conversion after several days. Diethyl 2-vinyl-cyclopropane-1,1-dicarboxylate (**xvi**) and 1,1-diphenyl-2-vinylcyclopropane (**xvii**) fail to give any detectable yield of polymers.



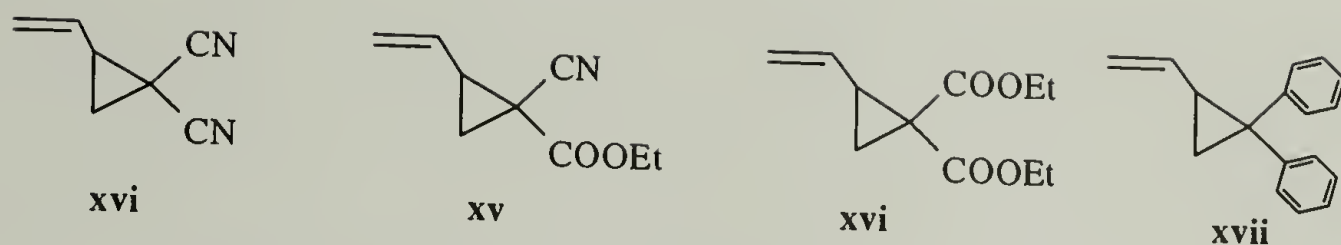


Figure 2.29. Structures of 2-Vinyl-1,1-Disubstituted Monomers

The lack of polymerizability of **xvi** and **xvii** was attributed to the insufficient stabilization of the propagating anion by the diphenyl and diester groups. However, recent work in our group showed that the anionic ring-opening polymerization of dialkyl cyclopropane-1,1-dicarboxylates can be achieved using stronger thiophenolate initiators (PhSNa(K)) at 130 °C. These results demonstrated that even without the contribution from the electron-donating vinyl substituent, the diester groups provide sufficient stabilization of the propagating anion, as predicted by the pKa scale as a measure of carbanion stabilization.<sup>84,85,87</sup> In the case of the gem-diphenyl monomer **xvii**, it was also suggested that its polymerizability was limited by steric hindrance of the two phenyl rings attached to the propagating carbanion. The poor polymerizability of this monomer can be predicted in accordance with the pKa value of (Ph<sub>2</sub>CH<sub>2</sub>) = 32.2 (in DMSO at 25 °C) as a measure of the carbanion stability upon ring-opening. It is apparent that the stabilization provided by the substituents is an order of magnitude less favorable than for **4**.

#### 2.3.4.3 Conclusions

In this study, the effect of the substituents on the cyclopropane ring on its reactivity towards anionic ring-opening polymerization was studied. It was determined that gem-substitution with electron-withdrawing groups is essential for the efficient ring-opening of these monomers. Thus, we can conclude that the poor tendency of

unsubstituted cyclopropanes to polymerize can be tremendously improved by placing substituents on the ring stabilize the carbanion upon ring-opening. The predicted order of reactivity of several 1,1-disubstituted cyclopropanes (**1**, **2a**, **3b**, **4**) was based on the pKa scale as a measure of carbanion stability. This crude reasoning proved to explain the general order of reactivity of gem-dinitrile **1**, nitrile-ester **2a** and gem-diester **3b** monomer, but proved unsuitable for the phenyl-nitrile **4**. In this case, it is proposed that the phenyl substituent provides additional destabilization to the ring due steric interactions; however, its effect on the constrained geometry of the ring (in relation to the nitrile substituent) needs to be further examined.

## 2.4 References

- (1) Kennedy, J. P.; Thomas, R. M. *Makromol. Chem.* **1962**, 53, 28.
- (2) Plesch, P. H. In *The Chemistry of Cationic Polymerization*; McMillan: New York, 1963; p 233.
- (3) Kennedy, J. P.; Minckler, L. S.; Wanless, G.; Thomas, R. M. *J. Polym. Sci.* **1964**, A2, 2093.
- (4) Coulson, C. A.; Moffit, W. E. *J. Chem. Phys.* **1947**, 15, 151.
- (5) Walsh, A. D. *Trans. Faraday Soc.* **1949**, 45, 179.
- (6) Weigert, R. *J. Am. Chem. Soc.* **1967**, 89, 5962.
- (7) Foote, C. S. *Tetrahedron Lett.* **1963**, 579.
- (8) Flygare, W. H. *Science* **1963**, 140, 1179.
- (9) Peters, D. *Tetrahedron* **1963**, 19, 1539.
- (10) Jones, W. J.; Stoicheff, B. P. *Can. J. Phys.* **1960**, 42, 2259.
- (11) Bastiansen, O.; Fritsch, F. N.; Hedberg, K. *Acta Crystallogr.* **1964**, 17, 538.

- (12) Wong, H. N. C.; Hon, M.; Tse, C.; Yip, Y. *Chem. Rev.* **1989**, 89, 165.
- (13) Kubisa, P. In *Cationic Polymerizations: Mechanisms, Synthesis and Applications*; Matyjaszewski, K., Ed.; Marcel Dekker: New York, 1996; pp 437-553.
- (14) Cox, J. D. *Tetrahedron* **1963**, 19, 1175.
- (15) Coffey, S. E. In *Rodd's Chemistry of Carbon Compounds*; Elsevier Scientific: Amsterdam, 1973; Vol. IV, p 2.
- (16) Kharasch, M. S.; Fineman, M.; Mayo, F. *J. Am. Chem. Soc.* **1939**, 61, 2139.
- (17) Shea, K. J.; Skell, P. S. *J. Am. Chem. Soc.* **1973**, 95, 6728.
- (18) Upton, C. J.; Incremona, J. H. *J. Org. Chem.* **1976**, 41, 523.
- (19) Maynes, G. C.; Applequist, D. E. *J. Am. Chem. Soc.* **1973**, 95, 856.
- (20) LaLonde, R. T.; Ferrara, P. B.; Debboli, A. D. *J. Org. Chem.* **1972**, 37, 1094.
- (21) Kuivila, H. G.; Cagwood, S. C.; Bayer, W. F.; Langrain, F. L. *J. Am. Chem. Soc.* **1955**, 77, 5175.
- (22) Walling, C.; Fredricks, P. S. *J. Am. Chem. Soc.* **1962**, 84, 3326.
- (23) Grob, C. A. *Angew. Chem., Int. Ed. Engl.* **1969**, 8, 535.
- (24) Grob, C. A.; Schiess, P. W. *Angew. Chem. Int. Ed. Engl.* **1967**, 6, 1.
- (25) Breslow, R. In *Molecular Rearrangements*; de Mayo, P., Ed.; Interscience: New York, 1963; p 233.
- (26) DePuy, C. H. *Top. Curr. Chem.* **1973**, 40, 73.
- (27) Kramer, G. M. *J. Am. Chem. Soc.* **1970**, 92, 4344.
- (28) Bone, W. A.; Perkin, W. H. *J. Chem. Soc.* **1895**, 67, 108.
- (29) Danishefsky, S. *Acc. Chem Res.* **1979**, 12, 66.
- (30) Stewart, J. M.; Westberg, H. H. *J. Org. Chem.* **1965**, 30, 1951.
- (31) Kohler, E. P.; Conant, J. B. *J. Am. Chem. Soc.* **1917**, 39, 1404.
- (32) Truce, W. E.; Lindy, L. B. *J. Org. Chem.* **1961**, 26, 1463.

- (33) Kierstead, R. W.; Linstead, R. P.; Weedon, B. C. L. *J. Chem. Soc.* **1952**, 3616.
- (34) Trost, B. M.; Cossy, J.; Burks, J. *J. Am. Chem. Soc.* **1983**, *105*, 1052.
- (35) Graziano, M. L.; Iesce, M. R. *Synthesis* **1985**, 1985, 762.
- (36) Danishefsky, S.; Rovnyak, G. *J. Chem. Soc., Chem. Commun.* **1972**, 820.
- (37) Danishefsky, S.; Rovnyak, G. *J. Org. Chem* **1975**, *40*, 114.
- (38) Neureiter, N. P. *J. Org. Chem.* **1959**, *24*, 2044.
- (39) Vogel, E. *Angew. Chem.* **1960**, *72*, 4.
- (40) Overberger, C. G.; Borchert, A. E. *J. Am. Chem. Soc.* **1960**, *82*, 1007, 4896.
- (41) Flowers, M. C.; Frey, H. M. *J. Chem. Soc.* **1961**, 3547.
- (42) Frey, H. M. *Adv. Phys. Org. Chem.* **1966**, *4*, 147.
- (43) Frey, H. M.; Walsh, R. *Chem. Rev.* **1969**, *69*, 103.
- (44) Stewart, J. M.; Pagenkopf, G. K. *J. Org. Chem.* **1969**, *34*, 7.
- (45) Eastham, A. M.; Darwent, B.; de B. and Beaubien, P. E. *Can. J. Chem.* **1951**, *29*, 575.
- (46) Virtanen, P. O.; Korhonen, R. *Acta Chem. Scand.* **1973**, *27*, 2650.
- (47) Dainton, F. S.; Ivin, K. J. *Quart. Rev. Chem. Soc.* **1958**, *12*, 61.
- (48) Ivin, K. J.; Busfield, W. K. In *Encyclopedia of Polymer Science and Technology*; Wiley: London, 19; Vol. 12, pp 555-605.
- (49) Ivin, K. J.; Saegusa, T. In *Ring-Opening Polymerization*; Ivin, K. J., Saegusa, T., Eds.; Elsevier Applied Science Publishers: New York, 1984; Vol. 1, pp 1-3.
- (50) Jessup, J. *J. Chem. Phys.* **1948**, *16*, 661.
- (51) Dainton, F. S.; Devlin, T. R. L.; Small, P. A. *Trans. Faraday Soc.* **1955**, *51*, 1710.
- (52) Hall, H. K. J.; Snow, L. G. In *Ring-Opening Polymerization*; Ivin, K. J., Saegusa, T., Eds.; Elsevier Applied Science Publishers: New York, 1984; Vol. 1, p 83.



- (53) Sawada, H. In *Thermodynamics of Polymerization*; Sawada, H., Ed.; Marcel Dekker: New York, 1976.
- (54) Tipper, C. F. H.; Walker, D. A. *J. Chem. Soc.* **1959**, 1352.
- (55) Pines, H.; Huntsman, W. D.; Ipatieff, V. N. *J. Am. Chem. Soc.* **1953**, 75, 2315.
- (56) Aoki, S.; Harita, Y.; Otsu, T.; Imoto, M. *Bull. Chem. Soc. Jpn.* **1966**, 39, 889.
- (57) Ketley, A. D. *J. Polym. Sci., Polym. Lett. Ed.* **1963**, 1, 313.
- (58) Naegele, W.; Haubenstock, H. *Tetrahedron Lett.* **1965**, 4283.
- (59) Worsfold, D. V.; Eastham, A. M. *J. Am. Chem. Soc.* **1957**, 79, 900.
- (60) Kobayashi, S.; Morikawa, K.; Saegusa, T. *Polym. J.* **1979**, 11, 405.
- (61) Olah, G. H. *Top. Curr. Chem.* **1979**, 80, 19.
- (62) Kirmse, W. *Top. Curr. Chem.* **1979**, 80, 125.
- (63) Takahashi, T. *J. Polym. Sci., Part A: Polym. Chem.* **1968**, 6, 403.
- (64) Takahashi, T.; Yamashita, I. *J. Polym. Sci., Part B: Polym. Lett.* **1965**, 3, 251.
- (65) Takahashi, T.; Yamashita, I.; Miyakawa, T. *Bull. Chem. Soc. Jpn.* **1964**, 37, 131.
- (66) Kennedy, J. P.; Elliott, J. J.; Butler, P. E. *J. Macromol. Sci.* **1968**, A2, 1415.
- (67) Ketley, A. D.; Berlin, A. J.; Fisher, L. P. *J. Polym. Sci., Part A: Polym. Chem.* **1967**, 5, 227.
- (68) Takahashi, T. *J. Polym. Sci., Part A: Polym. Chem.* **1968**, 6, 3327.
- (69) Pinazzi, C.; Pleurdeau, A.; Brosse, J. C. *C. R. Acad. Sci. Paris* **1968**, 266, 1032.
- (70) Ketley, A. D.; Ehrig, R. S. *J. Polym. Sci. Part A: Polym. Chem.* **1964**, 2, 4461.
- (71) Pinazzi, C.; Brosse, J. C.; Brossas, J.; Pleurdeau, A. *C. R. Acad. Sci. Paris* **1968**, 266, 443.
- (72) Pinazzi, C. B., J. C.; Brossas, J.; Pleurdeau, A. *C. R. Acad. Sci. Paris* **1970**, 270, 1650.
- (73) Pinazzi, C.; Brossas, J.; Brosse, J. C.; Pleurdeau, A. *Makromol. Chem.* **1971**, 144, 155.

- (74) Pinazzi, C.; Brosse, J. C.; Pleurdeau, A. *Makromol. Chem.* **1971**, *142*, 273.
- (75) Overberger, C. G.; Halek, G. W. *J. Polym. Sci. A-1* **1970**, *8*, 359.
- (76) Overberger, C. G.; Bochart, A. E.; Katchman, A. *J. Polym. Sci.* **1960**, *44*, 491.
- (77) Harris, L.; Ashdown, A. A.; Armstrong, R. T. *J. Am. Chem. Soc.* **1936**, *75*, 2315.
- (78) Ivin, K. J. *J. Chem. Soc.* **1959**, 1352.
- (79) Lishanskii, I. S.; Zak, A. G.; Fedorova, E. F.; Khachaturov, A. S. *Vysokomol. Soedin* **1965**, *7*, 966. Translated into English in *Polym. Sci. USSR*, **1965**, *1967*, 1066.
- (80) Lishanskii, I. S.; Zak, A. G.; Zhrebetskaya, Y.; Khachaturov, A. S. *Polym. Sci. USSR* **1967**, *A9*, 2138.
- (81) Cho, I.; Ahn, K.-D. *J. Polym. Sci., Part A: Polym. Chem.* **1979**, *17*, 3169.
- (82) Cho, I.; Ahn, K.-D. *J. Polym. Sci., Part A: Polym. Chem.* **1979**, *17*, 3183.
- (83) Cho, I.; Kim, J.-B. *J. Polym. Sci., Part A: Polym. Chem.* **1980**, *18*, 3053.
- (84) Penelle, J.; Herion, H.; Xie, T.; Gorissen, P. *Macromol. Chem. Phys.* **1998**, *199*, 1329.
- (85) Penelle, J.; Herion, H.; Soree, A.; Gorissen, P. *Polym. Prepr. (Am. Chem. Soc., Div. Polym. Chem.)* **1996**, *37 (1)*, 208.
- (86) Penelle, J.; Clarebout, G.; Balikdjian, I. *Polym. Bull. (Berlin)* **1994**, *32*, 395.
- (87) Penelle, J.; Xie, T. *Macromolecules* **2000**, *33*, 4667.
- (88) Penelle, J.; Xie, T., accepted for publication in *Macromolecules*.
- (89) Penelle, J. *Advanced Catalysis: New Polymer Syntheses and Modifications*, ACS Symposium Series; American Chemical Society: Washington, 2000.
- (90) Gilbert, H.; Miller, F. F.; Averill, S. J.; Schmidt, R. F.; Stewart, F. D.; Trumbull, H. L. *J. Am. Chem. Soc.* **1954**, *76*, 1074.
- (91) Kawai, H. In *Japan J. Appl. Phys.*, 1969; Vol. 8, pp 975-976.
- (92) Miyata, S.; Yoshikawa, M.; Tasaka, S.; Ko, M. *Polym. J.* **1980**, *12*, 857.

- (93) Danz, R.; Buechtemann, A.; Latour, M. *Mol. Cryst. Liq. Cryst. Sci. Technol., Sect. A* **1993**, 229, 181.
- (94) Davis, G. T.; McKinney, J. E.; Broadhurst, M. G.; Roth, S. C. *J. Appl. Phys.* **1978**, 51, 5095.
- (95) Sung Jo, Y.; Inoue, Y.; Chujo, R.; Saito, K.; Miyata, S. *Macromolecules* **1985**, 18, 1850.
- (96) Tasaka, S. A., K. M.; Yoshikawa, M.; Miyata, S.; Ko, M. *Ferroelectrics* **1984**, 57, 267.
- (97) Inoue, Y.; Kashiwazaki, A.; Maruyama, Y.; Jo, Y. S.; Chujo, R.; Kishimoto, M.; Seo, I. *Polymer* **1988**, 29, 144.
- (98) Maruyama, Y.; Jo, Y. S.; Inoue, Y.; Chujo, R.; Tasaka, S.; Miyata, S. *Polymer* **1987**, 28, 1087.
- (99) Inoue, Y.; Jo, Y. S.; Kashiwazaki, A.; Maruyama, Y.; Chujo, R.; Kishimoto, M.; Seo, I. *Polym. Commun.* **1988**, 29, 105.
- (100) Tasaka, S.; Inagaki, N.; Okutani, T.; Miyata, S. *Polymer* **1989**, 30, 1639.
- (101) Furukawa, T.; Date, M.; Nakajima, K.; Kosaka, T.; Seo, I. *Jpn. J. Appl. Phys.* **1986**, 25, 1178.
- (102) Furukawa, T.; Tada, M.; Nakajima, K.; Seo, I. *Jpn. J. Appl. Phys.* **1988**, 27, 200.
- (103) Jo, Y. S.; Maruyama, Y.; Inoue, Y.; Chujo, R.; Tasaka, S.; Miyata, S. *Polym. J.* **1987**, 19, 769.
- (104) Inoue, Y.; Maruyama, Y.; Sakurai, M.; Chujo, R. *Polymer* **1990**, 31, 850.
- (105) Sakurai, M.; Ohta, Y.; Inoue, Y.; Chujo, R. *Polym. Commun.* **1991**, 32, 397.
- (106) Inoue, Y.; Maruyama, Y.; Kawaguchi, K.; Ohta, Y.; Sakurai, M.; Jo, Y. S.; Chujo, R. *Polymer* **1991**, 32, 2958.
- (107) Inoue, Y.; Ohta, Y.; Sakurai, M.; Chujo, R.; Seo, I.; Kishimoto, M. *Polymer* **1994**, 35, 718.
- (108) Diez-Barra, E.; de la Hoz, A.; Moreno, A.; Sanchez-Verdu, P. *J. Chem. Soc., Perkin Trans. I* **1991**, 1, 2593.
- (109) Zefirov, N. S. K., T. S.; Kozhushkov, S. I.; Surmina, L. S.; Rashchupkina, Z. A. *Zh. Org. Khim. (Engl. Transl.)* **1983**, 19, 474.



- (110) Schmidt, R. F.; U.S. Patent 2,594,353 (April 29, 1952).
- (111) Ardis, A. E.; U.S. Patent 2,574,369 (November 6, 1951)
- (112) Swain, G. C.; Scott, C. B. *J. Am. Chem. Soc.* **1953**, 75, 141.
- (113) Wells, P. R. *Chem. Rev.* **1963**, 63, 171.
- (114) Ibne-Rasa, K. M. *J. Chem. Edu.* **1967**, 44, 89.
- (115) Ritchie, C. D. *Pure Appl. Chem.* **1978**, 50, 1281.
- (116) Hoz, S.; Speizman, D. *J. Org. Chem.* **1983**, 48, 2904.
- (117) Young, R. J.; Lovell, P. In *Introduction to Polymers*; Chapman & Hall: New York, 1991; p 251.
- (118) Besten, R. H., S.; Brandsma, L. *J. Org. Metallic Chem.* **1990**, 385, 153.
- (119) Harrelson, J. A., Ph.D. Dissertation, Duke University, 1986.
- (120) Arnett, E. M.; Maroldo, S. G.; Schilling, S. L.; Harrelson, J. A. *J. Am. Chem. Soc.* **1984**, 106, 6759.
- (121) Arnett, E. M.; Harrelson, J. A. *Gazz. Chim. Ital.* **1987**, 117, 237.
- (122) Brandsma, L.; Verkruijsse, H. *Preparative Polar Organometallic Chemistry*; Springer: Berlin, 1987 and 1990; Vol. 1 and Vol. 2.
- (123) Amstutz, R.; Dunitz, J.; Laube, T.; Schweizer, W. B.; Seebach, D. *Chem. Ber.* **1986**, 119, 434.
- (124) Boche, G. *Angew. Chem. Int. Ed. Engl.* **1989**, 28, 277.
- (125) Setzer, W.; Schleyer, P. v. R. *Adv. Organomet. Chem.* **1985**, 24, 353.
- (126) Reetz, M. T.; Hutte, S.; Goddard, R. *J. Am. Chem. Soc.* **1993**, 11, 9339.
- (127) Pepper, D. C. *J. Polym. Sci., Polym. Sym.* **1978**, 62, 65.
- (128) Pepper, D. C. *Polymer J.* **1980**, 12, 629.
- (129) Bordwell, F. G. *Acc. Chem. Res.* **1988**, 21, 456.
- (130) Raj, D. J. A.; Wadgaonkar, P. P.; Saviram, S. *Macromolecules* **1992**, 25, 2774.



- (131) Reetz, M. T.; Knauf, T.; Minet, U.; Bingel, C. *Angew. Chem. Int. Ed. Eng.* **1988**, *27*, 1373.
- (132) Woods, J. In *Polymeric Materials Encyclopedia*; Salamone, J. C., Ed.; CRC Press: N.Y, 1996; Vol. 2, p 1632.
- (133) Coover, H. W.; Dreifus, D. W.; O'Conner, J. T. In *Handbook of Adhesives, 3rd Ed.*; Skeist, I., Ed.; Van Nostrand Reinhold: NY, 1990; p 463.
- (134) Pepper, D. C.; Ryan, B. *Makromol. Chem.* **1983**, *184*, 383.
- (135) Coover, H. W.; McIntire, J. M. In *Encyclopedia of Polymer Science and Engineering*; Mark, H., Bikales, N. M., Overberger, C. G., Menges, G., Kroschwitz, J. I., Eds.; John Wiley and Sons: NY, 1985; Vol. 1, pp 299-305.
- (136) Rooney, J. M. *Br. Polym. J.* **1981**, *13*, 160.
- (137) Kukarni, R. K.; Porter, H. S.; Leonard, F. *J. Appl. Polym. Sci.* **1973**, *17*, 3509.
- (138) Cheung, K. H.; Guthrie, J. *Makromol. Chem.* **1987**, *188*, 3041.
- (139) Tseng, Y.-C.; Hyon, S.-H.; Ikada, Y. *Biomaterials* **1990**, *11*, 73.
- (140) Donnelly, E. F.; Pepper, D. C. *Macromol. Chem., Rapid Commun.* **1981**, *2*, 439.
- (141) Kagumba, L.; Penelle, J. *Polym. Prepr. (Am. Chem. Soc., Div. Polym. Chem.)* **2000**, *41*, 1313.
- (142) Kagumba, L.; Penelle, J. *Polym. Prepr. (Am. Chem. Soc., Div. Polym. Chem.)* **2000**, *41*, 1290.
- (143) Perry, S.; Hibbert, H. *J. Am. Chem. Soc.* **1940**, *62*, 2599.
- (144) Perry, S.; Hibbert, H. *Can. J. Chem.* **1933**, *8*, 102.
- (145) Bordwell, F. G.; Bares, J. E.; Bartmess, J. E.; McCollum, G. J.; Van Der Puy, M.; Vanier, N. R.; Matthews, W. *J. Org. Chem.* **1977**, *42*, 321.
- (146) Greenberg, A.; Stevenson, T. A. *J. Am. Chem. Soc.* **1985**, *107*, 3488.
- (147) Allen, F. H. *Acta Cryst.* **1980**, *B36*, 81.
- (148) Xie, T., Ph.D Dissertation, University of Massachussetts, Amherst **2001**.
- (149) Alder, R. W.; Anderson, K. R.; Benjes, P. A.; Butts, C. P.; Koutentis, P. A.; Orpen, A. G. *J. Chem. Commun.* **1998**, 309-310.

## STEREOCHEMICAL ANALYSIS OF POLY(ALKYL 1-CYANO-CYCLOPROPANECARBOXYLATES)

### 3.1 Introduction

The synthesis and characterization of several poly(alkyl 1-cyanoecyclopropanes) poly(**2a-d**) was described in Section 2.3.2. Unlike poly(1,1-dicyanocyclopropane) poly(**1**) and poly(dialkyl cyclopropane-1,1-dicarboxylate)s poly(**3**), these polymers contain a chiral carbon center, introducing the issue of tacticity for these poly(trimethylene) structures. A detailed analysis of the microstructure of poly(**2a-d**) using NMR spectroscopy is provided in this chapter. The term microstructure is principally used to describe specific repeat-unit structures, sequencing of repeat units, average compositions and composition distribution.<sup>1</sup> Analysis of the repeat structure also includes information about the stereochemical configuration and modes of monomer addition. In this chapter, the sequencing of repeat units in the polymer structure, and the factors influencing the stereochemistry of polymerization are discussed. These factors included temperature, nature of the initiator and counterion, solvent, and polymerization of a monomer with a chiral ester substituent (**2e**).

Due to the complexity of the <sup>1</sup>H-NMR spectra obtained, a model compound containing two chiral centers of the polymer backbone was synthesized to simplify the analysis. An NMR simulation program (WIN-DAISY) was used to assign the different resonances of the <sup>1</sup>H-NMR spectrum of the model compound, which were then correlated to the polymer microstructures.

It is well known that the tacticity of a polymer greatly affects its ability to crystallize. Crystalline polymers are usually composed of highly organized microstructures. The only known crystalline atactic vinyl polymers are poly(vinylchloride) and poly(vinyl alcohol), which are able to crystallize due to the relative small size of the chlorine atoms and strong hydrogen-bonding effects, respectively. Wide Angle X-ray Scattering (WAXS) analysis of powder samples of poly(**2a-d**) provided evidence that the polymers are semi-crystalline (Chapter 6). The evidence of crystallinity observed for these polymers strongly suggests that a significant amount of stereoregularity is obtained during the polymerization. This data prompted the detailed examination of the tacticity of poly(**2a-d**) that is provided in this chapter.

## 3.2 Background

### 3.2.1 Tacticity

The concept of tacticity in polymers was introduced to describe the order of the succession of configurational repeating units in the main chain of a polymer. There are defined forms of stereoregularity in polymers. Stereoregular polymers may either be *isotactic* or *syndiotactic*. Isotactic polymers are those composed only of one species of a configurational base unit in a single sequential arrangement, while syndiotactic polymers contain alternating configurational units that are enantiomeric.<sup>2</sup> Polymers with a random sequential distribution of configurational units are termed as *atactic*. Two different configurations are possible for each stereocenter, R and S, which make up the configurational base units. For isotactic polymers, each stereocenter along the



backbone has the same configuration (R or S), while for syndiotactic polymers the configuration of the stereocenter alternates from one repeat unit to the next (Figure 3.1).

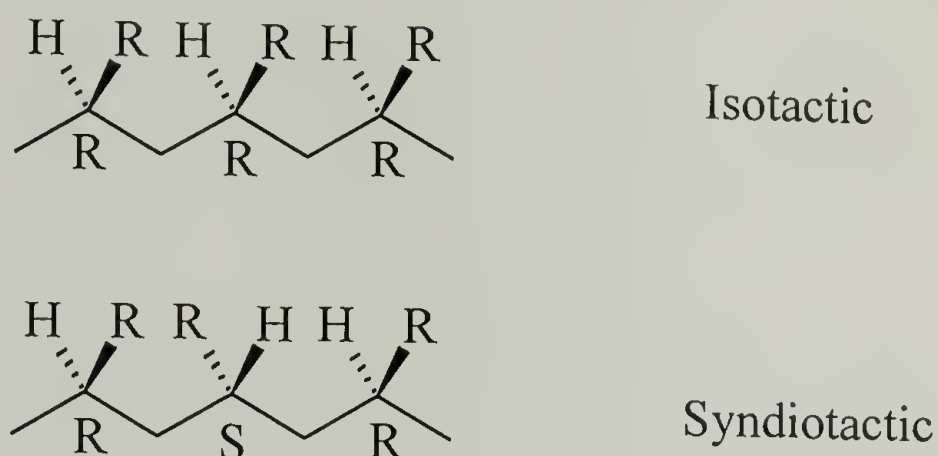


Figure 3.1. Stereoregular carbon-chain polymers with substituents on every second carbon.

The tacticity of carbon-chain polymers with a chiral center on every third carbon is described in Figure 3.2. While the definition of isotactic and syndiotacticity does not change, careful attention must be paid to the assignment of the configuration of the stereocenter.

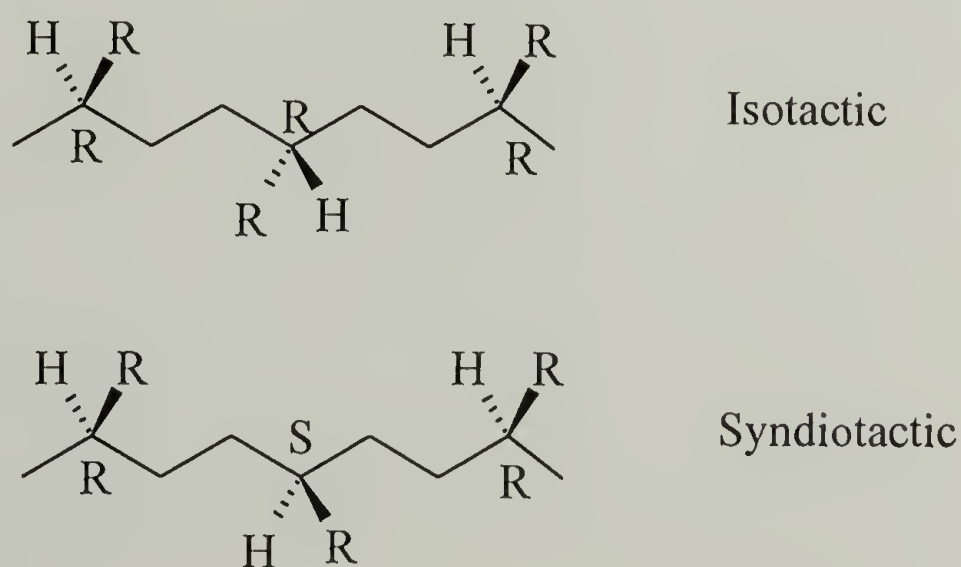
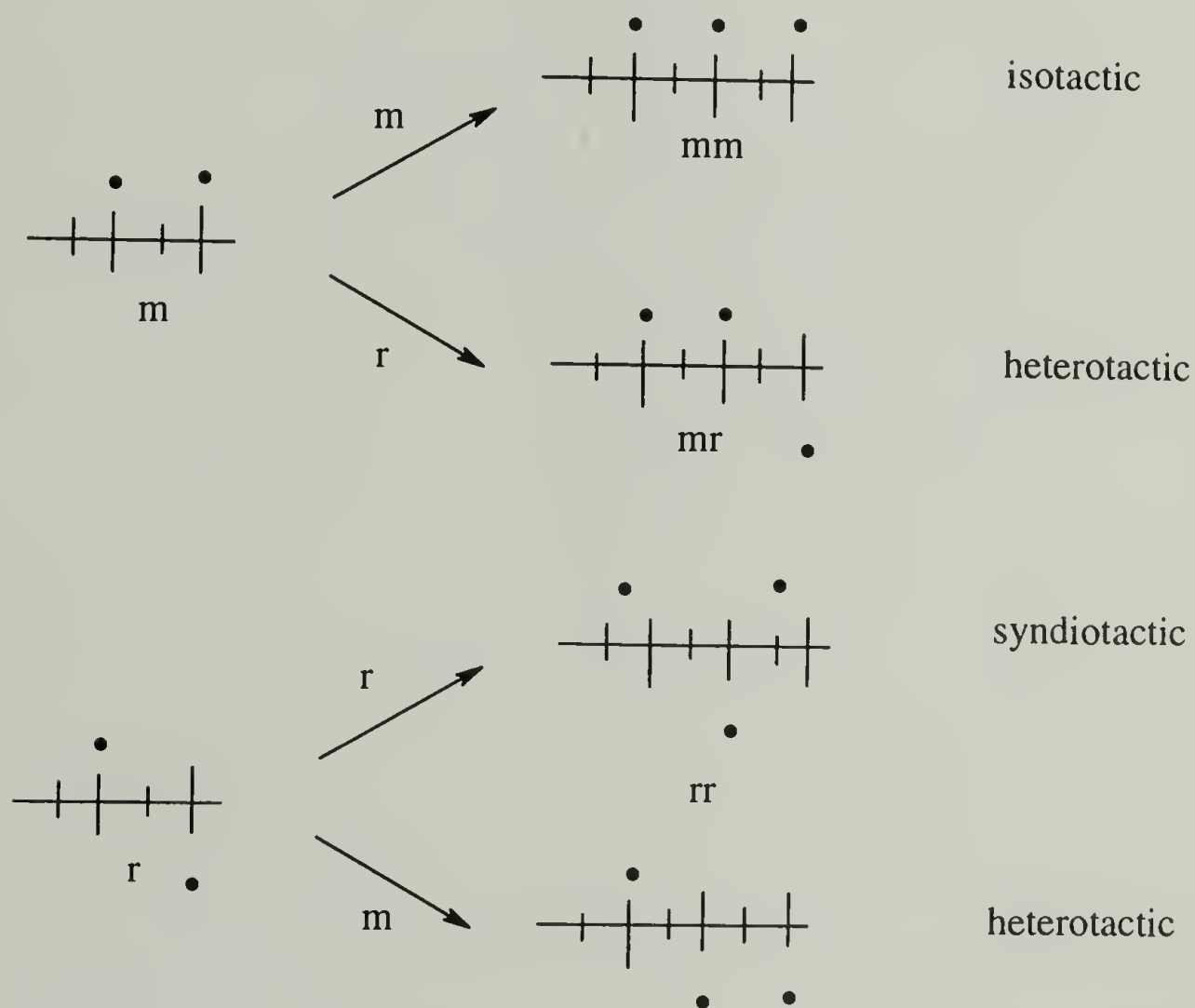


Figure 3.2. Stereoregular carbon-chain polymers with substituents on every third carbon.



The tacticity of polymers can be examined at various levels, such as diad, triad, tetrad level. Diad tacticity refers to pairs of adjacent repeating units that are iso or syndiotactic. *Meso* diads (*m*) are those whose adjacent units are isotactic, while *racemic* (*r*) is the term given to adjacent units that are syndiotactic. On a triad level, isotacticity is defined as *mm*, and syndiotacticity as *rr*. Heterotacticity is used to describe alternating sequences of meso and racemic diads, denoted as *rm* or *mr* (Scheme 3.1). Thus, heterotactic-specific polymerizations require high levels of organization during propagation.



Scheme 3.1. Iso-, syndio- and heterotactic diads

### 3.2.2 Stereochemical Control

A major breakthrough in the stereoregulation of polymer microstructures occurred in the 1950's, when Ziegler and Natta developed catalysts that promoted the stereospecific polymerizations of olefins.<sup>3-7</sup> These catalyst systems were based on metal halide-metal alkyl initiators and have been developed to polymerize a wide variety of vinyl and diene monomers with well-controlled microstructures. Control over the tacticity of the polymer also depends on the reaction conditions during polymerization. For example, numerous studies on the stereochemical polymerization of poly(methyl methacrylate) PMMA have demonstrated that the tacticity of PMMA can be controlled by changing the reaction conditions.<sup>8,9</sup> Isotactic PMMA is usually prepared by anionic initiators such as alkyllithium or Grignard reagents in non-polar solvents at -78 °C.<sup>10</sup> For example,  $t\text{-C}_4\text{H}_9\text{MgBr}$  gives highly isotactic PMMA with narrow molecular weight distribution.<sup>11</sup> Highly syndiotactic monodisperse PMMA can be obtained using  $t\text{-C}_4\text{H}_9\text{Li/R}_3\text{Al}$  ( $\text{Al/Li} > 3$ ) in toluene at -78 °C.<sup>12</sup> The nature of the initiator and its counterion affect the stereochemistry of polymerization. The use of excess  $\text{R}_3\text{Al}$  in the  $t\text{-BuLi/R}_3\text{Al}$  initiator system gives highly syndiotactic polymers. The  $\text{R}_3\text{Al}$  coordinates to the propagating chain end, and fixes the chain end conformation such that syndiotactic addition is favored.

Steric factors also play an important role in the stereochemistry of polymerization. For example, methacrylates with bulky ester groups like triphenylmethyl (trityl) groups, form isotactic polymers irrespective of polymerization conditions. For example, 1-phenylbenzosuberyl methacrylate is 98% isotactic under radical conditions (Figure 3.3).<sup>13</sup> Changing the solvent polarity from non-polar to polar

solvents also affects the stereochemistry of polymerization. For example, MMA polymerized in polar solvents using the typical alkyl lithium initiators or Grignard reagents give syndiotactic polymers.<sup>8</sup>

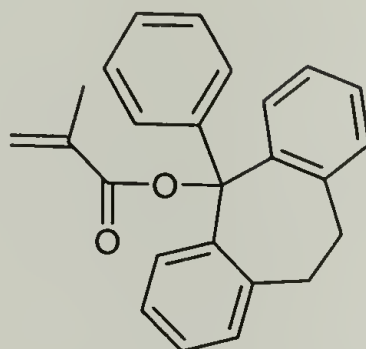


Figure 3.3. 1-phenylbenzosuberone methacrylate

Several properties of a polymer are tacticity dependent. For example, the  $T_g$  of PMMA increases with an increase in the degree of syndiotacticity reaching a maximum of 140 °C at 100%.<sup>14</sup> The ability of a polymer to crystallize is also largely dependent on the stereoregularity of the polymer microstructure. It is more energetically favorable for ordered structures (iso- or syndiotactic) to pack into crystalline lattices, than disordered (atactic) polymers. In turn, the degree of crystallinity of a polymer affects its properties such as solvent and chemical resistance and physical strength. For example, isotactic PMMA is hydrolyzed more rapidly than syndiotactic PMMA under basic conditions.<sup>15</sup>

### 3.2.3 Analytical Tools

Nuclear Magnetic Resonance (NMR) spectroscopy is currently the most powerful tool used to determine the stereochemical sequences of polymer microstructures. Both conventional one-dimensional (1D) and two-dimensional (2D) NMR are used to reveal details seen by no other technique.<sup>16</sup> The assignments of resonances in polymer microstructures often rely on the use of labeled isotopes, model

compounds, polymers of different tacticities, and modified polymers. The application of empirical rules and theoretical calculations have also been powerful tools.<sup>17</sup> Polymer stereosequence distributions obtained by NMR analysis are often analyzed by statistical methods such as Bernouillian statistics, or with the aid of computer programs that are designed to simulate high-resolution spectra. Typically, model compounds that consist of a section of the polymer backbone (such as two repeat units) are studied to simplify the analysis. <sup>13</sup>C-NMR is a powerful tool that can be used to distinguish between atactic, and tactic (iso-, syndio-, hetero-) structures. Details of the sensitivity of this method are provided in the discussion section.

### 3.3 Experimental

#### Measurements

<sup>1</sup>H-NMR and <sup>13</sup>C-NMR spectra were recorded on a Bruker AMX-2 500 spectrometer in (CD<sub>3</sub>)<sub>2</sub>SO. For the polymers, the spectra were obtained at 115 °C. NMR simulations were performed using the program WIN-DAISY available from Bruker.

#### Materials and Procedures

The synthesis of all the monomers and polymers discussed in this chapter were detailed in the experimental section (2.4.2), with the following exception:

**Synthesis of diethyl 2,5-dicyanoadipate (i)** (model compound). A mixture of ethyl 2-cyanopropionate (0.01 mol, 6.3 mL), potassium carbonate (0.02 mol, 2.8g), and dibromoethane (0.006mol, 0.52 mL) in DMSO (15 mL) was vigorously stirred for 15 hours using a mechanical stirrer. Water (30 mL) was added to the crude orange mixture and the product extracted with 3 x 15 mL portions of diethyl ether. The ether layer was



concentrated to yield an orange liquid. A Buchi Kugelrohr apparatus was used to remove the unreacted ethyl 2-cyanopropionate (under 1 mmHg vacuum). The residue of the distillation was the product diethyl 2,5-dicyanoadipate (i).  $^1\text{H}$  NMR ( $(\text{CD}_3)_2\text{SO}$ , 300 MHz):  $\delta(\text{ppm})$  1.29 (t,  $\text{CH}_3$ , 6H), 1.64 (s,  $\text{CH}_3$  6H), 1.85-2.1 (m,  $\text{CH}_2$ , 4H), 4.28 (q,  $\text{OCH}_2$ , 4H).  $^{13}\text{C}$  NMR ( $(\text{CD}_3)_2\text{SO}$ , 300 MHz):  $\delta(\text{ppm})$  14.6 ( $\underline{\text{C}}\text{H}_3$ ), 23.5 ( $\text{C}_{\text{quart.}}\underline{\text{C}}\text{H}_3$ ), 33.6 ( $\underline{\text{C}}\text{H}_2$ ), 44.0 ( $\underline{\text{C}}_{\text{quart.}}$ ), 63.6 ( $\text{O}\underline{\text{C}}\text{H}_2$ ), 120.3 ( $\underline{\text{C}}\text{N}$ ), 169.2 ( $\underline{\text{C}}=\text{O}$ ).

**Synthesis of sec-butyl cyanoacetate (ii).**<sup>18</sup> Benzene (50 mL) was added to a solution of cyanoacetic acid (8.5g, 0.1 mol) in 2-butanol (9.2 mL, 0.2 mol) and cooled in ice before slowly adding a few drops of concentrated sulfuric acid down the sides of the flask. The solution was refluxed for 2 hours, while collecting the water using a Dean Stark trap. After cooling the reaction mixture to room temperature, water (100 mL) was added and the product extracted using diethyl ether (75 mL). The ether layer was washed with water (50 mL), a 5% sodium bicarbonate solution (50 mL) and a saturated NaCl solution (50 mL), and dried overnight over sodium sulfate to yield 13.4g (95 %).  $^1\text{H}$  NMR ( $\delta(\text{ppm})$ ,  $\text{CDCl}_3$ ): 0.94 (t, 3H), 1.28 (d, 3H), 1.64 (m, 2H), 3.5 (s, 2H), 4.94 (m, 1H).  $^{13}\text{C}$  NMR ( $\delta(\text{ppm})$ ,  $\text{CDCl}_3$ ): 9.9 ( $\text{CH}_2\underline{\text{C}}\text{H}_3$ ), 19.5 ( $\text{CH}_3$ ), 25.3 ( $\underline{\text{C}}\text{H}(\text{CN}, \text{COOR})$ ), 28.9 ( $\underline{\text{C}}\text{H}_2\text{CH}_3$ ), 76.1 ( $\text{O}\underline{\text{C}}\text{H}$ ), 113.7 ( $\underline{\text{C}}\text{N}$ ), 163.2 ( $\underline{\text{C}}\text{OOR}$ ).

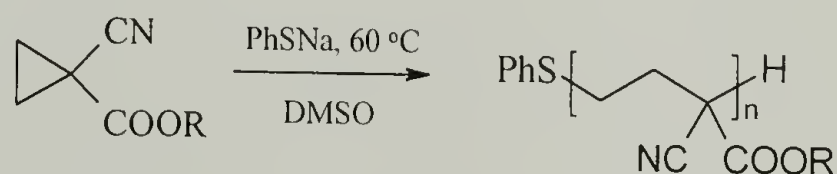
**Synthesis of sec-butyl 1-cyanocyclopropanecarboxylate 2e.** The monomer was synthesized according to the same procedure used for the alkyl 1-cyanocyclopropanecarboxylates **2a-d** (Section 2.3.3.2). Yield (38 %), b.p. 48/ 1mm Hg.  $^1\text{H}$  NMR ( $\delta(\text{ppm})$ ,  $\text{CDCl}_3$ ): 0.94 (t, 3H), 1.29 (d, 3H), 1.60 (m, 2H), 1.57-1.71(m, 4H), 3.5 (s, 2H), 4.90 (m, 1H).  $^{13}\text{C}$  NMR ( $\delta(\text{ppm})$ ,  $\text{CDCl}_3$ ): 9.9 ( $\text{CH}_2\underline{\text{C}}\text{H}_3$ ), 13.9 ( $\text{CH}_2$ , ring), 19.1 ( $\text{C}_{\text{quart.}}$ ), 19.6 ( $\text{CH}_3$ ), 28.9 ( $\underline{\text{C}}\text{H}_2\text{CH}_3$ ), 76.1 ( $\text{O}\underline{\text{C}}\text{H}$ ), 119.3 ( $\underline{\text{C}}\text{N}$ ), 167.7

19.1 ( $C_{\text{quart.}}$ ), 19.6 ( $\text{CH}_3$ ), 28.9 ( $\text{CH}_2\text{CH}_3$ ), 76.1 ( $\text{OCH}$ ), 119.3 ( $\text{CN}$ ), 167.7 ( $\text{COOR}$ ). Anal. Calc. for  $\text{C}_9\text{H}_{13}\text{NO}_2$  (167.23): C, 64.64; H, 8.38; N, 7.85. Found: C, 64.28; H, 8.54; N, 7.86.

**$^1\text{H}$ -NMR simulation method.** See APPENDIX section.

### 3.4 Results and Discussion

3.4.1. Polymer Synthesis and Characterization. Details of the anionic ring-opening polymerization of alkyl 1-cyanocyclopropanecarboxylates **2a-d** are provided in Section 2.3.2. Poly(**2a-c**) are soluble in highly polar solvents such as DMF and DMSO at  $100^\circ\text{C}$ , while poly(**2d**) dissolves in THF and chlorinated solvents at room temperature. The ring-opened structures of poly(**2a-d**) (Scheme 3.2) were confirmed by FT-IR and high temperature  $^1\text{H}$ - and  $^{13}\text{C}$ -NMR.



Poly(**2a-d**)

R = (a) ethyl, (b) i-propyl, (c) n-butyl, (d) n-octyl

Scheme 3.2. Synthesis of Poly(alkyl 1-cyanocyclopropanecarboxylate)s

The  $^1\text{H}$ -NMR spectrum of poly(**2a**) (500 MHz,  $(\text{CD}_3)_2\text{NCOD}$ ,  $115^\circ\text{C}$ ) with an expansion of the ethylene region ( $-\text{CH}_2\text{CH}_2-$ ) of the backbone is shown in Figure 3.4. Analysis of the  $-\text{CH}_2\text{CH}_2-$  region is key to unfolding the microstructure of the polymer. However, due to the complexity of the spectrum associated with AA'BB' spin-spin coupling systems, a model compound containing only two chiral units of poly(**2a**) was synthesized to simplify the analysis.

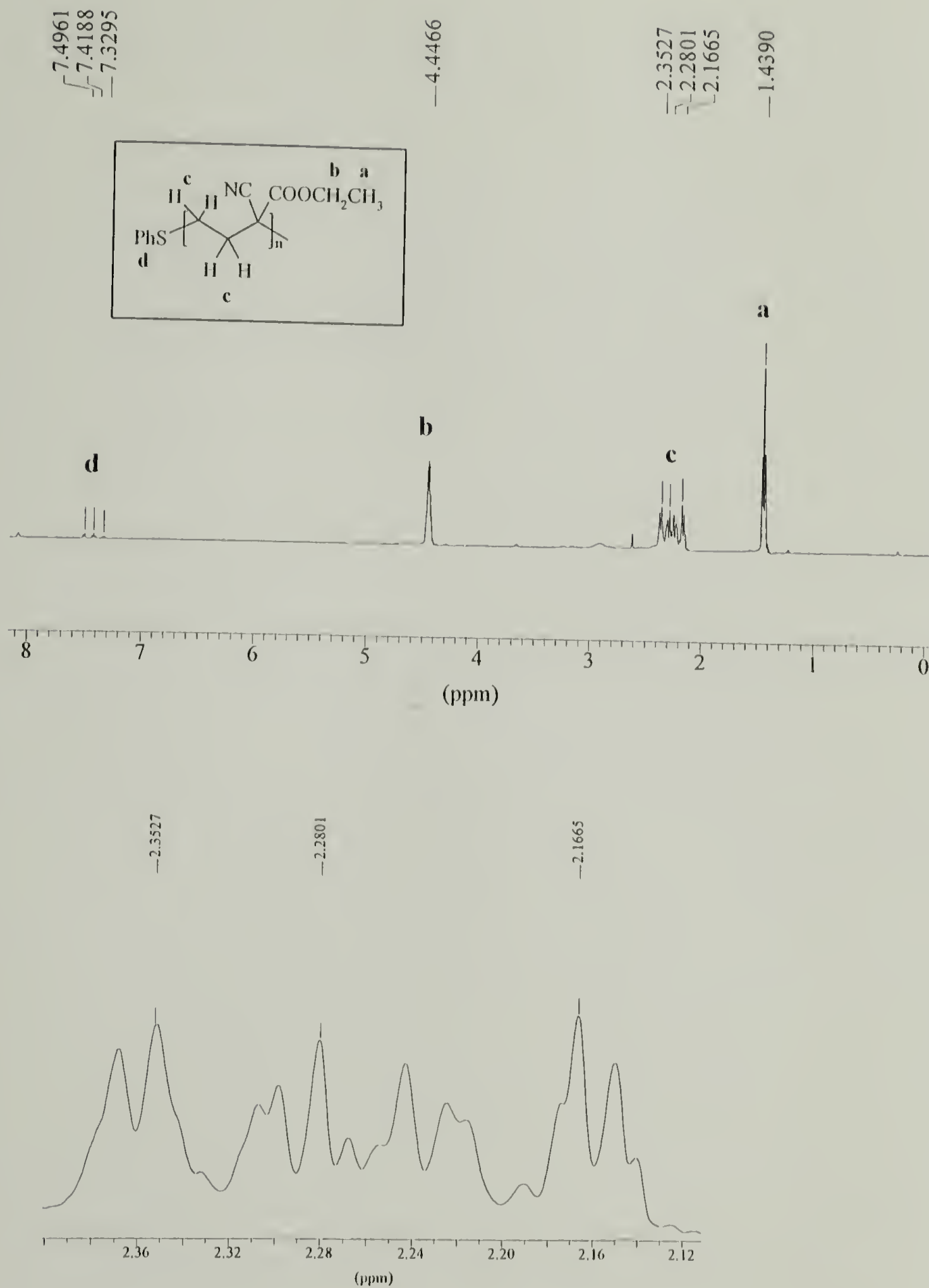
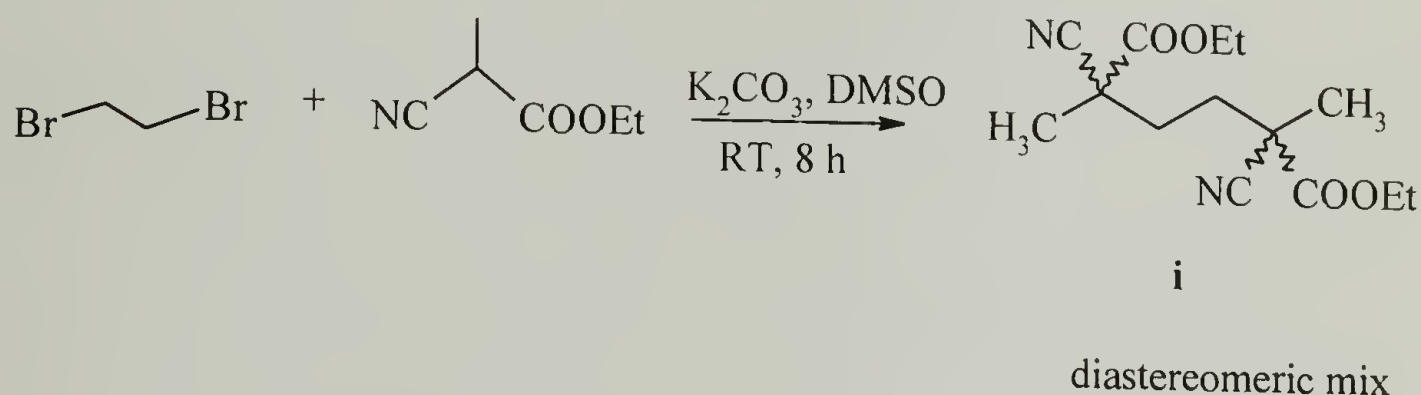


Figure 3.4.  $^1\text{H}$ -NMR Spectrum of Poly(2a) Showing the Expanded  $-\text{CH}_2\text{CH}_2-$  region (lower spectrum)

3.4.2 Analysis of model compound (i). The model compound, diethyl 2,5-dicyanoadipate (i), was synthesized in a one-step reaction involving the addition of a two-fold excess of ethyl 2-cyanopropionate to dibromoethane in the presence of a mild base (Scheme 3.3). The product was isolated by bulb-to-bulb distillation and analyzed by  $^1\text{H}$ -NMR spectroscopy to determine the diastereomeric content.



Scheme 3.3. Synthesis of diethyl 2,5-dicyanoadipate

The  $^1\text{H}$ -NMR spectrum of the model compound is shown in Figure 3.5. The compound contains two equivalent asymmetric carbon atoms with a cyano, carboxylate and methyl substituent on each carbon. The peaks corresponding to the ethylene ( $-\text{CH}_2-\text{CH}_2-$ ) protons have chemical shifts ranging from 1.75 - 2.05 ppm. An expansion of this region is shown in Figure 3.6.



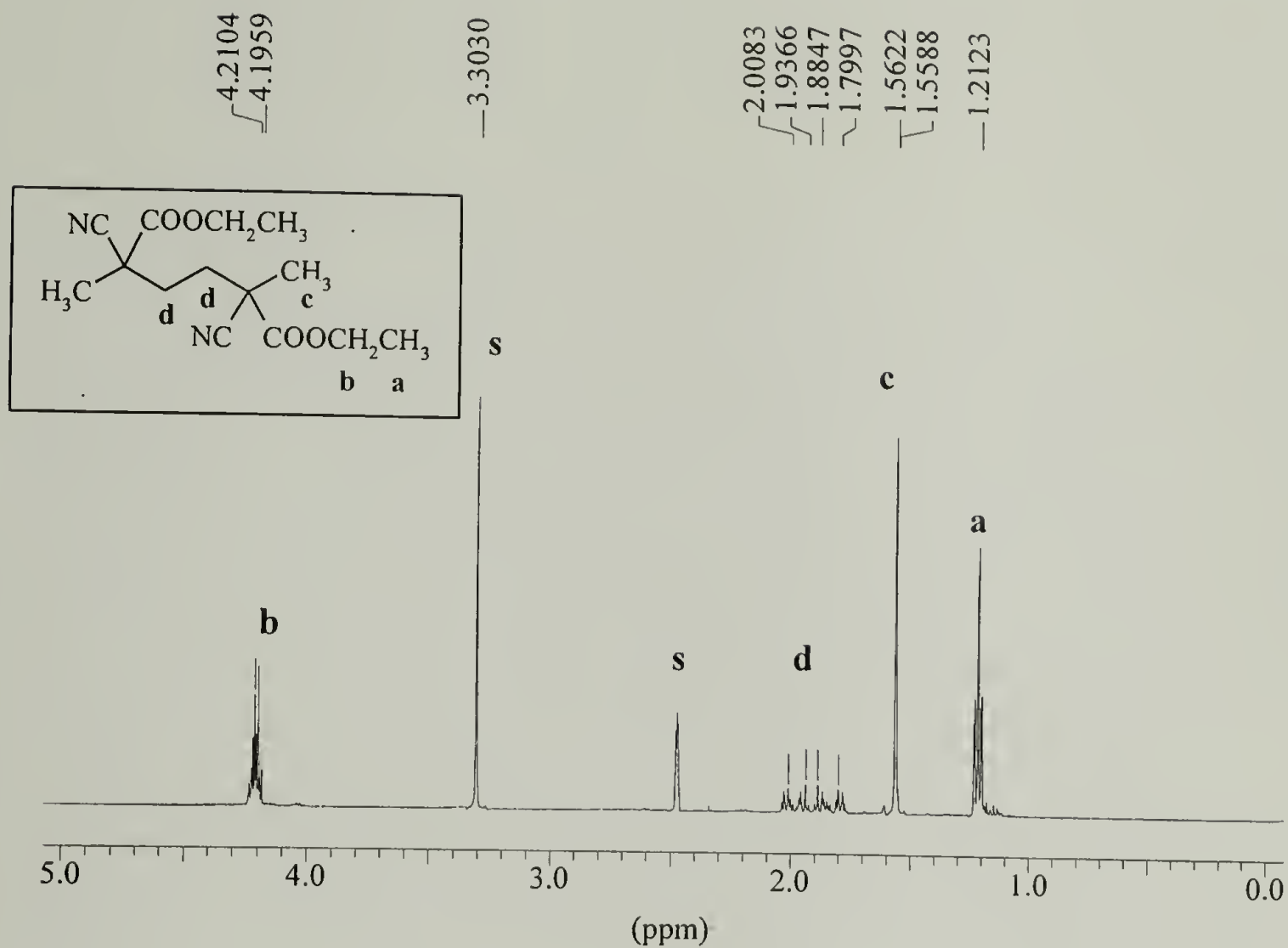


Figure 3.5.  $^1\text{H}$ -NMR Spectrum of Model Compound (i) (s = solvent peak)

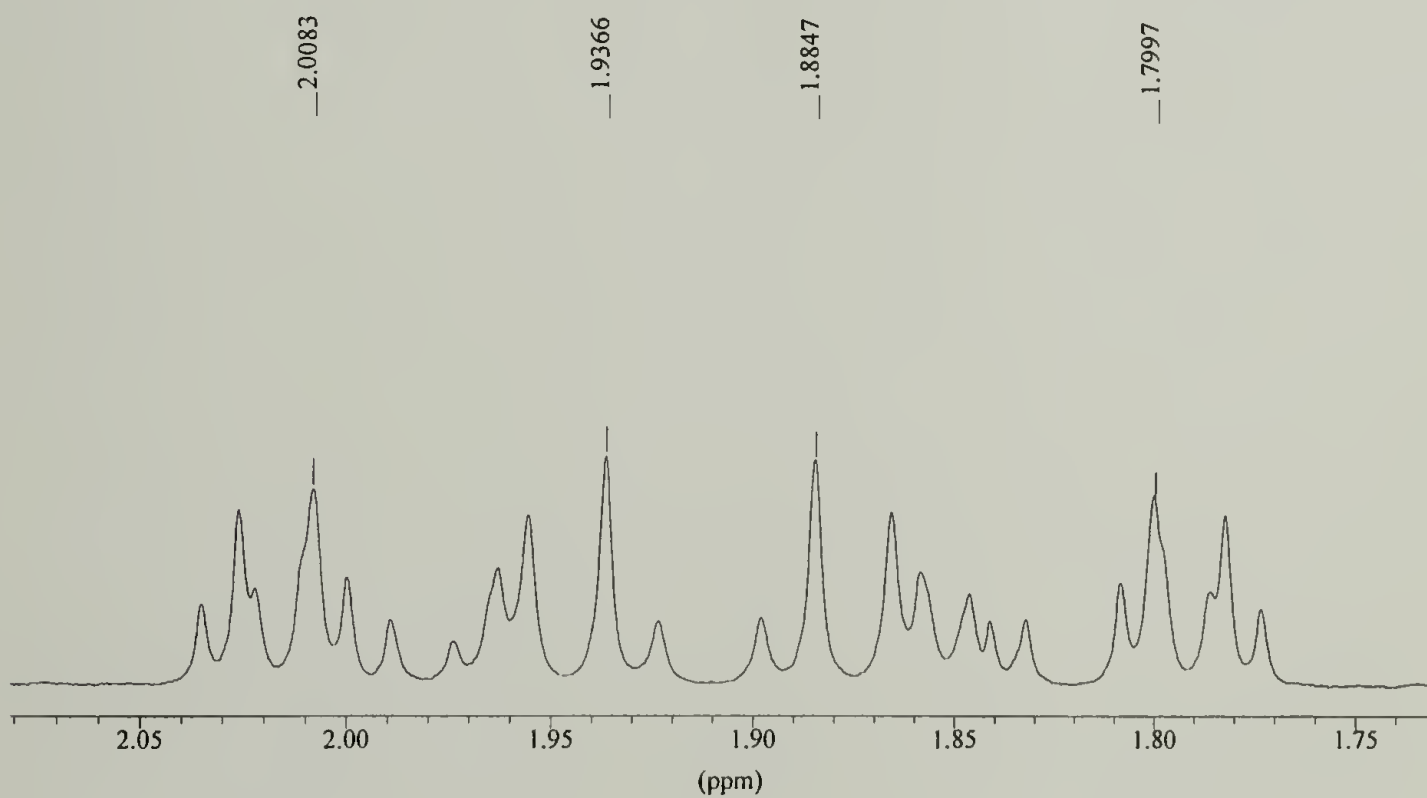


Figure 3.6.  $^1\text{H}$ -NMR Spectrum of  $-\text{CH}_2-\text{CH}_2-$  Region of the Model Compound (i)

There are two diastereoisomeric forms of the model compound, which are assigned *meso* and *dl* configurations (Figure 3.7). The *meso* diastereomer has a plane of symmetry and the -CH<sub>2</sub>-CH<sub>2</sub>- groups constitute an A<sub>2</sub>B<sub>2</sub> spin system. The *dl* diastereomer constitutes the more complex AA'BB' spin-spin coupling system. Since it was impossible to distinguish between the signals of the -CH<sub>2</sub>-CH<sub>2</sub>- region of each diastereomer by simple analysis of the <sup>1</sup>H-NMR spectrum, an NMR program was used to simulate the spectrum of each diastereomer in order to assign the resonances obtained from the experimental spectra.

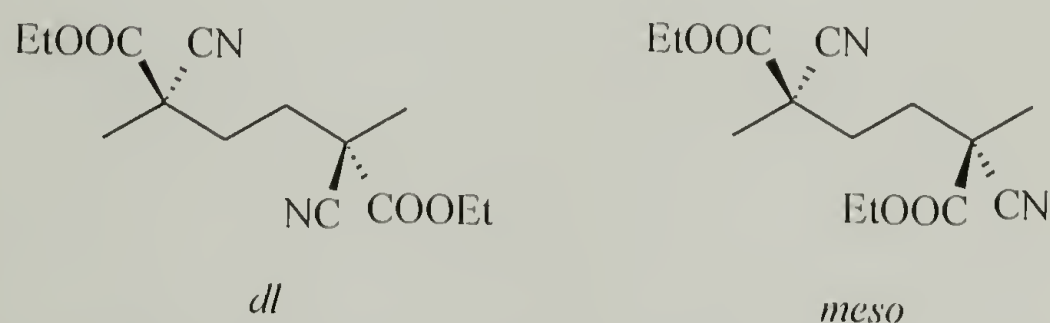
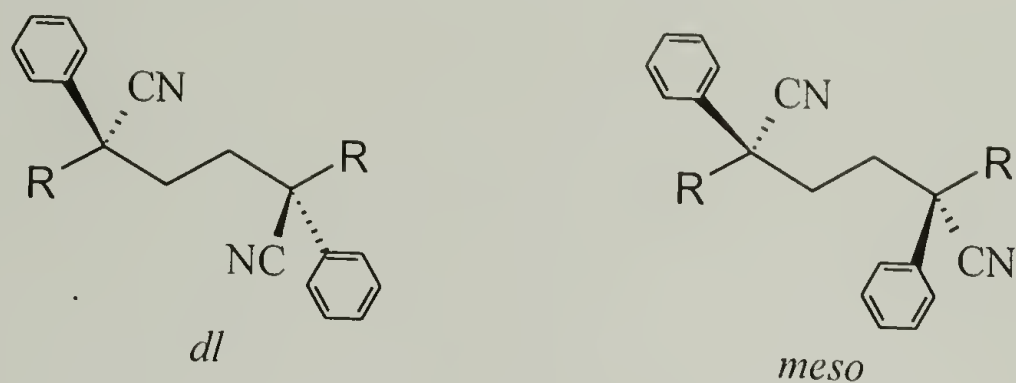


Figure 3.7. Structures of *meso* and *dl* Diastereomers of (i)

3.4.3. Analysis of NMR spectra of (i) via Simulation. Simulation of the <sup>1</sup>H-NMR spectrum of each diastereomer was performed using the WIN DAISY program described in the experimental section. Several input parameters such as the symmetry description, frequency (in Hz) and spin-spin coupling constants are required. Approximate values of the spin coupling constants were obtained by examining data obtained from the stereochemical analysis of  $\alpha$ - $\alpha'$ -diphenyl-substituted adiponitriles (ii) reported in the literature (Figure 3.8).<sup>19</sup> The two diastereomers of (ii) were isolated and conclusive assignments of the *meso* and *dl* configurations were made by analysis of the <sup>1</sup>H-NMR signals of the -CH<sub>2</sub>-CH<sub>2</sub>- region.



(ii (*meso*), ii' (*dl*))

R: (a) H; (b) COOEt; (c) Me; (d) Et

Figure 3.8. *Meso* and *dl* Diastereomers of Diphenyl-Substituted Adiponitriles (ii)

Except for **ii**a, the spectra of the ethylene region of the other diastereomers gave an AA'BB'-type multiplet. These were analyzed using an iterative computer program - LAOCN3.<sup>20</sup> The resultant spectral parameters were assigned to the *meso* and *dl* configurations in accordance with previous findings of Jung and Bothner-By, who studied substituted ethanes such as *meso*- and *dl*-2,5-diphenylhexanediol<sup>21</sup>. A summary of the NMR parameters obtained for  $\alpha$ - $\alpha'$ -diphenyl-substituted adiponitriles is provided in Table 3.1.

Table 3.1. NMR parameters for *meso* and *dl* forms (ii and ii'), expressed in Hz.\*

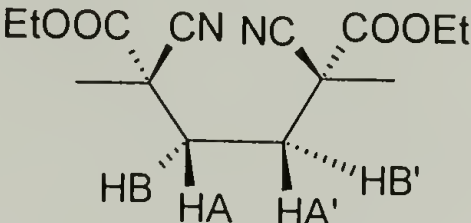
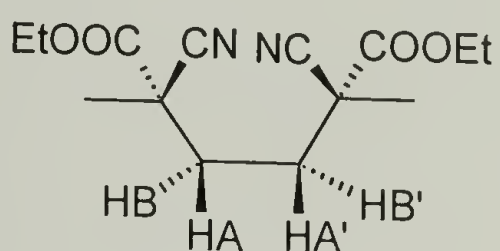
Derivative	$\delta_v$	$J_{AA'} = J_{BB'}$	$J_{AB'} = J_{A'B}$	$J_{AB} = J_{A'B'}$	Assign- ment
5a	$\sim 0$				<i>meso</i>
5a'	$\sim 0$	4.8	11.8		<i>dl</i>
5b	$\sim 0$				<i>meso</i>
5b'	$21.28 \pm 0.9$	$3.90 \pm 0.17$	$13.15 \pm 0.12$	$-13.52 \pm 0.12$	<i>dl</i>
5c	$19.92 \pm 0.3$	$13.19 \pm 0.26$	$4.10 \pm 0.04$	$-13.64 \pm 0.05$	<i>meso</i>
5c'	$23.30 \pm 0.12$	$4.80 \pm 0.24$	$11.80 \pm 0.16$	$-13.30 \pm 0.16$	<i>dl</i>
5d	$22.00 \pm 0.3$	$13.12 \pm 0.19$	$4.20 \pm 0.03$	$-13.50 \pm 0.04$	<i>meso</i>
5d'	$29.40 \pm 0.13$	$4.69 \pm 0.17$	$11.87 \pm 0.22$	$-13.58 \pm 0.19$	<i>dl</i>

\* see Figure 3.9 for the designation of  $H_A$ ,  $H_{A'}$ ,  $H_B$ ,  $H_{B'}$ .

Initial frequency parameters (chemical shifts in Hz) for the simulation of the individual spectrum of the  $-\text{CH}_2-\text{CH}_2-$  region of the *meso* and *dl* diastereomers of the model compound (i) were estimated from the experimental spectrum (Figure 3.4). Input values for the spin-spin coupling constants were estimated from Table 3.1. After the initial iteration, the parameters were refined and optimized in accordance with the experimental spectra. A summary of the input parameters (after refinement) for the simulation of the model compound (i) is shown in Table 3.2.



Table 3.2. Input Data for the Simulation of the  $^1\text{H}$ -NMR Spectra of the  $-\text{CH}_2\text{CH}_2-$  region of *meso* and *dl* diastereomers of (i).

Diastereomer	Meso	D, l (racemic)
Structure		
Symmetry element	$C_s$	$C_2$
Symmetry description	E, $\sigma_H$	E, $C_2$
Frequency	935, 1048 Hz	972, 1017 Hz
Spin-spin coupling constants		
$J_{AA'} = J_{BB'}$	12.0	4.5
$J_{AB'} = J_{A'B}$	4.1	12.8
$J_{AB} = J_{A'B'}$	-13.64	-13.30

Similar to  $\alpha, \alpha'$ -diphenyl-substituted adiponitriles (Table 3.1), a greater value for the  $J_{AA'}$  ( $J_{BB'}$ ) is seen for the *meso* form, while the *dl* form has a greater value for the  $J_{AB'}$  ( $J_{A'B}$ ) coupling constants. The relationship between the coupling constants is a Karplus-type<sup>22</sup> relationship often represented by the general formula

$$^3J = A \cos^2 \theta - B \cos \theta + c$$

where the coefficients A, B and C depend mainly on the nature of the four atoms in the pathway. Karplus equation defines the relationship between the vicinal coupling constant and the torsional angle  $\theta$  about the C-C bond (Figure 3.9).

The vicinal (or three bond) coupling constant ( $^3J$ ) between nuclei show a clear correlation with the dihedral angle between two planes defined by the three atoms. This correlation was first described by Lemieux and Schwarz.<sup>23,24</sup>

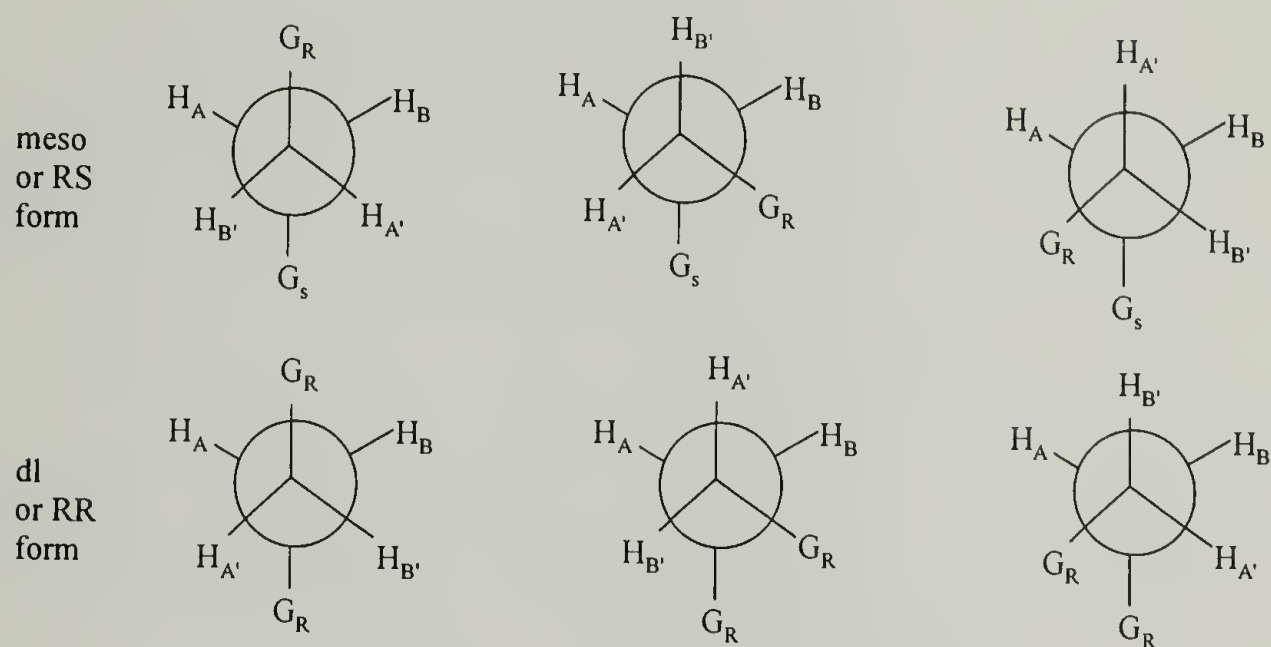


Figure 3.9. Conformations and equivalence relationships between the hydrogen atoms of  $-\text{CH}_2-\text{CH}_2-$  groups, for *meso* and *dl* conformations ( $G = \text{X}-\text{C}-(\text{COOEt}, \text{CN})$  where  $\text{X} = \text{CH}_3$  or  $\text{C}_6\text{H}_5$ )

Due to the notable steric hindrance of the  $G_R$  and  $G_S$  groups, the most stable conformation is the trans conformation, and thus most populated. Since the  $J_{\text{HH}}$  trans are larger than the gauche,<sup>25</sup> a greater value for  $J_{\text{AB'}}$  is expected in the *dl* form and  $J_{\text{AA'}}$  in the *meso* form. This relation was derived from Karplus equation established for  $\text{H}-\text{C}-\text{C}-\text{H}$  fragments.<sup>22</sup> Such Karplus type relationships between  $^3J$  values and the corresponding dihedral angle have been proved through theoretical and measurements of conformationally rigid molecules for a large number of molecular fragments.<sup>26</sup>

The  $^1\text{H}$ -NMR spectra of the ethylene region obtained from the simulation of the *meso* and *dl* diastereomers of the model compound (i) are shown in Figure 3.10.

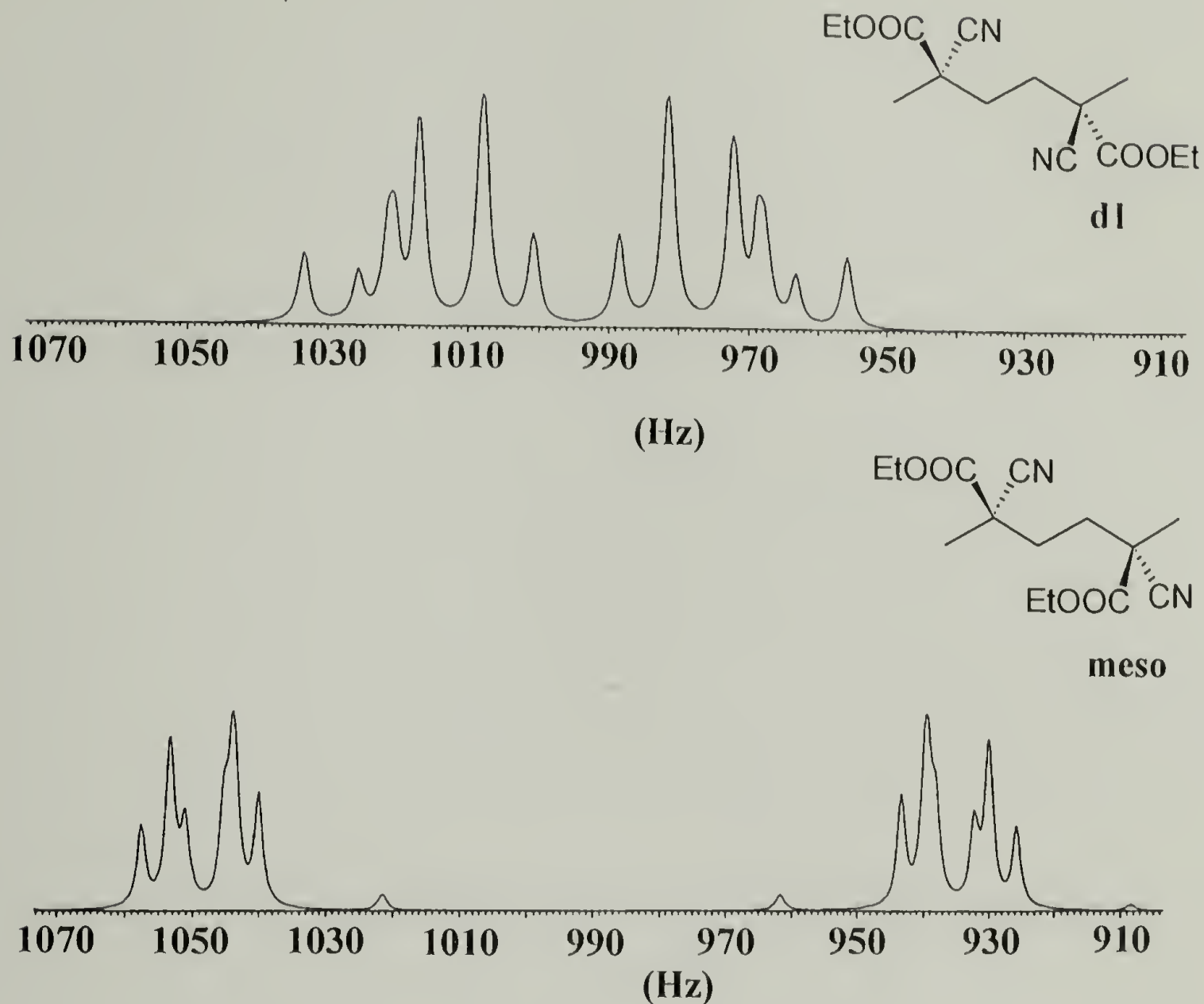


Figure 3.10.  $^1\text{H}$ -NMR Spectrum of the  $-\text{CH}_2\text{CH}_2-$  Region of the *meso* and *dl* Diastereomers obtained from the Simulation:

The simulation spectrum of a 50:50 mixture of the *meso* and *dl* forms is shown in Figure 3.11. From these spectra, it was evident that the model compound synthesized was a mixture of the *meso* and *dl* configurations. By integration of the peak areas of the experimental spectrum, the diastereomeric content of *meso:dl* was determined to be 50:50.

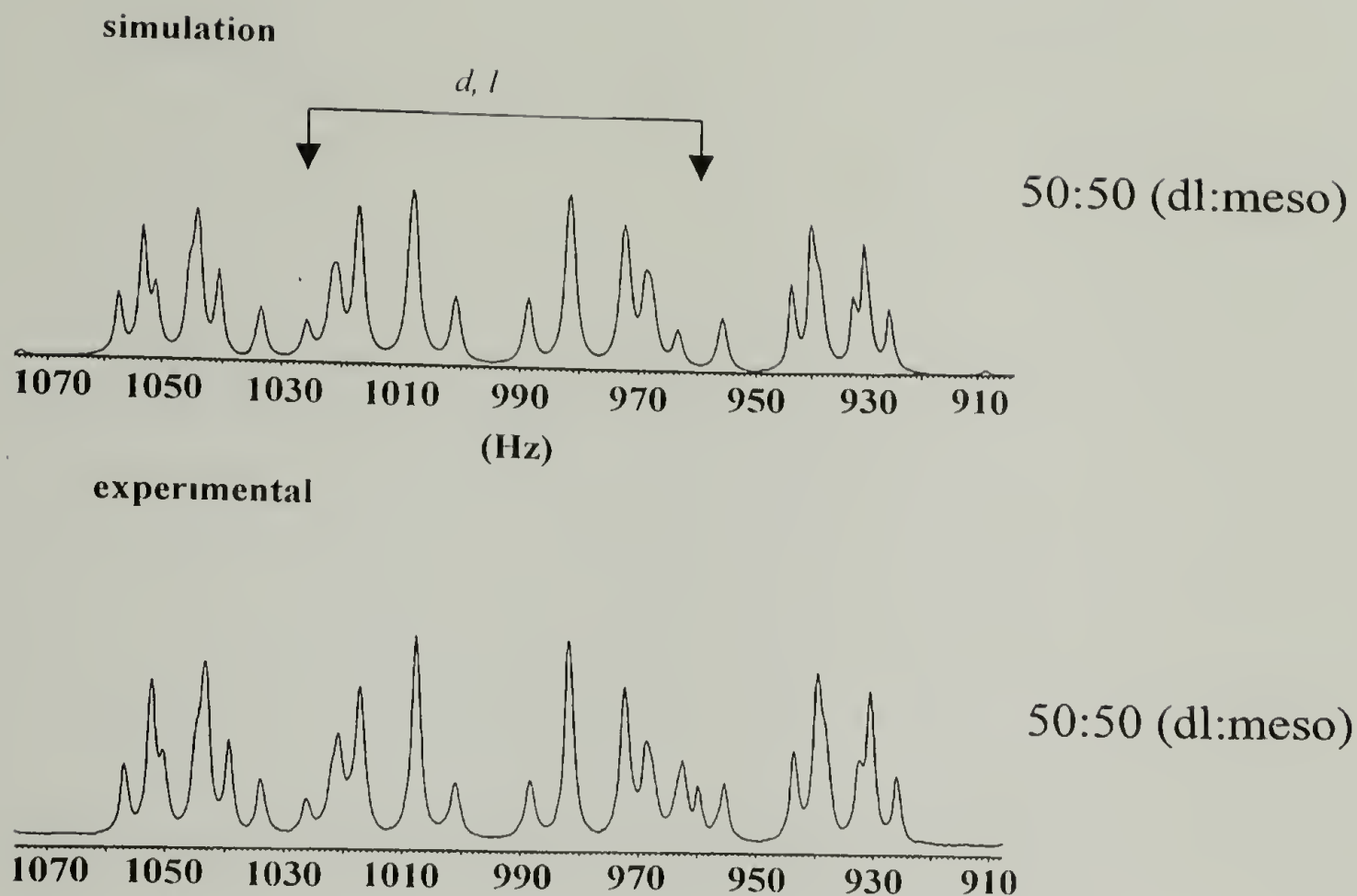


Figure 3.11. Theoretical and Experimental Spectra of a 50:50 diastereomeric mix of the model compound (i).

3.4.4. Analysis of the polymer microstructures. Simulation of the  $-\text{CH}_2\text{CH}_2-$  region of *meso* and *dl* diastereomers were obtained with increased line widths from 1.75 Hz to 3.75 Hz. The coupling constants initially used were those obtained from the model compound and optimized. Frequency input data was obtained from the experimental spectra of the polymers. The simulation spectrum of the  $-\text{CH}_2\text{CH}_2-$  region of a 50:50 mixture of *meso*:*dl* diastereomeric units is shown in Figure 3.12. The spectrum is representative of a segment of the polymer backbone containing two chiral centers. The spectra provide a method for the distinction between *meso* and *dl* configurations at the diad level in the polymer structure. Integration of the relative peak areas of the



experimental spectrum indicated that the polymer was composed of a 50:50 mixture of *meso:dl* diads (Figure 3.12).

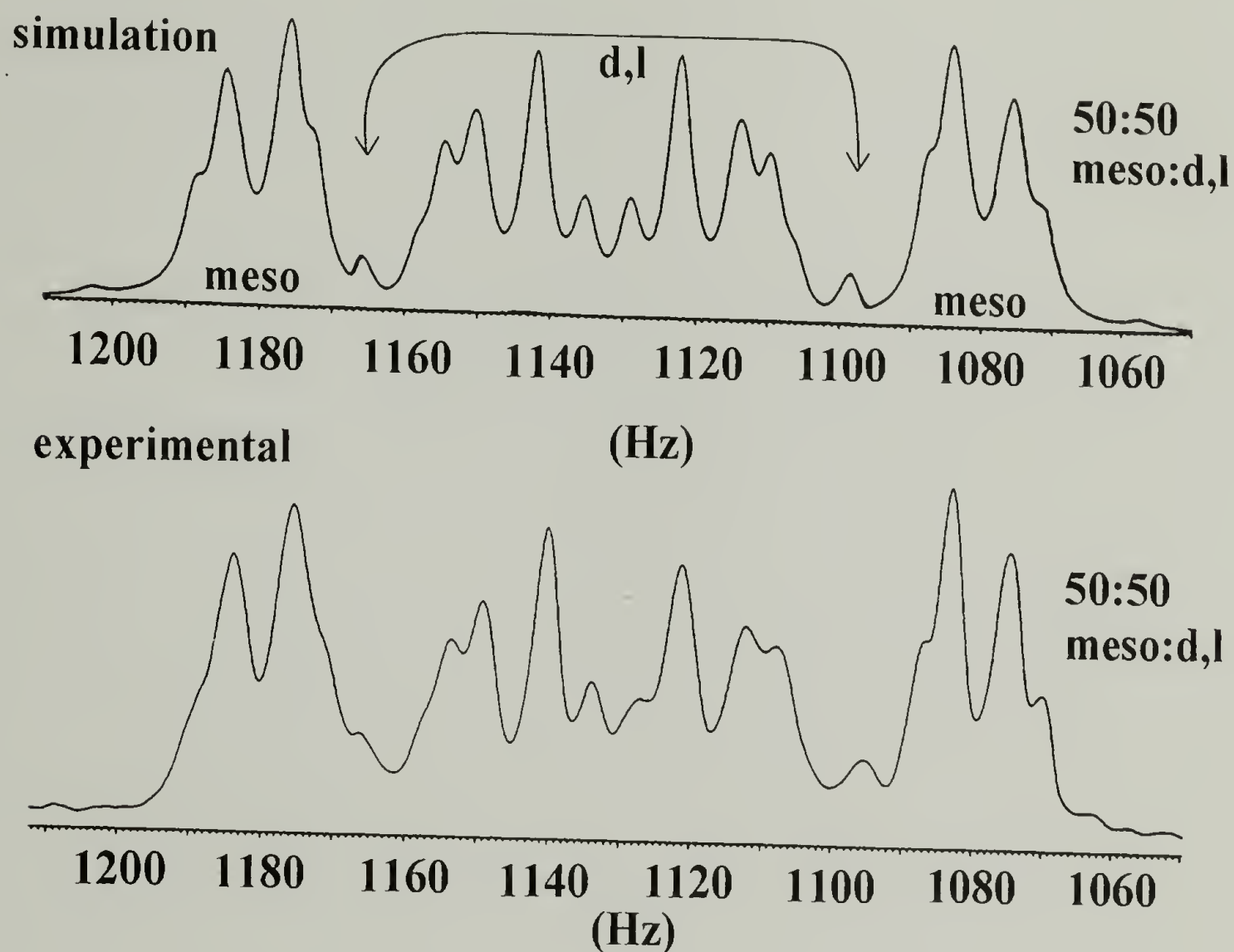


Figure 3.12. A Comparison of the Theoretical and Experimental Spectra of the  ${}^{-}\text{CH}_2\text{CH}_2{}^{-}$  Region of Poly(2a).

By definition, a polymer with a random mixture of *meso* and *dl* diads is considered atactic. However, if the microstructure consists of an alternating mixture of *meso* and *dl* diads, the polymer is considered heterotactic. The evidence provided by the NMR that at the diad level the polymer is made of an equal amount of *meso* and *dl* diads

is particularly interesting here, considering poly(**2a**) is a highly crystalline polymer. Polymer crystallinity is directly affected by the chain tacticity. For vinyl homopolymers, with the exception of polyvinyl alcohol and polyvinyl chloride, atactic polymers are non-crystalline. The crystallinity of poly(**2a**) is suggestive of a regular structure, which supports the *heterotactic* placement of diads units, rather than an atactic placement. Attempts to distinguish between the two microstructures using  $^{13}\text{C}$ -NMR were made.

3.4.5  $^{13}\text{C}$ -NMR Analysis. The long-range sensitivity of  $^{13}\text{C}$ -NMR to microstructural details makes it a valuable tool for probing polymer microstructures. Quantitative  $^{13}\text{C}$ -NMR spectra of poly(**2a**) is shown in Figure 3.13, with the expansion of the regions due to the ethylene carbons of the backbone and the side chain methylene carbons shown in Figure 3.14. The ethylene region shows a splitting in the peak (~10 Hz), but the methylene carbons of the side chain show a single peak.

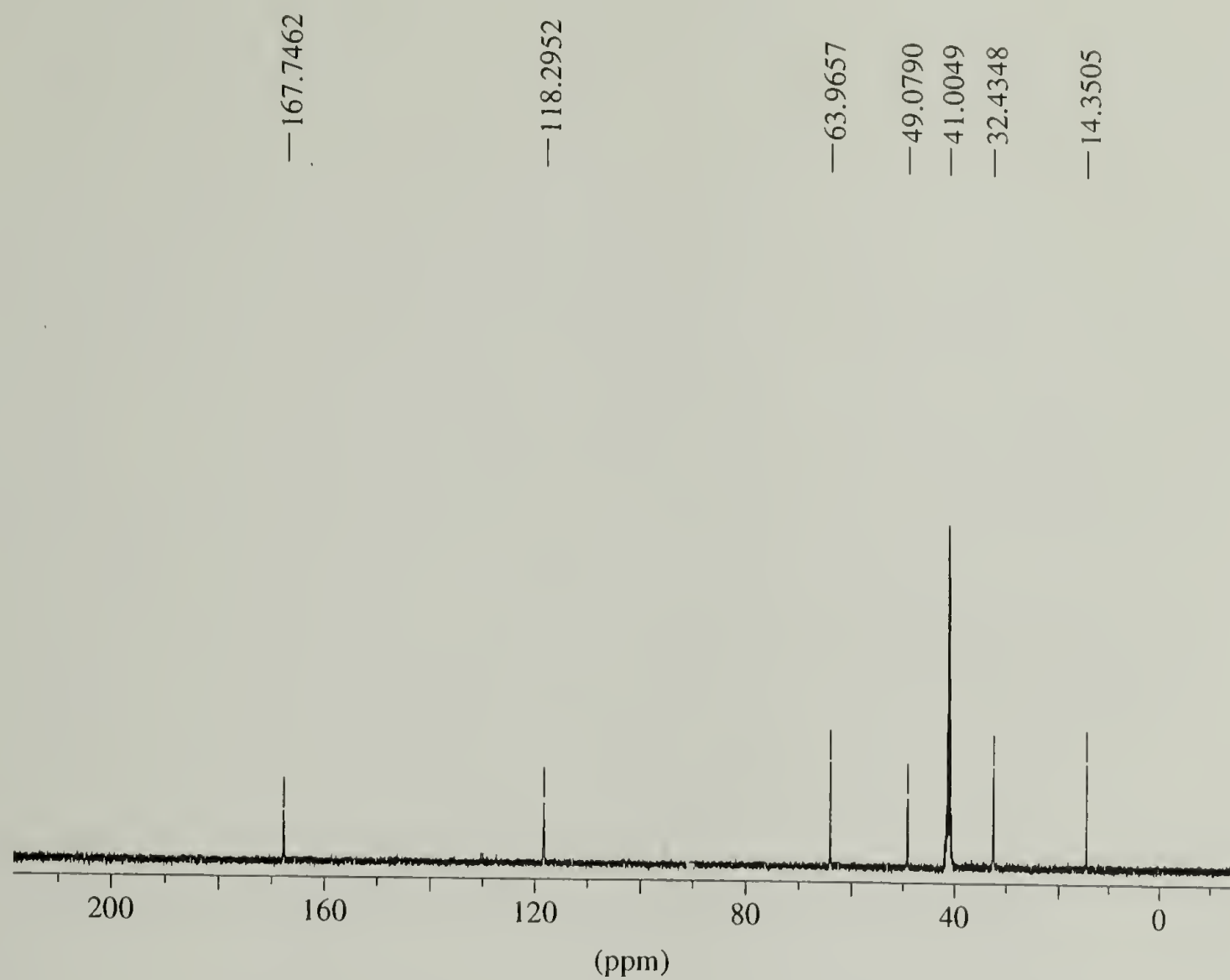


Figure 3.13. Quantitative  $^{13}\text{C}$ -NMR Spectrum of Poly(2a)  
(10 mm probe, 500 MHz NMR)

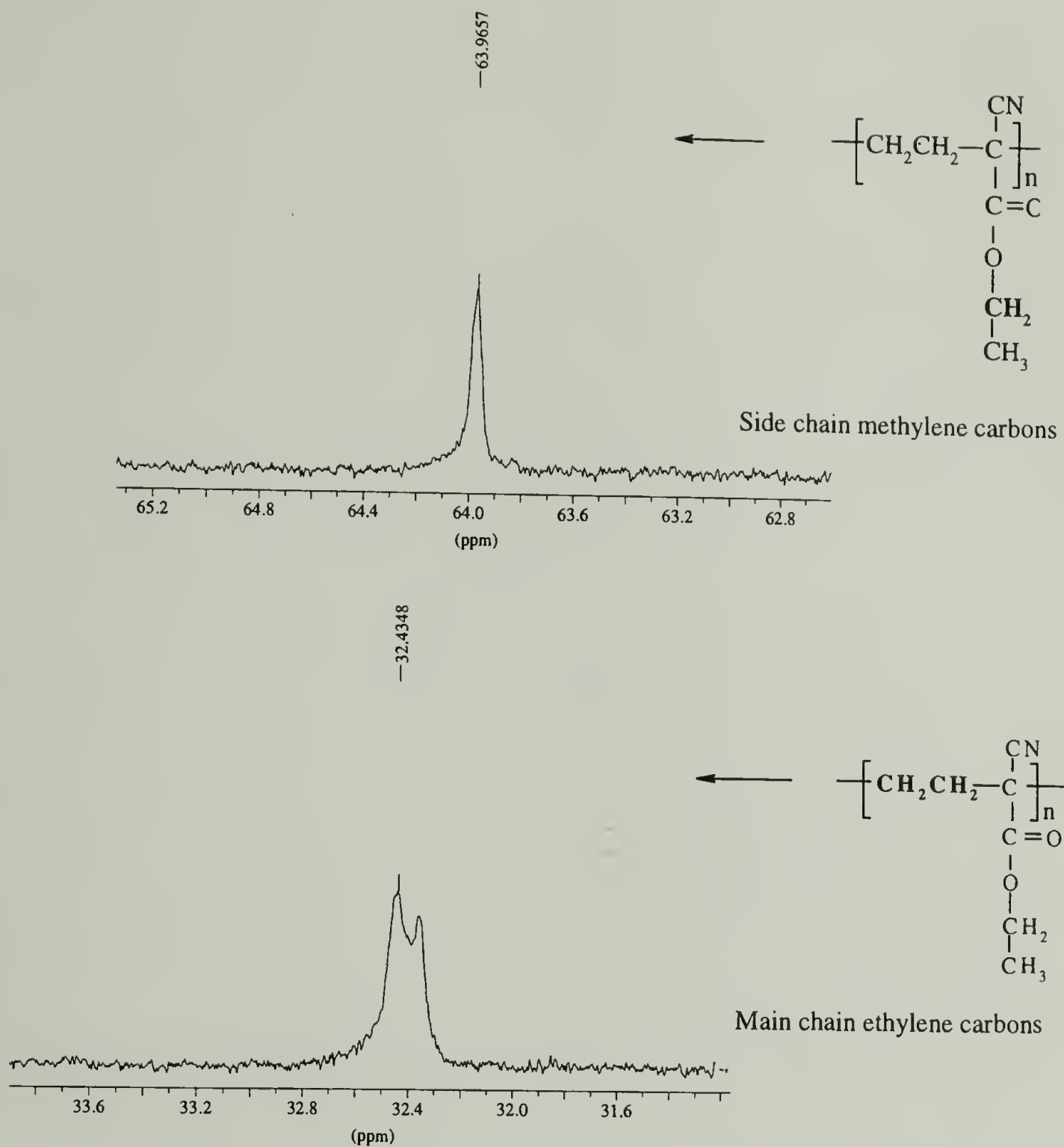


Figure 3.14.  $^{13}\text{C}$ -NMR Spectrum showing the Main Chain Ethylene and Side Chain Methylene Carbons of Poly(2a) (500 MHz NMR).



In order to analyze the above data, the  $^{13}\text{C}$ -NMR spectrum of the model compound (i) was obtained (Figure 3.15). Previous analysis of the  $^1\text{H}$ -NMR spectrum of the model compound confirmed that sample contained a mixture of both *meso* and *dl* diastereomers, with the distinction of resonances for each diastereomer made possible via simulation analysis. However, the  $^{13}\text{C}$ -NMR spectrum of (i) showed that there is little difference in the chemical shifts of the carbons of each diastereomer even at 500 MHz. For the ethylene carbon region at 33.5 ppm, the difference in the resonance is only 10 Hz, while the methylene carbons of the ester are indistinguishable.

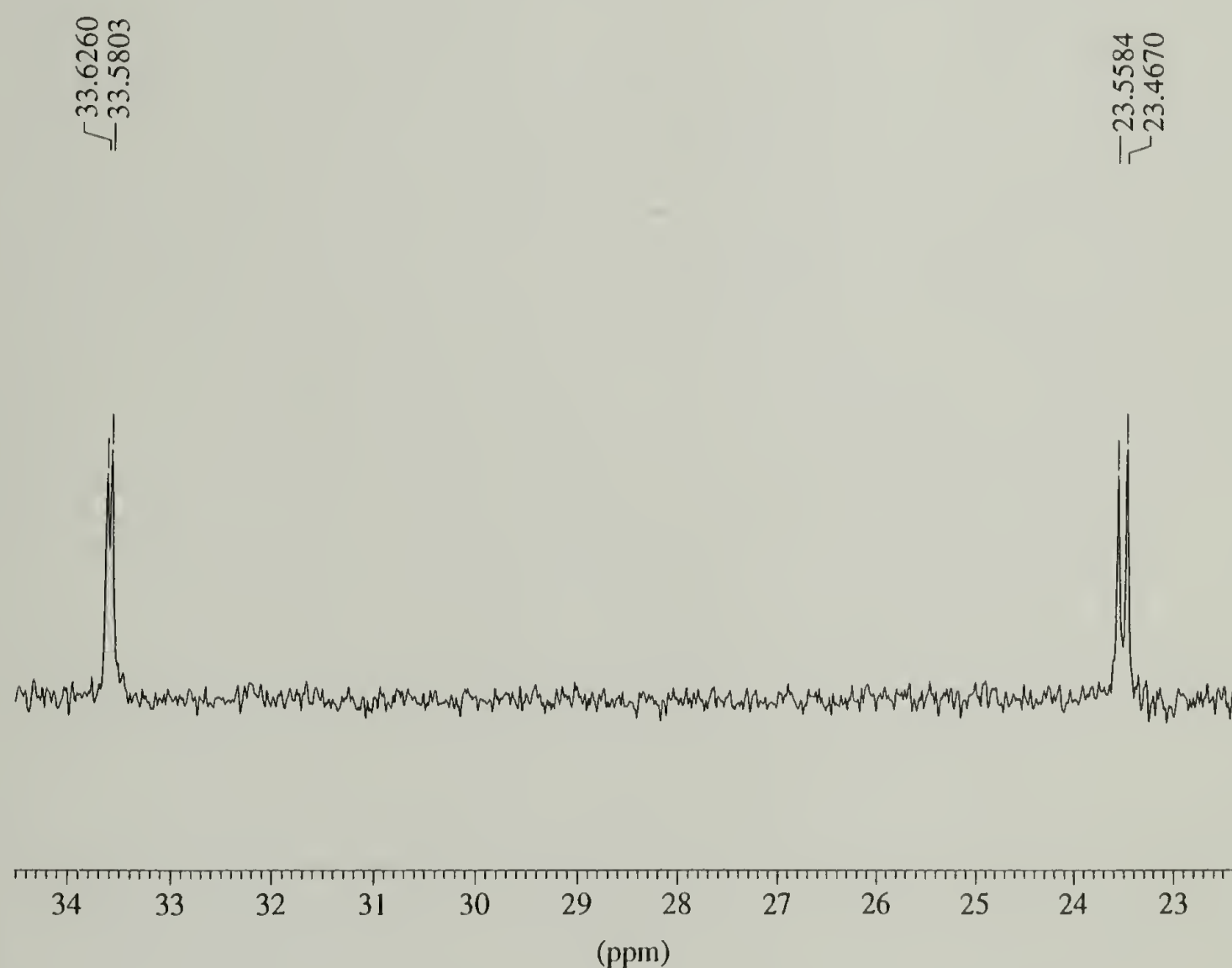


Figure 3.15.  $^{13}\text{C}$ -NMR Spectrum showing the Ethylene Carbons (33 ppm) of the model compound (i). (500 MHz NMR).

Based on the  $^{13}\text{C}$ -NMR spectrum of the model compound, the splitting observed for the peak due to the main chain ethylene carbons of poly(2a) can be attributed to the difference in resonance between the *meso* and *dl* configurations at the diad level. This result is consistent with the findings of the  $^1\text{H}$ -NMR analysis, which provided conclusive evidence for a mixture of *meso* and *dl* diastereomers at the diad level.

In order to distinguish between atacticity and heterotacticity, a higher-level order of sensitivity (such as at the triad or tetrad level) is required. For some polymers such as PMMA,  $^1\text{H}$ -NMR has been used to identify the stereochemical configuration at the triad level.<sup>27</sup> However, for many other polymers such as polypropylene, configurational information could not be unambiguously assigned due to the overlap of the resonances from the various triads.<sup>28</sup> This problem was resolved with the use of  $^{13}\text{C}$ -NMR spectroscopy in the early 1970's. The advantages of  $^{13}\text{C}$ -NMR is the increased range in chemical shift ( $\sim 20\times$  that of  $^1\text{H}$ -NMR).<sup>29</sup> The structural sensitivity is enhanced through the existence of well separated resonances for the different carbon atoms. In many examples, the chemical shifts of the carbons can be dissected in a strictly additive manner, into contributions from neighbouring carbons and constituents. This additive behavior was defined by Grant and Paul.<sup>30</sup> However, in many cases model compounds that closely resemble the polymer structure are needed, which can be synthetically challenging. In  $^{13}\text{C}$ -NMR, the connecting unit sequence can be observed at the diad, triad, tetrad, and sometimes pentad level, with the simplest level being the diad level. However, for the sequence distribution of the greatest utility is the triad level, which provides more information on the long range microstructure of the polymer compared to the diad level.

The general trend among vinyl polymers is that the backbone methylene carbons exhibit greater configurational sensitivity than the methine carbons.<sup>29</sup> For the 1,1-disubstituted poly(trimethylene)s poly(**2a-d**), the additional methylene carbon in the backbone makes a significant difference in the level of sensitivity observed. In order to examine this difference, the diad, triad and tetrad level in the structure of poly(ethyl cyanoacrylate) PECA were compared to poly(**2a**). For the <sup>13</sup>C-NMR spectrum of an atactic sample of poly(ethyl cyanoacrylate) PECA, several signals for the main chain and side chain methylene carbons were observed.<sup>31,32</sup> Since the main-chain methylene and methine carbons have overlapping resonances, these carbons were distinguished using a DEPT pulse sequence for which only carbons bearing hydrogens were observed. The DEPT spectrum of a sample of PECA is shown in Figure 3.16.<sup>31</sup> The peaks between 43-46 ppm correspond to the methylene carbons of the backbone, while the peaks around 65 ppm correspond to the side chain methylene units. The intensities were assigned to the various triads (mm, mr, rr) and tetrads (rrr, mrm, mmm, etc) as indicated. From this spectrum it is clear that the side chain methylene carbons show sensitivity at the triad level, while the main-chain methylene carbons show sensitivity at the tetrad level.

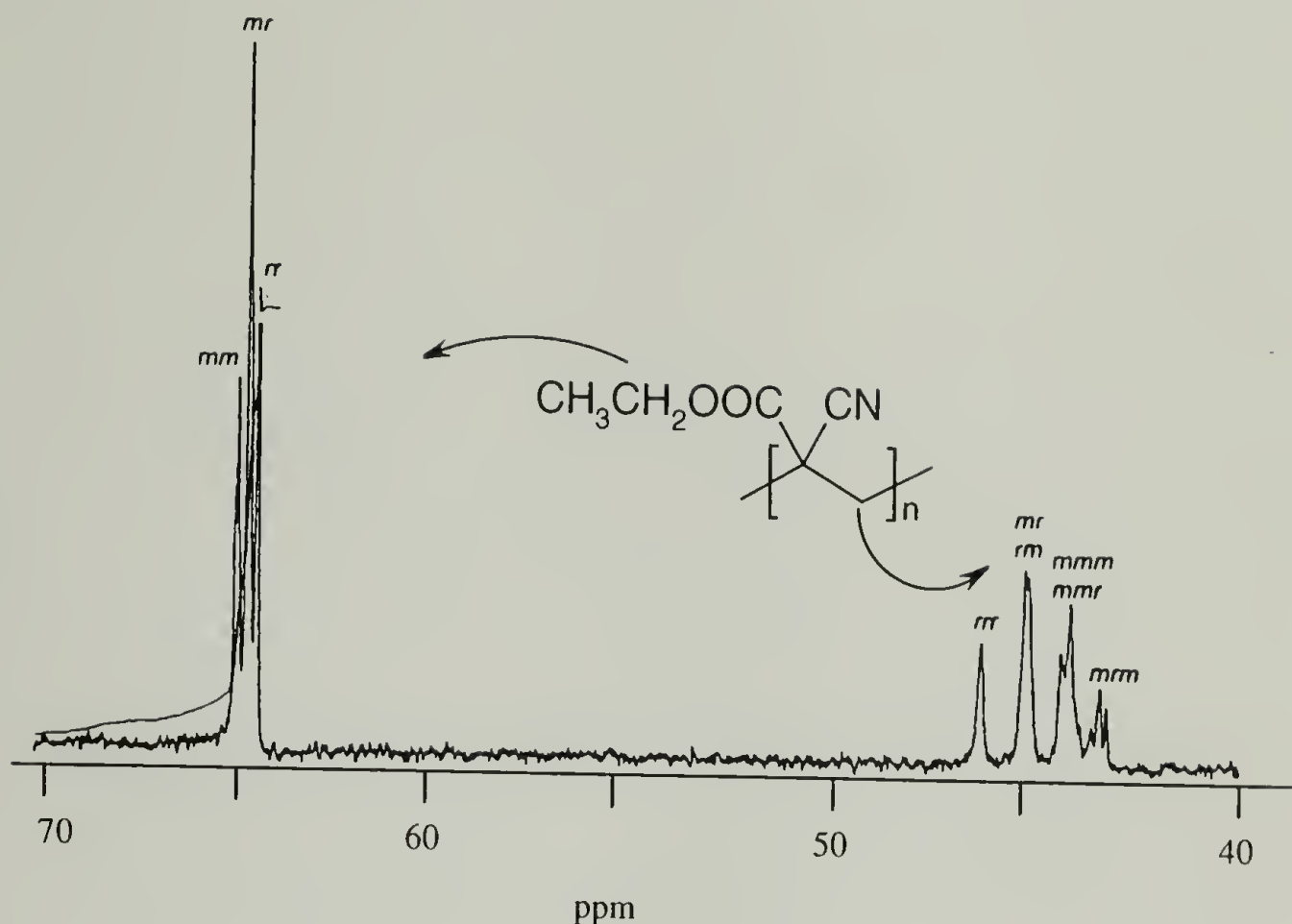


Figure 3.16. DEPT Spectrum of an atactic PECA Sample

In contrast to poly(ethyl cyanoacrylate), the quaternary carbon centers in the backbone of poly(**2a**) are separated by two methylene carbons instead of one. In order to examine the difference between the diad, triad and tetrad sensitivity for the two polymers, the structural symmetry of each carbon atom in the various possible monomer sequences was examined. For the methylene carbons of the backbone of vinyl polymers, the sensitivity is due to an even number of structural units, the simplest being at the diad level. Figure 3.17 demonstrates sensitivity at the diad level for both PECA and poly(**2a**). For PECA, the chiral carbons on each side are adjacent to the methylene carbon. However, for poly(**2a**), the chiral centers are separated by an extra methylene carbon. This distinction is not dramatic at the diad level, however, if the methylene carbons are





Figure 3.18. Triad level sensitivity of the side chain carbons of PECA and Poly(2a)

If more than three peaks are observed, the sensitivity to the *next* nearest neighbour must be considered, and up to 10 unique pentad configurations may be observed. Therefore, it is evident that the contrast in the resolution between PECA and poly(2a) is significantly affected by the additional methylene unit in the backbone structure. For poly(2a), sensitivity of the main chain and side chain methylene carbons at the triad or tetrad level is significantly lower.

3.4.6 Analysis of the stereochemistry of polymerization. The stereochemistry of a polymer is influenced by the reaction conditions during its polymerization. Examples of the influence of reaction conditions on the tacticity of poly(methylmethacrylate) were provided in Section 3.1.2 of this chapter. Another example includes poly(ethyl cyanoacrylate) PECA, for which a sample made with *t*-butyl magnesium bromide initiator displays an equal distribution of stereoisomers, while polymers made by initiation with amines tended towards syndiotacticity.<sup>31</sup> It was proposed that the difference in tacticity between the two samples is attributable to the counterion effect. The counterion influences the chain conformation at the growing end, and may also affect the accessibility of the incoming monomer.

As a result, the influence of various reactions conditions on the tacticity of poly(alkyl 1-cyanocyclopropanecarboxylates) was investigated.

**Results.** Monomers **2a-d** were polymerized under a variety of reaction conditions in order to determine the influence of various parameters on the resulting tacticity of the polymers. The following variables were examined:

*Influence of the counterion.* Thiophenolate salts with potassium, sodium, lithium and tetrabutylammonium counterions were used to polymerize **2a-d**.

*Temperature effects.* The polymerization of **2a** was carried out at ambient temperature, 60, 100, 120 and 140 °C.

*Solvent effects.* The polymerization of **2a** and **2b** were carried out in DMSO, DMF, THF, toluene and acetonitrile.

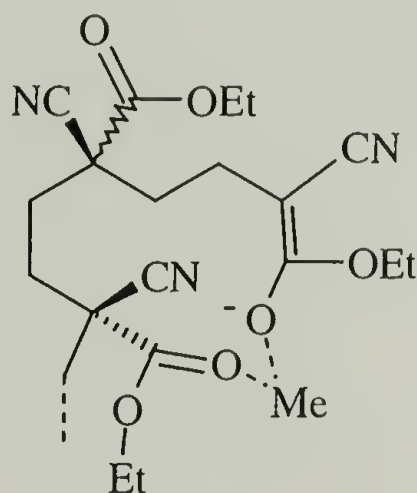
*Polymerization of a monomer containing a chiral ester (enantiomeric mixture).* Sec-butyl 1-cyanocyclopropane **2e** was synthesized and polymerized in DMSO at 60 °C.

The tacticity of the samples was analyzed by examining the ethylene region of the backbone protons using <sup>1</sup>H-NMR spectroscopy as previously described. Analysis of the resulting polymer microstructures indicated that the polymers in all cases were composed of an equal mixture of *meso* and *racemic* diads, regardless of the reaction conditions.

**Discussion.** It is evident from the <sup>1</sup>H-NMR data that there was no observable influence of reaction conditions on the stereochemistry of polymerization of poly(**2a-e**) at the diad level. Unfortunately, due to the lack of a significant experiment(s), we do not have a way to determine whether the stereochemistry at the triad level is influenced by the reaction conditions. From the spectra obtained of these polymers, it is proposed that the 50:50 mixture of *meso* and *racemic* diads present in the microstructure are alternating and

not randomly placed. This is mainly based on the indirect evidence of the crystallinity of these polymers (WAXS data-details in Chapter 6), that suggests that there is a high degree of stereoregularity in the microstructure of poly(**2a-d**).

Based on the above conclusions, it is suggested that the stereochemistry of the polymer chain end unit is determined relative to the penultimate unit upon the addition of incoming monomer. In this case, the formation of a favored 12-membered cycle between the propagating carbanion and the carboxylate group of the penultimate unit (Figure 3.19) Based on classical arguments for ring formation, the 12-membered cyclic intermediate is more favorable kinetically than an 8-membered ring, which would be formed if coordination occurred with the previous unit and not the penultimate unit on the backbone. This results in the alternation of configuration at each stereocenter, yielding a heterotactic polymer microstructure.



Me = metal

Figure 3.19. Proposed 12-membered cyclic intermediate formed during the polymerization of **2a**

sensitive to their next nearest neighbor, then greater differences in tetrad sensitivity will be observed for the two polymers. For poly(**2a**), sensitivity at the tetrad level will not be observed due to the increased distance between the chiral carbon centers from 5 carbons at the diad level to 8 carbons at the tetrad level. Based on the poor sensitivity observed at the diad level for poly(**2a**), the resolution at 500 MHz will most definitely not be good enough to distinguish at the tetrad level.

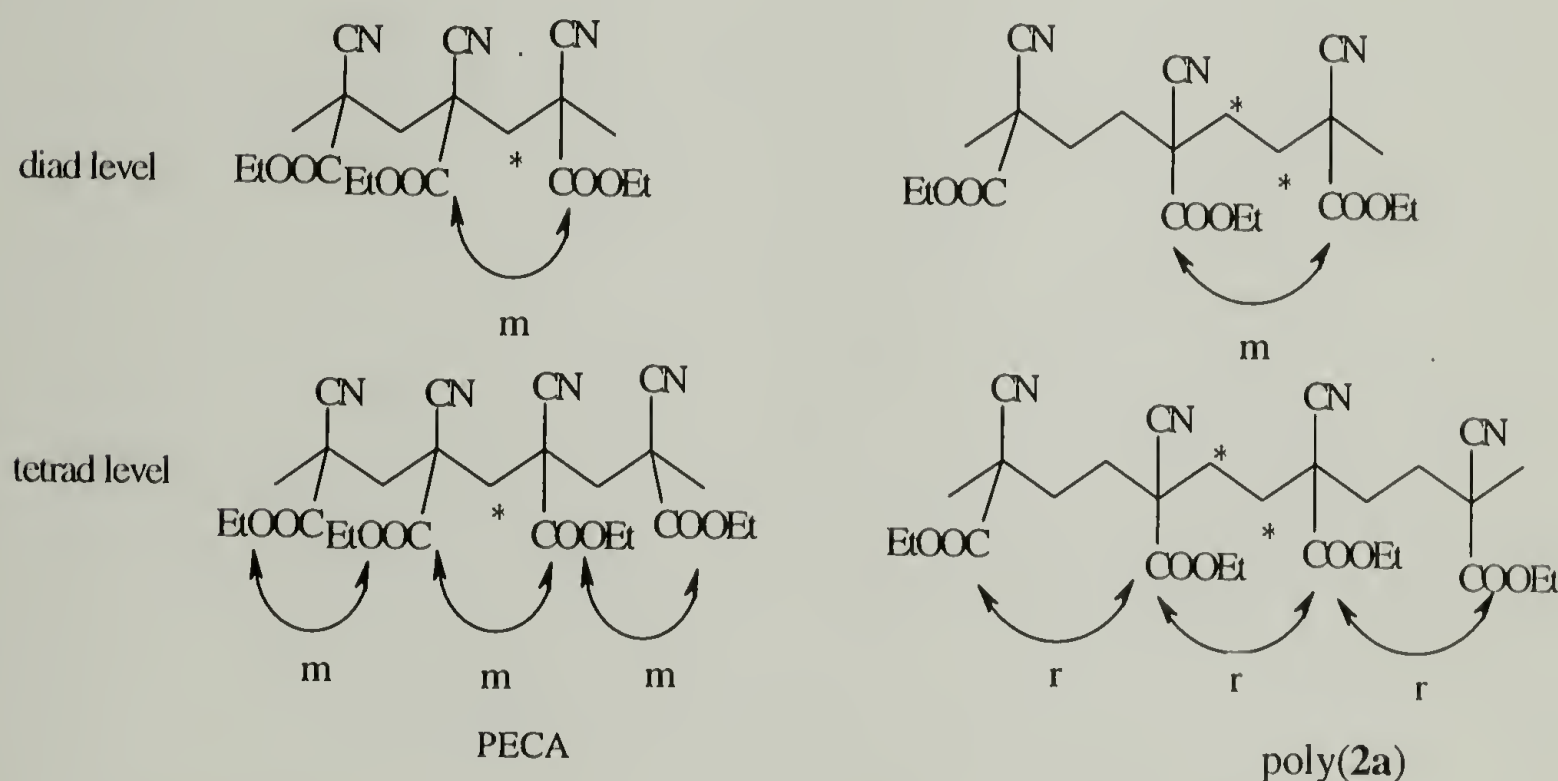


Figure 3.17. Comparison of the diad and tetrad levels of PECA and Poly(**2a**).

Similar differences will be observed for the ester or nitrile substituents on the chain. In this case however, for vinyl polymers, the side chain groups will be configurationally sensitive to an odd sequence of structural units, similar to the methine carbons. For example, Figure 3.18 shows carbonyl atoms on the ester side chains that are sensitive to the nearest neighbor configuration, i.e. sensitivity at the triad level where, three resonances mm, mr, rr are expected.



### 3.5 Conclusions

High temperature  $^1\text{H}$ -NMR analysis combined with simulation experiments provided evidence that the microstructure of samples poly(**2a-d**) is a stoichiometric mixture of *meso* and *dl* diads, suggesting that the polymers are either atactic or heterotactic. Further investigation of the tacticity using  $^{13}\text{C}$ -NMR analysis did not provide conclusive evidence for the stereoregularity beyond the diad level, due to the poor sensitivity afforded by the increased distance between the chiral carbon centers along the poly(trimethylene) backbone. No further experiments that could confirm the tacticity of poly(**2a-d**) beyond the diad level were identified. However, WAXS data provided evidence that poly(**2a-d**) are highly crystalline, which supports the highly ordered heterotactic arrangement of the diads over a disordered atactic microstructure.

Changing the polymerization conditions such as temperature, solvent and counterion did not influence the *meso:dl* ratio at the diad level. In contrast to vinyl polymers, poly(trimethylene)s will require significantly higher resolution in NMR spectroscopy to probe the microstructure beyond the diad level.

### 3.6 References

- (1) Randall, J. C. In *Encyclopedia of Polymer Science and Engineering*; Mark, H., Bikales, N. M., Overberger, C. G., Menges, G., Kroschwitz, J. I., Eds.; Wiley-Interscience: New York, 1985; Vol. 9, p 797.
- (2) IUPAC Macromolecular Division, Commission on Macromolecular Nomenclature, *Compendium of Macromolecular Nomenclature*, Blackwell Scientific: Oxford, 1991.
- (3) Natta, G.; Danuso, F.; Sianesi, D. *Makromol. Chem.* **1959**, 30, 238.
- (4) Natta, G.; Pino, P.; Corradini, P.; Danusso, F.; Mantica, E.; Mazzanti, G.; Moraglio, G. *J. Am. Chem. Soc.* **1955**, 77, 1708.
- (5) Natta, G. P., I.; Zambelli, A.; Gatti, G. *J. Polym. Sci.* **1961**, 51, 387.

- (6) Natta, G.; Danuso, F.; Sianesi, D. *Makromol. Chem.* **1958**, 28, 253.
- (7) Natta, G. *J. Polym. Sci.* **1955**, 16, 143.
- (8) Hatada, K.; Kitayama, T.; Ute, K. *Prog. Polym. Sci.* **1988**, 13, 189.
- (9) Yuki, Y.; Hatada, K. *Adv. Polym. Sci.* **1979**, 31, 1.
- (10) Hatada, K.; Ute, K.; Tanaka, K.; Okamoto, Y.; Kitayama, T. *Polym. J.* **1986**, 18, 1037.
- (11) Kitayama, T.; Zhang, Y.; Hatada, K. *Polym. J.* **1994**, 26, 868.
- (12) Hatada, K. *J. Polym. Sci., Part A: Polym. Chem.* **1999**, 37, 245.
- (13) Nakano, T.; Mori, M.; Okamoto, Y. *Macromolecules* **1993**, 26, 867.
- (14) Kitayama, T.; Masuda, E.; Yamaguchi, M.; Nishiura, T.; Hatada, K. *Polym. J.* **1992**, 24, 81.
- (15) Semen, J.; Lando, J. B. **1969**, 2, 570.
- (16) Tonelli, A. E. In *NMR Spectroscopy and Polymer Microstructure: the conformational connection*; VCH: New York, 1989.
- (17) Bovey, F. A. In *Chain Structure and Conformation of Macromolecules*; Academic Press: New York, 1982.
- (18) Bowic, J. H.; Williams, D. H.; Madsen, P.; Schroll, G.; Lawesson, S. O. *Tetrahedron* **1967**, 23, 305.
- (19) Casini, G.; Ferappi, M.; Pietroni, B. R. *Tetrahedron* **1972**, 28, 1497.
- (20) Castellano, S. *LAOCN3* **1972**, Mellon Institute, Pittsburg USA.
- (21) Jung, D.; Bothner-By, A. A. *J. Am. Chem. Soc.* **1964**, 86, 4025.
- (22) Karplus, M. *J. Chem. Phys.* **1956**, 30, 11.
- (23) Schwarcz, J. A.; Perlin, A. S. *Can. J. Chem.* **1972**, 50, 3667.
- (24) Lemieux, R.-U.; Nagabhushan, T. L.; Paul, B. *Can. J. Chem.* **1972**, 50, 773.
- (25) Emsley, J. W.; Feeney, J.; Sutcliffe, L. H. *High Resolution Nuclear Magnetic Resonance*; Pergemon: London, 1965; Vol. II.

- (26) Hansen, P. E. *Prog. Nucl. Magn. Reson. Spectros.* **1981**, *14*, 175.
- (27) Bovey, F. A.; Tiers, G. V. D. *J. Polym. Sci.* **1960**, *44*, 173.
- (28) Bovey, F. A. In *Polymer Conformation and Configuration*; Academic Press: NY, 1969; p 32.
- (29) Randall, J. C. In *Carbon-13 NMR and Polymer Stereochemical Configuration, ACS Symposium Series*; Pasika, W. M., Ed.: Washington, D.C., 1979; pp 291-318.
- (30) Grant, D. M.; Paul, E. G. *J. Am. Chem. Soc.* **1964**, *86*, 2984.
- (31) Robello, D. R.; Eldridge, T. D.; Michaels, F. M. *J. Polym. Sci., Part A: Polym. Chem.* **1999**, *37*, 2219.
- (32) Fawcett, A. H.; Guthrie, J.; Otterburn, M. S.; Szeto, D. S. *J. Polym. Sci., Part C: Polym. Lett.* **1988**, *26*, 459.

## RING-OPENING POLYMERIZATION OF CYCLOBUTANES

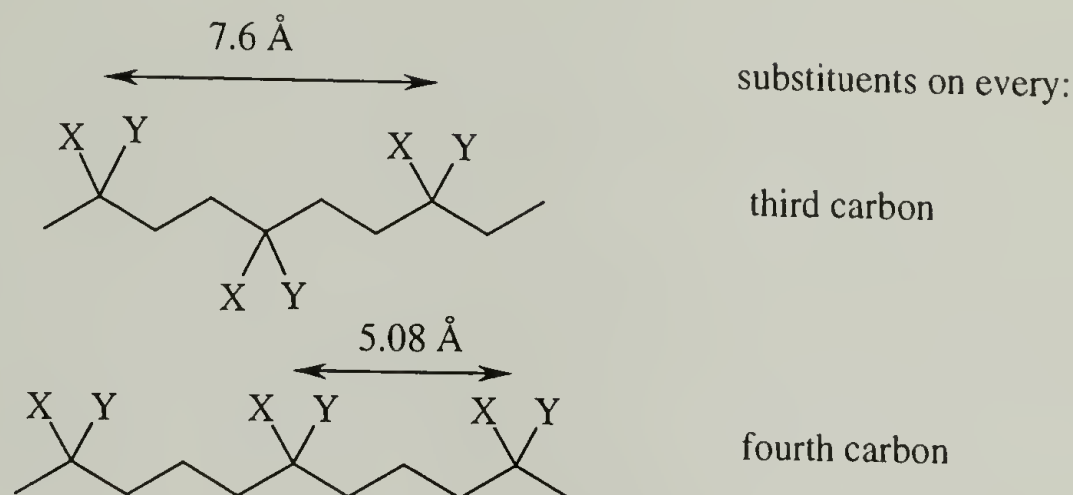
## 4.1 Introduction

In an effort to obtain synthetic control over the location of substituents on every fourth atom along the backbone of carbon-chain polymers, the synthesis of 1,1-disubstituted poly(tetramethylene)s ( $\text{CH}_2\text{CH}_2\text{CH}_2(\text{CXY})_n$ ) was attempted via the ring-opening polymerization of activated cyclobutanes. The purpose of the work presented in this chapter was to investigate the reactivity of several 1,1-disubstituted cyclobutanes towards anionic ring-opening polymerization. The activated cyclobutanes include dialkyl 1,1-cyclobutanedicarboxylates (**5a-c**), ethyl 1-cyanocyclobutanecarboxylate (**6**), and 1,1-dicyanocyclobutane (**8**). Comparisons of their polymerizability were made with similarly activated cyclopropane monomers presented in chapter 2 of this dissertation and previously investigated in our group<sup>1,2</sup>

Carbon-chain polymers with substituents on every fourth carbon atom along the backbone provide a unique structure that would allow highly polar and/or bulky ester substituents to be placed at regular intervals along the backbone. In theory, the distance between these substituents (assuming an all trans conformation of the backbone) increases from 2.54 Å (for a vinyl architecture) to 5.08 Å. In addition, with this substitution pattern, the moieties are not oriented in an alternating mode along the backbone (up and down) as in the case of the polymers with substituents on every third carbon with an all-trans conformation (Scheme 4.1). Instead, the substituents assume a position on the same side of the backbone (always up or always down), providing a non-



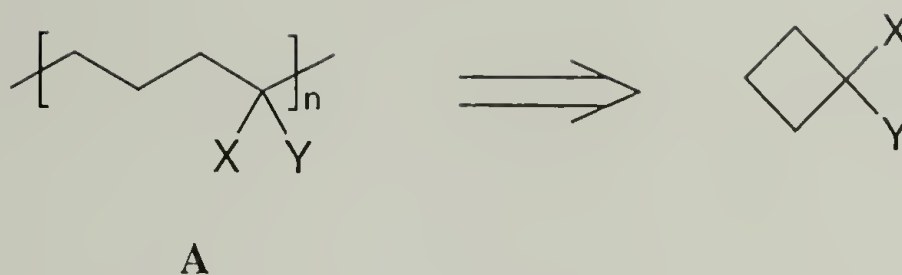
centrosymmetric environment for the side-substituent(s). This is crucial in applications requiring the specific co-alignment of substituents such as pyro- and piezoelectricity or some non-linear optical properties.



Scheme 4.1. Carbon-chain polymers with substituents on every third and every fourth carbon atom

From a retrosynthetic point of view, one of the ways to achieve the target polymer (A) is via the ring opening of 1,1-difunctionalized cyclobutanes (Scheme 4.2). The cyclobutane ring has a strain energy ( $26.5 \text{ kcal}\cdot\text{mol}^{-1}$ ) that is similar to cyclopropane ( $27.5 \text{ kcal}\cdot\text{mol}^{-1}$ ). It is the relief of this ring strain that provides the thermodynamic driving force for the ring-opening polymerization of the cyclic monomers. Previous reports on the polymerization of highly functionalized cyclobutanes with strong activating electron-withdrawing and electron-donating substituents (section 4.2) suggested that these polymerizations might be feasible.<sup>3-5</sup>

In order to determine the feasibility of polymerization of cyclobutanes via ring-opening, thermodynamic and kinetic factors were considered. The chemistry of cyclobutanes will be examined and compared to cyclopropanes, in order to gain a better understanding of the reactivity of these small alkanes towards polymerization.



Scheme 4.2. Ring-Opening Polymerization of Functionalized Cyclobutanes

## 4.2 Background: The Chemistry of Cyclobutanes

### 4.2.1 Structure and Bonding

A planar structure for the cyclobutane ring was accepted by organic chemists for many years.<sup>6</sup> However, a “bent” or “folded” cyclobutane ring has gained increasing acceptance based on experimental evidence.<sup>7</sup> X-ray and electron diffraction studies indicate that the three main conformations are the  $D_{4h}$  planar,  $D_{2d}$  non-planar and  $D_{2d}$  planar (Figure 4.1). Unsubstituted cyclobutanes tend to display a folded ring  $D_{2d}$  symmetry. Electron diffraction and X-ray studies on a variety of substituted cyclobutanes such as octafluorocyclobutane also show evidence of the same  $D_{2d}$  non-planar conformations.

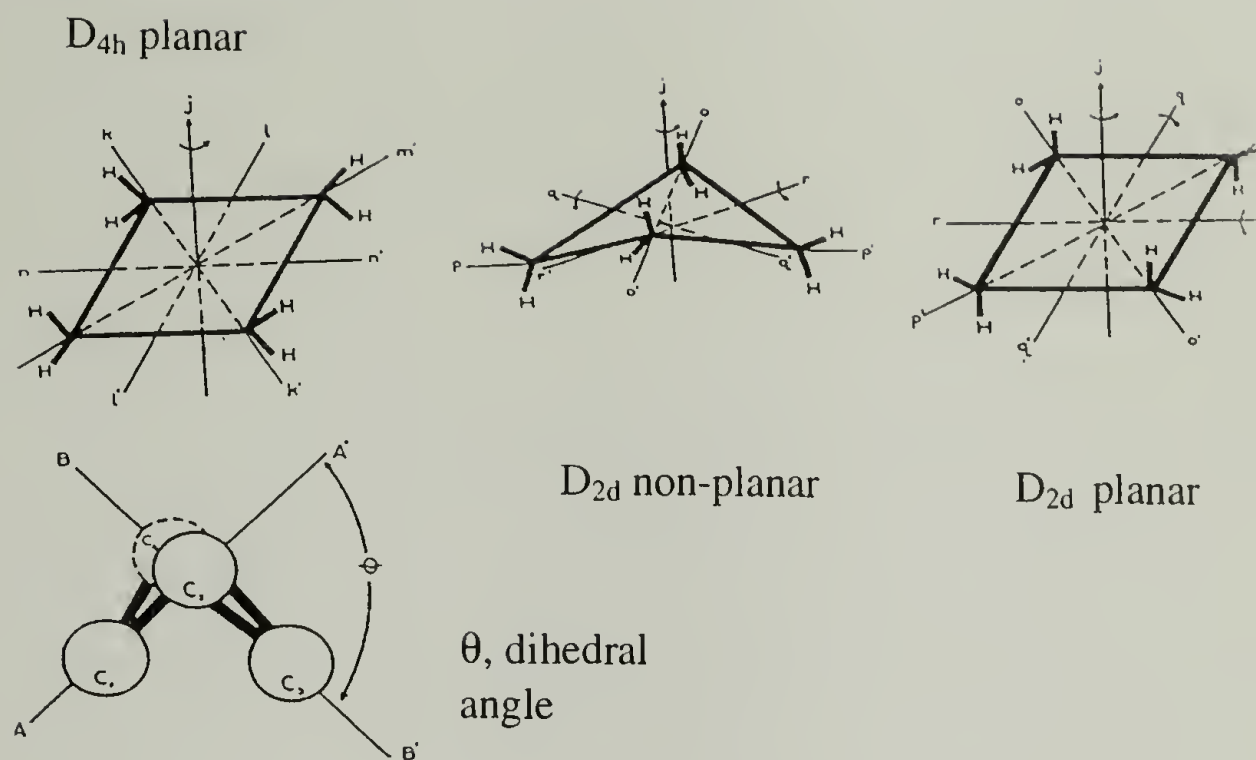
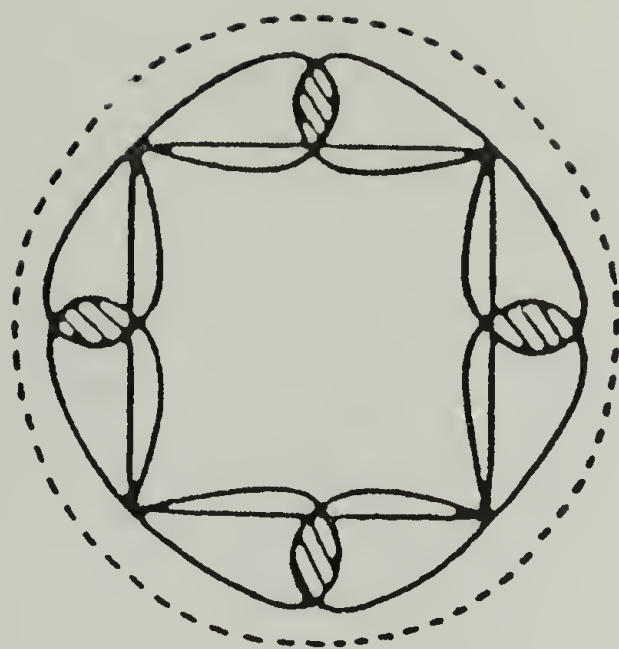


Figure 4.1. Conformations of cyclobutane

According to the model proposed by Möffitt for cyclopropanes, the orbitals are not regular  $sp^3$  hybridized (as for tetrahedral carbons), but actually bent outward (by  $22^\circ$ ) from the hypothetical inter-nuclear straight line.<sup>8</sup> This effect is also present in cyclobutanes, but to a lesser extent of 20% as compared to cyclopropane (Figure 4.2). The resulting poor overlap of the orbitals provides a certain amount of electron delocalization ( $\pi$  character), which contributes to the stability of the ring bonds. The residual  $\pi$  orbital is shown by the dotted lines in Figure 4.2. Similar to the cyclopropane rings, the inherent  $\pi$  character (“ethylene like behavior”) of the bent bonds is empirically known. This molecular orbital analysis of cyclobutanes explains some of its unusual reactivity, but does not explain others like its stability to oxidizing agents such as ozone.<sup>9</sup>



Cyclobutane  
(top view)

//// : area of carbon orbital  
overlap

Figure 4.2. "Bent" orbitals of the cyclobutane ring

#### 4.2.2 Reactivity in Ring-Opening Reactions: Comparison with Cyclopropanes

As previously mentioned, a cyclobutane ring has a similar strain energy of 26.5 kcal mol<sup>-1</sup>, compared to 27.5 kcal mol<sup>-1</sup> for a cyclopropane ring. This similarity in strain energies is generally true irrespective of the constitution of the rings, provided the atoms are singly bonded.<sup>10,11</sup> For example, the energy required for the homolytic C-C cleavage of  $c\text{-(CH}_2\text{)}_{n+2} \rightarrow \cdot\text{CH}_2(\text{CH}_2)_n\text{CH}_2\cdot$  is 61 kcal·mol<sup>-1</sup> for  $n = 1$  (cyclopropane) and 62.5 kcal·mol<sup>-1</sup> for  $n = 2$  (cyclobutane).<sup>12</sup>

Even though cyclobutane rings exhibit bond strain energies similar to cyclopropanes, they are much less reactive towards ring-opening.<sup>10</sup> This trend is also true for heterocycles (such as oxirane vs. oxetane). Since the ring-opening of unsubstituted three- and four membered rings is kinetically unfavorable, additional



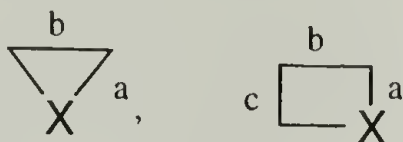
activating groups on the ring or a change in the nature of the ring (heterocycles) are necessary to activate these cycles. Studies on the ring-opening of similarly activated three- and four-membered rings showed that cyclobutanes are up to 3-4 orders of magnitude less reactive than their cyclopropane analogues.<sup>13</sup> For example, the ring-opening of 1-cyano-2-phenylsulphonyl-methylcyclobutane is  $4.8 \times 10^3$  times slower than for the cyclopropane analogue. In some cases, variations of 7-9 orders of magnitude in the rate constants between three- and four-membered rings towards ring-opening have been reported.<sup>14</sup>

Thermodynamic considerations do not completely explain the relative inertness of the four-membered rings relative to cyclopropanes.<sup>15</sup> Studies showed that the differences in enthalpies of activation for ring fission between cyclopropane and cyclobutane greatly exceed the overall ring strain energy difference.<sup>14</sup> This difference in reactivity was attributed to a difference in the mode of strain release in the two compounds.<sup>16</sup> A simple molecular mechanics calculation of the ring strain as a function of bond extension (leading to the strain-free open-chain structure) showed that the release of the strain for a given bond extension is less for cyclobutane than for cyclopropane, except at very small extensions. This difference was accounted for by the varying components of strain. For cyclopropane, 75% of the excess enthalpy is attributed to valence deformation (angle) strain and 25% to torsional strain. For cyclobutanes, 50% is due to the contribution of 1,3 non-bonded interactions and the remainder due to the valence deformation and torsional strain.<sup>17,18</sup>

### 4.2.3 Comparison of Three- and Four-membered ring Heterocycles

A summary of the strain energies, bond angles and bond lengths of various three- and four-membered saturated cycles is shown in Table 4.1. It is evident that irrespective of constitution, both the rings have very similar strain energies, as long as all the bonds are single. With the exception of sulfur-heterocycles, the ring strain of cycloalkanes and cyclic ethers vary by only 1-2 kcal·mol<sup>-1</sup>.

Table 4.1. Strain Energies (kcal·mol<sup>-1</sup>), Bond Angles and Bond Lengths of Three and Four- Membered Cycles<sup>19</sup>




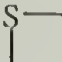


	X = (CH <sub>2</sub> )		X = O		X = S	
(CH <sub>2</sub> ) <sub>n</sub>	n = 2	n = 3	n = 2	n = 3	n = 2	n = 3
Ring Strain (kcal·mol <sup>-1</sup> )	27.5	26.5	27.3	25.5	19.8	19.6
Bond lengths (Å)						
a	1.51		1.44	1.443	1.815	1.847
b	1.51		1.47	1.517	1.484	1.549
c			1.44	1.517	1.815	1.549
d				1.443		1.847
Bond Angles (°)						
ca	60		61.24	90.5	48.3	76.8
ab	60		59.18	91.89		90.6
bc			59.18	85.0		95.6
da				92.61		90.6

Despite their similar strain energies, cyclobutane heterocycles are generally up to 3-4 orders of magnitude less reactive towards ring-opening than their cyclopropane analogues. For example, Sterling and coworkers studied the reactivity of some three- and

four-membered heterocycles.<sup>16</sup> In this study, a higher reactivity of oxirane and thiirane by several orders of magnitude in comparison to their four-membered ring analogues was demonstrated. The results for a nucleophilic addition using a thiosulfate ion are summarized in Table 4.2.

Table 4.2 Nucleophilic fission of strained saturated heterocycles<sup>16</sup>

		
$k_{\text{rel}}^{\text{a}}$ (120°)	1	$5.4 \times 10^{-4}$
strain energy (kcal·mol <sup>-1</sup> )	27.3	25.5
		
$k_{\text{rel}}^{\text{a}}$ (120°)	0.8	$3.7 \times 10^{-5}$
strain energy (kcal·mol <sup>-1</sup> )	19.8	19.6

<sup>a</sup> Reactions in sodium thiosulphate-water. Values for 3- and 4- rings extrapolated from values at *ca* 50°.

These results were similar to previous studies on hydroxyl ion reactions,<sup>20</sup> but showed a much larger difference in reactivity. Again, the small difference in the total strain energy between the two heterocycles does not account for the large difference (orders of magnitude) in reactivity. As discussed in the previous section (section 4.2.2), it is believed that the difference in reactivity is accounted for, at least in part, by the difference in distribution of the strain in four-membered rings compared to the three-membered rings.

## 4.2.4 Polymerizability of Cyclobutanes

### 4.2.4.1 Thermodynamics of Polymerization

The free energy of polymerization ( $\Delta G_{lc}$ ) for cyclobutanes was estimated from thermodynamic data at 298 K and determined to be largely negative: ( $\Delta G_{lc} = -21.2$  kcal·mol<sup>-1</sup>). (Table 2.2, Section 2.2.4.1).<sup>21,22</sup> This  $\Delta G_{lc}$  for cyclobutanes is very close to the value determined for cyclopropane (-22.1 kcal mol<sup>-1</sup>), and strongly favors the ring-opening polymerization of cyclobutanes from a thermodynamic viewpoint. Similar to cyclopropanes, the relief of the ring strain provides the potent thermodynamic driving force for the ring-opening polymerization.

### 4.2.4.2 Kinetics of Polymerization

Even though thermodynamics strongly favor the ring-opening polymerization of cyclobutanes, a suitable reaction pathway must exist for these monomers (and their derivatives), for polymerization to occur. Unsubstituted cyclobutanes, like cyclopropanes, but contrary to polar four-membered rings such as oxetanes or lactones, do not polymerize because of the lack of polarizability in potentially cleavable bonds.<sup>22</sup> In chapter 2, it was demonstrated that adding activating electron-withdrawing and/or electron-donating groups on cyclopropane, provided a mechanism for electron transfer from nucleophilic to electrophilic centers. These substituents also serve to stabilize the propagating centers upon ring-opening. In this chapter, attempts to polymerize similarly activated cyclobutanes is described.

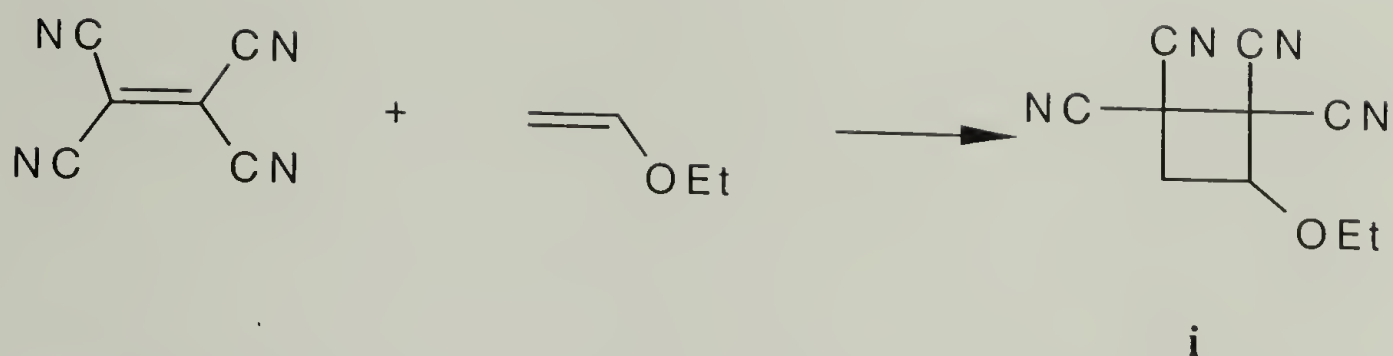


#### 4.2.5 Ring-Opening Polymerization of Cyclobutanes: Literature Survey

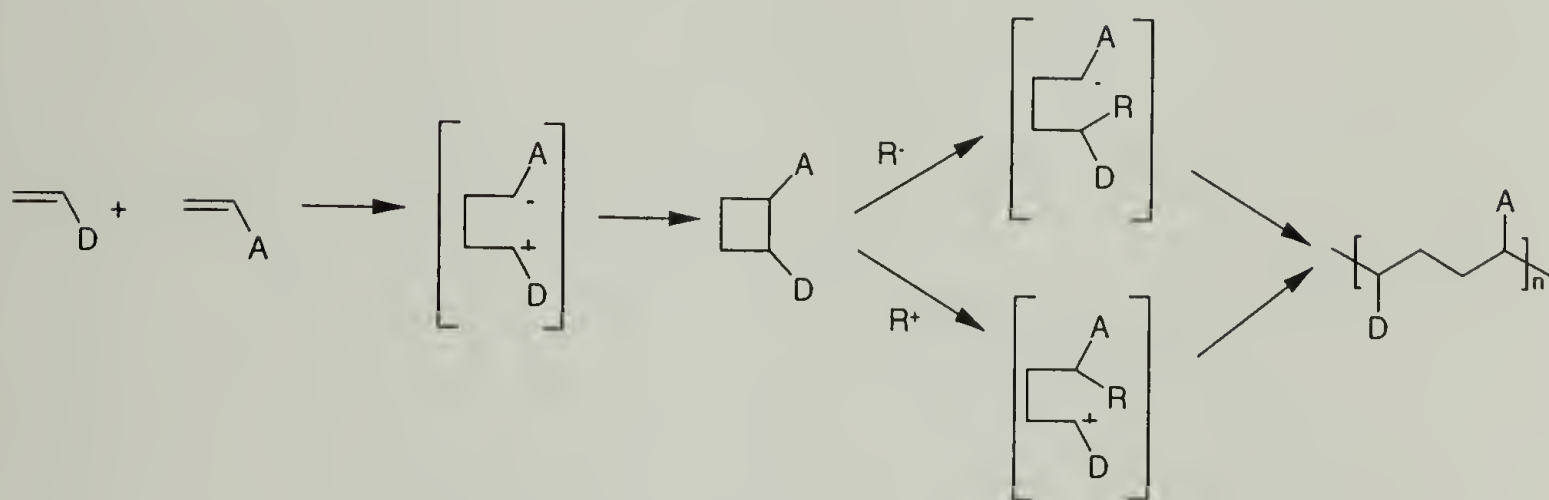
As previously mentioned, the reactivity of cyclobutanes towards ring-opening reactions is several orders of magnitude less than for cyclopropane rings.<sup>13</sup> Therefore, it was expected that cyclobutane rings must be highly activated or harsher reaction conditions must be used in order to favor their polymerization. In comparison to cyclopropanes, there are relatively fewer examples of ring-opening polymerization (oligomerization) available in the literature for cyclobutanes. Several examples of these polymerizations are provided in the discussion in following.

##### 4.2.5.1 Anionic Polymerization

The spontaneous thermal reaction of electron-rich olefins with electron-poor olefins forms a variety of small organic molecules and polymers. For example, the spontaneous reaction of tetracyanoethylene (TCNE) with ethyl vinyl ether (EVE) yields a cyclobutane adduct via zwitterionic tetramethylene derivatives (Scheme 4.3).<sup>23,24</sup> Since these cyclobutanes are derived from zwitterionic tetramethylenes, they can undergo both anionic and cationic ring-opening polymerizations (Scheme 4.4).<sup>5</sup> For example, the anionic polymerization of 1,1,2,2-tetracyano-3-ethoxycyclobutane **i** can be achieved at ambient temperature using various initiators such as triethylamine and various sodium salts such as CH<sub>3</sub>ONa. Polymers with moderate molecular weights ( $\overline{M}_n = 17$  K, GPC, DMF, PS standards) and broad PDI's (1.65-2.12) were obtained.



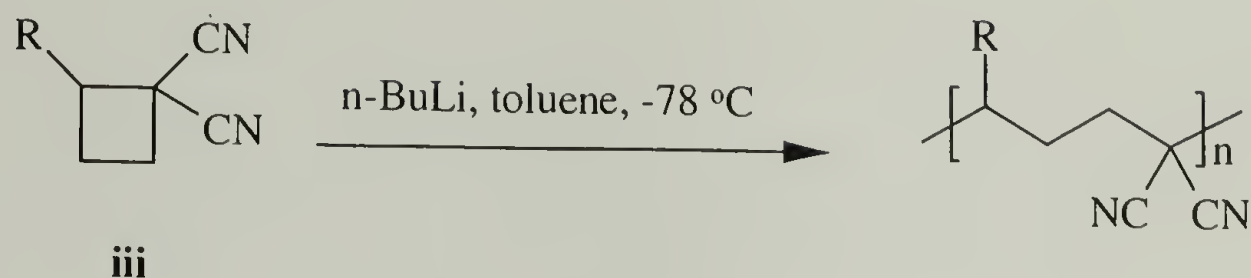
Scheme 4.3. Spontaneous reaction of TCNE and EVE to yield 1,1,2,2-tetracyano-3-ethoxycyclobutane (i)



Scheme 4.4. Ring-Opening Polymerization of Cyclobutanes

Individual reports have also been published on the ring-opening polymerization of activated cyclobutanes such as 1-isobutoxy-2-nitrocyclobutane **ii**<sup>4</sup> and 1,1-dicyano-2-ethoxycyclobutane **iii**.<sup>3</sup> The polymerization of **iiia** was carried out in DMSO using NaCN at 25 °C and in toluene using n-BuLi at -78 °C (Scheme 4.5). However, under these conditions, viscosity measurements suggest that only low molecular weights polymers were obtained. Monomer **iiib** failed to polymerize anionically under equivalent conditions. It was suggested that this was due to the lack of sufficient activation of the cyclobutane ring, given the phenyl group is a relatively poor electron-donating group in comparison to the ether group.

The electron-donating and electron-withdrawing substituents activate the ring by the heterolytic polarization of the 1,2 bond as described in Scheme 4.4. Both monomers are inert to radical polymerization.



**iiia** : R = OEt

**iiib** : R = C<sub>6</sub>H<sub>5</sub>

Scheme 4.5. Ring-Opening Polymerization of **iii**.

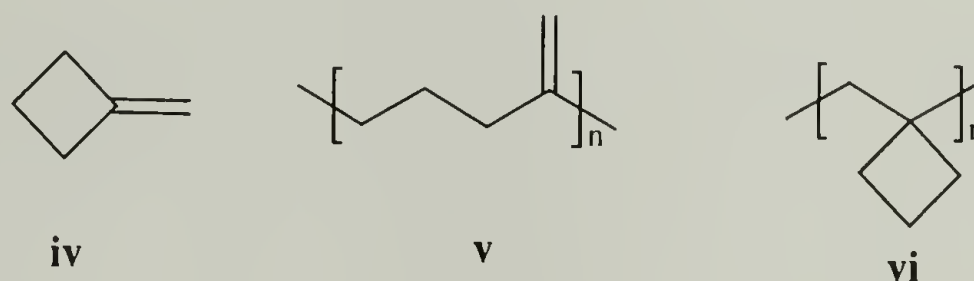
#### 4.2.5.2. Cationic Polymerization

Activated monomers derived from zwitterionic intermediates can also undergo cationic ring-opening polymerizations. Protic acids do not polymerize **i** at all. However, moderate molecular weight polymers ( $\overline{Mn} = 30$  K) were obtained when weaker Lewis acids such as ZnX<sub>2</sub> (X= Cl, Br, I) were used as initiators. The cationic polymerization of oxacyclobutanes (oxetanes) has been reported and is discussed under polymerization of heterocyclic cycles (Section 4.2.5.4).

#### 4.2.5.3 Coordination Polymerization

The ring-opening polymerization of methylene cyclobutane **iv** using heterogeneous Ziegler-Natta catalysts was reported to undergo sluggish reactivity at 25 °C. Low molecular weight polymers with mixed ring-opened (**v**) and unopened structures (**vi**) were observed (Scheme 4.6).<sup>25-27</sup>

Using the Ring-Opening Metathesis Polymerization (ROMP) catalyst  $(1,2\text{-Me}_2\text{C}_5\text{H}_3)_2\text{ZrMe}^+\text{MeB}(\text{C}_6\text{F}_5)_3^-$ , the polymerization proceeds rapidly at 20 °C in toluene to yield polymethylenecyclobutene of exclusively the ring-opened structure (v) ( $\geq 95\%$ ) with quantitative conversion.<sup>28</sup>



Scheme 4.6. Ring-opening polymerization of methylene cyclobutane (iv)

The ring-opening polymerization of various cyclobutenes have also been reported using ROMP catalysts. For example, the polymerization of 3,3-dipropylcyclobutane was achieved using the Schrock initiator  $\text{Mo}(=\text{CHR})(=\text{NAr})(\text{OR}')_2$  where R is  $\text{C}_6\text{H}_5\text{C}(\text{Me})_2$ -, Ar is 2,6-diisopropyl phenyl and R' is  $(\text{Me})_3\text{C}$ .<sup>29</sup> Polymers of medium molecular weights ( $\overline{Mn} = 51,700$ ) were obtained with a PDI of 1.27. The polymerization is completely regiospecific (HT) and stereospecific (trans).

#### 4.2.5.4 Polymerization of three- and four-membered Heterocycles

Ethylene oxide (oxirane) is the only cyclic ether that is readily polymerized by both anionic and cationic mechanisms due to its unusual electronic structure.<sup>30</sup> The polymerization of oxirane under anionic conditions can even be achieved using sodium hydroxide.<sup>31,32</sup> Under cationic conditions, oxirane readily polymerizes using Lewis acids such as  $\text{BF}_3$  or  $\text{AlCl}_3$ . However, the cationic polymerization is characterized by side reactions (mainly cyclization), due to the higher basicity of the linear ether group in the



polymer chain compared to the epoxide monomer.<sup>33</sup> Unlike oxiranes, oxacyclobutanes do not polymerize anionic conditions. However, one exception is the polymerization of oxetane with amorphous zinc dimethoxide. It was suggested that coordination of the oxetane to the catalyst facilitates the nucleophilic attack of the growing species on the monomer.<sup>34</sup> Under cationic conditions, oxacyclobutanes polymerize in the presence of catalytic quantities of  $\text{BF}_3$  to yield a mixture of linear polyether and cyclic tetramer.<sup>35</sup>

Three-membered rings with a sulfur heteroatom (thiirane) are also highly reactive and polymerize by initiation with a variety of nucleophiles such as sodium ethoxide/thiophenolate, or potassium t-butoxide.<sup>30</sup> However, the polymer is insoluble in most solvents even at high temperature, resulting in heterogeneous reaction conditions and limitations in molecular weight determination. Thiiranes also readily polymerizes under cationic conditions using Lewis acids or strong acids such as  $\text{HCl}$ . Unlike oxetane, thietane polymerizes under both anionic and cationic conditions.<sup>36</sup> Specific initiators such as thiolates with bulky counterions (such as tetrabutyl(ethyl)ammonium) are effective initiators for the initiation of thietane at room temperature.<sup>37</sup> On the other hand, anionic initiators such as Grignard reagents are very slow initiators, requiring days at  $70\text{ }^\circ\text{C}$  or hours at  $100\text{ }^\circ\text{C}$ .<sup>38</sup> Thietanes also readily polymerize under cationic conditions when initiated with strong acids at room temperature, or using Lewis acids such as  $\text{BF}_3\cdot\text{OEt}_2$ . For both cyclic ethers and sulfides, 3-membered rings are much more reactive than 4-membered rings.

## 4.3 Ring-Opening Polymerization of 1,1-Disubstituted Cyclobutanes

### 4.3.1 Experimental

#### Measurements

Solution NMR spectra were recorded on a Bruker 300 spectrometer in  $\text{CDCl}_3$  using TMS as the internal reference for  $^1\text{H}$ -NMR and  $\text{CDCl}_3$  for  $^{13}\text{C}$ -NMR. IR spectra were recorded on a BioRad FTS 175C FT-IR spectrometer and elemental analysis was performed at the Microanalytical Laboratory of the University of Massachusetts, Amherst. Melting point determinations were made using an Electrothermal melting point apparatus.

#### Materials

Methyl, ethyl and diisopropyl malonate (99+%), ethyl cyanoacetate (98%) and 1,3-dibromopropane (99%) were obtained from Aldrich and used without further purification. Potassium carbonate (anhydrous, p.a.) was obtained from Acros. DMSO used for the polymerization reactions was purified by distillation under vacuum (40 °C/2mm Hg), discarding the first and last 25%, and drying over 4Å molecular sieves.

**General Procedure for the Synthesis of Dialkyl Cyclobutane-1,1-Dicarboxylates 5a-c.** The corresponding dialkyl malonate (0.456 mol), 1,3-dibromopropane (96.71g, 0.479 mol), potassium carbonate (374g, 2.70 mol) and 510 mL DMSO were mixed into a round bottom flask equipped with a mechanical stirrer. After vigorous stirring at room temperature for 48 h, the yellow mixture was treated with 1 L distilled water and the product was extracted with 3 x 400 mL portions of diethyl ether. The combined ether layers were concentrated and the residue washed several times with

The combined ether layers were concentrated and the residue washed several times with water before drying over  $\text{MgSO}_4$ . The crude product was distilled under vacuum to yield the respective cyclobutane monomer.

**Dimethyl cyclobutane-1,1-dicarboxylate 5a.** Yield 27%, colorless liquid, b.p.  $50\text{ }^\circ\text{C}/1\text{ mmHg}$ .  $^1\text{H}$  NMR ( $\text{CDCl}_3$ , 300 MHz):  $\delta$  (ppm) 1.99 (m, 2H, cyclobutyl  $\text{CH}_2$ ), 2.56 (t, 4H, cyclobutyl  $\text{CH}_2$ ), 3.75 (s, 6H,  $\text{OCH}_3$ ).  $^{13}\text{C}$  NMR ( $\text{CDCl}_3$ , 300 MHz):  $\delta$  (ppm) 16.2 (cyclobutyl,  $\text{C}_{\text{quart.}}$ ), 28.9 (cyclobutyl  $\text{CH}_2\text{CH}_2$ ), 52.6 ( $\text{OCH}_3$ ), 172.3 ( $\text{C}=\text{O}$ ). IR (liquid film,  $\text{cm}^{-1}$ ): 3000, 2955, 2850, 1735, 1435, 1270, 1200, 1130, 1060, 970, 930, 870. Anal. Calc. for  $\text{C}_8\text{H}_{12}\text{O}_4$  (172.2): C, 55.79; H, 7.04. Found: C, 54.01; H, 7.12.

**Diethyl cyclobutane-1,1-dicarboxylate 5b.** Yield 30%, colorless liquid, b.p.  $50\text{--}55\text{ }^\circ\text{C}/1\text{ mmHg}$ .  $^1\text{H}$  NMR ( $\text{CDCl}_3$ , 300 MHz):  $\delta$  (ppm) 1.26 (t, 6H,  $\text{CH}_3$ ), 1.98 (m, 2H, cyclobutyl  $\text{CH}_2$ ), 2.54 (t, 4H, cyclobutyl  $2\text{CH}_2$ ), 4.21 (q, 4H,  $\text{OCH}_2$ ).  $^{13}\text{C}$  NMR ( $\text{CDCl}_3$ , 300 MHz):  $\delta$  (ppm) 14.4 ( $\text{CH}_3$ ), 16.5 (cyclobutyl,  $\text{C}_{\text{quart.}}$ ), 28.9 (cyclobutyl,  $\text{CH}_2\text{CH}_2$ ), 53.0 (cyclobutyl,  $\text{CH}_2(\text{C}_{\text{quart.}})$ ), 61.6 ( $\text{OCH}_2$ ), 172.2 ( $\text{C}=\text{O}$ ). IR (liquid film,  $\text{cm}^{-1}$ ): 2980, 2900, 2870, 1730, 1450, 1390, 1367, 1265, 1200, 1130, 1110, 1065, 1015, 860. Anal. Calc. for  $\text{C}_{10}\text{H}_{16}\text{O}_4$  (200.26): C, 59.97; H, 8.07. Found: C, 59.36; H, 8.09.

**Diisopropyl cyclobutane-1,1-dicarboxylate 5c.** Yield, 24%, colorless liquid, b.p.  $90\text{ }^\circ\text{C}/3\text{ mmHg}$ .  $^1\text{H}$  NMR ( $\text{CDCl}_3$ , 300 MHz),  $\delta$  (ppm): 1.23 (d, 12H,  $\text{CH}_3$ ), 1.95 (m, 2H, cyclobutyl  $\text{CH}_2$ ), 2.50 (t, 4H, cyclobutyl  $2\text{CH}_2$ ), 5.06 (m, 2H,  $\text{CH}$ ).  $^{13}\text{C}$  NMR ( $\text{CDCl}_3$ , 300 MHz),  $\delta$  (ppm): 16.0 (cyclobutyl,  $\text{C}_{\text{quart.}}$ ), 21.5 ( $\text{CH}_3$ ), 28.4 (cyclobutyl  $\text{CH}_2\text{CH}_2$ ), 52.8 (cyclobutyl,  $\text{CH}_2(\text{C}_{\text{quart.}})$ ), 68.5 ( $\text{OCH}$ ), 171.3 ( $\text{C}=\text{O}$ ). IR (liquid film,  $\text{cm}^{-1}$ ): 2980, 2950, 2870, 1725, 1450, 1375, 1270, 1200, 1100, 930, 912, 890, 825. Anal. Calc. for  $\text{C}_{12}\text{H}_{20}\text{O}_4$  (228.32): C, 63.12; H, 8.85. Found: C, 62.54; H, 8.82.



**Ethyl 1-cyanocyclobutanecarboxylate 6.** The same procedure as described for 5a-c was followed. The molar equivalent of ethyl cyanoacetate was used instead of the corresponding dialkyl malonate. Yield: 8%, colorless liquid, b.p. 96-100 °C/ 1mmHg.  $^1\text{H}$  NMR ( $\text{CD}_3)_2\text{SO}$ , 300 MHz):  $\delta$  (ppm) 1.34 (t, 3H,  $\text{CH}_3$ ), 2.09-2.36 (m, 2H, cyclobutyl  $\text{CH}_2$ ), 2.58-2.77 (m, 4H, cyclobutyl  $\text{CH}_2$ ), 4.27 (q, 2H,  $\text{OCH}_2$ ). Anal. Calc. for  $\text{C}_8\text{H}_{11}\text{NO}_2$  (153.19): C, 62.72; H, 7.25; N, 9.14. Found: C, 62.51; H, 7.23; N, 9.11.

**Cyclobutane-1,1-dicarboxamide 7.** Diethyl cyclobutane-1,1-dicarboxylate **5b** (15.9g, 0.079 mol) was added to a 1.0 M sodium ethanolate solution. Ammonia was bubbled through the solution for 10 minutes and the reagents were allowed to react for 20 hours. The white precipitate was filtered and recrystallized from ethanol/water. Yield 90%, m.p. 276-278 °C.  $^1\text{H}$  NMR ( $(\text{CD}_3)_2\text{SO}$ , 300 MHz):  $\delta$  (ppm) 1.79 (m, 2H,  $\text{CH}_2$ ), 2.45 (t, 4H,  $\text{CH}_2$ ), 7.1 (d, 4H,  $\text{NH}_2$ ).

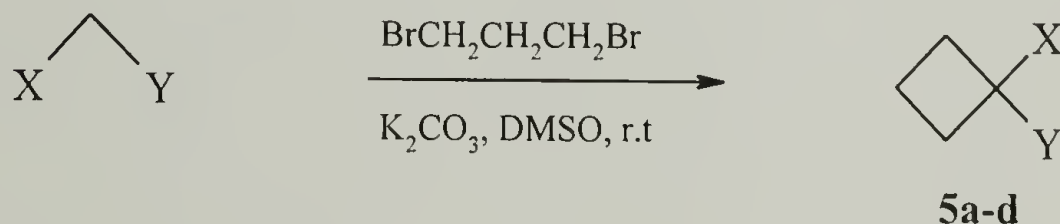
**1,1-Dicyanocyclobutane 8.** A finely ground mixture of cyclobutane-1,1-dicarboxamide (2.17g, 0.015 mol) and phosphorus pentoxide (5.32g, 0.0375 mol) was slowly heated in a Büchi Kugelrohr apparatus to 120 °C /1 mmHg. The collection flask was cooled in ice and clear crystals were obtained. Yield: 20 %, m.p. 37 °C (lit. 37°C<sup>39</sup>).  $^1\text{H}$  NMR ( $\text{CDCl}_3$ , 300 MHz):  $\delta$  (ppm) 2.40 (m, 2H,  $\text{CH}_2$ ), 2.87 (t, 4H,  $\text{CH}_2$ ).  $^{13}\text{C}$  NMR ( $\text{CDCl}_3$ , 300 MHz):  $\delta$  (ppm) 18.4 ( $\text{CH}_2\text{CH}_2$ ), 25.8 ( $\text{CH}_2\text{C}_{\text{quart.}}$ ), 33.8 ( $\text{C}_{\text{quart.}}$ ), 116.3 ( $\text{CN}$ ). Anal. Calc. for  $\text{C}_6\text{H}_6\text{N}_2 \cdot (\text{H}_2\text{O})_{1.5}$  (133.12): C, 54.13; H, 6.82; N, 21.03. Found: C, 54.25; H, 4.84; N, 21.00.



**General Polymerization Procedure.** Potassium and sodium thiophenolate initiators were dried just before use at 200 °C for 2 hours under vacuum (1 mmHg) using a Büchi Kugelrohr apparatus. The cyclobutane monomer was added to a solution of the initiator in DMSO under nitrogen. The polymerization tube was sealed and placed in an oil bath and heated to the desired temperature.

### 4.3.2 Results and Discussion

4.3.2.1 Monomer Synthesis. Several 1,1-disubstituted cyclobutane monomers **5a-c**, **6**, and **8** were synthesized following a slightly modified procedure previously reported by Zefirov et. al. (Scheme 4.7).<sup>40</sup> This procedure involves the cycloalkylation of active methylene compounds by 1,3-dibromopropane in the presence of excess potassium carbonate in DMSO solvent.



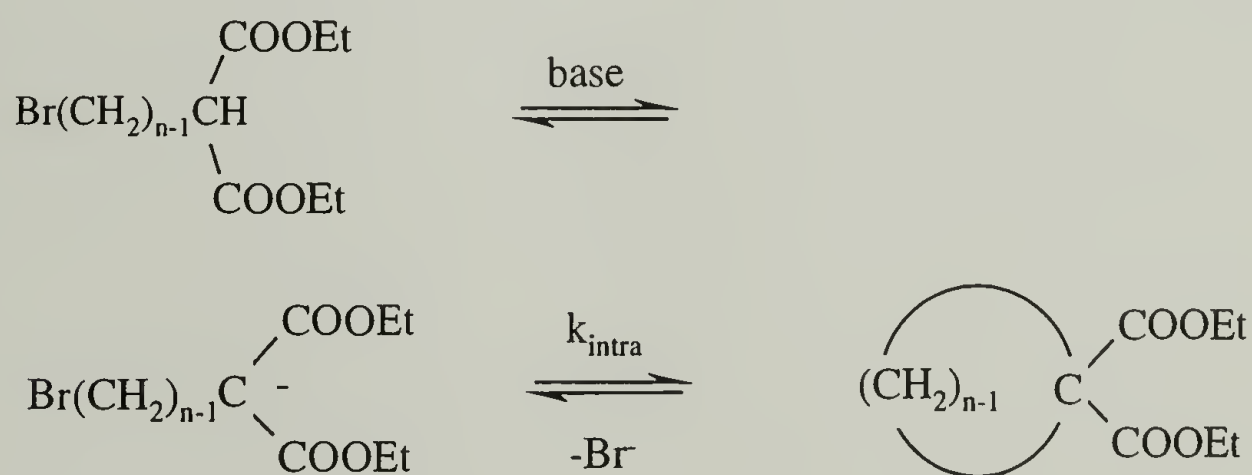
**5:** X = Y = COOR;  
**5a:** R = Me **5b:** R = Et **5c:** R = i-Pr  
**5d:** X = COOEt, Y = CN

Scheme 4.7. Synthesis of 1,1-disubstituted cyclobutanes

The cyclization of bifunctional reagents generally suffers from two main competitive reactions: oligomerization via intermolecular stepwise substitution and decay of the carbanionic species by reaction with adventitious impurities.

However, a previous study on the cyclization of ( $\omega$ -bromopropyl)malonate anions indicated that the reaction leading to the formation of 4-membered rings is not significantly affected by either one of these competitive reactions.<sup>41</sup>

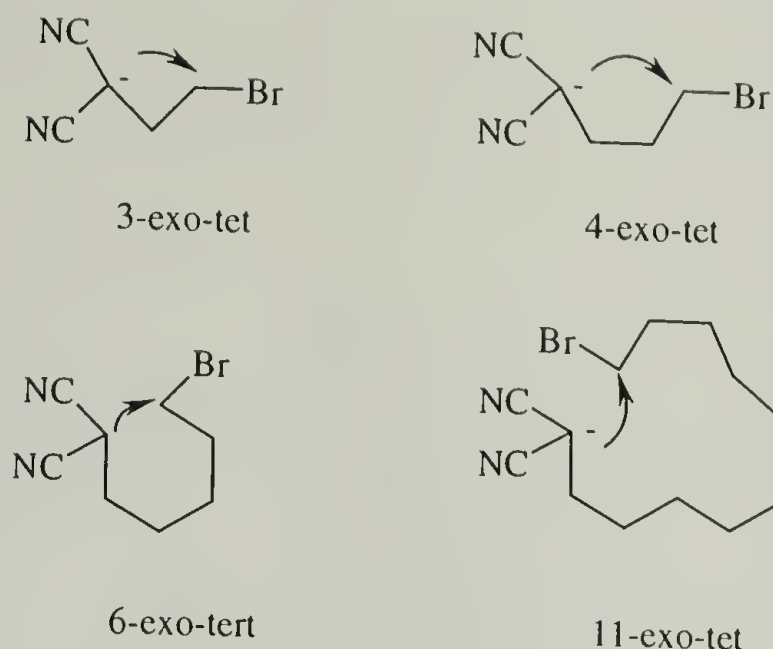
Significantly lower yields were obtained for the formation of cyclobutanes than for the corresponding cyclopropane derivatives, with the main side product being the monosubstituted product. This was not unexpected based on several studies described in the literature on the kinetics of ring formation. For example, the kinetics of cyclization of diethyl ( $\omega$ -halogenoalkyl)malonic esters in tert-butyl alcohol and in ethanol was studied by Knipe and Sterling.<sup>42</sup> In this study, the rate of formation of 3-membered rings was too fast to measure, implying a minimum ratio of 100:1 for the relative rates of formation of 3- over 5-membered rings. The kinetics of cyclization of diethyl ( $\omega$ -bromoalkyl) malonates (in DMSO at 25 °C) was also independently studied by Mandolini et al. (Scheme 4.8).<sup>41,43]</sup>



Scheme 4.8. Cyclization of diethyl ( $\omega$ -bromoalkyl) malonates

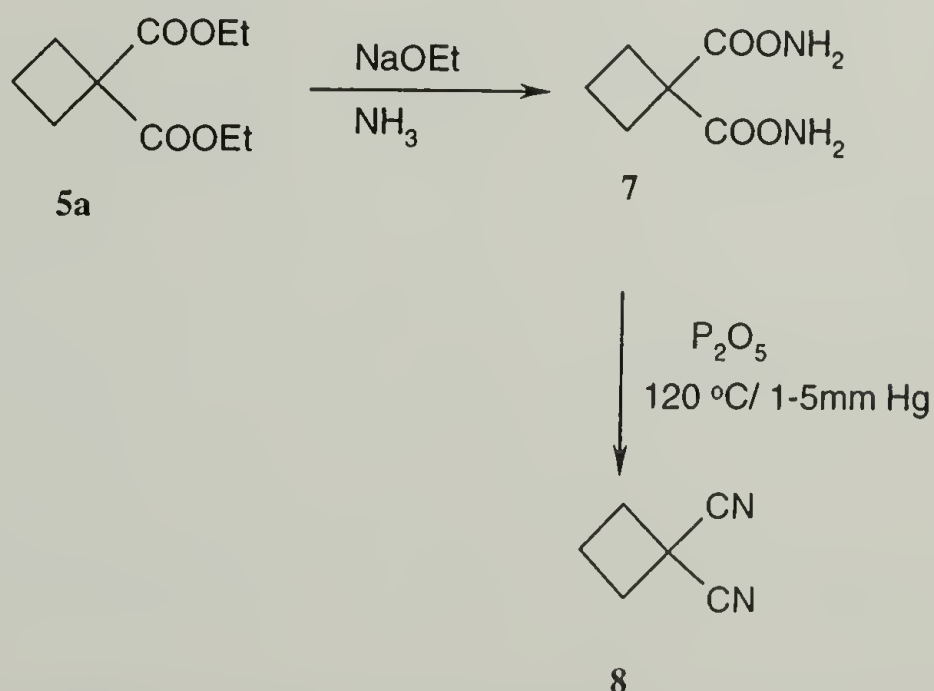
In their kinetic study, the reactivity profile for the malonate cyclization of 4 to 21-membered rings was determined. In comparison to five-membered rings, which exhibited the highest ease of formation, four-membered rings displayed almost two orders of magnitude less reactivity towards ring-formation. Assuming that the previously determined minimum ratio of 100:1 for the formation of 3- and 5-membered rings holds in DMSO, these results demonstrate that the kinetics of cyclization for cyclobutanes is at least four orders of magnitude less favorable than for cyclopropanes.

The synthesis of 1,1-dicyanocyclopropane **8** via the alkylation of malononitrile with 1,3-dibromopropane using a mild base ( $K_2CO_3$ ) afforded very low yields (< 5%). Low yields for this reaction have previously been reported in the literature.<sup>39</sup> Slightly improved yields were obtained when a 1:1 mixture of  $K_2CO_3$ :KOH was used. The ease of formation of 3-, 5- and 6-membered rings over 4- and 11-membered rings can be explained in light of Baldwin's rules which examine the stereochemical requirement in the transition state for the cyclization process.<sup>44</sup> These cyclizations are exo-tet processes, which depend on the probability that the intermediate adopts the appropriate conformation for the cyclization and on the distance between the reactive centers in this conformation (Scheme 4.9).



Scheme 4.9. Cyclization of 3, 4, 6 and 11-membered rings

Due to poor yields obtained during the synthesis of 1,1-dicyanocyclobutane **8** via the cyclization reaction, an alternative procedure was used (Scheme 4.10). In this procedure, diamide **7** was first synthesized in high yield by the reaction of diethyl cyclobutane-1,1-dicarboxylate **5a** with ammonia. Attempts to completely dehydrate the diamide using an imminium salt<sup>45</sup>, phosphorus oxychloride and thionyl chloride<sup>46</sup> were unsuccessful due to the poor solubility of the diamide. The final product **8** was obtained by dehydration with phosphorus pentoxide in 20% yield.



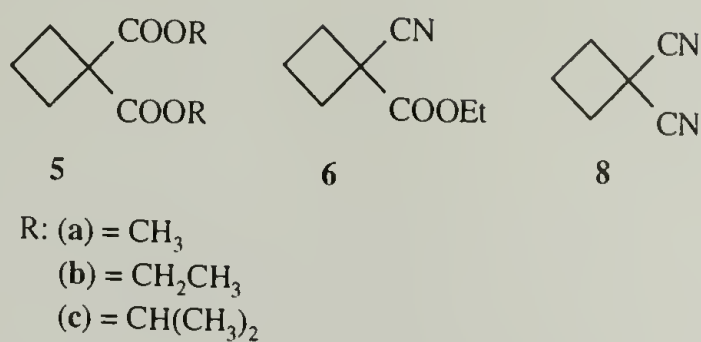
Scheme 4.10. Synthesis of Cyclobutane-1,1-Dicarbonitrile **8**



4.3.2.2 Anionic Polymerization. Thiophenolate salts (PhSK/Na) are efficient initiators for the anionic ring-opening polymerization of various 1,1-disubstituted cyclopropanes.<sup>1,2,47-49</sup> As discussed in chapter 2, the reactivity of these cyclopropanes towards anionic ring-opening polymerization depends on the ability of the electron-withdrawing substituents on the ring to stabilize the propagating carbanion generated upon opening of the ring. In our study, it was demonstrated that nitrile groups on the ring are highly stabilizing substituents and significantly increase the reactivity of the cyclopropane ring over ester substituents (section 2.3.4).

Based on these results, the ring-opening polymerization of 1,1-disubstituted cyclobutane monomers **5a-d**, **6**, and **8** was attempted using potassium and sodium thiophenolate initiators. Due to the expected lower reactivity of the cyclobutane monomers over the analogous cyclopropanes, higher reaction temperatures between 140 and 180 °C were employed. A summary of the polymerization data is shown in Table 4.3. The reactions were monitored using <sup>1</sup>H-NMR spectroscopy.

Table 4.3. Reaction Conditions for **5a-d**, **6** and **8** with Sodium (Na) and Potassium (K) Thiophenolates in DMSO.



Expt. #	Monomer	[M] mmol	[I] mmol	DMSO (mL)	Temp. (°C)	Time (h)
1	<b>5b</b>	4.5	0.21 (Na)	1	160	64
2	<b>6</b>	3.3	0.33 (Na)	0.7	140	24
3	<b>5a</b>	0.33	0.33 (K)	0.5	140	24
4	<b>5b</b>	0.33	0.33 (K)	0.5	140	76
5	<b>6</b>	0.33	0.33 (K)	0.5	140	24
6	<b>5b</b>	0.2	0.2 (Na)	1	160	66
7	<b>5c</b>	0.4	0.4 (Na)	1.5	160	168
8	<b>8</b>	4.76	0.18(Na)	0.2	140	72
9	<b>8</b>	2.87	0.11(Na)	0.15	180	6

<sup>1</sup>H-NMR analysis of the reaction mixture of **5a-c** with PhSK(/Na) showed that no reaction occurred below 140 °C after 2 days. Attempts to polymerize **5b** and **6** (Exp. #1 and #2) using PhSNa at 160 and 140 °C respectively, afforded no polymer even after long reaction times. In order to investigate the efficiency of the initiation reaction, stoichiometric amounts of PhSK(/Na) (Exp. #3-7) at 140 and 160 °C were used. In these experiments, the disappearance of the monomer after several hours was evident by <sup>1</sup>H-NMR analysis of the reaction mixture.

The  $^1\text{H}$ -NMR spectrum of the reaction mixture after 5 h (Expt. 4) is shown in Figure 4.3. Analysis of the spectrum indicated that the main products of the reaction of **5b** with PhSNa were diethyl cyclobutanecarboxylate (**i**) and ethyl phenyl thioether (**ii**).

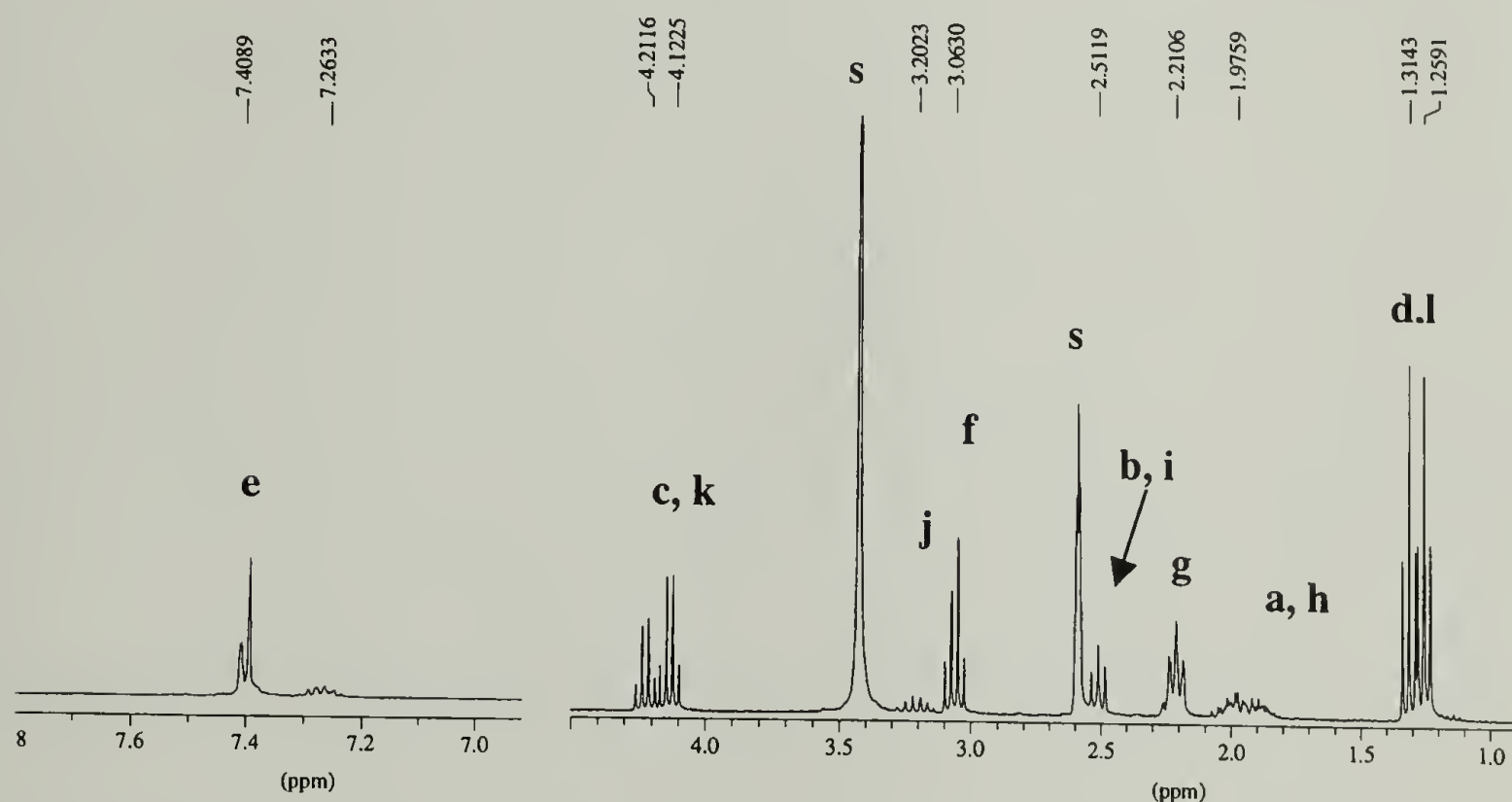
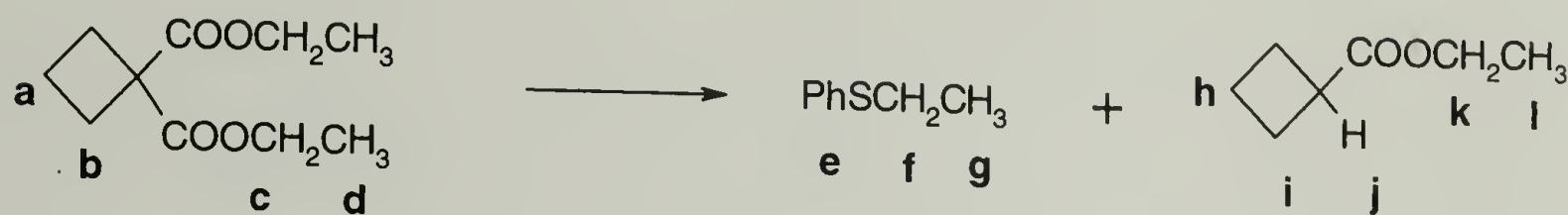
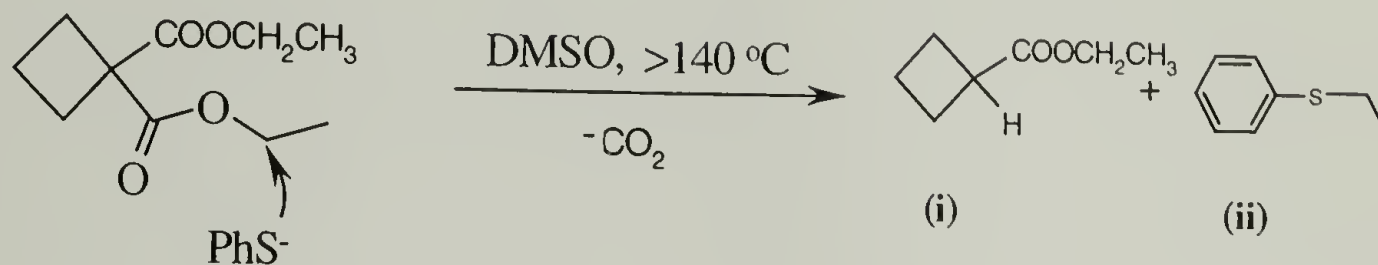


Figure 4.3.  $^1\text{H}$ -NMR spectrum of reaction of **5b** with PhSK (Expt. 4) in  $(\text{CD}_3)_2\text{SO}$

Figure 4.3 provided evidence that the main reaction is the attack of PhSNa on the alkyl carbon of the ester group and not on the ring. This reaction is known as the Krapcho reaction<sup>50</sup> and is summarized in Scheme 4.11.



**Scheme 4.11.** Competitive Krapcho reaction

Similarly, the reaction of sodium thiophenolate with ethyl 1-cyanocyclopropane carboxylate **6** yielded cyanocyclobutane and ethyl phenyl thioether as the main products. No polymers(oligomers) were isolated for any of the reactions of **5a-c**, and **6** with PhSK/Na at 160 °C, even after long reaction times.

For the polymerization of 1,1-dicyanocyclopropane **8** at 140 °C (Expt. 8), precipitation was observed after 1 hour. Analysis of the product by <sup>1</sup>H-NMR showed that ring-opening of the cyclobutane monomer occurred. However, after long reaction times (72 h), endgroup analysis indicated that only oligomers ( $\overline{Xn} = 3-5$ ) had been formed. An additional attempt was carried out for the same reaction at 180 °C (Expt. 9), but again only oligomers were obtained even after long reaction times.

The anionic polymerization of several 1,1-disubstituted cyclopropanes (**1**, **2a-d**, **4**) at 60 °C (using PhSK(/Na)) was described in chapter 2. In the case of similarly activated cyclobutanes, no polymerization with could be observed even at high temperatures (>140 °C) with the same initiators. For reactions with equimolar amounts of ester-



containing monomer (**5a-c**, **6**) and initiator (PhSK/Na), <sup>1</sup>H-NMR analysis showed that the preferred reaction was a nucleophilic attack on the ester group and not on the ring as desired. As previously discussed in section 4.2.2., despite the similar strain energies of cyclopropanes and cyclobutanes (26.5 kcal·mol<sup>-1</sup> vs. 27.5 kcal·mol<sup>-1</sup>, respectively), cyclobutanes are several orders of magnitude less reactive. Our experiments demonstrated a similar trend and a poor tendency of cyclobutane monomers to polymerize via ring-opening. In the case of 1,1-dicyanocyclobutane **8**, ring-opening occurs at 140 °C, but the rate of propagation was very slow which limited high molecular weight polymers from being obtained.

Literature reports on the ring-opening polymerization of cyclobutane adducts derived from electron-rich and electron-poor olefins (Scheme 4.4),<sup>5</sup> suggest that the strong electron-donor and acceptor substituents on the cyclobutane ring provide the necessary activation and a kinetic pathway that favor the polymerization of these monomers. According to the "bond-forming initiation theory" proposed by Hall, these monomers are in equilibrium with zwitterionic intermediates and are capable of undergoing both anionic and cationic polymerization.<sup>51</sup> For example, 1,1,2,2-tetracyano-3-ethoxycyclobutane (**iii**) is highly reactive, undergoing anionic ring-opening polymerization in the presence of weak bases such as triethylamine at ambient temperature. As expected, lower reactivity towards ring-opening polymerization was evident in the homopolymerization of dimethyl dicyanoethylenedicarboxylate (**iv**) and 1,1-dicyano-2-ethoxycyclobutane (**v**) in comparison to the highly activated tetracyano derivative (**iii**).<sup>52</sup>

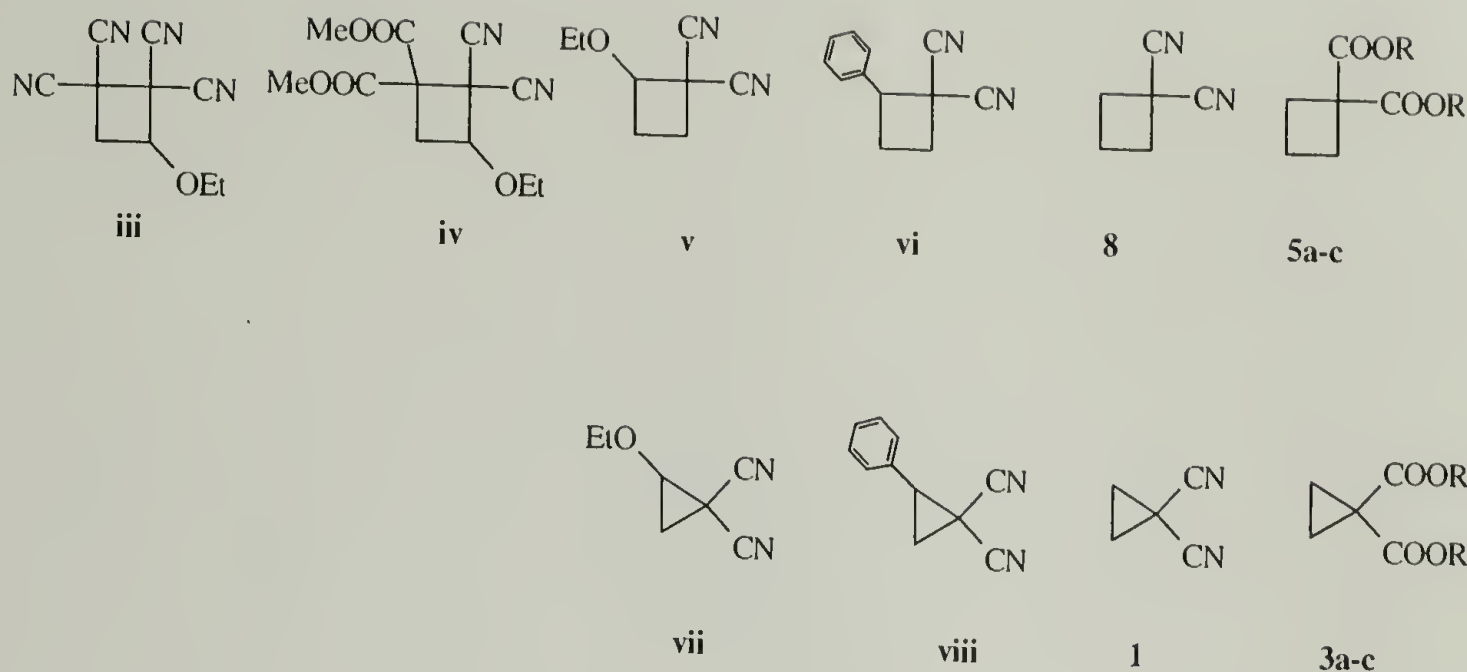


Figure 4.4. Activated Cyclobutane and Cyclopropane Derivatives

All the cyclopropane monomers investigated thus far, are much more reactive than the cyclobutanes bearing the same substituents. For example, while 1,1-dicyanocyclopropane **1** polymerizes rapidly at 60 °C (3.8 mol-% PhSNa), 1,1-dicyanocyclobutane **8** polymerizes very slowly at 140 °C under the same conditions. The addition of an activating electron-donor substituent on the cyclopropane ring (**vii**) increases its reactivity so much that the monomer becomes too reactive to isolate in its monomeric form.<sup>3</sup> In contrast, its cyclobutane analogue (**v**) yielded only oligomers after long reaction times at high temperatures. From these examples, it is evident that due to the low kinetic propensity of cyclobutanes to polymerize, the ring must be activated by several activating substituents in order to achieve high molecular weight polymers under moderate conditions.

## 4.4 Conclusions

Attempts to synthesize poly(1,1-difunctionalized tetramethylene)s via the anionic ring-opening polymerization of 1,1-disubstituted cyclobutanes using sodium and/or potassium thiophenolate at 140–180 °C was unsuccessful. Despite the similar strain energies of 3- and 4-membered rings, cyclobutane rings are much less reactive and require highly activating substituents on the ring in order to obtain acceptable polymerization rates. In this study, the use of strong nucleophiles at high temperatures did lead to the formation of high molecular weight polymers. For the dialkyl 1,1-cyclopropanedicarboxylate monomers, a side reaction (preferential attack on the ester substituent) was the favored reaction. Therefore, an alternative synthetic route to achieve our target poly(tetramethylene)s structures via the polymerization of 1,1-difunctionalized butadienes was attempted, with the results discussed in chapter 5.

## 4.5 References

- (1) Penelle, J.; Herion, H.; Xie, T.; Gorissen, P. *Macromol. Chem. Phys.* **1998**, *199*, 1329.
- (2) Penelle, J.; Xie, T. *Macromolecules* **2000**, *33*, 4667.
- (3) Lee, J.-Y.; Cho, I. *Bull. Korean Chem. Soc.* **1986**, *7*, 210.
- (4) Kushibiki, N.; Irie, M.; Hayashi, K. *J. Polym. Sci., Polym. Chem. Ed.* **1975**, *13*, 77.
- (5) Yokozawa, T.; Miyamoto, Y.; Futamura, S. *Makromol. Chem., Rapid Commun.* **1993**, *14*, 245.
- (6) Roberts, J. R.; Sharts, C. M. In *Organic Reactions*; John Wiley and Sons: New York, 1962; Vol. 12, p 1.
- (7) Wilson, A.; Goldhamer, D. *J. Chem. Edu.* **1963**, *40*, 504.

- (8) Coulson, C. A.; Moffit, W. E. *J. Chem. Phys.* **1947**, *15*, 151.
- (9) Fieser, L. F.; Fieser, M. In *Advanced Organic Chemistry*; Reinhold: New York, 1961; pp 535,544.
- (10) Pell, A. S.; Pilcher, G. *Trans. Faraday Soc.* **1965**, *61*, 71.
- (11) Baird, N. C.; Dewar, M. J. S. *J. Am. Chem. Soc.* **1967**, *89*, 3967.
- (12) Benson, S. W. In *Thermochemical Kinetics*; Wiley: New York, 1968.
- (13) Earl, H.; Stirling, C. J. M. *J. Chem. Soc., Perkin Trans. II* **1987**, *9*, 1273.
- (14) Bury, A.; Earl, H.; Stirling, C. J. M. *J. Chem. Soc., Perkin Trans. II* **1987**, *9*, 1281.
- (15) Wong, H. N. C.; Hon, M.; Tse, C.; Yip, Y. *Chem. Rev.* **1989**, *89*, 165.
- (16) Stirling, C. J. M. *Tetrahedron* **1985**, *41*, 1613.
- (17) Bauld, N.; Cessac, J.; Holloway, R. H. *J. Am. Chem. Soc.* **1977**, *99*, 8140.
- (18) Dunitz, J.; Schomaker, V. *J. Chem. Phys.* **1952**, *20*, 1703.
- (19) *Heterocycl. Chem.* **1972**, *5*, 12.
- (20) Pritchard, G.; Long, F. A. *J. Am. Chem. Soc.* **1958**, *80*, 4162.
- (21) Dainton, F. S.; Ivin, K. J. *Quart. Rev. Chem. Soc.* **1958**, *12*, 61.
- (22) Ivin, K. J.; Saegusa, T. In *Ring-Opening Polymerization*; Ivin, K. J., Saegusa, T., Eds.; Elsevier Applied Science Publishers: New York, 1984; Vol. 1, pp 1-3.
- (23) Williams, K. K.; Wiley, D. W.; McKusick, B. C. *J. Am. Chem. Soc.* **1962**, *84*, 2210.
- (24) Huisgen, R. *Acc. Chem. Res.* **1977**, *10*, 117.
- (25) Pinazzi, C.; Brossas, J.; Clouet, G. *Makromol. Chem.* **1971**, *148*, 81.
- (26) Pinazzi, C.; Brossas, J. *Makromol. Chem.* **1969**, *122*, 105; **1971**, *1147*, 1915.
- (27) Rossi, R.; Diversi, P.; Porri, L. *Macromolecules* **1972**, *5*, 247.
- (28) Yang, X.; Jia, L.; Marks, T. J. *J. Am. Chem. Soc.* **1993**, *115*, 3392.
- (29) Alder, R.; Allen, P. R.; Khosravi, E. *J. Chem. Soc., Chem. Commun.* **1994**, 1235.



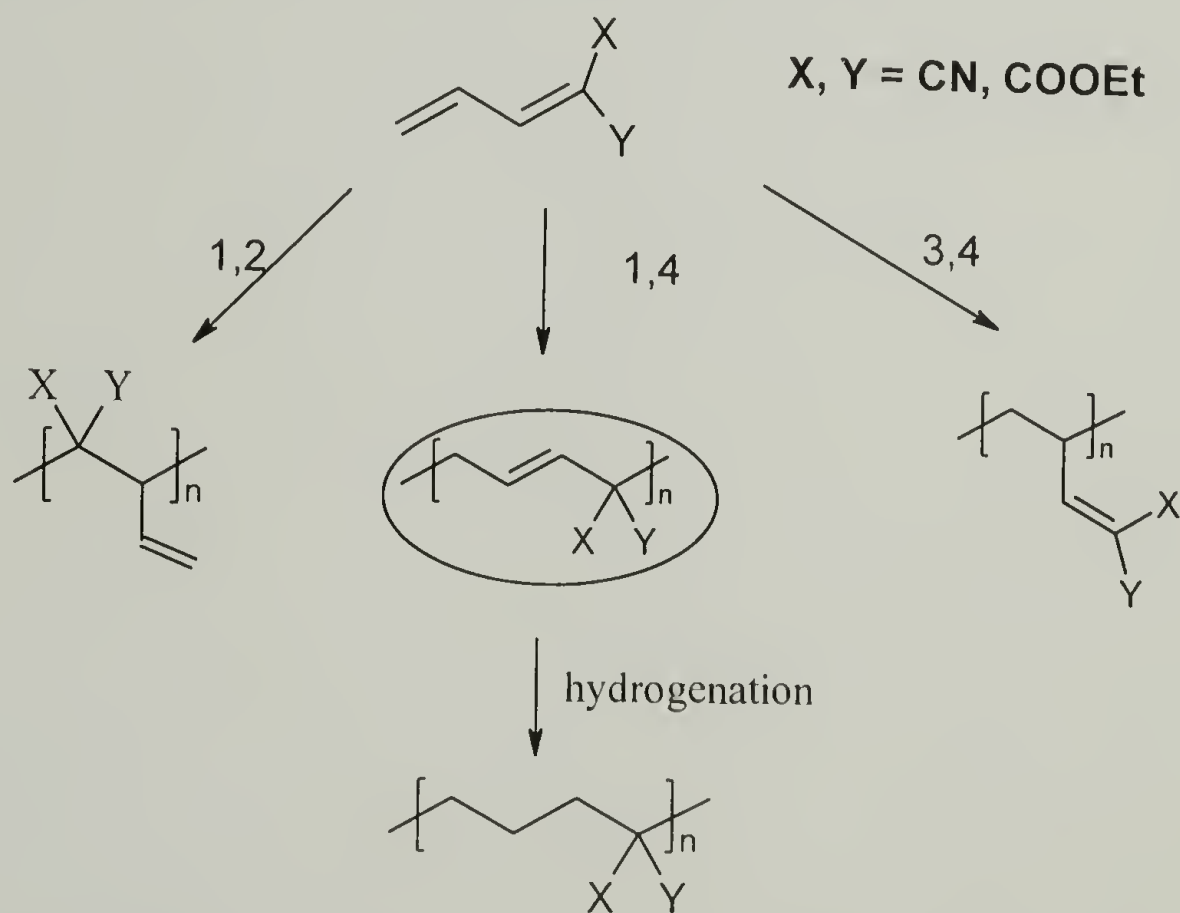
- (30) Inoue, S.; Aida, T. In *Ring-Opening Polymerization*; Ivin, K. J., Saegusa, T., Eds.; Elsevier Applied Science Publishers: New York, 1984; Vol. 1, pp 185-298.
- (31) Perry, S.; Hibbert, H. *J. Am. Chem. Soc.* **1940**, 62, 2599.
- (32) Perry, S.; Hibbert, H. *Can. J. Chem.* **1933**, 8, 102.
- (33) Pasika, W. M. *J. Polym. Sci.* **1965**, A3, 4287.
- (34) Hirano, T.; Nakayama, S.; Tsuruta, T. *Makromol. Chem.* **1975**, 176, 1897.
- (35) Rose, J. B. *J. Chem. Soc.* **1956**, 542.
- (36) Sigwalt, P.; Spassky, N. In *Ring-Opening Polymerization*; Ivin, K. J., Saegusa, T., Eds.; Elsevier Applied Science Publishers: New York, 1984; Vol. 2, pp 603-714.
- (37) Machon, J. P.; Nicco, A. *Europ. Polym. J.* **1971**, 7, 353.
- (38) Price, C. C.; Blair, E. A. *J. Polym. Sci., Part A: Polym. Chem.* **1967**, 5, 171.
- (39) Diez-Barra, E.; de la Hoz, A.; Moreno, A.; Sanchez-Verdu, P. *J. Chem. Soc., Perkin Trans. 1* **1991**, 1, 2593.
- (40) Zefirov, N. S. K., T. S.; Kozhushkov, S. I.; Surmina, L. S.; Rashchupkina, Z. A. *Zh. Org. Khim. (Engl. Transl.)* **1983**, 19, 474.
- (41) Casadei, M. A.; Galli, C.; Mandolini, L. *J. Am. Chem. Soc.* **1984**, 106, 1051.
- (42) Knipe, A. C.; Sterling, C. J. M. *J. Chem. Soc. B* **1968**, 67.
- (43) Illuminati, G.; Mandolini, L. *Acc. Chem. Res.* **1981**, 14, 95.
- (44) Baldwin, J. E. *J. Chem. Soc., Chem. Commun.* **1976**, 734.
- (45) Bargar, T. M.; Riley, C. M. *Synthetic Commun.* **1980**, 10, 479.
- (46) Rickborn, B.; Jensen, F. R. *J. Org. Chem.* **1962**, 4608.
- (47) Kagumba, L.; Penelle, J. *Polym. Prepr. (Am. Chem. Soc., Div. Polym. Chem.)* **2000**, 41, 1313.
- (48) Kagumba, L.; Penelle, J. *Polym. Prepr. (Am. Chem. Soc., Div. Polym. Chem.)* **2000**, 41, 1290.
- (49) Penelle, J.; Herion, H.; Soree, A.; Gorrissen, P. *Polym. Prepr. (Am. Chem. Soc., Div. Polym. Chem.)* **1996**, 37 (1), 208.

- (50) Krapcho, A. *Synthesis* **1982**, 893.
- (51) Hall, H. K. J.; Padias, A. B. *Acc. Chem Res.* **1990**, 23, 3.
- (52) Yokozawa, T.; Wakabayashi, Y.; Kimura, T. *J. Polym. Sci., Polym. Chem. Ed.* **1997**, 35, 1563.

## ANIONIC POLYMERIZATION OF 1,1-DIFUNCTIONALIZED BUTADIENES

## 5.1 Introduction

The synthetic methodology designed toward the formation of poly(1,1-difunctionalized tetramethylenes)  $\text{CH}_2\text{CH}_2\text{CH}_2\text{C}(\text{XY})_n$  ( $\text{X}, \text{Y} = \text{CN}/\text{COOR}$ ) via the ring-opening polymerization of 1,1-disubstituted cyclobutanes was unsuccessful under the conditions described in chapter 4. Therefore, an alternative strategy to via the anionic polymerization of 1,1-difunctionalized butadienes was designed and is described in this chapter. Control of the microstructure of the 1,1-difunctionalized polybutadiene is essential in this approach because subsequent hydrogenation of the 1,4-microstructure must be performed to obtain the desired poly(tetramethylene) structure (Scheme 5.1).



Scheme 5.1. Synthesis of Poly(1,1-difunctionalized tetramethylene)s

Only the microstructure resulting from the 1,4 addition will yield the desired polymers with two substituents on every fourth carbon upon hydrogenation. In this chapter, the synthesis and characterization of the polymer microstructure resulting from the polymerization of butadienes 1,1-disubstituted by ester and/or cyano groups are discussed in detail.

## 5.2 Background

### 5.2.1 Butadiene Polymerization

About 99% of the world's natural rubber is obtained from the Hevea tree (*Hevea brasiliensis*) as a natural latex or submicroscopic dispersion in a saplike material.<sup>1</sup> Natural rubber has been used for many centuries, but the most significant period in the history of rubber was during World War I and II.<sup>2</sup> The dramatic increase in the demand for rubber led to the development of synthetic rubber substitutes and the emergence of the polybutadiene rubber industry.

The polymerization of 1,3-butadienes yields polymer structures containing unsaturated units, which can exist in three different isomeric forms: cis-1,4; trans-1,4; and vinyl (1,2) (Figure 5.1). The vinyl polymer can be iso, syndio or atactic.

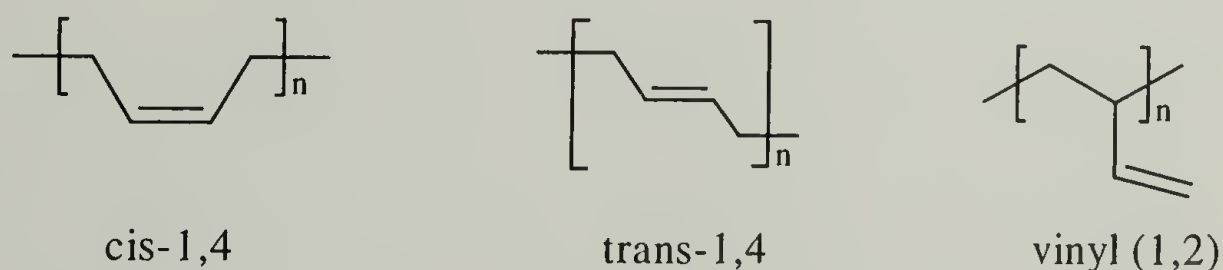


Figure 5.1. Polybutadiene microstructures



Monosubstituted butadienes such as 1-methylbutadiene have also been polymerized, and yield additional 3,4-vinyl structures due to the difference in substitution of the two double bonds (Figure 5.2). The polybutadiene microstructure significantly affects its properties.<sup>3,4</sup> For example, natural rubber consists of poly(cis-1,4-isoprene) which is an amorphous solid with a glass transition temperature ( $T_g$ ) of  $-72\text{ }^{\circ}\text{C}$  and melting temperature ( $T_m$ ) of  $28\text{ }^{\circ}\text{C}$  if crystallized. The polymer is an excellent elastomer over a considerable temperature range, broadening its use for a variety of applications especially at ambient conditions. The trans isomer (gutta percha/balata) is highly crystalline with a  $T_m \sim 97\text{ }^{\circ}\text{C}$ . Due to its high crystallinity, high melting temperature, and resulting processing difficulties, the trans isomer has fewer applications, although properties such as its good resistance to abrasion are useful for applications such as golf covers. The microstructures of various butadiene polymers is generally determined by IR<sup>5-7</sup> and/or NMR spectroscopy.<sup>8-11</sup>

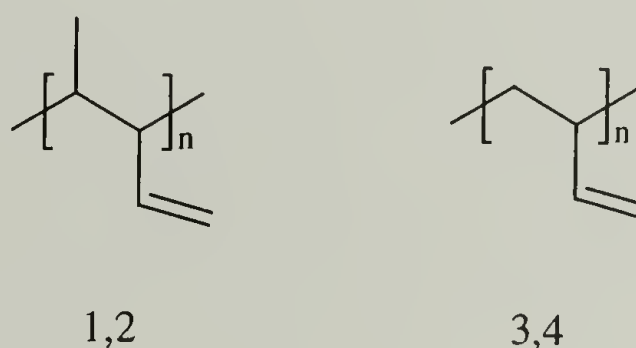


Figure 5.2. Polymer microstructures arising from 1,2- and 3,4- additions to 1-methyl butadiene

### 5.2.2 Stereochemistry of butadiene polymerization

Polybutadienes can be prepared by free-radical, anionic or coordination polymerization. The polymerizations are typically via emulsion (free-radical) or solution methods. Free radical polymerization of polybutadienes in solution leads to low molecular weight polymers (1000-4000 g/mol),<sup>12</sup> while high molecular weight amorphous polymers with high trans-1,4 content are obtained under emulsion polymerization. The anionic polymerization of isoprene (2-methylbutadiene) can be obtained using organolithiums, yielding polymers with 1,2-, 1,4- or 3,4- repeating units. Both the alkali metal (or derivative) and the solvent greatly affect the chain microstructure. For example, aliphatic solvents like cyclohexane or hexane give higher cis-1,4 units than aromatic solvents like benzene. The use of polar solvents (like THF) leads to an increase in the 3,4 microstructure, presumably due to the solvation of the lithium cation leading to a carbon-lithium bond with more ionic character.<sup>13,14</sup>

With the development of Ziegler-Natta organometallic catalysts in the late 1950s, control over the microstructure, polydispersity and branching was achieved in polybutadienes. The use of Ziegler-Natta catalysts to synthesize highly stereoregular polybutadienes and other polymers has been reviewed.<sup>15</sup>

### 5.2.3 Hydrogenation of polybutadienes

Unsaturated polymers can be hydrogenated to yield new products with distinct properties.<sup>16-19</sup> For example, the hydrogenation of elastomeric 1,4-polybutadiene gives a crystalline polyethylene plastic. The structures and properties of the hydrogenated polymers depend on the extent of hydrogenation. The hydrogenation of polymers can be

achieved by catalytic (homogeneous or heterogeneous) and non-catalytic (diimide, hydroboration) methods.<sup>20</sup> The use of heterogeneous catalysts is difficult due to the high tendency of polymer molecules to become absorbed on the catalyst, rendering them inefficient.<sup>21</sup> High temperatures, large amounts of catalysts and high hydrogen pressure can be employed to achieve effective hydrogenation.<sup>22-25</sup> However, chain cleavage reactions occur under such conditions and low molecular weight products are often obtained. Homogeneous hydrogenation using boranes can also be used, but these are only effective at high temperatures and chain degradation is also sometimes observed.<sup>26</sup> Homogeneous metal-organic hydrogenation catalysts<sup>27,28</sup> are effective and useful for the hydrogenation of unsaturated polymers under mild conditions.<sup>29-34</sup>

Non-catalytic hydrogenation of polymers can be achieved using boranes or diimides. The reduction of carbon-carbon double bonds using hydrazine was reported as early as 1905, but it was not until the early 1960's that it was recognized that diimide ( $\text{HN} = \text{NH}$ ) was the actual reducing agent.<sup>35-37</sup> Initially, diimide was used as a general hydrogenation reagent of non-polar low molecular weight compounds,<sup>37-39</sup> but its potential usefulness to hydrogenate polymers was soon realized.<sup>40</sup> The technique is attractive due to its relatively simple procedure, with a reaction carried out at atmospheric pressure (under nitrogen), typically at temperatures below 160 °C.<sup>41</sup> In addition, this method can be used to hydrogenate unsaturated polymers with functional groups. Many functional groups coordinate with organometallic hydrogenation catalysts, greatly reducing their efficiency. In extreme cases, highly coordinating functionalities such as amino and carboxyl groups poison the catalyst and prevent hydrogenation. Some unsaturated polymers containing  $-\text{Cl}$ ,  $-\text{CN}$ ,  $-\text{SO}_3\text{Na}$ , and  $-\text{PO}(\text{OCH}_3)_2$  groups have been



hydrogenated using diimides.<sup>20</sup> Many methods have been used to generate diimide<sup>41</sup> in solution, such as via the oxidation of hydrazine<sup>42</sup>, decarboxylation of potassium azodicarboxylate,<sup>36,37</sup> or via the thermolysis of arylsulfonylhydrazides.<sup>35,43,44</sup> Systematic studies on the use of diimide as a hydrogenating agent for polymers have been made.<sup>21,41,45-48</sup> Due the versatility of the reagent, the procedure has since been used to generate a wide variety of hydrogenated polymers on a laboratory scale.<sup>49-53</sup>

## 5.3 Experimental

### Measurements

<sup>1</sup>H- and <sup>13</sup>C-NMR spectra were recorded on a Bruker DPX 300 spectrometer in CDCl<sub>3</sub>. IR spectra were recorded on a BioRad FTS 175C FT-IR spectrometer. Elemental analysis was performed at the Microanalysis Laboratory of University of Massachusetts, Amherst. Thermogravimetric analysis (TGA) were performed on a Perkin-Elmer TAC 7/DX instrument using heating rates of 10 °C/min. Molecular weights were obtained via Gel Permeation Chromatography (GPC) analysis using a PL LC 1120 pump, Waters R403 Differential Refractometer detector, and three PLgel columns (105 Å, 104 Å, 103 Å). THF was used as the eluent with a flow rate of 1 mL·min<sup>-1</sup> and the samples calibrated to poly(methyl methacrylate) standards.

### Materials

All the chemicals were purchased from Aldrich. Acrolein was purified by fractional distillation. TiCl(i-PrO)<sub>3</sub> was purchased as a 1.0 M solution in hexane. p-toluenesulfonyl hydrazide was recrystallized from methanol and dried in vacuo at 40 °C for 8 h prior to use. o-Xylene was filtered through activated alumina before use.



THF and benzene were distilled over sodium/benzophenone, and tri-n-propyl amine was distilled from  $\text{CaH}_2$ . All other solvents were reagent grade and used without further purification.

**Synthesis of ethyl 2-cyano-2,4-pentadienoate 9.** The monomer was synthesized by modification of Gerber's procedure<sup>54</sup> as follows: Zinc chloride (37 mmol, 5.04g) was added to 40 mL dioxane and heated to 70 °C while stirring for 30 min. The reaction mixture was cooled to room temperature before adding ethyl cyanoacetate (60 mmol, 6.78 g) and then acrolein (75 mmol, 5.0 mL). After stirring for 3 hours, 50 mL hexane was added to the reaction mixture and washed with 3 x 100 mL portions of a cold 3% hydrochloric acid solution. The organic layer was separated and concentrated. The crude product was recrystallized from a 1:1 petroleum ether-diethyl ether mixture. Yield 60%. m.p 40 °C.  $^1\text{H}$  NMR ( $\text{CDCl}_3$ , 300 MHz):  $\delta$  (ppm) 1.37 (t, 3H,  $\text{CH}_3$ ), 4.33 (q, 2H,  $\text{OCH}_2$ ), 5.89-6.20 (dd, 2H,  $\text{CH}_2=\text{CH}-$ ), 6.85-6.97 (ddd, 1H,  $\text{CH}_2=\text{CH}-$ ), 7.84 (d, 1H,  $\text{CH}_2=\text{CH}-\text{CH}=\text{C}(\text{COOR},\text{CN})$ ).  $^{13}\text{C}$  NMR ( $\text{CDCl}_3$ , 300 MHz):  $\delta$  (ppm) 14.1 ( $\text{CH}_3$ ), 62.6 ( $\text{OCH}_2$ ), 107.0 ( $\text{CH}=\text{C}(\text{COOR},\text{CN})$ ), 113.7 (CN), 132.0 ( $\text{CH}_2=\text{CH}-$ ), 134.0 ( $\text{CH}_2=\text{CH}-$ ), 155.2 ( $=\text{CH}=\text{C}=\text{C}$ ), 161.7 ( $\text{C}=\text{O}$ ). Anal. Calc.  $\text{C}_8\text{H}_9\text{NO}_2$  (151.8): C, 63.55; H, 6.01; N, 9.27. Found: C, 63.50; H, 5.84; N, 9.23.

**Synthesis of diethyl 2-propenylidenemalonate 10.** The monomer was synthesized by slight modification of a literature procedure<sup>55</sup> as follows: Diethyl malonate (3.8 mL, 25 mmol) was added dropwise to a suspension of sodium hydride (25 mmol, 0.6g) in 80 mL THF. The mixture was stirred at 0 °C for 30 min. and cooled to -78 °C. The  $(i\text{-PrO})_3\text{TiCl}$  solution (1.0 M, 25 mL) was added dropwise and stirred for 1 hour before adding acrolein (45 mmol, 3.0 mL). The mixture was warmed to room temperature

while stirring for 3 hours. The solution was then hydrolyzed using 150 mL of a 3% aqueous hydrochloric acid solution. The product was extracted with 3 x 100 mL portions of diethyl ether. The ether layer was washed with 100 mL of a 10% sodium bicarbonate aqueous solution, with 3 x 100 mL portions of water and then dried over magnesium sulfate. The product was isolated by concentration and distillation using a Buchi Kugelrohr apparatus. Yield: 40% (colorless oil), b.p. 63-65 °C/0.12 mmHg.  $^1\text{H}$  NMR ( $\text{CDCl}_3$ , 300 MHz):  $\delta$  (ppm) 1.34 (t, 3H,  $\text{CH}_3$ ), 1.39 (t, 3H,  $\text{CH}_3$ ), 4.22 (q, 2H,  $\text{OCH}_2$ ), 4.25 (q, 2H,  $\text{OCH}_2$ ), 5.65-5.74 (dd, 2H,  $\text{CH}_2=\text{CH}-$ ), 6.75 (ddd, 1H,  $\text{CH}_2=\text{CH}-$ ), 7.00 (d, 1H,  $\text{CH}_2=\text{CH}-\text{CH}=\text{CH}-$ ).  $^{13}\text{C}$  NMR ( $\text{CDCl}_3$ , 300 MHz):  $\delta$  (ppm) 14.5 ( $\text{CH}_3$ ), 61.8 ( $\text{OCH}_2$ ), 107.0 ( $\text{CH}=\text{C}(\text{COOR})_2$ ), 132.0 ( $\text{CH}_2=\text{CH}-$ ), 134.0 ( $\text{CH}_2=\text{CH}-$ ), 155.2 ( $=\text{CH}-\text{C}=\text{C}$ ), 161.7 ( $\text{C}=\text{O}$ ). IR spectrum,  $\text{cm}^{-1}$ : 3100, 1740, 1635, 1595, 940, 860, 795, 770.

**Anionic polymerization of 9.** Due to the high reactivity of these butadienes, the monomers were weighed in a dry box and all the polymerizations carried out under nitrogen. The initiator (0.066 mmol equivalent) was added to a solution of the monomer **2** (0.5g, 3.3 mmol) in 3 mL benzene. The solution was stirred at room temperature for 16 hours and precipitated in hexane. The final product was isolated by filtration, washed several times with ether and dried in vacuo at room temperature.

**Radical polymerization of 9.** AIBN (5.4 mg, 0.03 mmol) was added to a solution of the monomer (0.5g, 3.3 mmol) in 3 mL benzene. The reaction was heated at 80 °C for 16 hours. The polymer was isolated by precipitation in hexane.

**Anionic polymerization of 10.** The initiator (0.25 mmol equivalent) was added to a solution of the monomer **2** (0.5g, 2.5 mmol) dissolved in 5 mL benzene and allowed to react while stirring at room temperature for 4 hours. The polymer was isolated by precipitation in hexane.

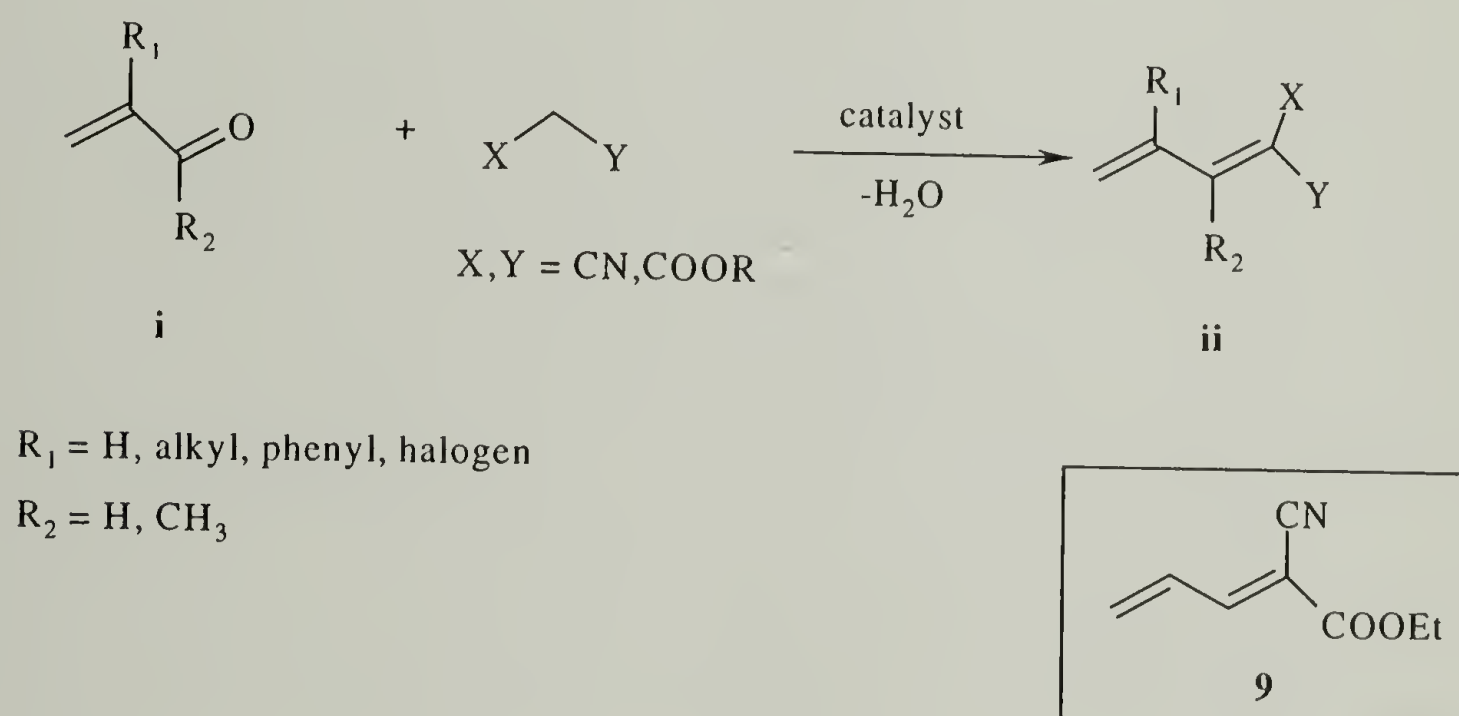
**Hydrogenation.** A three-neck round bottom flask equipped with a magnetic stirrer was supplied with a positive pressure of nitrogen through a gas inlet adapter atop the reflux condensor. In this vessel, 5 g of polybutadiene was dissolved in 250 mL o-xylene. In some cases, DMF was also used as an alternative solvent. After complete dissolution of the polymer, p-toluenesulfonyl hydrazide (12.29g, 0.066 mol) and tri-n-propylamine (9.46g, 0.066 mol) were added. The vessel was heated to reflux of the solvent (135-140 °C) for 4 hours. The o-xylene solution was washed twice with 500 mL deionized water, and the organic layer filtered through a ¼ inch layer of activated alumina in a coarse sintered glass filtered funnel. The polymer was isolated by precipitation in methanol and dried in vacuo at 90 °C for 3 hours.

## 5.4 Results and Discussion

5.4.1 Monomer Synthesis. Ethyl 2-cyano-2,4-pentadienoate **9** was synthesized in good yield via the reaction of ethyl cyanoacetate and acrolein in dioxane using zinc chloride as a catalyst. This procedure for the synthesis of 1,1-disubstituted-1,3-butadienes by the reaction of active methylene compounds with  $\alpha,\beta$ -unsaturated carbonyl compounds was previously reported by Gerber (Scheme 5.2).<sup>54</sup> The use of classical aldol condensation catalysts (such as pyridine, piperidine, hydroxides or alkoxides of alkali metals) suffers from a competitive Michael addition<sup>56</sup> and polymerization of both



acrolein and (ii).<sup>57</sup> In this condensation process, the use of a metal salt catalyst under slightly acidic conditions favors the direct formation of the highly reactive butadienes. Reaction under low pH hinders the polymerization and Michael addition side reactions. Halides, nitrates, and carboxylate salts of Zn, Cu, Mn, Cr, Cu, Ni, Ca, Mg, and Li were previously studied, but no quantitative relationship was derived help in the selection of an optimum catalyst under a given set of conditions. Monomer **9** is highly reactive towards anionic and radical initiation and must be stored at room temperature with anionic and radical inhibitors.

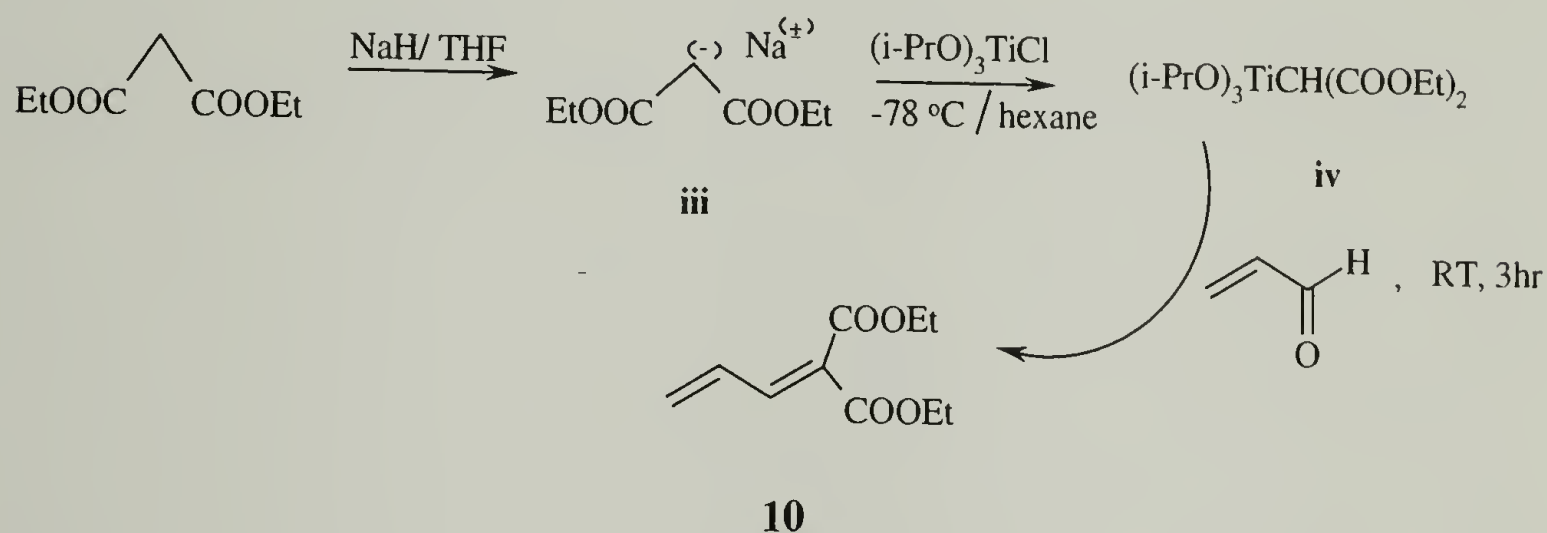


Scheme 5.2. General Synthesis of 1,1-difunctionalized-1,3-butadienes

The synthesis of diethyl 2-propenylidene malonate **10** was achieved via the reaction of the titanium derivative of diethyl malonate with acrolein at 20 °C (Scheme 5.3). The titanium derivative was obtained from the reaction of the sodium salt of diethyl malonate (**iii**) with one equivalent of chlorotriisopropoxytitanium in THF at -78 °C. It is known that the condensation of alkali-metal salts of CH acids  $\text{XCH}_2\text{Y}$  ( $\text{X, Y} = \text{CO}_2\text{R}$ ,



CN, COR) with aldehydes does not take place due to the easy dissociation of the products into the initial reagents.<sup>58,59</sup> The reaction of the titanium complex (iv) with various  $\alpha,\beta$ -unsaturated aldehydes (such as acrolein, crotonaldehyde, or sorbaldehyde) takes place under mild conditions, leading to the condensation products containing a conjugated diene or triene system (with moderate to good yields).



Scheme 5.3. Synthesis of diethyl-propenylidenemalonate **10**

Monomers **9** and **10** were characterized using FT-IR,  $^1\text{H}$ - and  $^{13}\text{C}$ -NMR spectroscopy and elemental analysis. Presence of a trace amount of residual diethyl malonate and diisopropyl malonate formed via transesterification with the catalyst was observed in the  $^1\text{H}$ -NMR spectra of **10**, even after purification by both flash chromatography and bulb-to-bulb distillation. The monomers are soluble in aromatic hydrocarbons, chloroform, acetone and diethyl ether.

The  $^1\text{H}$ - and  $^{13}\text{C}$ -NMR spectra of ethyl 2-cyano-2,4-pentadienoate **9** are shown in Figure 5.3 and 5.5, respectively. The special location of the nitrile and the ester groups with respect to the conjugated system was previously determined via analysis of the

proton spectra using some empirical additive methods.<sup>60,61</sup> It was determined that the chemical shift for the methyne proton of the ( $=\underline{\text{CH}}\text{-CH=CH}_2$ ) group is at 7.75 ppm for the Z isomer and at 8.0 ppm for the E isomer (Figure 5.4). The methylene proton of **9** is at 7.75 ppm indicating that the Z isomer is the preferred structure (regardless of the size of the ester).<sup>60</sup>

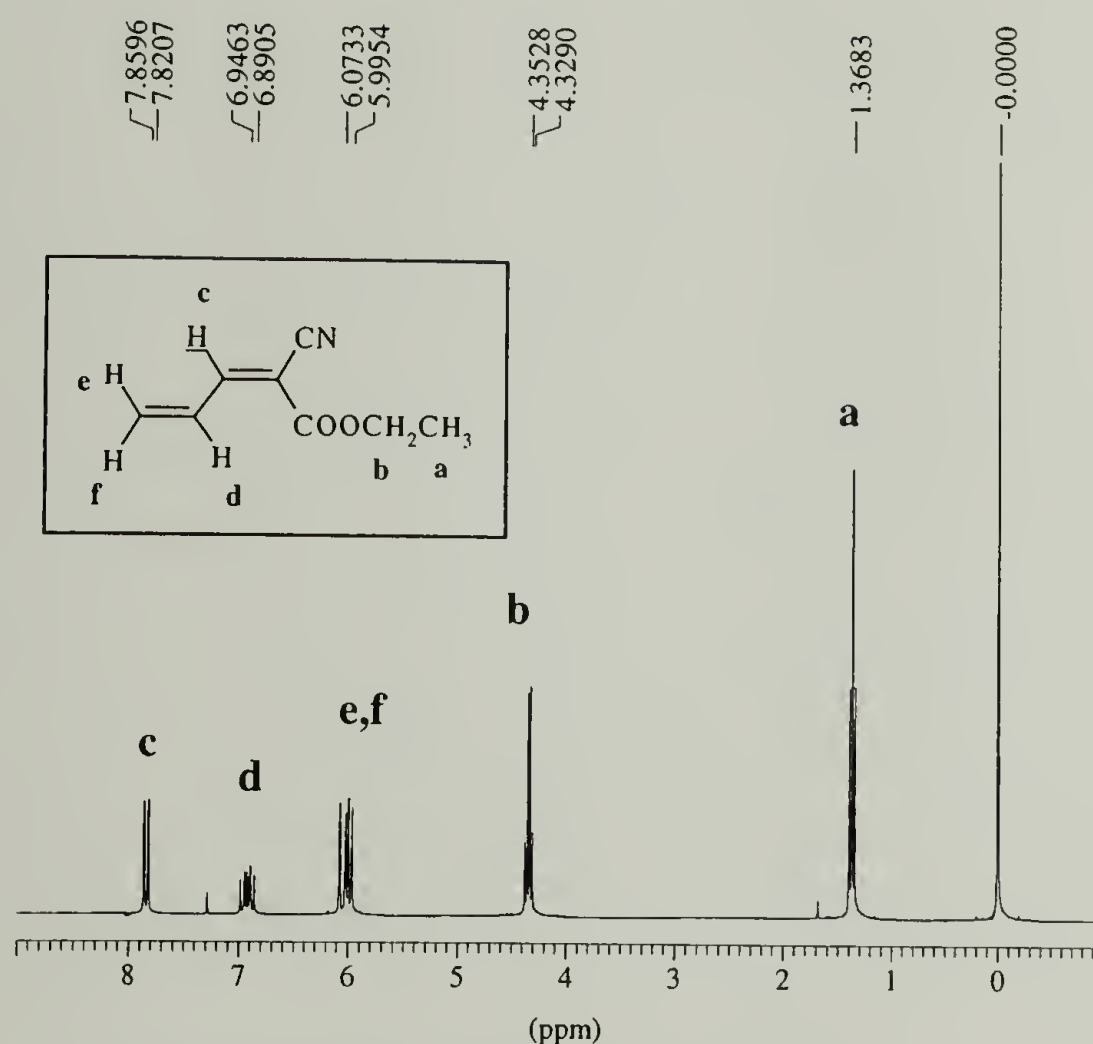


Figure 5.3.  $^1\text{H}$ -NMR Spectrum of **9** ( $\text{CDCl}_3$ )

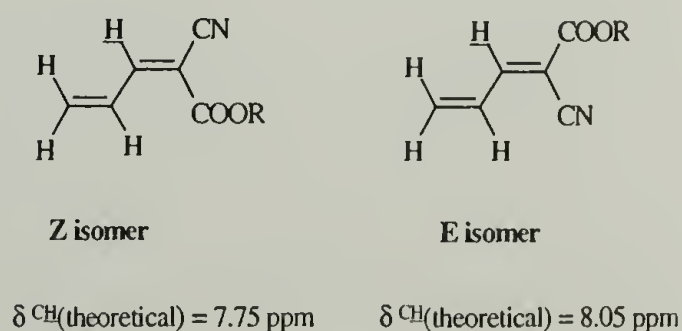


Figure 5.4. Isomers of **9**

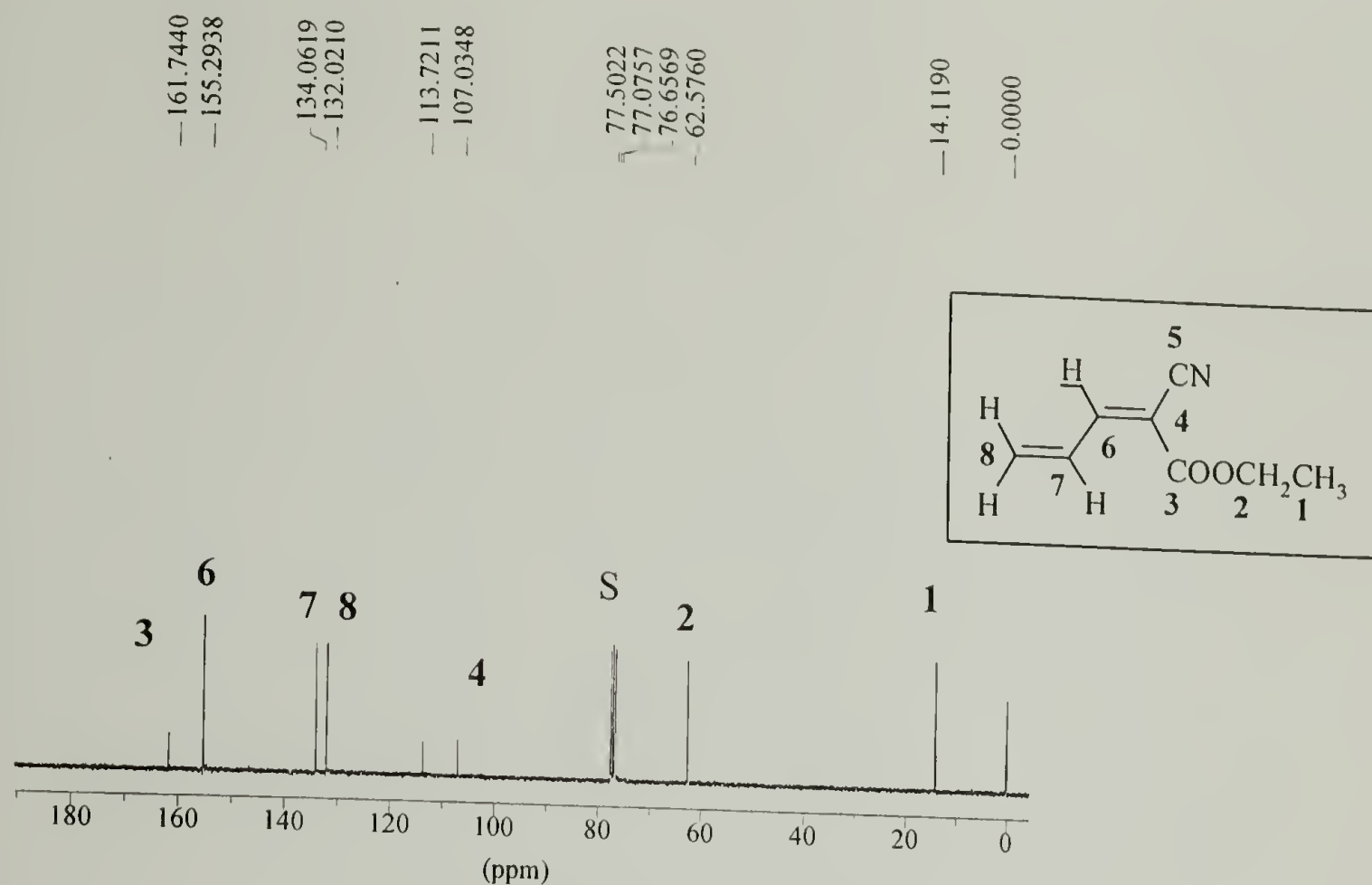


Figure 5.5.  $^{13}\text{C}$ -NMR Spectrum of **9** ( $\text{CDCl}_3$ )  
(S = solvent peak)

5.4.2 Anionic Polymerization. The anionic polymerization of **9** and **10** was achieved under various conditions described in Table 5.1. The data represents initial experimental conditions selected based on previous reports on the polymerization of **9**<sup>54,60</sup>, using piperidine in benzene at ambient temperature as an initiator. Under the examined conditions, relatively high molecular weight polymers with broad distributions (PDI 1.8-2.9) were obtained for the polymerization of **9**. The ‘spontaneous’ polymerization of highly purified monomer **9** upon dissolution in polar solvents such as DMSO or acetone was also observed at room temperature. The use of the term ‘spontaneous’ here refers to polymerization without any purposely added initiator. The resulting polybutadienes were soluble in THF, acetone, benzene, and chlorinated solvents. Initiation with triethylamine yielded quantitative conversion after 17 h. These

preliminary set of experiments were carried out to examine the influence of the reaction conditions on the microstructure of the resulting polybutadienes.

Table 5.1. Polymerization of **9** and **10**

$M^a$	I	$[M]_0/[I]_0$	Temp. (°C)	Time (h)	$\overline{M}_n^c$	$\overline{M}_w$	PDI	Yield (%)
<b>9</b> <sup>*</sup>	piperidine	27	RT	4	44K	78K	1.8	31
<b>9</b>	piperidine	10	RT	12	6K	19K	2.9	40
<b>10</b>	piperidine	10	RT	12	-	-	-	<1% <sup>d</sup>
<b>9</b>	Et <sub>3</sub> N	50	RT	17	51K	96K	1.8	100
<b>9</b> <sup>b</sup>	AIBN	100	60	24	-	-	-	81 <sup>e</sup>

<sup>a</sup> dissolved in benzene, except for \* which was carried out in acetone

<sup>b</sup> with 0.8 mmol benzoic acid

<sup>c</sup> GPC in THF calibrated to poly(methylmethacrylate standards)

<sup>d</sup> fine ppte was formed in hexane

<sup>e</sup> insoluble in THF at room temperature

It must be noted that the anionic polymerization of **9** had first been reported by Gerber in 1968.<sup>54</sup> The monomer was found to be highly reactive and to polymerize in the presence of alcohols, organic and inorganic bases. The hydroxyl (HO<sup>-</sup>) ion resulting from the dissociation of water was nucleophilic enough to initiate the anionic polymerization. During the anionic polymerization of **9**, the resulting dienoate carbanion is stabilized by the nitrile and ester substituents. This stabilizing effect is also observed in  $\alpha$ -cyanoacrylate polymerizations, with some additional stabilization arising from the allylic structure in the butadiene case. As usual, the two electron-withdrawing substituents strongly influence the distribution of the electrons in the  $\pi$ -system by combined mesomeric and inductive effects.<sup>60</sup> The chain propagates via nucleophilic attack of the anionic active end on the double bond of the monomer. A discussion of the various possible modes of addition (1,2-; 1,4- or 3,4-) is presented in the following section.



The anionic polymerization of **10** initiated with piperidine at room temperature, yielded a fine precipitate in hexane, which was isolated by evaporation of the solvent (Table 5.1). The low yields obtained are believed to be mainly due to the presence of residual malonate impurities in the monomer, which act as termination agents.

5.4.3 Radical polymerization. Gerber had also previously reported on the radical polymerization of **9** using benzoyl peroxide in benzene at 75 °C (with benzoic acid added to retard the anionic polymerization). A control experiment without the benzoyl peroxide initiator yielded no polymer after 19 hours at 75 °C.<sup>54</sup> In our study, the radical polymerization of **9** was initiated with AIBN in benzene at 60 °C. Benzoic acid was added to inhibit the anionic polymerization. After 24 h, a rubbery product was obtained, which was insoluble in THF at room temperature. <sup>1</sup>H-NMR analysis (in CDCl<sub>3</sub>) provided evidence that the polymer was crosslinked. Further experiments under free-radical conditions were not performed in this study, but according to a study done by Gerber, the monomer **9** demonstrated reactivity comparable to 2,3-dichlorobutadiene, which is much more reactive than styrene or (meth)acrylate monomers under free-radical conditions<sup>54</sup>. This high reactivity was attributed to a combination of allylic resonance and carbonyl- and nitrile-conjugated resonance in the resulting radical.

5.4.4. **Structural Analysis of Poly(9) and Poly(10).** A detailed characterization of the microstructure of poly(**9**) and poly(**10**) was performed using FT-IR and <sup>1</sup>H- and <sup>13</sup>C-NMR spectroscopy. The <sup>1</sup>H-NMR spectrum of poly(**9**) (Et<sub>3</sub>N, C<sub>6</sub>H<sub>6</sub>, 17 h, RT) is shown in Figure 5.6. Analysis of the microstructure was performed by comparing the

theoretical chemical shifts (in ppm) of the vinyl protons for the three possible units: 1,2-; 1,4-; and 3,4-. These theoretical values were calculated from NMR tables and are distinct for each microstructure (Figure 5.7). The vinylic protons in the spectra at 5.8-5.9 ppm are consistent with the theoretical values expected from the 1,4 microstructure, while the absence of vinylic protons around 5.0 ppm and 7.0 ppm discounted the presence of 1,2 and 3,4 units, respectively.

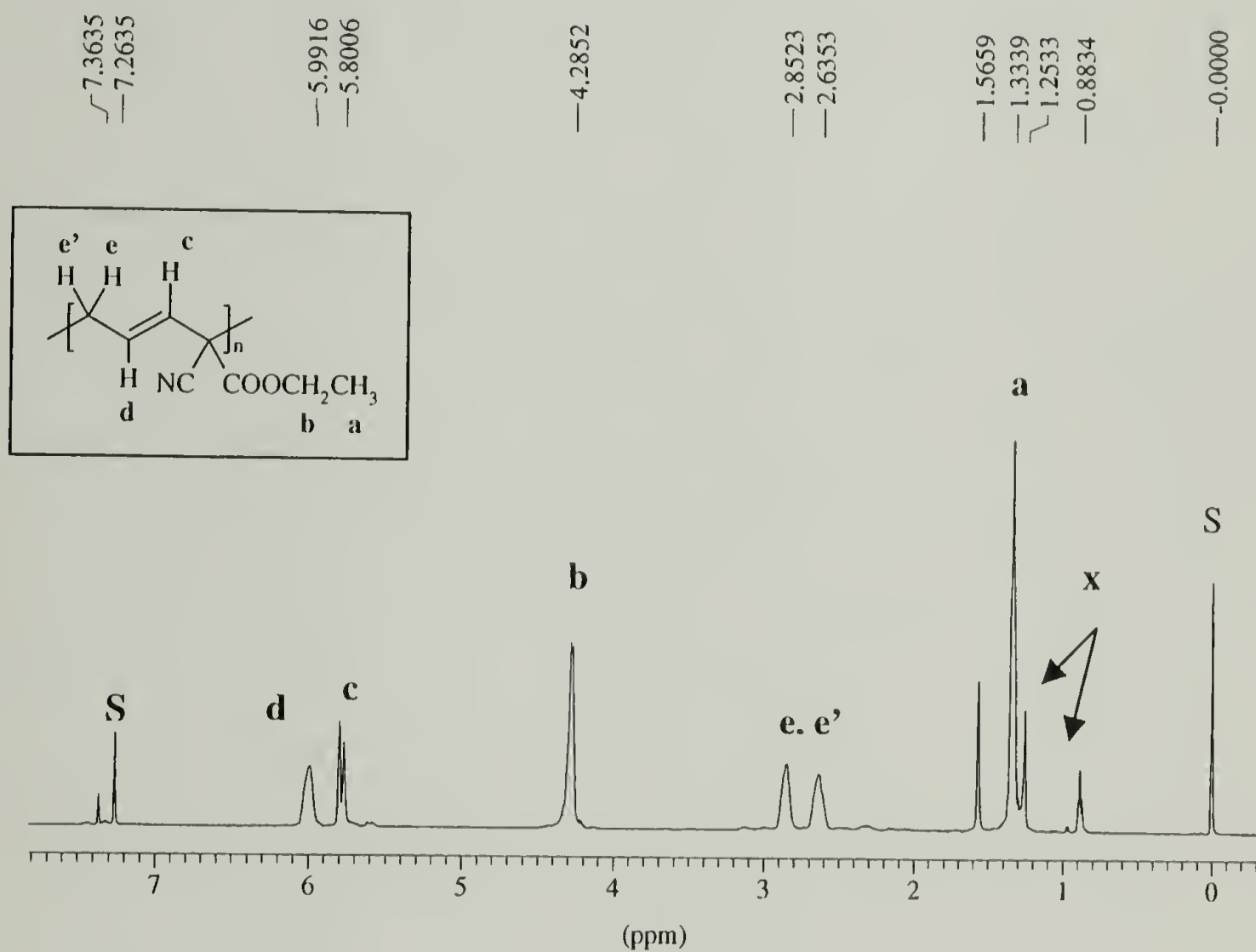


Figure 5.6.  $^1\text{H}$ -NMR spectrum of Poly(9) in  $\text{CDCl}_3$  (S- reference solvent, x – indicates residual solvent peaks)

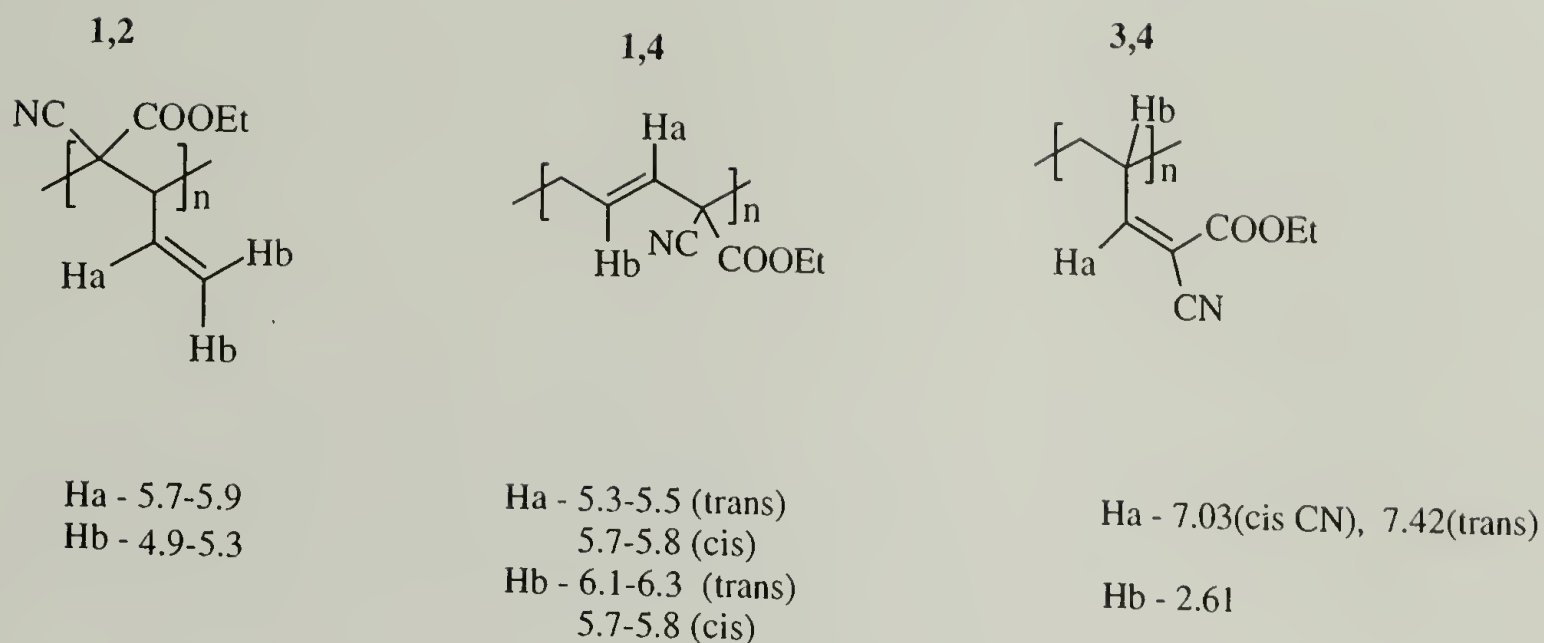


Figure 5.7. Theoretical Chemical shifts (ppm) of vinylic protons for 1,2-; 1,4- and 3,4- units as calculated from NMR tables.

The vinyl carbon peaks in the  $^{13}\text{C}$ -NMR spectrum of the polymer at 127 and 130 ppm are also consistent with the assignment of the 1,4-microstructure (Figure 5.8). The resonances of the vinyl carbons resulting from 1,2-addition are predicted to occur around 114 and 135 ( $\pm 5$ ) ppm, and at 103 and 144 ppm ( $\pm 10$ ) ppm for 3,4-addition units.

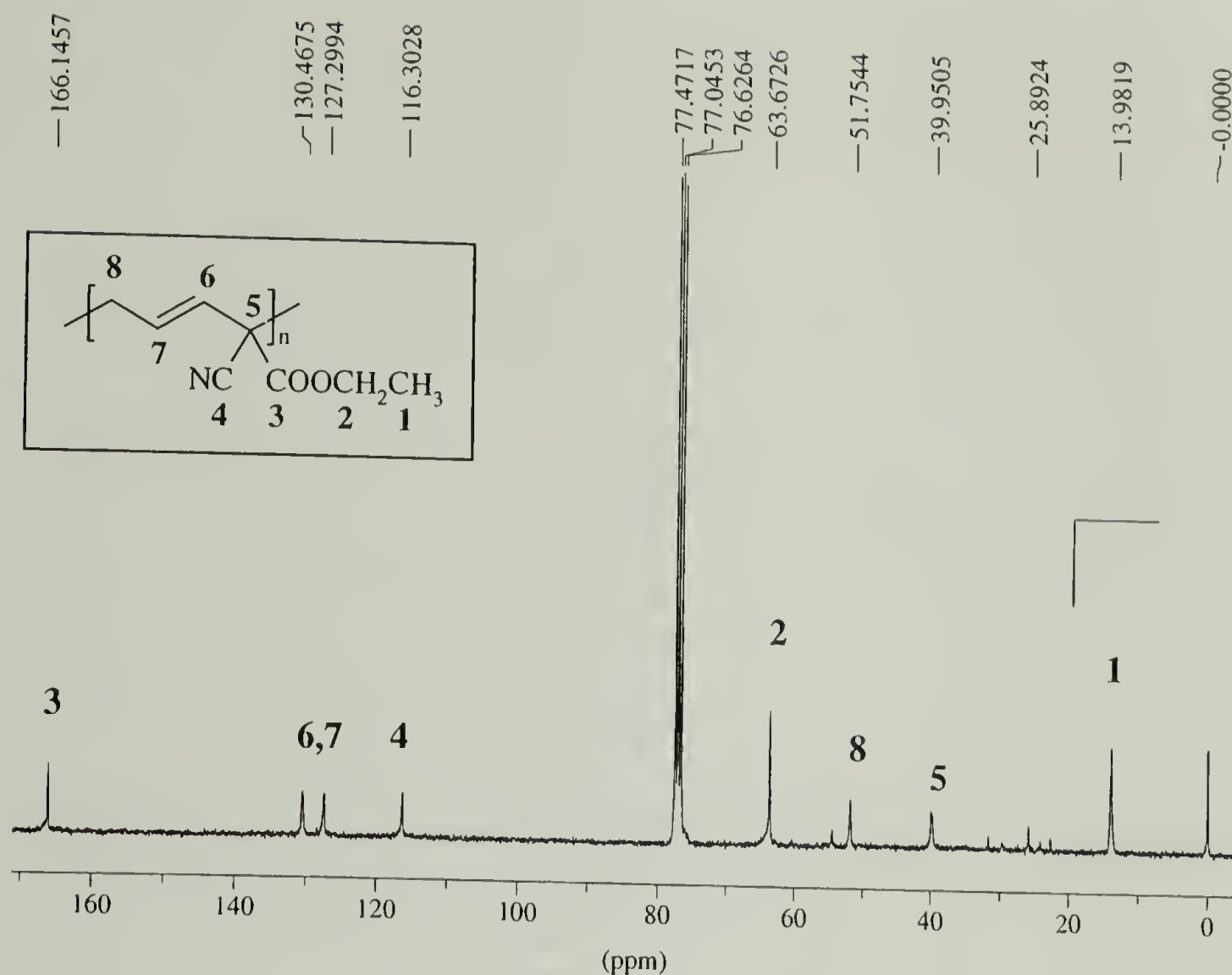


Figure 5.8.  $^{13}\text{C}$ -NMR spectrum of Poly(9) ( $\text{CDCl}_3$ )

The IR spectrum of poly(9) ( $\text{Et}_3\text{N}$ ,  $\text{C}_6\text{H}_6$ , 17 h, RT) is shown in Figure 5.9. The predicted values for the out-of-plane C-H bending in the vinylic region for the various microstructures are shown in Figure 5.10. The IR data provided only evidence for trans 1,4-units in the polymer microstructure at  $967\text{ cm}^{-1}$ . The peaks due to the stretching of the terminal vinyl carbons characteristic of the 1,2-addition product at  $995\text{--}985\text{ cm}^{-1}$  and  $915\text{--}905\text{ cm}^{-1}$  and of the 3,4-addition product at  $850\text{--}790\text{ cm}^{-1}$  are absent. These findings corroborate the results obtained from  $^1\text{H}$ -NMR spectroscopy.



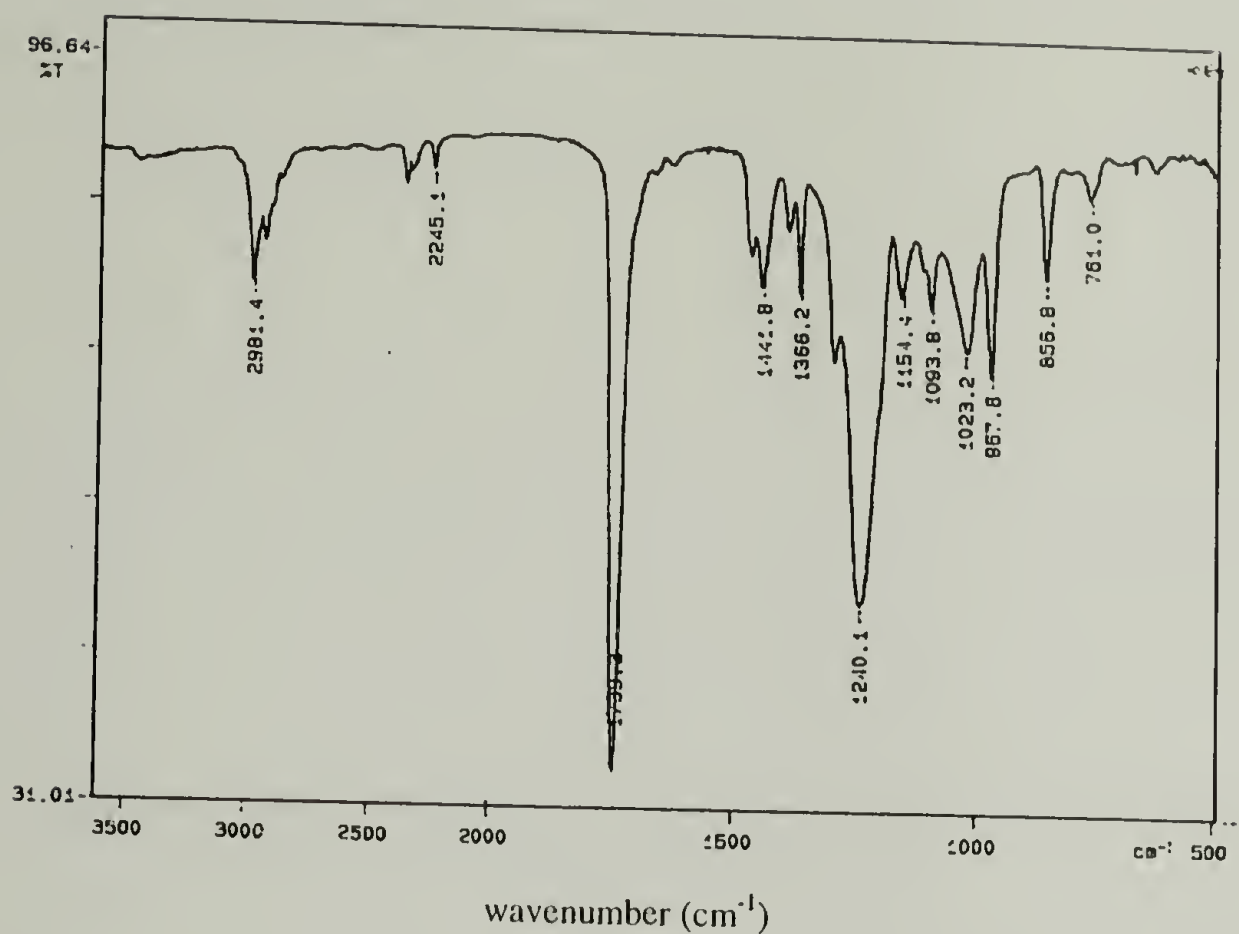


Figure 5.9. IR spectrum of Poly(9)

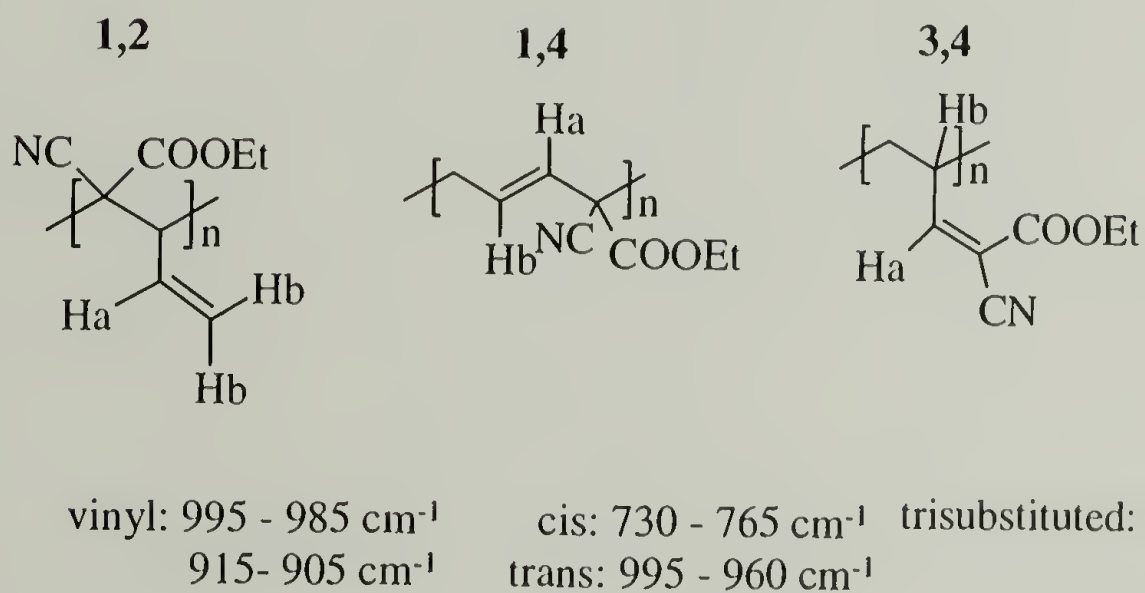
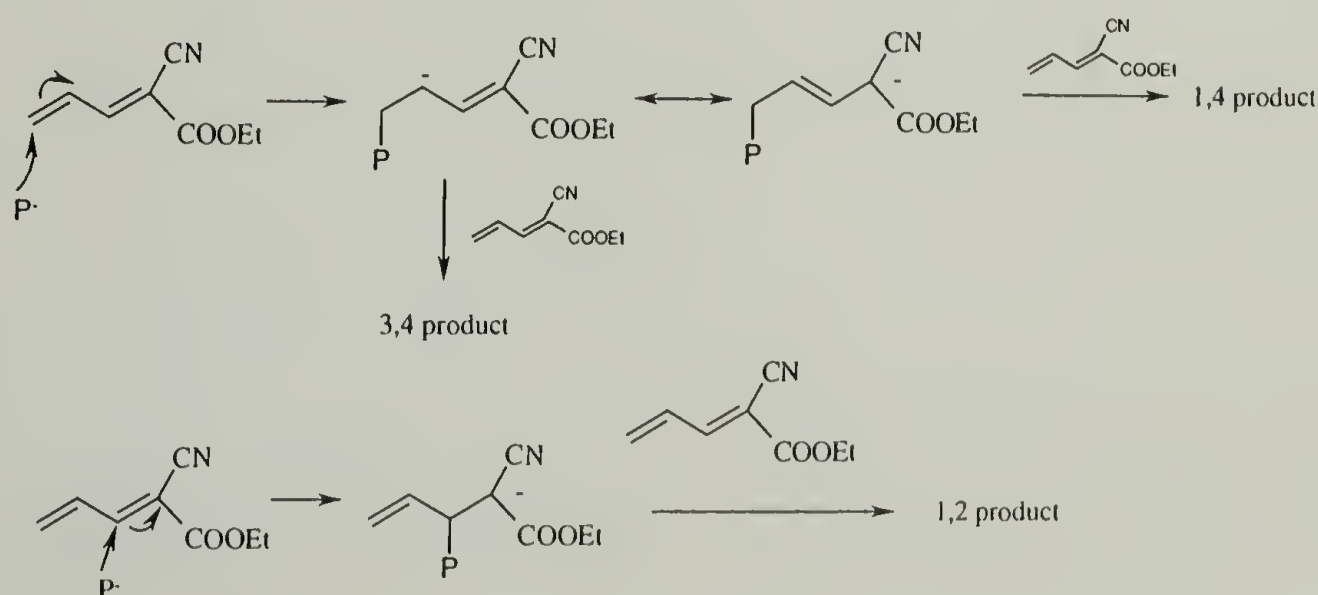


Figure 5.10. IR analysis of out-of-plane C-H bending for 1,2-; 1,4- and 3,4-units

These results contradict the previous report by Gerber, which, on the basis of UV-Vis spectroscopy, concluded that 15% of the microstructure was composed of 3,4-units and 75 % of 1,4-addition units. NMR and IR analysis of a sample polymerized under equivalent conditions provided strong evidence that this conclusion is incorrect. A similar analysis of the microstructure of a sample of poly(**10**) (piperidine, benzene - Table 5.1) indicated that the polymer consisted of a mixture of 1,2- (17%); 1,4- (17%) and 3,4- (66%) units. A discussion of these results is provided in following.

Stereochemical control of the microstructure of poly(**9**) and poly(**10**) was the main focus of this study. The targeted polybutadiene microstructure was the 1,4-product, which after subsequent hydrogenation would yield the desired poly(tetramethylene) (Figure 5.1). In this study, the data provided by NMR spectroscopy unambiguously proved that the microstructure of poly(**9**) obtained under anionic conditions consists only of units resulting from the 1,4-addition. Scheme 5.4 shows the various possible mechanisms of addition during the anionic polymerization of **9**. The stabilization of the propagating carbanion by the allylic structure favors the propagation via 1,4-addition over the 3,4-addition.



Scheme 5.4. Mechanisms for 1,2-; 1,4-; and 3,4-additions

The 1,2 addition product is less favored over the 1,4 addition probably due to the steric and electronic repulsion associated with the presence of nitrile and ester substituents on the carbon atom of the propagating carbanion. Under the free-radical conditions described, the 1,4-addition product was also the only product for poly(**9**) observed via NMR spectroscopy.

For poly(**10**), a mixture of microstructures was observed. The 3,4-addition product becomes favored (66%), but 1,4- (17%) and 1,2- (17%) products can be observed as well. These results are surprising, in particular the clear preference for the formation of the 3,4-microstructure that implies the preferred formation of a less stabilized intermediate (loss of the allylic stabilization) during the polymerization. A direct attack on the  $\beta$  rather than the  $\delta$  position also involves a much larger steric strain in the transition state. We propose that the formation a complex involving the propagating piperidinium carbanion and one monomer molecule acting as a ligand (bidentate?) is responsible for the observed stereochemistry (Figure 5.11). Although this is strictly hypothetical, tetrahedral intermediates such as **i** or **ii**, where the nucleophilic site and butadienyl moieties are prearranged, could explain the preferred addition on the  $\beta$  position of the butadiene.

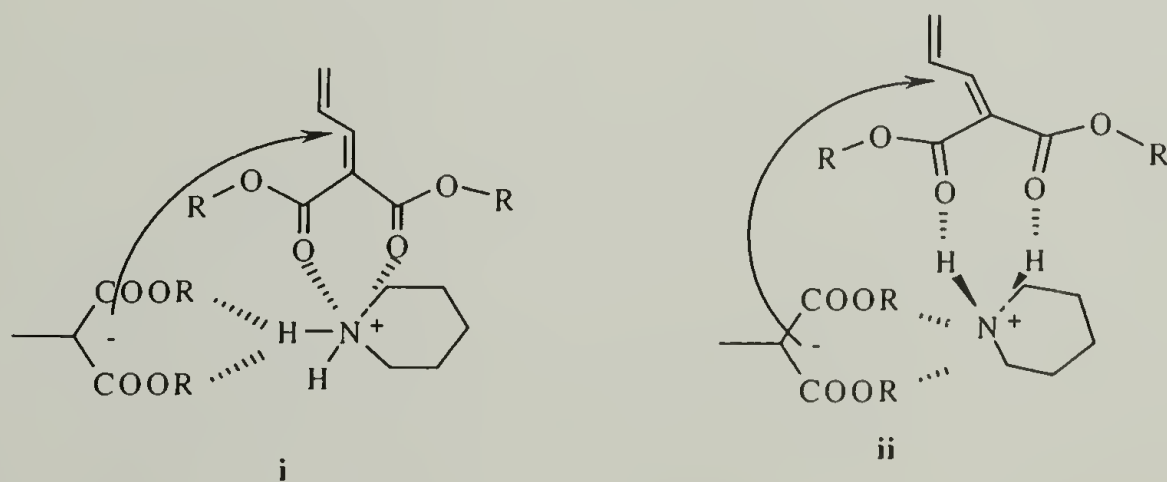


Figure 5.11. Proposed Tetrahedral Intermediates **i** and **ii**

It is known that for ammonium ions, the positive centers are on the adjacent carbons and hydrogens, rather than on the nitrogen as suggested by the Lewis structure. X-ray analysis of organic ammonium salts with bidentate anions has indicated that the geometry where the electron-rich sites on the anion interact strongly with the atoms directly attached to the central nitrogen is the preferred one in the solid state.<sup>62,63</sup> The fact that the cyanoester butadiene **9** is not attacked on the  $\delta$  position might reflect the difficulty for the cyanoester moiety to effectively act as a bidentate ligand, the lone pair on the cyano group being colinear with the CN bond.

5.4.5 Hydrogenation Results. Attempts to hydrogenate 1,4 poly(**9**) were performed using the diimide generated in situ by the thermal decomposition of p-toluenesulfonylhydrazide. This method has been successfully used to hydrogenate polymers with functional groups such as nitrile groups.<sup>58</sup> Analysis of the <sup>1</sup>H-NMR spectrum of the product indicated 66% of the hydrogenation had occurred after refluxing for 4 hours in o-xylene. Previous work on the hydrogenation of unsaturated polymers using this method had indicated that complete hydrogenation was usually achieved by adding a second amount of p-TSH and the tri-n-propyl amine with additional reflux time. However, in the case of the hydrogenation of poly(**9**), it was initially suspected that incomplete hydrogenation occurred due to precipitation of the hydrogenated product as the reaction proceeded. Changing the solvent to a good solvent for the hydrogenated product, such as DMF, showed improved conversion (80%), but was still not quantitative under the conditions described above. Optimization of the experimental conditions in order to achieve quantitative hydrogenation needs further pursuit.



## 5.5 Conclusions

The synthesis of unsaturated poly(tetramethylene)s was achieved via the anionic polymerization of 1,1-difunctionalized-1,3-butadienes. The anionic polymerization of ethyl 2-cyano-2,4-pentadienoate **9** yielded polymers with only the 1,4-microstructure, while the anionic polymerization of diethyl 2-propenylidenemalonate **10** yielded a mixture of 1,2-; 1,4- and 3,4-microstructures. Subsequent hydrogenation of poly(**9**) yielded partially hydrogenated (80 %) polymers using diimide as the reducing agent. Further work will be needed to identify conditions that yield only the 1,4-microstructure for **10**, and complete hydrogenation of poly(1,4) structures thereafter. This study showed that this strategy provides a feasible method to achieving the desired poly(1,1-difunctionalized tetramethylene)s, however, stereochemical control of the butadiene polymerization is crucial.

## 5.6 References

- (1) In *Encyclopedia of Polymer Science and Engineering*; Mark, H., Bikales, N. M., Overberger, C. G., Menges, G., Kroschwitz, J. I., Eds.; Wiley-Interscience: New York, 1985; Vol. 12, p 668.
- (2) Woods, J. In *Polymeric Materials Encyclopedia*; Salamone, J. C., Ed.; CRC Press: N.Y, 1996; Vol. 2, p 1632.
- (3) Ulrich, H. In *Introduction to Industrial Polymers*; Hanser: Munich, 1993; pp 48, 63-64, 180.
- (4) Stempel, G. H. In *Polymer Handbook*; Brandrup, J., Immergut, E. H., Eds.; Wiley: New York, 1975; Vol. V-1 - V-5.
- (5) Silas, R. S.; Yates, J.; Thornton, N. *Anal. Chem.* **1959**, *31*, 529.
- (6) Binder, J. L. *J. Polym. Sci.* **1963**, *A-1*, 47.
- (7) Binder, J. L. *J. Polym. Sci.* **1965**, *A-3*, 1587.

- (8) Santee, E. R.; Chang, R.; Morton, M. *J. Polym. Sci. Polym. Lett. Ed.* **1973**, *11*, 449.
- (9) Mochel, V. D. *J. Polym. Sci., Part A: Polym. Chem.* **1972**, *10*, 1009.
- (10) Duch, M. W.; Grant, D. M. *Macromolecules* **1970**, *3*, 165.
- (11) Clague, A. D. H.; Van Brockhaven, J. A. M.; Blaauw, L. P. *Macromolecules* **1973**, *7*, 348.
- (12) Dreyfuss, P. In *Polymeric Materials Encyclopedia*; Salamone, J. C., Ed.; CRC Press: N.Y Vol. 8, pp 5657-5662, and references therein.
- (13) Tobolsky, A. V.; Rogers, C. E. *J. Polym. Sci.* **1959**, *40*, 73.
- (14) Morton, M.; Fetters, L. J. *J. Polym. Sci.* **1964**, *A2*, 3311.
- (15) Tate, D. P.; Bethea, T. W. In *Encyclopedia of Polymer Science and Engineering*; John Wiley & Sons: New York, 1985; Vol. 2, p 537.
- (16) Schultz, D. N.; Turner, S. R.; Golub, M. A. *Rubber Chem. Technol.* **1982**, *55*, 809.
- (17) Wicklatz, J. In *Chemical Reactions of Polymers*; Fetters, E. M., Ed.; Wiley-Interscience: N.Y, 1964; Chapt. 2F.
- (18) Golub, M. A. In *The Chemistry of Alkenes, Vol. 2*; Zabicky, J., Ed.; Wiley-Interscience: London, 1970, Chapt. 9.
- (19) Moberly, C. W. In *Encyclopedia of Polymer Science and Engineering*; Mark, H., Bikales, N. M., Overberger, C. G., Menges, G., Kroschwitz, J. I., Eds.; Interscience: N.Y, 1967; Vol. 7, p 557.
- (20) Schultz, D. N. In *Encyclopedia of Polymer Science and Engineering*; Mark, H., Bikales, N. M., Overberger, C. G., Menges, G., Kroschwitz, J. I., Eds.; Wiley-Interscience: N. Y, 1985; Vol. 7, pp 807-817 and references therein.
- (21) Harwood, H. J.; Russell, D. B.; Verthe, J. J. A.; Zymonas, J. *Makromol. Chem.* **1973**, *163*, 1.
- (22) Yakubchik, A. I.; Tikhomirov, B. I.; Sulimov, V. S. *Rubber Chem. Technol.* **1962**, *35*, 1063.
- (23) Yakubchik, A. I.; Gromova, G. N. *Rubber Chem. Technol.* **1958**, *31*, 156.
- (24) Jones, R. V.; Moberly, C. W.; Reynolds, W. B. *Ind. Eng. Chem.* **1953**, *45*, 1117.

- (25) Gregg, E. C. *Am. Chem. Soc., Div. Polym. Chem.* **1967**, 8, 851.
- (26) Ramp, F. L.; DeWitt, E. J.; Trapasso, L. E. *J. Org. Chem* **1962**, 27, 4368.
- (27) Falk, J. C.; Schlott, R. C. *J. Org. Chem.* **1971**, 36, 1445, and references included therein.
- (28) Vol'pint, M. E.; Kolomnnikov, I. S. *Russ. Chem. Rev. (English Trans.)* **1969**, 38, 273.
- (29) Gippin, M. *Rubber Chem. Technol.* **1962**, 35, 1066.
- (30) Sloan, M. F.; Matlack, A. S.; Breslow, R. *J. Am. Chem. Soc.* **1963**, 85, 4014.
- (31) Witt, D. R.; Hogan, J. P. *J. Polym. Sci., Part A: Polym. Chem.* **1970**, 8, 2689.
- (32) Falk, J. C.; Schlott, R. C. *Macromolecules* **1971**, 4, 152.
- (33) Duck, E. W.; Locke, J. M.; Mallinson, C. J. *Ann. Chem.* **1968**, 719, 69.
- (34) Taylor, G. L.; Davison, S. *J. Polym. Sci., Part B: Polym. Lett.* **1968**, 6, 699.
- (35) van Tamelen, E. E.; Dewey, R. S.; Timmons, R. J. *J. Am. Chem. Soc.* **1961**, 83, 3729.
- (36) Hunig, S.; Muller, R.; Thier, W. *Tetrahedron Lett.* **1961**, 353.
- (37) Corey, E. J.; Mock, W. Y.; Pasto, D. J. *Tetrahedron Lett.* **1961**, 11, 347.
- (38) Miller, C. E. *J. Chem. Ed.* **1965**, 42, 254.
- (39) Hunig, S.; Muller, R.; Thier, W. *Angew. Chem. Int. Ed. Eng.* **1965**, 4, 271.
- (40) Nakagawa, T.; Okawara, M. *J. Polym. Sci., Part A: Polym. Chem.* **1968**, 6, 1795.
- (41) Mango, L. A.; Lenz, R. W. *Makromol. Chem.* **1973**, 163, 13.
- (42) Aylward, F.; Sawistowska, M. *Chem. Ind.* **1962**, 404, 484.
- (43) Cusack, N. J.; Reese, C. B.; Risius, A. C.; Rozpeikar, B. *Tetrahedron* **1976**, 32, 2157.
- (44) Hunig, S.; Muller, R.; Thier, W. *Angew. Chem. Int. Ed. Eng.* **1963**, 2, 214.
- (45) O'Gara, J. E.; Wagener, K. B.; Hahn, S. F. *Makromol. Chem.* **1993**, 14, 657.



- (46) Hahn, S. F. *J. Polym. Sci., Part A: Polym. Chem.* **1992**, 30, 397.
- (47) Shroff, R.; Prasad, A.; Lee, C. J. *J. Polym. Sci., Part B: Polym. Phys.* **1996**, 34, 2317.
- (48) Gerum, W.; Hohne, G. W. H.; Wilke, W.; Arnold, M.; Wegner, T. *Macromol. Chem. Phys.* **1996**, 197, 1691.
- (49) Chen, H. Y. *J. Polym. Sci., Polym. Lett. Ed.* **1977**, 15, 271.
- (50) Mohajer, Y.; Wilkes, G. L.; Wang, I. C.; McGrath, J. E. *Polymer* **1982**, 23, 1523.
- (51) Storey, R. F.; George, S. E. *Proc. Am. Chem. Soc. Div. Polym. Mat. Sci. Eng.* **1988**, 58, 985.
- (52) Rachapudy, H.; Smith, G. G.; Raju, V. R.; Graessley, W. W. *J. Polym. Sci., Polym. Phys. Ed.* **1979**, 17, 1211.
- (53) Sanui, K.; MacKnight, W. J.; Lenz, R. W. *J. Polym. Sci., Polym. Lett. Ed.* **1973**, 11, 427.
- (54) Gerber, A. H. *Polym. Prepr. (Am. Chem. Soc., Div. Polym. Chem.)* **1968**, 9, 434.
- (55) Kasatkin, A. N.; Biktimirov, R. K.; Tolstikov, G. A.; Khalilov, L. M. *Zh. Org. Khim. (Engl. Transl.)* **1990**, 26, 1191.
- (56) Warner, D. T.; Moe, O. A. *J. Am. Chem. Soc.* **1948**, 70, 3470.
- (57) Gerber, A. H.; U.S Patent 1967, 3,316,227.
- (58) Wittig, G.; Todt, U.; Nagel, K. *Chem. Ber.* **1950**, 83, 110.
- (59) Beletskaya, I. P.; Gulyukina, N. S.; Ali, M. A.; Solov'yanov, A. A.; Reutov, O. A. *Zh. Org. Khim.* **1987**, 23, 730.
- (60) Denchev, Z. Z.; Kabaivanov, V. S. *J. Polym. Sci.* **1991**, 42, 2933.
- (61) Matter, U.; Pascual, C.; Pretsch, E.; Pross, W. S.; Sternhell, S. *Tetrahedron* **1969**, 25, 691.
- (62) Reetz, M. T.; Knauf, T.; Minet, U.; Bingel, C. *Angew. Chem. Int. Ed. Eng.* **1988**, 27, 1373.
- (63) Reetz, M. T.; Hutte, S.; Goddard, R. *J. Am. Chem. Soc.* **1993**, 11, 9339.



## ANALYSIS OF THE CRYSTAL STRUCTURE OF POLY(1,1-DISUBSTITUTED TRIMETHYLENE)S

### 6.1 Introduction

It is well known that polyethylene PE chains crystallize in the all-trans (*TT*)<sup>1</sup> conformation, which is a straightforward 2-fold helix, or planar zig-zag with a stereochemical periodicity of 0.125 nm. The nature and the density of substituents present on the carbon backbone strongly influence the conformation of the chains in polymer crystals. For example, poly(vinylidene fluoride) will adopt conformations other than the all-trans in order to minimize unfavorable repulsive interactions between adjacent substituents.<sup>2</sup> In some examples such as isotactic polystyrene, the phenyl ring on every second carbon changes the conformation such that the backbone consists of a selective repetitive combination of *trans* and *gauche* (*G*) bonds (*TGTGTG*).<sup>3</sup> The introduction of *gauche* bonds into the backbone reduces the axially projected advance (along the *c*-axis) per carbon atom and generates a distinct chain axis periodicity.

Contrary to the typical repeat pattern of vinyl polymers with substituents on every second carbon, 1,1-disubstituted poly(trimethylene)s have geminal substituents on every third carbon. In this study, the polymers were synthesized via the anionic ring-opening polymerization of 1,1-disubstituted cyclopropanes as described in chapter 2 of this dissertation. The obtained polymers containing dicyano, cyano-ester, cyano-phenyl, and diester substituents on every third carbon are all semi-crystalline as provided by WAXS data. The aim of this study was to study the influence of the substitution pattern over the

conformation of the chains in the crystal. With this substitution pattern, an all-trans conformation (TTTTTT) of the backbone chains would generate a two-fold helical conformation with a c-repeat of 0.750 nm. This represents a three-fold increase from 0.250 nm expected for polymer chains with substituents on every second carbon in an all-trans conformation (such as polyethylene). It is proposed that due to this increased distance, the strong repulsive interactions between the substituents along the backbone are minimized, allowing the chains to maintain an all-trans backbone conformation. In contrast, analogous polymers with similar substituents on every second carbon (such as poly( $\alpha$ -cyanoacrylates) are all completely amorphous,.

Difficulties arising from the insolubility and decomposition before melting of poly(dicyanocyclopropane) poly(**1**) prevented a detailed analysis of its crystal structure since the necessary orientation of the chains could not be achieved. WAXS patterns of the powder samples of poly(**2a-d**) also provided evidence of crystallinity, however, a detailed study of their crystalline structure remains to be investigated. In this chapter, a detailed analysis of the crystal structure of poly(diethyl-1,1-cyclopropanedicarboxylate) poly(**3b**) is reported, including the dimensions of the unit cell.

## 6.2 Background

### 6.2.1 Crystallinity in Polymers

The ability of a polymer to crystallize depends on the structure of polymer and its tacticity. Unlike small molecules, long chain molecules generally do not form long-range continuous and exact periodic structures in three dimensions.<sup>4</sup> Crystallinity exists in regions within the polymer matrix where the molecules order themselves in a

thermodynamically favorable alignment. Therefore, polymers generally consist of regions of both ordered regions and regions characterized by almost complete lack of order (randomness) among the molecules. The regions of disorder are referred to as amorphous regions, while the ordered regions are composed of molecules that are oriented or aligned in a regular array analogous to crystalline packing in non-polymeric solids. Polymers never achieve 100% crystallinity, and are therefore referred to as semi-crystalline. This is evident in the measurement of the density of crystalline polymers, which is normally between that expected for a fully crystalline sample and that of an amorphous polymer.

In polymers, the basic chemical repeat unit consists of covalently attached molecules along the backbone. This differs from the spacial bonding patterns and organization in other directions, where the molecules are held by weak van der Waal forces between the chains. Several models have been proposed for the organization of macromolecules in a crystal. The fringed-micelle model was first proposed in the 1930s. It described polymer crystallinity in terms of localized highly ordered regions -crystallites- embedded in an amorphous matrix. In the 1950s, X-Ray diffraction experiments provided evidence for the folded-chain lamella theory. In 1957, the first single polymer crystals were grown from dilute solution.<sup>5</sup> The polyethylene crystals were plate-like (lamellar) with a crystal thickness on the order of 100 Å. Chain folding of the polymer chains was proposed since the chains are longer than the typical thickness observed for these crystals. Two modes of chain folding were described. Adjacent reentry describes the regular, uniform fold period, while non adjacent- re-entry describes the irregular manner in which the chains loop in and out of the lamellae. This chain folded lamella morphology was also observed for polymers crystallized from the melt. The



process of crystallization in polymers has been widely studied and been the subject of much debate. Some of the reported theories are highly sophisticated involving lengthy mathematical treatments, but are based on the main concept of nucleation and growth.

### 6.2.2 Factors determining crystal structure

The degree of crystallinity in a polymer depends on both thermodynamic and kinetic factors. Under thermodynamic considerations, the main parameter used to characterize the process of crystallization is Gibbs free energy,  $G$ . The Gibbs free energy is related to the enthalpy  $H$  and entropy  $S$  by the equation  $G = H - TS$ , where  $T$  is the thermodynamic temperature. During crystallization, the polymer molecules orient into ordered structures leading to a considerable reduction in the entropy,  $S$ . This entropy penalty is offset by the large reduction in enthalpy that occurs during crystallization. A negative value of the overall change in the Gibbs free energy,  $\Delta G$  on crystallization favors the thermodynamics of crystallization. The packing of polymer chains into a crystalline lattice is highly dependent on its structure and on the magnitude of secondary forces between the polymer chains. Regarding the structure, the linearity of the chains, and the tacticity are important factors in determining the extent of crystallization and the crystal structure. For example, the simple and regular structure of polyethylene favors its crystallization. Less simple structures such as polyamides are also highly crystalline, favored by the secondary forces provided by hydrogen bonding between the polar groups on the chains. Chain flexibility is also an important factor, since it allows the chains to easily achieve the required conformation for packing. Substituents in the main chain or side chains that stiffen the backbone, often lead to increased difficulties in packing. The



size of pendant groups along the backbone will also influence the crystallization behavior of a polymer. In general, less bulky functional groups are more easily incorporated into the crystal structure than larger groups.

Polymer crystallization is also greatly influenced by kinetic factors. Rapid cooling from the melt significantly decreases the degree of crystallinity, since little time is allowed for the cooperative movement of the chains to form ordered structures. Crystallization can be induced by annealing the amorphous polymer at a temperature between the glass transition temperature and the melting point of the crystals. PE crystallizes in lamellar form with a chain folded structure when slowly cooled from dilute solution. On the other hand, slow cooling from the melt results in spherulite formation, in which lamellar crystals are stacked and grow radially from the center of the spherulite crystal. Under high pressure and at high temperature, PE forms an extended chain crystal of several micron (length) in which the chains are fully extended.

The degree of crystallinity and the size and arrangement of the crystallites in a semi-crystalline polymer greatly affect its physical and chemical properties. Crystalline polymers are generally tougher, stiffer, more opaque and more resistant to solvent than their amorphous counterparts. Crystalline polymers also demonstrate superior mechanical properties resulting from the increase in the cohesive strength due to the more effective intermolecular secondary forces that arise from the close packing of molecules in the crystalline structure.<sup>6</sup>

### 6.2.3 Crystal structure determination

The structure of a crystalline solid is defined by a regular repeating pattern of atoms in three dimensions. The repeat unit is known as the *unit cell* and the crystals are made up of stacks of these unit cells in three dimensions. The dimensions of the unit cell are labeled  $a$ ,  $b$  and  $c$ . The crystal structure of small molecules can easily be determined from X-ray diffraction patterns of a single crystal sample. The relative positions of the atoms are determined from the measurement of the positions and intensities of the X-ray maxima obtained from diffractometers at different angles. The unit cell of the sample is calculated from this data.

In the case of macromolecules, the chains pack together side by side and generally lie along one particular direction in the crystals. The unit cells are made up of repeating segments of the polymer chains, often with several segments in one unit cell composed of tens or hundreds of atoms. The atoms along the chains are held by covalent bonds, while the chains are held together in the crystal by secondary forces such as van der Waal forces or hydrogen bonding. Since macromolecules do not form long range continuous and exact periodic structures in three dimensions, the crystals have anisotropic physical properties.

Determination of the crystal structure of a semi-crystalline polymer is more complicated. For most polymers large single crystals are difficult to obtain. Therefore, instead of using single crystals, samples are normally oriented prior to analysis. Orienting samples induces crystallinity in polymers, and can be achieved by drawing, stretching or rolling.

Highly stretched samples form long, slender crystallites with many hundreds of repeats along the crystalline axis, also known as the fibre or chain axis. For polymers, the chain axis is normally indexed as  $c$  in the unit cell.

X-Ray diffraction patterns of oriented samples are obtained on film and are known as fibre patterns. The polymer molecules are orientated approximately parallel to the fibre axis, which is parallel to the  $c$  direction in the crystal lattice. X-Ray photographs capture the spread of crystal orientation about the chain axis, and a fibre pattern obtained is analogous to the rotation photographs performed on a single crystal about the same crystallographic axis. The fibre patterns provide information on the unit cell dimensions of the polymer crystal. This is determined by assignment of the spots (or arcs) in the fibre patterns to the crystallographic indices ( $hkl$ ). Bragg's equation (1) is used to calculate the  $d$ -spacings ( $d_{hkl}$ )

$$n\lambda = 2d_{hkl} \sin \theta \quad (1)$$

where  $d$  is the spacing of the atomic net planes ( $hkl$ ),  $2\theta$  is the Bragg diffraction angle and  $\lambda$  is the x-ray wavelength. The diffraction angle  $2\theta$  is measured for all reflections and the used to calculate the  $d$ -spacing. A set of  $d_{hkl}$  is a function of the unit cell parameters.

The unit cell of a crystalline lattice is assigned to one of the seven basic crystal systems such as orthorhombic, or triclinic unit cells. Depending on the unit cell, several different equations relate the  $hkl$  indices to the  $d$ -spacings, which are a measure of the interplanar spacing of the regularly arranged atoms. For example, for the orthorhombic unit cell (2),

$$a \neq b \neq c \quad \alpha = \beta = \delta = 90^\circ \quad d_{hkl} = \left( \frac{h^2}{a^2} + \frac{k^2}{b^2} + \frac{l^2}{c^2} \right)^{-\frac{1}{2}} \quad (2)$$



The fibre patterns are usually calibrated with calcite, which has a strong diffraction ring of known  $d$ -spacing at 0.3035 nm ( $d_{111}$ ). The measure  $d$ -spacings are then compared with various sets of  $hkl$  planes of unit cells with different dimensions. All reflections on the equator have index  $l = 0$ , while for those on the first layer line  $l = 1$ , and so on. The value of  $c$  in the unit cell can be easily calculated from this layer line spacing since  $h$  and  $k = 0$ . Difficulties arise for semi-crystalline polymers because the reflections tend to be in the form of arcs due to imperfect orientation of the crystals. The arcs can also be diffuse due to the small dimensions of the crystallites and lattice imperfections. Once the position and intensities of the reflections are assigned, the unit cell dimensions can be calculated. This assignment is not simple, and often, theoretical calculations must be made of plausible crystal structures. The number of chains and the chain repeat units per unit cell can be determined from crystallographic data. Simulations of diffraction patterns are then compared with the experimental and the best fit is used as a model for the crystal structure of the polymer.

Transmission Electron Microscopy (TEM) analysis is also important in crystal structure determination. Imaging by electron microscopy provides evidence of the crystal size and thickness. These factors are dependent on the crystallization conditions, such as solvent used and crystallization time. Electron diffraction patterns are also used to calculate the  $d$ -spacings, which are indexed to a particular unit cell using the  $hkl$  indices, similar to the method described for X-ray diffraction. These patterns are typically calibrated with gold. This information is then used to calculate the unit cell dimensions, which should correlate to the X-ray diffraction data.



## 6.3 Experimental

### Materials

The polymers used in this study were synthesized according to a general procedure described in chapter 2 of this dissertation (pg 58). The poor solubility of poly-(1,1-dicyanocyclopropane) poly(1) and poly(phenyl 1-cyclopropanecarbonitrile) poly(4) limited the determination of their  $\overline{Mn}$ . For the other polymers  $\overline{Mn}$  values were measured by GPC (DMF at 100 °C, PS standards) and re-calibrated by end-group analysis via NMR. Poly(alkyl 1-cyanocyclopropanecarboxylates) poly(2a-d); poly(2a) ( $\overline{Mn}$  = 5000), poly(2b) ( $\overline{Mn}$  = 5370), poly(2c) ( $\overline{Mn}$  = 7730), poly(2d) ( $\overline{Mn}$  = 7000). Poly(diethyl cyclopropane-1,1-dicarboxylate) poly(3b) ( $\overline{Mn}$  = 12000) was obtained from a colleague Xie Tao in our research group. The chemical synthesis and characterization of the polymer is reported in the literature.<sup>7</sup>

### **Sample Preparation.**

**Isothermal Crystallization from Solution.** Poly(diethyl cyclopropane-1,1-dicarboxylate) poly(3b) was dissolved in benzene (1% w/v) at 70 °C for 30 min. Crystals of the polymer were grown by isothermal crystallization at 30 °C for 12 h before cooling to room temperature. At room temperature the turbid mixture was diluted to a 0.01% w/v solution. Oriented mats suitable for X-ray diffraction were prepared by filtering the crystalline suspension through a 0.2  $\mu\text{m}$  Millipore filter contained in a stainless steel filter holder. The filter holder was connected to a water aspirator to extract the solvent. A thin film of the crystals was obtained after drying the sample.

**Crystallization from the melt.** Fiber samples of poly(**3b**) suitable for X-ray diffraction were prepared by drawing samples from the melt ( $T_m \sim 176^\circ\text{C}$ ) and allowed to cool to room temperature. The density ( $\rho$ ) was measured at  $25^\circ\text{C}$  by floatation in a mixture of perfluorodecalin ( $\rho = 1.908\text{ gcm}^{-3}$ ) and pentane ( $\rho = 0.626\text{ gcm}^{-3}$ ). The density of crystalline Poly(**3b**) was found to be  $1.17 \pm 0.03\text{ gcm}^{-3}$ .

### Measurements

**Transmission Electron Microscopy.** Samples for TEM were prepared by depositing drops of the crystalline suspension (0.01% w/v) in benzene onto carbon-coated grids. Gradual evaporation of the solvent was achieved overnight. Some of the grids were coated with gold to calibrate the diffraction patterns and to decorate the crystals for imaging. In some cases, the crystals were also decorated with platinum/palladium to enhance the contrast of the TEM images. The grids were examined at room temperature in both imaging and diffraction modes using a JEOL 100 CX electron microscope operating at an accelerating voltage of 100 kV.

**X-ray Diffraction.** X-ray diffraction patterns were obtained from sedimented mats and from fibers of poly(**3b**). Both wide and low-angle X-ray diffraction patterns were obtained at room temperature using a nickel-filtered Cu  $K_\alpha$  radiation of wavelength 0.1542 nm. The data was recorded on film, using a point-collimated beam, in an evacuated Statton camera. The diffraction patterns were obtained with the incident beam directed parallel and orthogonal to the surface of the mats. Calcite ( $d_B = 0.3035\text{ nm}$ ) was dusted onto the samples for calibration purposes.

**Wide angle X-ray scattering (WAXS).** WAXS patterns of the polymers were obtained at room temperature using Siemens D500 diffractometer, operating in transmission mode with Ni-filtered  $\text{CuK}_\alpha$  radiation of wavelength 0.1542 nm.

### **Model Building and Analyses of Structure**

*Torsional angle calculations.* The potential energy profiles for backbone torsional angles were calculated using the InsightII computer program and the CVFF force field. For each backbone bond, the torsion angles at the center of successive trimers of the poly(**3b**) molecule, translating one backbone carbon at a time, were examined. Scans were performed by setting the torsion angle under investigation at given value between  $0^\circ$  and  $360^\circ$  in  $10^\circ$  steps and minimizing the energy of the system.

*Modeling.* The software package Cerius2, version 3.8 (MSI) was used in the structural modeling and diffraction simulations. The basic strategy was to determine the molecular conformation of the poly(**3b**) molecule and the molecular packing arrangement within the experimental unit cell. After the initial model building stage, a combination of energy minimization (EMin), using the CVFF force field, and simulations of diffraction patterns was used. It was ensured that the model was stereochemically sound and that the simulated diffraction patterns were in good agreement with the experimental data.

*Diffraction Pattern Simulations.* In the computer simulated X-ray diffraction patterns, the temperature factor, degree of arcing and relative intensity were chosen to match the experimental X-ray diffraction pattern(s). At each reciprocal lattice point we compared the calculated intensity with the observed intensity to ensure that the final refined structure had no unacceptable discrepancies.<sup>8</sup>



## 6.4 Structure and Morphology of Poly(diethyl-1,1-cyclopropane dicarboxylate).

### 6.4.1 Results

6.4.1.1 Electron Microscopy - Imaging. Figure 6.1 (a, b, c) show a series of TEM images of lamellae-like crystals of poly(**3b**) grown isothermally from a benzene solution. Figure 6.1(a) shows a common scene of gently overlaying lamellar-like crystals with no particular azimuthal interrelationship. In general, the crystals are crudely ellipsoidal in shape a few microns in length. Figure 6.1(b) shows a higher magnification picture of two adjacent individual crystals and the metal shadowing gives a value of 7–8 nm for the thickness. In some instances the poly(**3b**) crystals form of a terraced stack in azimuthal register, as shown in Figure 6.1(c) ( $\approx 10$  layers). It is probable that this type of architecture is a consequence of epitaxial crystallization.

Figure 6.1. Transmission electron micrographs of the Poly(**3b**) lamellar-like crystals isothermally crystallized from benzene. (a) Groups of the gently overlaid ellipsoidal crystals shadowed with gold to enhance contrast. (b) A pair of individual crystals at higher magnification, also shadowed with gold. Inset: selected area ( $hk0$ ) electron diffraction pattern taken with the electron beam normal to the lamellar surface to show the relative orientation with respect to the crystals. (c) A terraced stack ( $\approx 10$  layers) of crystals in azimuthal register; shadowed with Pt-Pd. Note: scale bars 1  $\mu\text{m}$ .



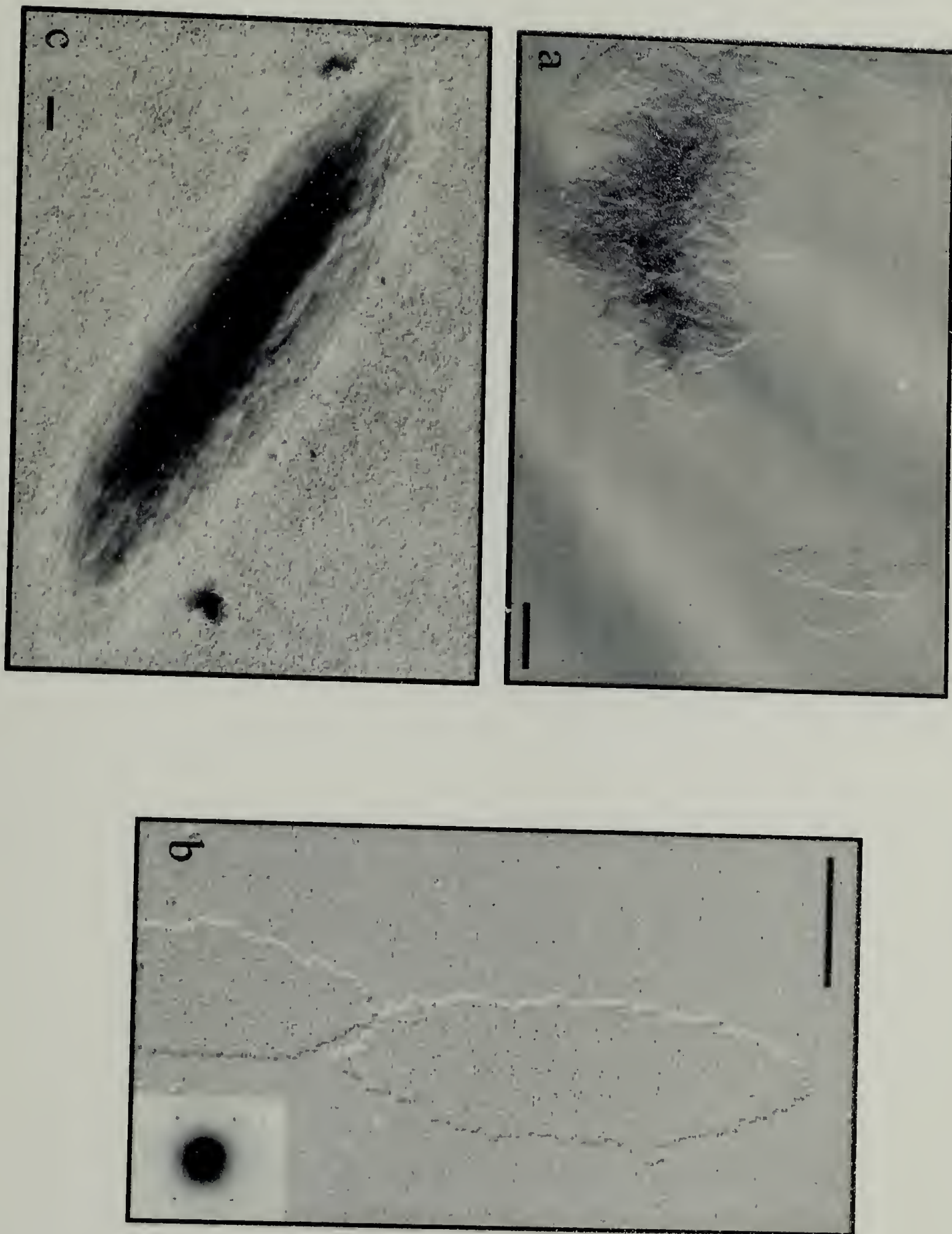
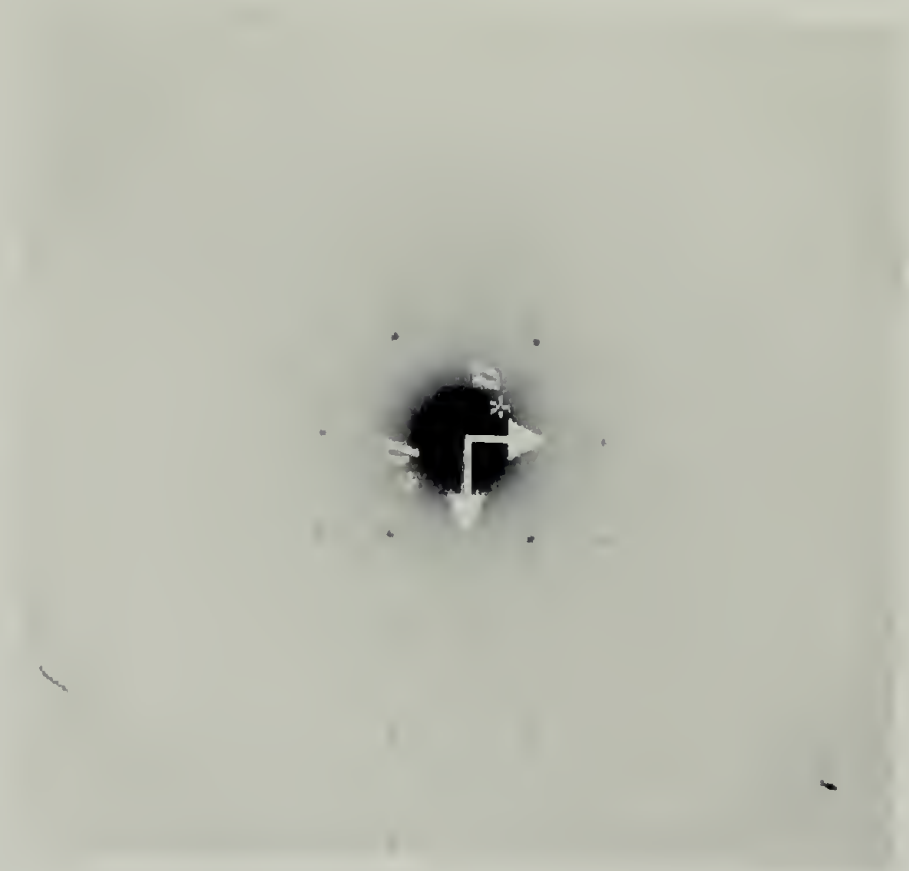


Figure 6.1

6.4.1.2 Electron Diffraction. The electron diffraction pattern of single crystals of poly(**3b**) is shown in Figure 6.2(a). The pattern was obtained with the beam normal to the lamellar crystal surface. The diffraction signals lie on a rectangular net, which we believe corresponds to the  $hk0$  reciprocal lattice, i.e. the chains are normal to the lamellar surface (this is proven by X-ray diffraction results provided later). From the gold calibration, all the electron diffraction spots can be indexed in terms of rectangular real lattice with parameters:  $a = 1.554$  nm,  $b = 1.136$  nm and  $\gamma = 90^\circ$ . The electron diffraction spacings, together with estimated intensities, are given in Table 6.1. The relative azimuthal orientation of the electron diffraction pattern to the crystals is shown by the inset in Figure 6.2(b). There are systematic absences for  $h00$  and  $0k0$  for odd  $h$  and  $k$ , respectively, a feature consistent with a  $p2gg$  two-dimensional space group. This, together with the strong intensities of the  $\{110\}$  diffraction signals, supports a model with molecules sited at the corners and center of the  $ab$ -rectangular lattice.

Figure 6.2. Selected area  $hk0$  electron diffraction patterns. (a) Taken with the electron beam normal to the lamellar-like crystal surface (001). The diffraction signals index on a rectangular reciprocal lattice with  $a^* = 0.644 \text{ nm}^{-1}$ ,  $b^* = 0.880 \text{ nm}^{-1}$  and the strong  $\{110\}$  family of diffraction signals suggest the molecules are sited at the corner(s) and center of the  $ab$ -basal plane. The metal calibration ring is just visible on the periphery of the pattern. (b) Calculated weighted  $hk0$  reciprocal net. The circular spot diameter is proportional to the relative intensity.

a



b

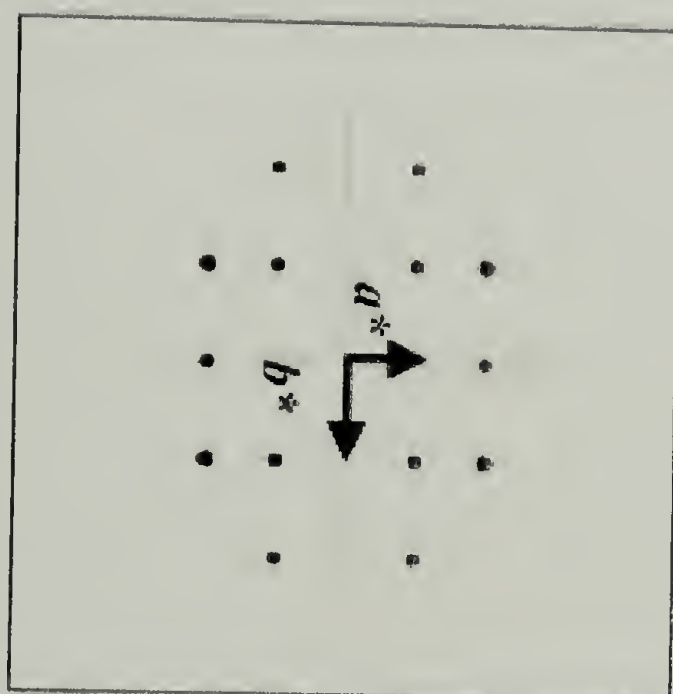


Figure 6.2



**Table 6.1.** Comparison of Observed and Calculated Diffraction Spacings (nm) and Relative Intensities: Electron Diffraction Data ( $hk0$ ) from Individual Poly(**3b**) Lamellar Crystals

$hkl^a$	$d_{obs}$	$d_{calc}$	$I_{obs.}^b$
100	s	1.554	
010	s	1.136	
110	0.917	0.917	vs
200	0.777	0.777	s
210	0.640	0.641	s
120	0.533	0.533	s
300	s	0.515	
320	0.383	0.383	w
030	s	0.379	

<sup>a</sup> Indexed on a rectangular lattice with parameters:  $a = 1.554$  nm,  $b = 1.136$  nm.

<sup>b</sup> vs: very strong; s: strong. <sup>s</sup> Systematic absence

6.4.1.3 X-Ray Diffraction. The wide-angle diffraction pattern from an oriented, sedimented mat of poly(**3b**) (isothermally-crystallized from benzene) is shown in Figure 6.3(a), with the incident beam parallel parallel to the mat surface (mat normal vertical). We believe that the diffraction signals on the first and higher layer lines are broader as a consequence of the shorter ( $\approx 7$  nm) coherent length along the molecular axis. The wide-angle X-ray diffraction pattern obtained with the incident beam directed orthogonal to the melt-crystallized poly(**3b**) fibers is shown in Figure 6.3(b). The pattern is similar to that obtained from the sedimented mats of isothermally solution-grown crystals (Figure 6.3(a), but the diffraction signals ( $hk1$ ) on the first layer line are more clearly defined, a feature which we will consider in the discussion section later.

The equatorial diffraction signals matched those obtained by electron diffraction and confirm that the electron diffraction pattern (Figure 6.2(a)) represents the  $hk0$  reciprocal lattice. Systematic absences for  $h00$  and  $0k0$  for odd  $h$  and  $k$ , respectively, were found.

**Figure 6.3.** Wide-angle X-ray diffraction patterns of Poly(**3b**) (a) Isothermally crystallized from benzene and sedimented into oriented mats; the incident beam directed parallel to the mat surface (mat normal vertical). The circles in the top half represent the calculated reciprocal lattice points; the diameters are proportional to the calculated relative intensity after appropriate Lorentz (incorporating Cox & Shaw factor) and polarization factors have been applied. (b) The wide-angle X-ray diffraction pattern from a melt-crystallized fiber of Poly(**3b**) obtained with the incident beam directed orthogonal to the fiber axis (vertical). Note the increased sharpness of the first layer line diffraction signals. (c) The low-angle X-ray diffraction pattern showing a pair of diffraction arcs at  $7.26 \pm 0.03$  nm spacing. The diffraction arc(s) near the periphery (top, right-hand and bottom left-hand) is the wide-angle 110 diffraction signal which provides a useful calibration.

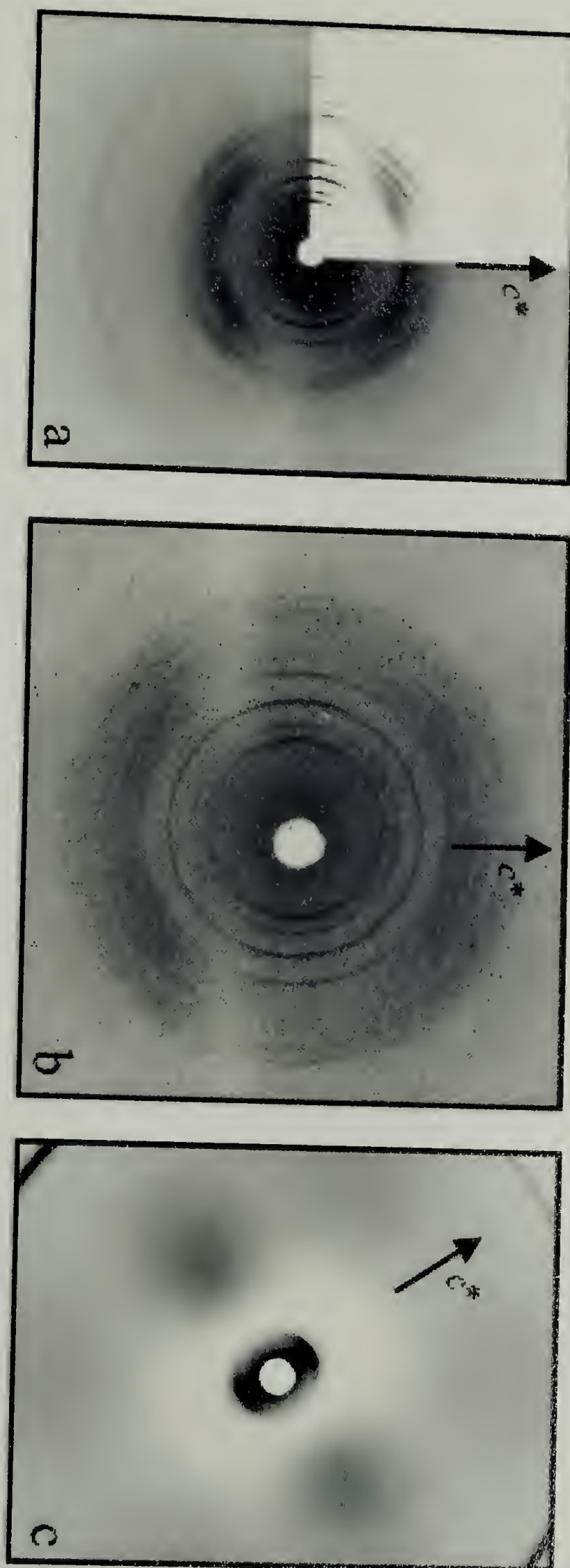


Figure 6.3

Knowing the spacings and indices of the  $hk0$  diffraction signals we were able, by following the row lines, to unambiguously identify six independent  $hk1$  first layer line signals (111, 201, 211, 121, 411, 511). The measured spacings of these  $hk1$  diffraction signals were used to establish, with confidence, a  $c$ -value of  $0.585 \pm 0.002$  nm. A second order layer line also appears together with a weak (002) meridional diffraction signal. This distribution of layer line intensity suggests a 2-fold helical conformation for the PDEE molecule, which when coupled with the other systematic absences mentioned above, enables the space group  $P2_12_12_1$  to be assigned.

The diffraction signals in both patterns (Figures 6.3(a) and 6.3(b)) index on an orthorhombic unit cell with parameters:  $a = 1.554 \pm 0.002$  nm,  $b = 1.136 \pm 0.002$  nm,  $c$  (chain axis) =  $0.585 \pm 0.002$  nm. The wide-angle X-ray diffraction pattern, obtained with the incident beam orthogonal to the sedimented mat surface, shows a set of diffraction rings that index on the same crystallographic lattice. A summary of the measured diffraction spacings, indexing and relative intensities are given in Table 6.2.



Table 6.2. X-ray Diffraction Data from Oriented, Sedimented Poly(3b) Lamellar-like Crystals.

$hkl^a$	$d_{obs}$	$d_{calc}$	$I_{obs.}^b$	$hkl^a$	$d_{obs}$	$d_{calc}$	$I_{obs.}^b$
100	s	1.554		001	s	0.585	
010	s	1.136		111	0.492	0.493	m
110	0.917	0.917	vs	201	0.466	0.467	m
200	0.779	0.777	s	211	0.433	0.432	m
210	0.639	0.641	vs	121	0.397	0.394	s
020	0.567	0.568	vw	411	0.311	0.312	w
120	0.533	0.533	s	511	0.269	0.267	w
300	s	0.515					
320	0.384	0.383	w	002	0.293	0.293	vw
030	s	0.379		112	0.280	0.279	w
410	0.369	0.368	m	202	0.272	0.274	w
230	0.339	0.340	w	312	0.249	0.248	m
510	0.301	0.300	m				

<sup>a</sup> Indexed on an orthorhombic unit cell with parameters:

$a = 1.554 \pm 0.002$  nm,  $b = 1.136 \pm 0.002$  nm,  $c$  (chain axis) =  $0.585 \pm 0.02$  nm.

<sup>b</sup> vs: very strong; s: strong; m: medium; w: weak, vw: very weak.

<sup>s</sup> Systematic absence.

The low-angle X-ray diffraction pattern (Figure 6.3(c)) shows a pair of arcs on the meridian, at spacing  $7.26 \pm 0.03$  nm, that we believe represents the lamellar stacking periodicity (LSP). We are able to record this pattern simultaneously with the 110 wide angle diffraction signal allowing a direct calibration, and therefore, we are able to measure the LSP spacing with better than usual confidence.

## 6.4.2 Discussion

6.4.2.1 Backbone Conformation. The measured  $c = 0.585$  nm value is 22% lower than that expected for an all-trans cyclopropane backbone conformation with substituents located on every third carbon atom (see Introduction).<sup>9</sup> This suggests that the backbone conformation is compressed, for example, by introduction of gauche bonds. The evidence from the oriented X-ray diffraction patterns suggests a 2-fold helical conformation for the backbone of poly(**3b**) molecules. We also know from the observed intensity distributions, in both the electron and X-ray diffraction patterns, that we have two molecules passing through the *ab*-basal plane, at the corner(s) and center;<sup>10</sup> thus, four chemical units per unit cell. Indeed, the assignment of space group  $P2_12_12_1$  defines the coupling between molecules rather precisely and means that the molecules are arranged in an antiparallel fashion.

Before proceeding, it is perhaps worth pausing to consider if a model with an all-trans backbone is at all credible for the poly(**3b**) molecule. Afterall, this is the backbone conformation found in the case of spiro(cyclopropane-1,9'-fluorene),<sup>9</sup> as discussed in the Introduction. If we imagine a *c*-axis spacing of 0.75 nm for poly(**3b**), the calculated fully crystalline density would be  $0.93 \text{ gcm}^{-3}$ , a value 21% less than the  $1.17 \pm 0.03 \text{ gcm}^{-3}$  measured value. Since calculated densities are invariably greater than measured densities, there is a serious and fundamental problem for a crystalline structure of PDEE based on an all-trans backbone conformation.

For polymers where the side groups have the potential flexibility to decouple themselves from the symmetry of the backbone, as is the case for poly(**3b**), it is also prudent to consider if the side groups within in the crystal could conspire in some way to

generate unexpected periodicities.<sup>11</sup> We were unable to find any structures that would generate even the basic features of the experimental diffraction pattern, while maintaining an all-trans backbone conformation.

Thus, we return to consideration of a structural model where the backbone conformation is compressed. In this case the calculated density is  $1.20 \text{ gcm}^{-3}$ , 3% more than the measured value, and gives an appropriate fit with the measured density. Based on the concepts outlined in the Introduction, chain conformations were considered involving combinations of trans and gauche bonds, while still maintaining the 2-fold helical character for the backbone. It turns out that the backbone sequence  $TG\overline{G}TG\overline{G}$  meets these two criteria exactly and the basic conformation is illustrated in Figure 6.4.<sup>12</sup>

**Figure 6.4.** Two orthogonal views (perpendicular to the  $c$ -axis) of the basic backbone ( $TG\overline{G}TG\overline{G}$ ) conformation for Poly(**3b**). This backbone conformation is a 2-fold helix with a  $c$ -repeat of 0.585 nm. Note the trans conformation (arrowed) is the  $CX_2-CH_2-CH_2-CX_2$  bond(s). The shaded side features represent the  $-X$  side groups.



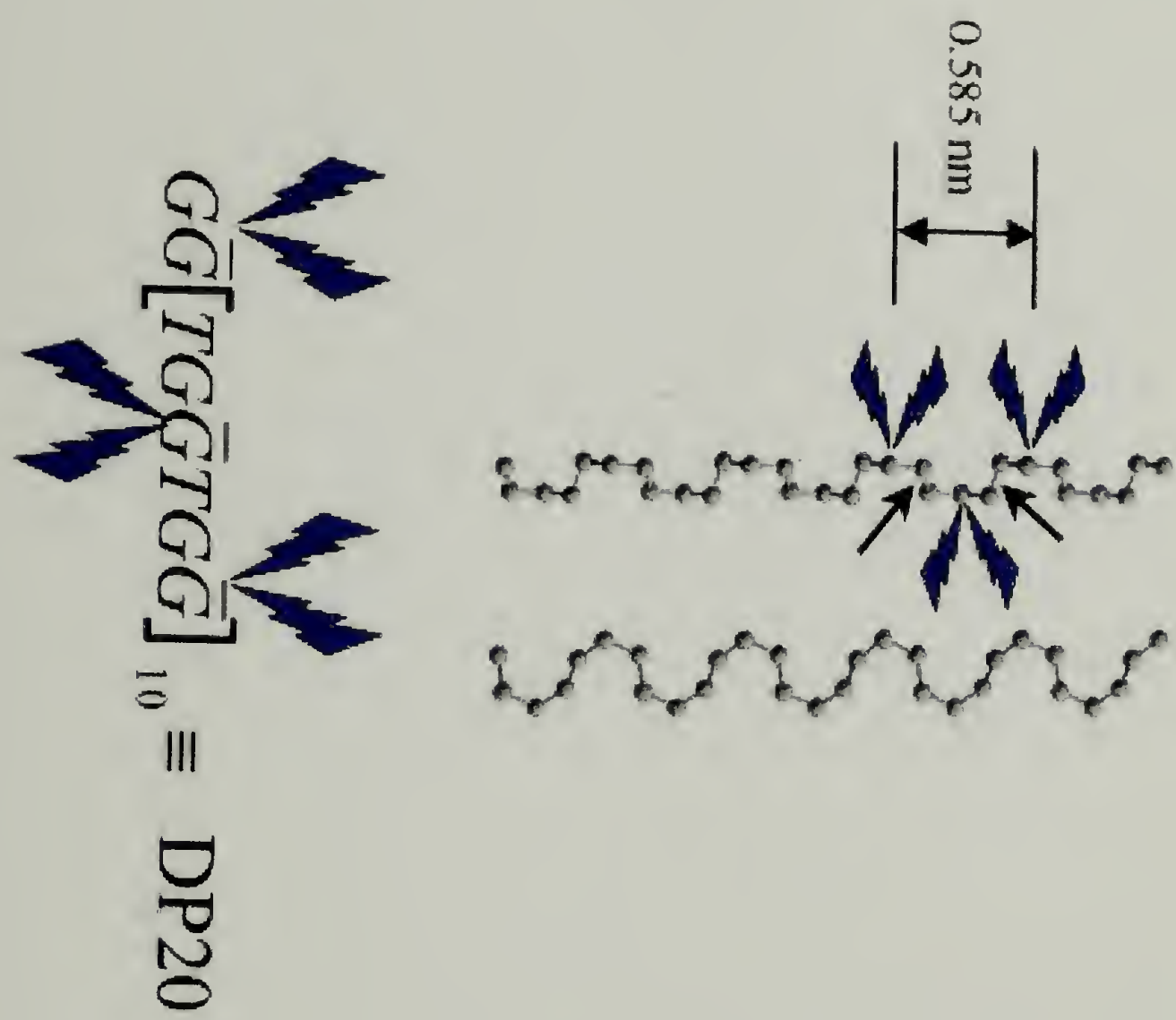


Figure 6.4

At this stage, the potential energy profiles of the torsional angles for  $\text{-CX}_2\text{-CH}_2\text{-CH}_2\text{-CX}_2\text{-}$ ,  $\text{-CH}_2\text{-CX}_2\text{-CH}_2\text{-CH}_2\text{-}$  and  $\text{-CH}_2\text{-CH}_2\text{-CX}_2\text{-CH}_2\text{-}$  bonds were calculated. We wished to be sure that conformation  $TG\overline{G}TG\overline{G}$  is indeed both energetically and stereochemically feasible, i.e. that the backbone is comfortably in an energy minimum rather than being driven into this conformation by side group packing considerations. This could be the case if not all possible chain conformations were examined during the structural modeling process. The calculated potential energy profiles for the torsional angles are plotted in Figure 6.5. It can be seen that for the  $\text{-CX}_2\text{-CH}_2\text{-CH}_2\text{-CX}_2\text{-}$  bond the trans conformation is noticeably preferable. However, the situation is different for the  $\text{-CH}_2\text{-CX}_2\text{-CH}_2\text{-CH}_2\text{-}$  and  $\text{CH}_2\text{-CH}_2\text{-CX}_2\text{-CH}_2\text{-}$  bonds; in these cases the  $G$  and  $\overline{G}$  conformations are marginally (2.2 Kcal/mol) favored. Thus, these results provide supporting evidence for the proposed  $TG\overline{G}TG\overline{G}$  backbone conformation favored by the X-ray diffraction data. It should be noted that this backbone conformation imparts a direction to the chain in addition to the different terminal end groups.

**Figure 6.5.** Calculated potential energy profiles for the various bond torsional angles of the backbone of Poly(**3b**). (a) the -CH<sub>2</sub>-CH<sub>2</sub>- bond, showing the lower minimum for the *T* conformation, and (b) the lower energy of the gauche bonds, adjacent to the CX<sub>2</sub> unit.

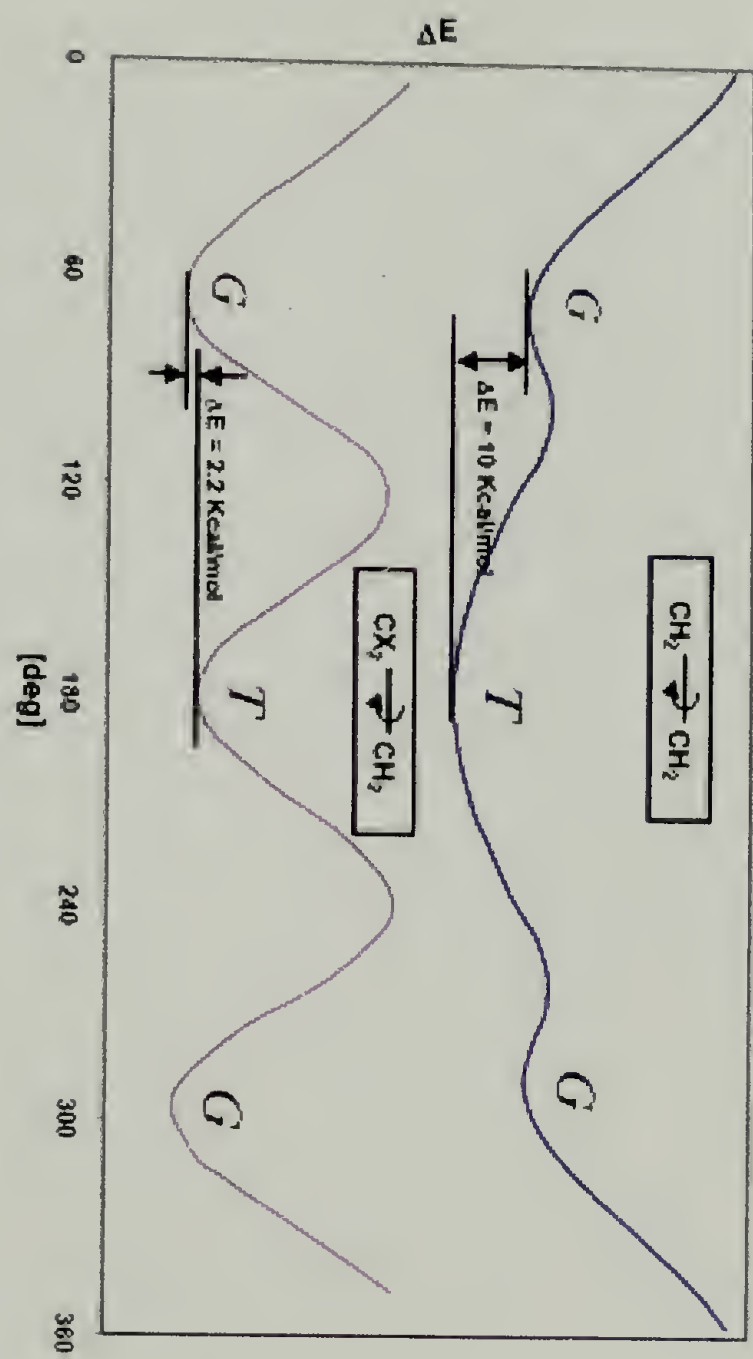


Figure 6.5



6.4.2.2 Consideration of Side Group Geometry. Figures 6.6(a & b) illustrate the situation if the carbon and oxygen atoms in the pair of ethyl carboxylate side groups are arranged in a plane orthogonal to the polymeric backbone. The adjacent ethoxy oxygen atoms clash (interatomic distance 0.16 nm) and as a consequence counter torsional rotations of  $\approx 60^\circ$  about the C-C-C=O bonds, respectively, are necessary to relieve congestion, as shown in Figure 6.6(c & d).

**Figure 6.6.** Two orthogonal views, parallel and perpendicular to *c*-axis showing the carbon and oxygen atoms for the pair of -COOCH<sub>2</sub>CH<sub>3</sub> side groups: (a) & (b) if all the atoms lie in a plane orthogonal to chain axis. (Backbone chain carbon atoms in black). This conformation is not sterically feasible since the two adjacent ethoxy oxygen atoms are too close (arrowed distance). Thus, torsional rotations occur about the C-C-C=O bonds, as illustrated by curved arrows, to relieve congestion. (c) & (d) showing the final conformation of the side groups. Backbone chain carbon atoms in black. There is now no interatomic clash between the ethoxy oxygen atoms.

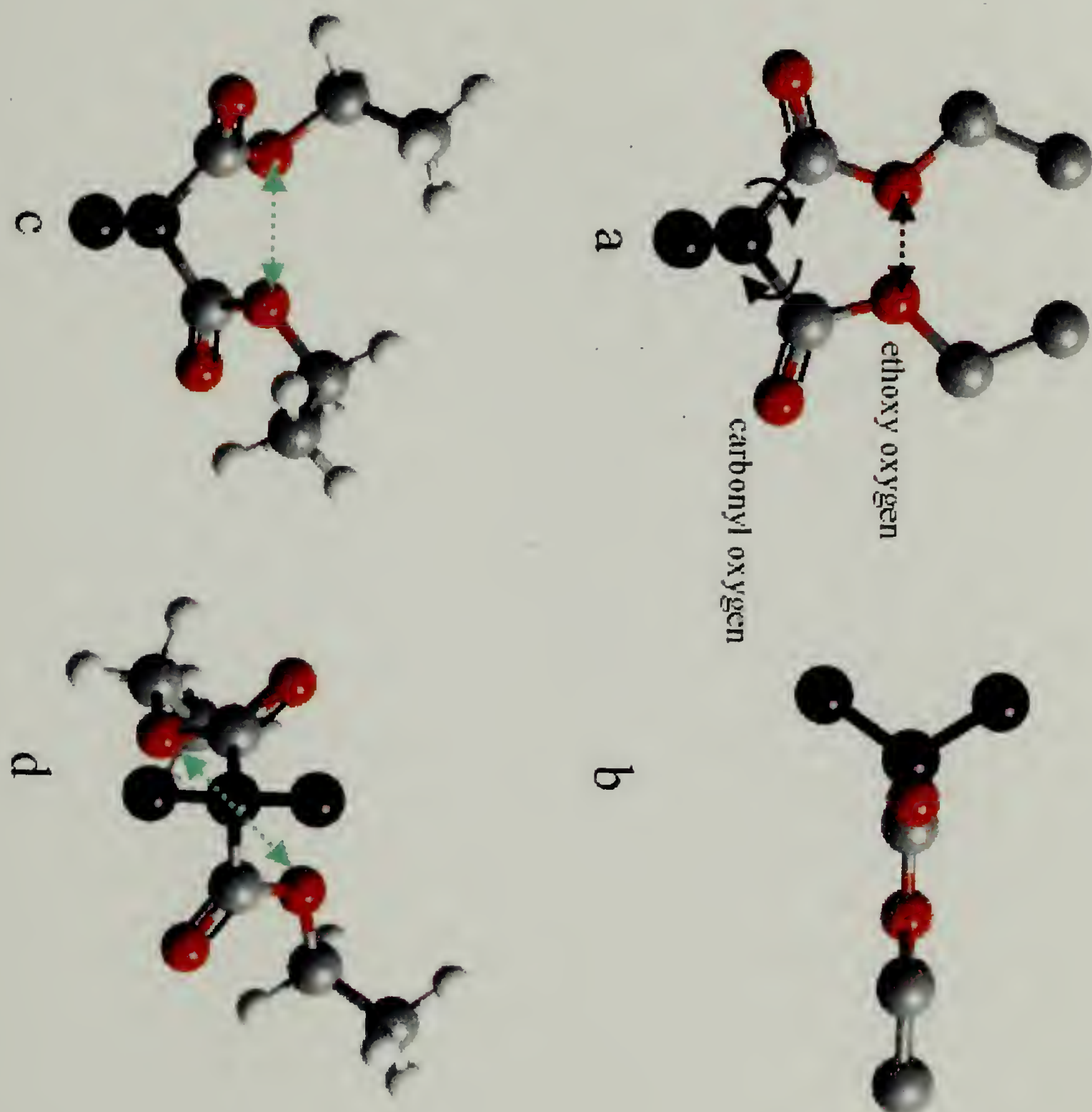


Figure 6.6

6.4.2.3 Chain Packing and Crystal Structure Refinement. Two energy minimized poly(**3b**) chain segments were placed into the orthorhombic unit cell, subject to symmetry requirements, and the initial setting angle(s) (in the *ab*-plane) found by best fit with the observed electron and equatorial X-ray diffraction intensities. The full set of observed X-ray *hkl* intensities were then used to search for possible relative *z*-shifts of the molecules. For each of the contending starting structures the potential energy of the whole crystal structure was minimized until we were satisfied that we had established the best fit with the experimental data for a model with no stereochemical clashes and minimum potential energy. The final torsion angles for the backbone and side chains are given in Table 6.3. It should be noted that the refined values for the backbone torsional angles are about 10° off the formal gauche values and 20° off for the trans value for -CX<sub>2</sub>-CH<sub>2</sub>-CH<sub>2</sub>-CX<sub>2</sub>- dimethylene bond. This backbone conformation gives a closer fit with the experimental intensities and matches the measured *c*-repeat exactly.

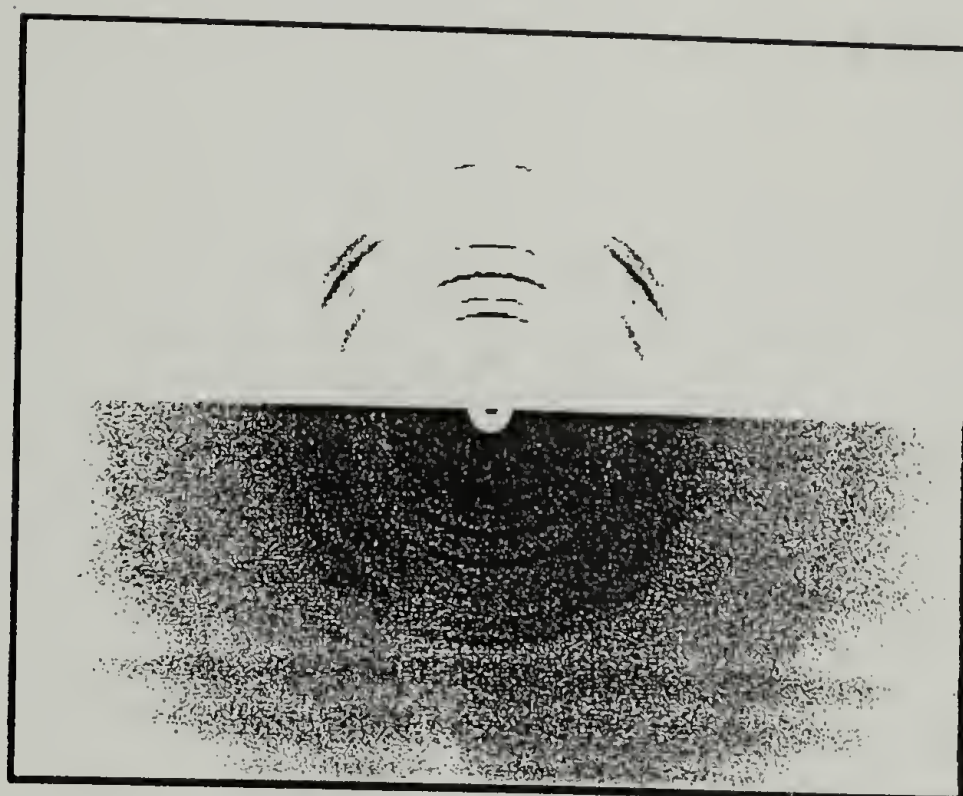
**Table 6.3.** Torsional Rotation Angles for the Backbone and Side Group Bonds in the Refined Poly(**3b**) Crystal Structure.

Backbone	[deg]	Side Group	[deg]
CX <sub>2</sub> -CH <sub>2</sub> -CH <sub>2</sub> -CX <sub>2</sub>	160 ( <i>T</i> )	CH <sub>2</sub> -CX <sub>2</sub> -C=O	0 (for <b>X1</b> ) 120 (for <b>X2</b> )
CH <sub>2</sub> -CH <sub>2</sub> -CX <sub>2</sub> -CH <sub>2</sub>	72 ( <i>G</i> )	CX <sub>2</sub> -C <sub>c</sub> -O-CH <sub>2</sub>	176 ( <i>T</i> )
CH <sub>2</sub> -CX <sub>2</sub> -CH <sub>2</sub> -CH <sub>2</sub>	-71 ( <i>G</i> )	C <sub>c</sub> -O-CH <sub>2</sub> -CH <sub>3</sub>	-100 (for <b>X1</b> ) 80 (for <b>X2</b> )

C<sub>c</sub>: carbonyl side group carbon atom

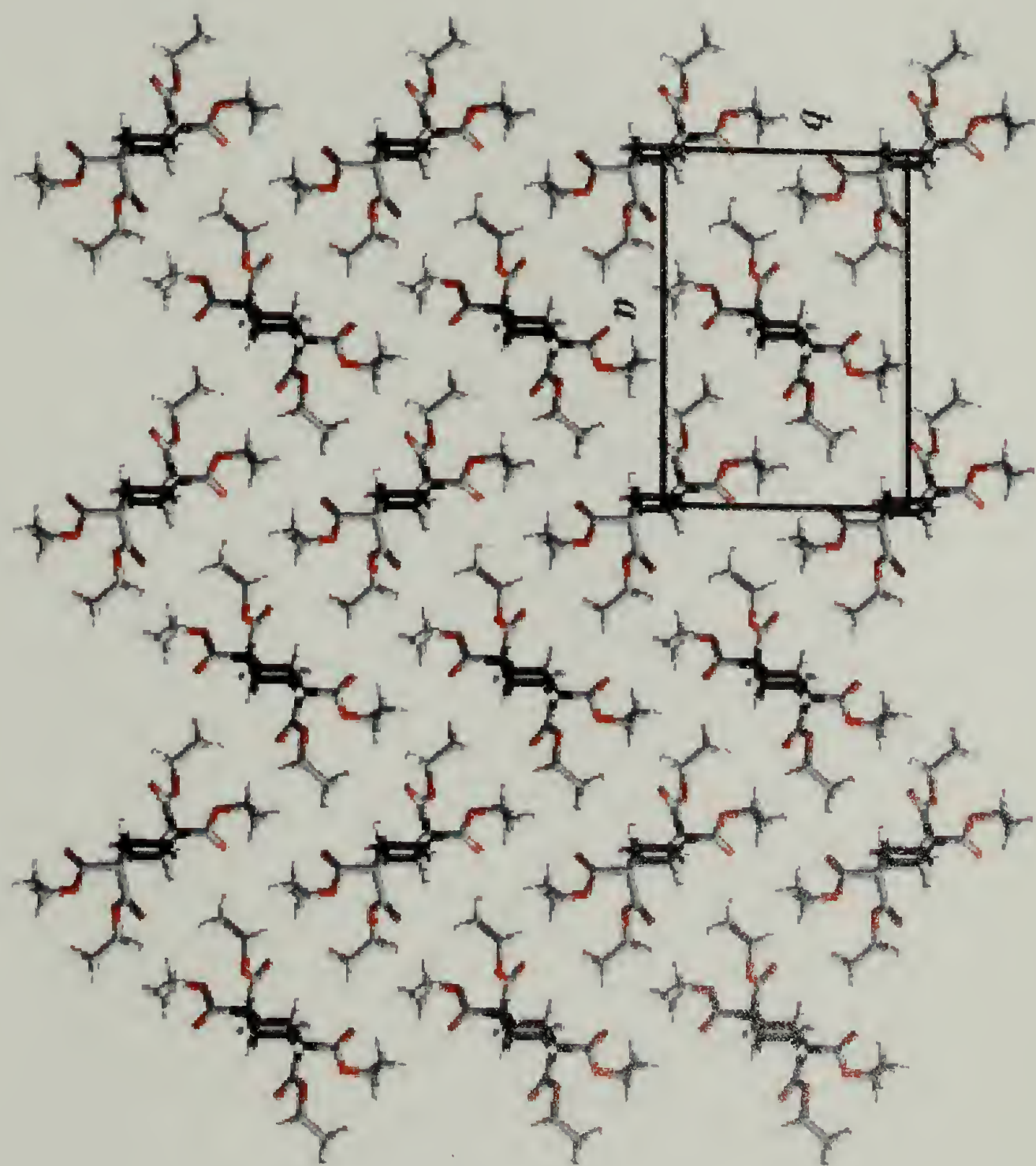
Interestingly, Alder<sup>13</sup> has also noticed a similar off-trans perturbation for the dimethylene bond in spiro(cyclopropane-1,9'-fluorene). The calculated  $hk0$  electron diffraction pattern for final structure is shown in Figure 6.2(b) for convenient comparison with the experimental pattern. The computer simulated wide-angle X-ray diffraction pattern is compared with the experimental pattern in Figure 6.7. As can be seen the match is exceedingly good.<sup>8</sup> Two projections of the crystal structure are shown in Figure 6.8. Thus, in the case of poly(**3b**), we judge that it is the mutual interaction between the pair(s) of  $-\text{COOCH}_2\text{CH}_3$  side groups that in turn controls the backbone conformation.



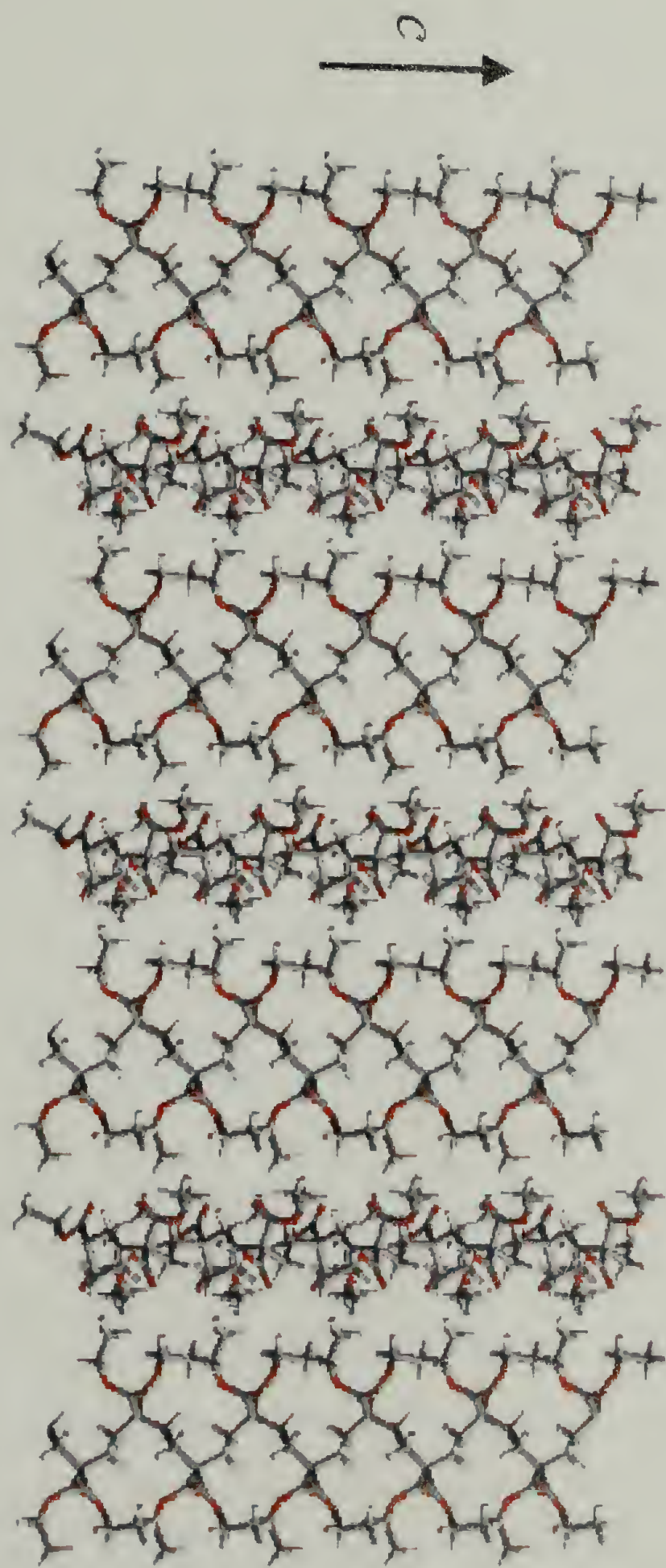


**Figure 6.7.** Computer simulated X-ray diffraction pattern from refined model (top) compared with the experimental X-ray pattern (bottom).

**Figure 6.8.** Views of the refined structure of the Poly(**3b**) crystal in stick mode. **(a)** Parallel to *c*-axis; the backbone is highlighted in black. The unit cell contains two antiparallel molecules, or four monomer units of poly(**3b**). **(b)** A view orthogonal to the diagonal (110) plane (*c*-axis vertical) showing, successively, corner and center (antiparallel) chains.



a

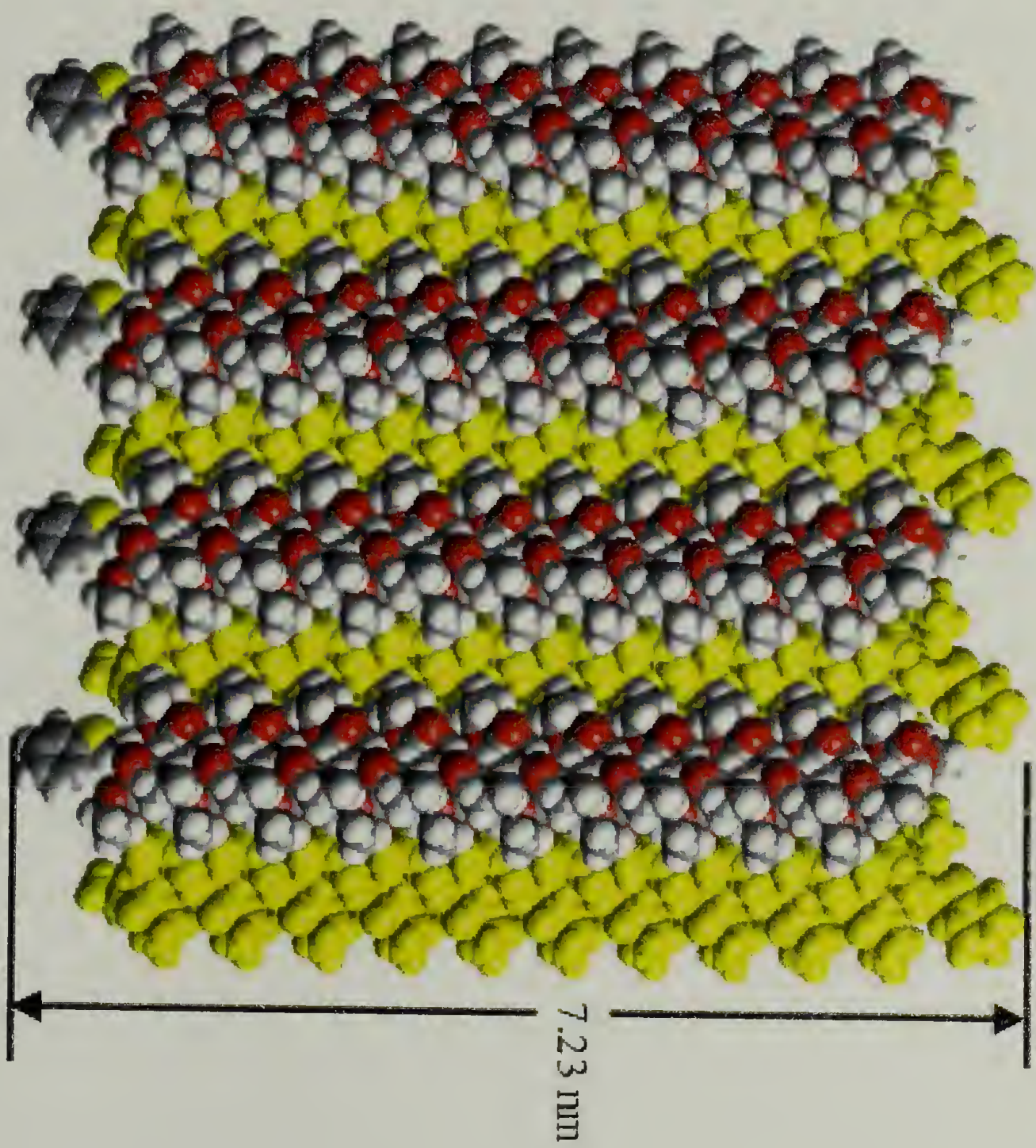


**b**



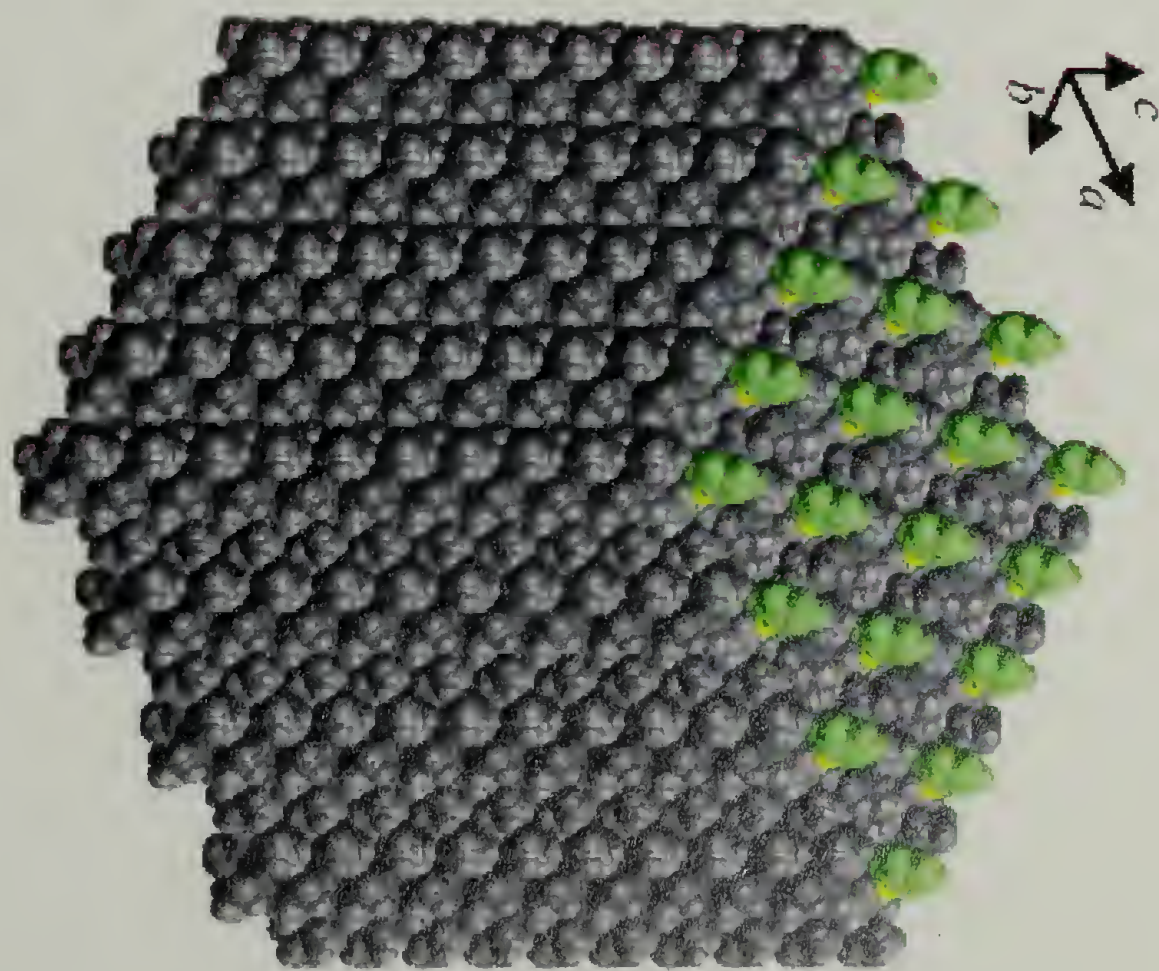
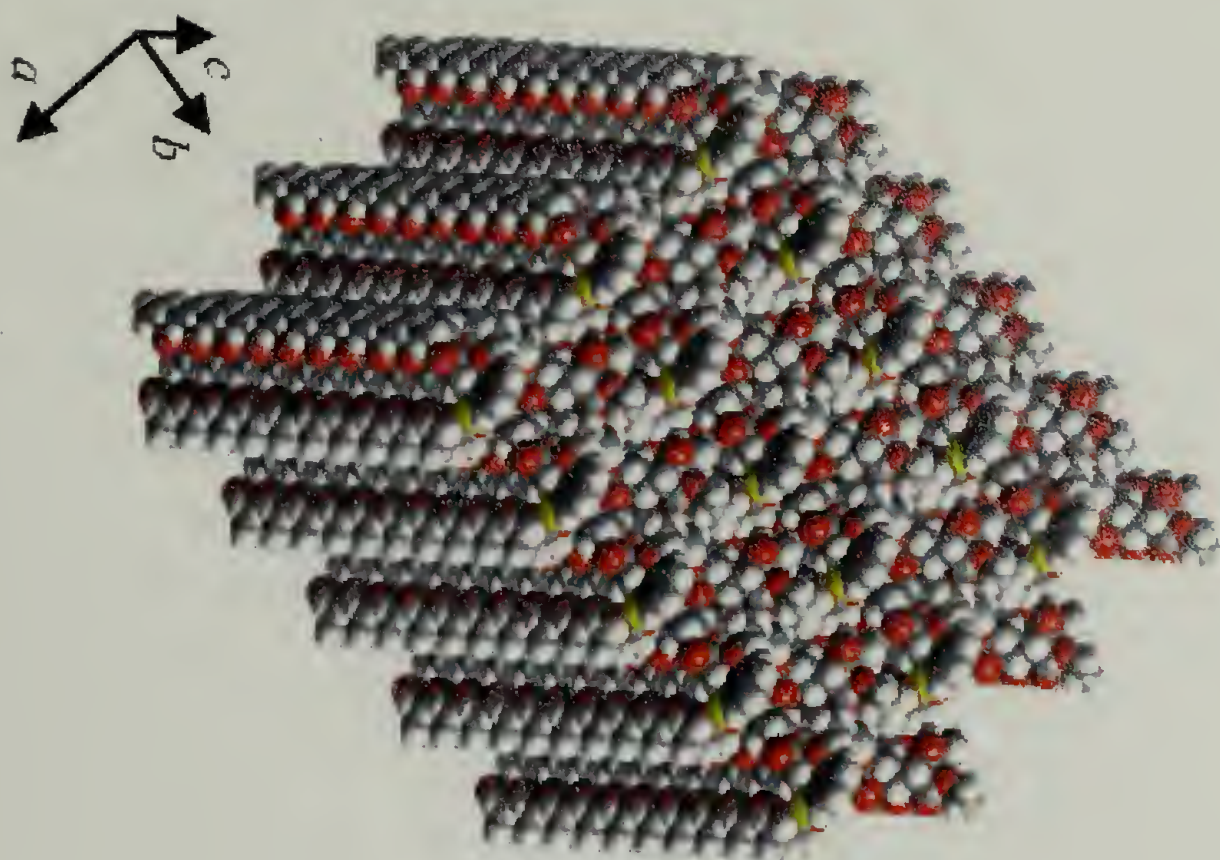
6.4.2.4 Nature of the Lamellar-like Crystals. The electron microscopic images of the poly(**3b**) crystals grown by isothermal crystallization from benzene (Figure 6.1) show a constant thickness over the whole crystal surface ( $\sim \mu\text{m}^2$ ). This constant thickness feature is also supported by the occurrence of the discrete low angle (LSP) diffraction signal obtained from sedimented mats; indeed, it provides us with a direct measure of the *maximum* crystal thickness:  $7.26 \pm 0.03$  nm. We know, from both electron and X-ray diffraction, that the PDEE molecules are directed orthogonal to the large crystal surface (*ab*-plane) and that the molecules pack in an antiparallel fashion. Figure 6.9 shows views of an individual PDEE molecule, including terminal groups together with views of the lamellar-like structure. The outer limit thickness of the crystal is 7.23 nm for poly(**3b**) molecules with 20 monomers.<sup>14</sup> We suggest that the degree of molecular dispersion in these poly(**3b**) crystals, isothermally crystallized from benzene, is small: we estimate the order of one or two monomers about a mean of 19. The experimental support for this statement is the relative sharpness of the LSP arc and the smoothness of the crystal surfaces<sup>15</sup> (see Figure 6.1). It is, perhaps, not too surprising to discover that these crystals, isothermally-grown from solution are close to monodisperse entities. The very nature of this crystallization process is selective. Figure 6.9 conveniently illustrates that the terminal  $-\text{S-Ph}$  group can fit into the poly(**3b**) crystalline lattice without frustrating the crystal<sup>16</sup> and so a proportion of the molecules in the crystal could have DPs lower than 20 but larger DPs would cause interlamellar congestion, a feature not consistent with the experimental evidence.

**Figure 6.9.** Space filling model of the lamellar-like crystal structure of Poly(**3b**). (a) A view orthogonal to the chain axis (vertical) for a complete 20 DP molecule (upward pointing chains in yellow). Note the terminal phenyl rings connected via a sulfur atom to the molecular chain. The outer limit thickness is 7.23 nm (lamellar stacking periodicity, LSP = 7.26 nm). (b) An oblique view showing the crystal surface; sulfur atom yellow, phenyl ring green. The box represents the *ab*-unit cell. (c) A single polymer chain (*c*-axis vertical) of DP 20: (left) backbone atoms in space-filling mode and side groups in stick mode; (center) backbone atoms in stick and side groups in space-filling mode; (right) center chain rotated  $\pi/2$  around *c*-axis.



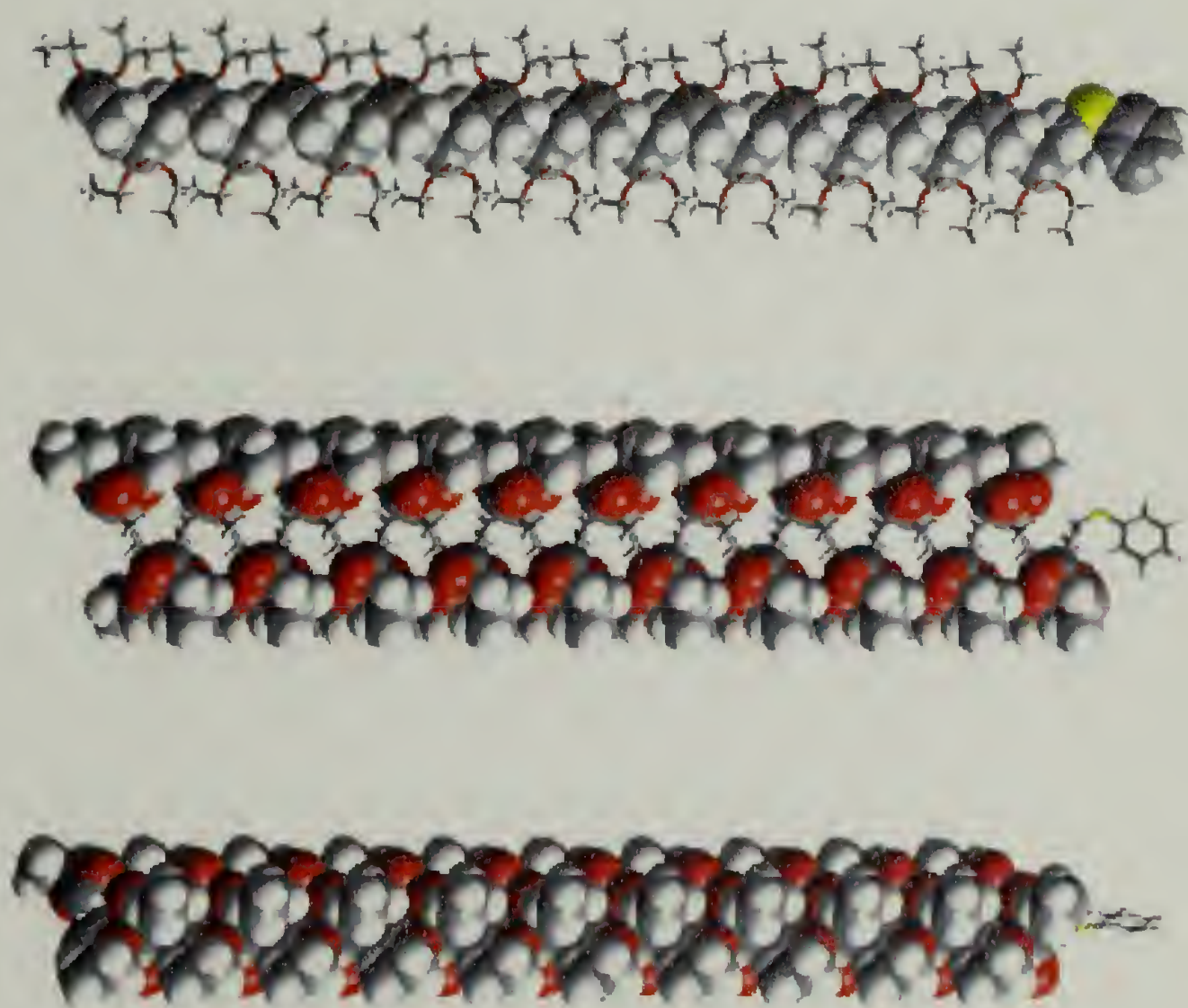
**a**





**b**





c

In the case of the melt crystallized poly(**3b**) sample, a wider molecular length range will be expected to crystallize out; indeed, the X-ray diffraction results support this expectation. The wide-angle X-ray diffraction pattern (Figure 6.3b) of melt-crystallized poly(**3b**), although it represents the same crystal structure as the solution-grown crystals, has noticeably sharper  $hkl$ , for  $l \neq 0$ , diffraction signals. Also, we do not observe a LSP signal in the low-angle diffraction region.<sup>17</sup> These results are consistent with crystals where no segregation takes place in layers orthogonal to the molecular axis, i.e. we envision an architecture where the poly(**3b**) molecules shown in Figure 6.9, but in this case with a larger range of individual lengths, can interpenetrate. Although such a structure has defects<sup>18</sup> (terminal groups) incorporated the overall coherent length in the  $c$ -direction is increased, and consequently the  $hkl$ , for  $l \neq 0$ , diffraction signals sharpen.

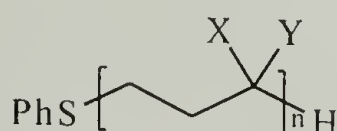
6.4.2.5 General Considerations Relating to Decorated Alkanes. If alkane polymers, in the all-trans extended backbone conformation, are decorated with a side group(s) on every second backbone carbon atom then interatomic clashes can occur between the contiguous side groups (only  $\approx 0.25$  nm apart) along the chain. This congestion is often relieved by the introduction of backbone gauche bonds, e.g. as for *i*-polypropylene<sup>19,20</sup> and *i*-polystyrene<sup>21,22</sup> where the backbone conformation is  $(TG)_3$ . When the backbone repetitive decoration frequency is reduced, the distances between spatially near-neighbor side groups jumps dramatically to  $\approx 0.75$  nm for decoration on every third backbone carbon atom (the polycyclopropanes), and to  $\approx 0.50$  nm in the case of decoration sites on every fourth backbone carbon atom.

For these families of polymers, the interatomic interactions between side group and backbone atoms will be the primary mechanism for influencing and controlling the overall conformation.<sup>9</sup>

## 6.5. Structure of Poly(1), Poly(2a-d), and Poly(4).

### 6.5.1 Results and Discussion

6.5.1.1 Wide-angle X-ray Scattering. WAXS patterns were obtained of powder samples of 1,1-disubstituted poly(trimethylene)s with the chemical structures shown in Figure 6.10.



poly(1); X = Y = CN

poly(2); X = CN, Y = COOR; R = Et (2a), R = i-Pr (2b)  
R = n-Bu (2c), R = octyl (2d)

poly(3b); X = Y = COOEt

poly(4); X = CN, Y = phenyl

Figure 6.10. Structures of Various Poly(1,1-disubstituted trimethylene)s.

The WAXS patterns of powder samples of the polymers are shown in Figure 6.11. The intensity of the X-ray scattering is plotted against the diffraction angle,  $2\theta$ . The sharp peaks are due to the scattering from the crystalline regions, while the broad underlying “halo” is due to the scattering from the amorphous regions.

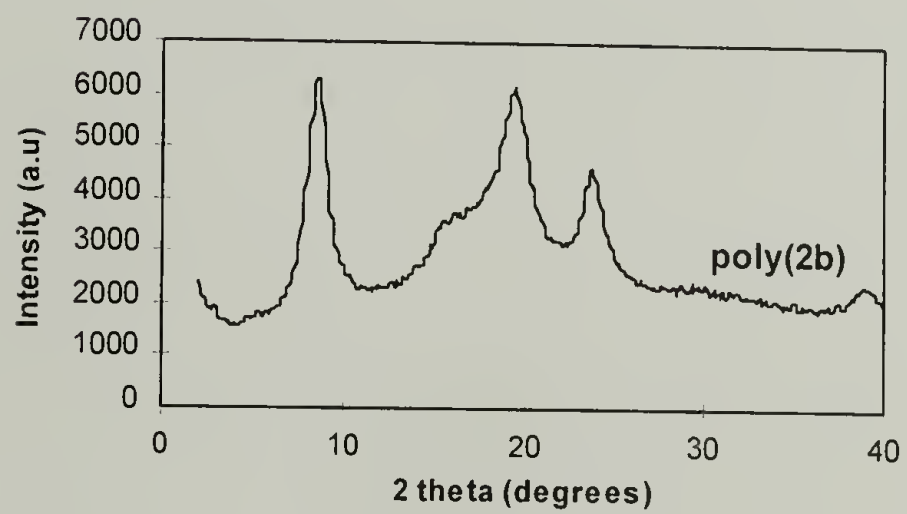
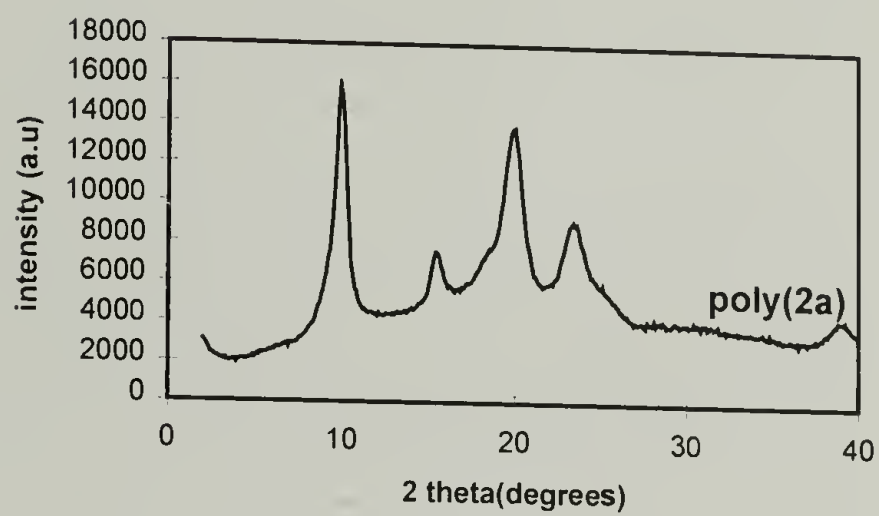
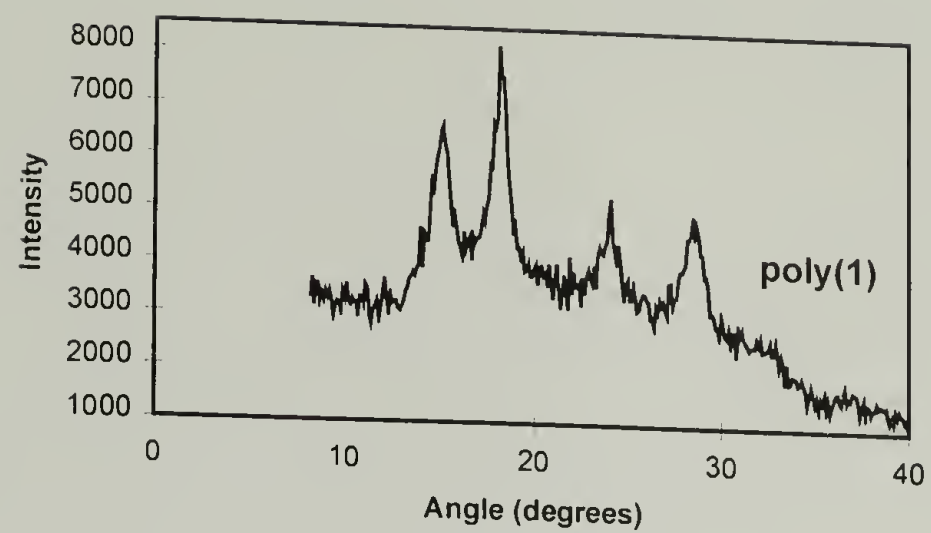
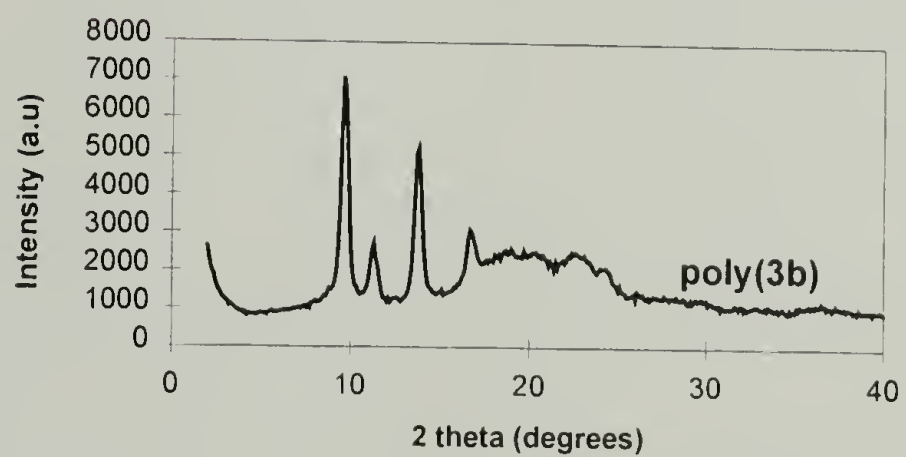
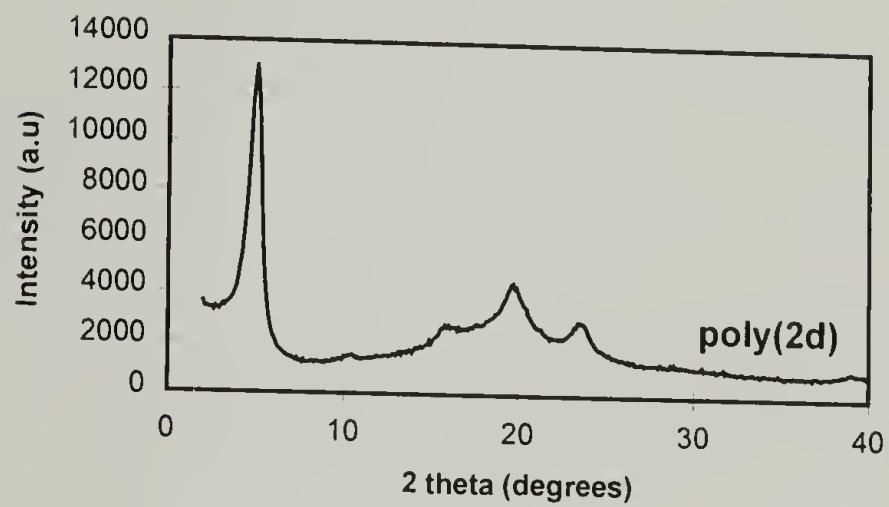
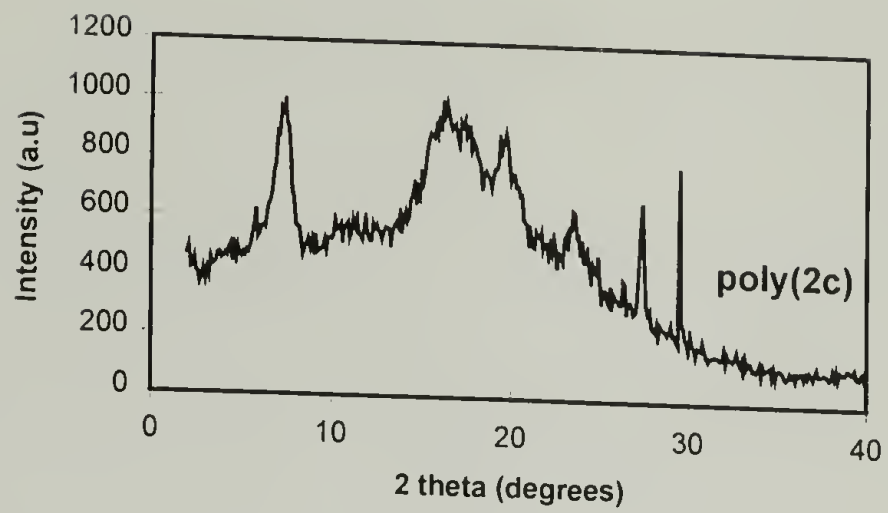


Figure 6.11. WAXS patterns of Poly(1,1-disubstituted trimethylene)s

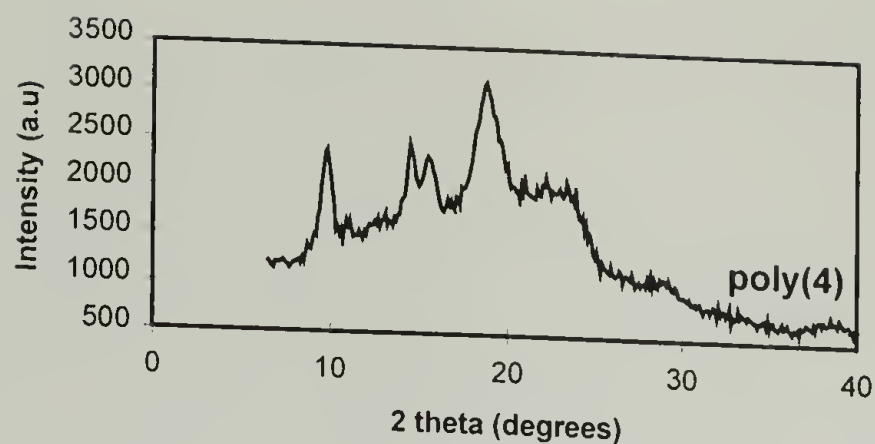


Figure 6.11 CONTINUED



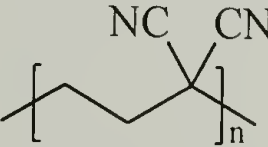
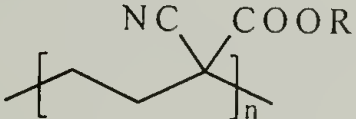
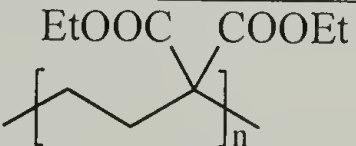
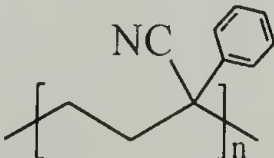
CONTINUED

Figure 6.11 CONTINUED



The d-spacings were calculated based on the values of the angles (two theta) obtained from the peak maxima. These d-spacings correspond to periodicities within the polymer structure. The results are summarized in Table 6.4.

Table 6.4. Measured d-spacings from WAXS patterns

#	Polymer structure	d-spacings (Å)
1		3.13, 3.73, 4.85, 5.83
2		<b>2a</b> 2.30, 3.80, 4.44, 5.75, 8.93 <b>2b</b> 2.32, 3.74, 4.58, 5.21, 10.40 <b>2c</b> 3.78, 4.51, 5.44, 11.95 <b>2d</b> 3.79, 4.51, 5.54, 17.67
3b		5.33, 6.39, 7.79, 9.17
4		4.72, 5.72, 6.11, 9.03

R = ethyl (**2a**); isopropyl (**2b**); n-butyl (**2c**); n-octyl (**2d**)

## BIBLIOGRAPHY

- Alder, R. W.; Anderson, K. R.; Benjes, P. A.; Koutentis, P. A.; Orpen, A. G. *J. Chem. Soc., Chem. Commun.* **1998**, 309.
- Alder, R. W.; Anderson, K. R.; Benjes, P. A.; Butts, C. P.; Koutentis, P. A.; Orpen, A. G. *J. Chem. Commun.* **1998**, 309-310.
- Alder, R.; Allen, P. R.; Khosravi, E. *J. Chem. Soc., Chem. Commun.* **1994**, 1235.
- Allcock, H. R.; Lampe, F. W. In *Contemporary Polymer Chemistry*; Prentice-Hall: New Jersey, 1990.
- Allen, F. H. *Acta Cryst.* **1980**, B36, 81.
- Amstutz, R.; Dunitz, J.; Laube, T.; Schweizer, W. B.; Seebach, D. *Chem. Ber.* **1986**, 119, 434.
- Andrews, R. J.; Grulke, E. A. In *Polymer Handbook*; Brandrup, J., Immergut, E. H., Grulke, E. A., Eds.; Wiley-Interscience: New York, 1999; Vol. VI, p 207.
- Aoki, S.; Harita, Y.; Otsu, T.; Imoto, M. *Bull. Chem. Soc. Jpn.* **1966**, 39, 889.
- Ardis, A. E.; U.S. Patent 2,574,369 (November 6, 1951)
- Arnett, E. M.; Harrelson, J. A. *Gazz. Chim. Ital.* **1987**, 117, 237.
- Arnett, E. M.; Maroldo, S. G.; Schilling, S. L.; Harrelson, J. A. *J. Am. Chem. Soc.* **1984**, 106, 6759.
- Atkins, E. A. T. In *Comprehensive Polymer Science*; Booth, C., Price, C., Eds.; Pergamon: London, 1990 pp. 613-650.
- Aylward, F.; Sawistowska, M. *Chem. Ind.* **1962**, 404, 484.
- Baird, N. C.; Dewar, M. J. S. *J. Am. Chem. Soc.* **1967**, 89, 3967.
- Baldwin, J. E. *J. Chem. Soc., Chem. Commun.* **1976**, 734.
- Bargar, T. M.; Riley, C. M. *Synthetic Commun.* **1980**, 10, 479.
- Bastiansen, O.; Fritsch, F. N.; Hedberg, K. *Acta Crystallogr.* **1964**, 17, 538.
- Bauld, N.; Cessac, J.; Holloway, R. H. *J. Am. Chem. Soc.* **1977**, 99, 8140.

- Beletskaya, I. P.; Gulyukina, N. S.; Ali, M. A.; Solov'yanov, A. A.; Reutov, O. A. *Zh. Org. Khim.* **1987**, 23, 730.
- Benson, S. W. In *Thermochemical Kinetics*; Wiley: New York, 1968.
- Besten, R. H., S.; Brandsma, L. *J. Org. Metallic Chem.* **1990**, 385, 153.
- Binder, J. L. *J. Polym. Sci.* **1965**, A-3, 1587.
- Binder, J. L. *J. Polym. Sci.* **1963**, A-1, 47.
- Boche, G. *Angew. Chem. Int. Ed. Engl.* **1989**, 28, 277.
- Bone, W. A.; Perkin, W. H. *J. Chem. Soc.* **1895**, 67, 108.
- Bordwell, F. G. *Acc. Chem. Res.* **1988**, 21, 456.
- Bordwell, F. G.; Bares, J. E.; Bartmess, J. E.; McCollum, G. J.; Van Der Puy, M.; Vanier, N. R.; Matthews, W. *J. Org. Chem.* **1977**, 42, 321.
- Bovey, F. A. In *Chain Structure and Conformation of Macromolecules*; Academic Press: New York, 1982.
- Bovey, F. A. In *Polymer Conformation and Configuration*; Academic Press: NY, 1969; p 32.
- Bovey, F. A.; Tiers, G. V. D. *J. Polym. Sci.* **1960**, 44, 173.
- Bowie, J. H.; Williams, D. H.; Madsen, P.; Schroll, G.; Lawesson, S. O. *Tetrahedron* **1967**, 23, 305.
- Brandsma, L.; Verkruijsse, H. *Preparative Polar Organometallic Chemistry*; Springer: Berlin, 1987 and 1990; Vol. 1 and Vol. 2.
- Brasure, D.; Ebnesajjad, S. In *Encyclopedia of Polymer Science and Engineering*; Mark, H., Bikales, N. M., Overberger, C. G., Menges, G., Kroschwitz, J. I., Eds.; Wiley-Interscience: New York, 1985; Vol. 17, p 476.
- Breslow, R. In *Molecular Rearrangements*; de Mayo, P., Ed.; Interscience: New York, 1963; p 233.
- Buncel; Shaik; Um; Wolfe *J. Am. Chem. Soc.* **1988**, 110, 1275.
- Bunn, C. W.; Howells *J. Polym. Sci.* **1955**, 18, 307.



- Bunn, C. W. *J. Polym. Sci.* **1955**, *16*, 322.
- Bunn, C. W. *Proc. Roy. Soc., (London)* **1942**, *A180*, 67.
- Bury, A.; Earl, H.; Stirling, C. J. M. *J. Chem. Soc., Perkin Trans. II* **1987**, *9*, 1281.
- Chamberlin, Y.; Gole, J.; Pascault, J. P.; Durand, J. P.; Dawans, F. *Makromol. Chem.* **1979**, *180*, 2309.
- Casadei, M. A.; Galli, C.; Mandolini, L. *J. Am. Chem. Soc.* **1984**, *106*, 1051.
- Casini, G.; Ferappi, M.; Pietroni, B. R. *Tetrahedron* **1972**, *28*, 1497.
- Castellano, S. *LAOCN3* **1972**, Mellon Institute, Pittsburg USA.
- Chen, H. Y. *J. Polym. Sci., Polym. Lett. Ed.* **1977**, *15*, 271.
- Cheung, K. H.; Guthrie, J. *Makromol. Chem.* **1987**, *188*, 3041.
- Cho, I.; Kim, J.-B. *J. Polym. Sci., Part A: Polym. Chem.* **1980**, *18*, 3053.
- Cho, I.; Ahn, K.-D. *J. Polym. Sci., Part A: Polym. Chem.* **1979**, *17*, 3169.
- Cho, I.; Ahn, K.-D. *J. Polym. Sci., Part A: Polym. Chem.* **1979**, *17*, 3183.
- Choi, S. B.; Takahara, A.; Amaya, N.; Murata, Y.; Kajiyama, T. *Polym. J.* **1989**, *21*, 215.
- Clague, A. D. H.; Van Brockhaven, J. A. M.; Blaauw, L. P. *Macromolecules* **1973**, *7*, 348.
- Coffey, S. E. In *Rodd's Chemistry of Carbon Compounds*; Elsevier Scientific: Amsterdam, 1973; Vol. IV, p 2.
- Coles, H. J.; Simon, R.; Chapoy, L. L. In *Recent Advances in Crystalline Polymers*; Elsevier Applied Science Publishers: Barking, UK, 1984; p 324.
- Coover, H. W.; Dreifus, D. W.; O'Conner, J. T. In *Handbook of Adhesives*, 3rd Ed.; Skeist, I., Ed.; Van Nostrand Reinhold: NY, 1990; p 463.
- Coover, H. W.; McIntire, J. M. In *Encyclopedia of Polymer Science and Engineering*; Mark, H., Bikales, N. M., Overberger, C. G., Menges, G., Kroschwitz, J. I., Eds.; John Wiley and Sons: NY, 1985; Vol. 1, pp 299-305.
- Corey, E. J.; Mock, W. Y.; Pasto, D. J. *Tetrahedron Lett.* **1961**, *11*, 347.

- Coulson, C. A.; Moffit, W. E. *J. Chem. Phys.* **1947**, *15*, 151.
- Cox, J. D. *Tetrahedron* **1963**, *19*, 1175.
- Cusack, N. J.; Reese, C. B.; Risius, A. C.; Rozpeikar, B. *Tetrahedron* **1976**, *32*, 2157.
- Dainton, F. S.; Ivin, K. J. *Quart. Rev. Chem. Soc.* **1958**, *12*, 61.
- Dainton, F. S.; Devlin, T. R. L.; Small, P. A. *Trans. Faraday Soc.* **1955**, *51*, 1710.
- Danishefsky, S. *Acc. Chem Res.* **1979**, *12*, 66.
- Danishefsky, S.; Singh, R. K. *J. Org. Chem* **1975**, *40*, 3807.
- Danishefsky, S.; Rovnyak, G. *J. Org. Chem* **1975**, *40*, 114.
- Danishefsky, S.; Rovnyak, G. *J. Chem. Soc., Chem. Commun.* **1972**, 820.
- Danz, R.; Buechtemann, A.; Latour, M. *Mol. Cryst. Liq. Cryst. Sci. Technol., Sect. A* **1993**, *229*, 181.
- Davis, G. T. In *The application of ferroelectric Polymers*; Wang, T. T., Herbert, J. M., Glass, A. M., Eds.; Blackie: Glasgow and London, 1988; Vol. 37.
- Davis, G. T.; McKinney, J. E.; Broadhurst, M. G.; Roth, S. C. *J. Appl. Phys.* **1978**, *51*, 5095.
- Denchev, Z. Z.; Kabaivanov, V. S. *J. Polym. Sci.* **1991**, *42*, 2933.
- DePuy, C. H. *Top. Curr. Chem.* **1973**, *40*, 73.
- Diez-Barra, E.; de la Hoz, A.; Moreno, A.; Sanchez-Verdu, P. *J. Chem. Soc., Perkin Trans. 1* **1991**, *1*, 2593.
- Dohany, E. J.; Humphrey, J. S. In *Encyclopedia of Polymer Science and Engineering*; Mark, H., Bikales, N. M., Overberger, C. G., Menges, G., Kroschwitz, J. I., Eds.; Wiley-Interscience: New York, 1985; Vol. 17, pp 536-538.
- Donnelly, E. F.; Pepper, D. C. *Macromol. Chem., Rapid Commun.* **1981**, *2*, 439.
- Donnelly, E. F. J., D. S.; Pepper, D. C.; Dunn, D. J. *J. Polym. Sci., Polym. Lett. Ed.* **1977**, *15*, 399.

- Dox, A. W.; Yoder, L. J. *J. Am. Chem. Soc.* **1921**, *12*, 66.
- Dreyfuss, P. In *Polymeric Materials Encyclopedia*; Salamone, J. C., Ed.; CRC Press: N.Y Vol. 8, pp 5657-5662, and references therein.
- Duch, M. W.; Grant, D. M. *Macromolecules* **1970**, *3*, 165.
- Duck, E. W.; Locke, J. M.; Mallinson, C. J. *Ann. Chem.* **1968**, *719*, 69.
- Dunitz, J.; Schomaker, V. *J. Chem. Phys.* **1952**, *20*, 1703.
- Earl, H.; Stirling, C. J. M. *J. Chem. Soc., Perkin Trans. II* **1987**, *9*, 1273.
- Eastham, A. M.; Darwent, B.; de B. and Beaubien, P. E. *Can. J. Chem.* **1951**, *29*, 575.
- Edwards; Pearson, J. *J. Am. Chem. Soc.* **1962**, *84*, 16.
- Emsley, J. W.; Feeney, J.; Sutcliffe, L. H. *High Resolution Nuclear Magnetic Resonance*; Pergemon: London, 1965; Vol. II.
- Falk, J. C.; Schlott, R. C. *Macromolecules* **1971**, *4*, 152.
- Falk, J. C.; Schlott, R. C. *J. Org. Chem.* **1971**, *36*, 1445,
- Farina, M.; Silvestro, G. D.; Sozzani, P. *Macromolecules* **1982**, *15*, 1451.
- Fawcett, A. H.; Guthrie, J.; Otterburn, M. S.; Szeto, D. S. *J. Polym. Sci., Part C: Polym. Lett.* **1988**, *26*, 459.
- Fieser, L. F.; Fieser, M. In *Advanced Organic Chemistry*; Reinhold: New York, 1961.
- Finkelmann, H.; Rehage, G.; Gordon, M. In *Liquid Crystal Polymers II/III, Advances in Polymer Science Series*; Springer-Verlag: New York, 1984; Vol. 60/61.
- Flowers, M. C.; Frey, H. M. *J. Chem. Soc.* **1961**, 3547.
- Flygare, W. H. *Science* **1963**, *140*, 1179.
- Foote, C. S. *Tetrahedron Lett.* **1963**, 579.
- Frey, H. M.; Walsh, R. *Chem. Rev.* **1969**, *69*, 103.
- Frey, H. M. *Adv. Phys. Org. Chem.* **1966**, *4*, 147.

- Furukawa, T.; Tada, M.; Nakajima, K.; Seo, I. *Jpn. J. Appl. Phys.* **1988**, 27, 200.
- Furukawa, T.; Date, M.; Nakajima, K.; Kosaka, T.; Seo, I. *Jpn. J. Appl. Phys.* **1986**, 25, 1178.
- Gangal, S. V. In *Encyclopedia of Polymer Science and Engineering*; Mark, H., Bikales, N. M., Overberger, C. G., Menges, G., Kroschwitz, J. I., Eds.; Wiley-Interscience: New York, 1985; Vol. 16, pp 577-613.
- Gerber, A. H. *Polym. Prepr. (Am. Chem. Soc., Div. Polym. Chem.)* **1968**, 9, 434.
- Gerber, A. H. U.S Patent 1967, 3,316,227.
- Gerum, W.; Hohne, G. W. H.; Wilke, W.; Arnold, M.; Wegner, T. *Macromol. Chem. Phys.* **1996**, 197, 1691.
- Gilbert, H.; Miller, F. F.; Averill, S. J.; Schmidt, R. F.; Stewart, F. D.; Trumbull, H. L. *J. Am. Chem. Soc.* **1954**, 76, 1074.
- Gippin, M. *Rubber Chem. Technol.* **1962**, 35, 1066.
- Golub, M. A. In *The Chemistry of Alkenes, Vol. 2*; Zabicky, J., Ed.; Wiley-Interscience: London, 1970, Chapt. 9.
- Grant, D. M.; Paul, E. G. *J. Am. Chem. Soc.* **1964**, 86, 2984.
- Graziano, M. L.; Iesce, M. R. *Synthesis* **1985**, 1985, 762.
- Greenberg, A.; Stevenson, T. A. *J. Am. Chem. Soc.* **1985**, 107, 3488.
- Gregg, E. C. *Am. Chem. Soc., Div. Polym. Chem.* **1967**, 8, 851.
- Grob, C. A. *Angew. Chem., Int. Ed. Engl.* **1969**, 8, 535.
- Grob, C. A.; Schiess, P. W. *Angew. Chem. Int. Ed. Engl.* **1967**, 6, 1.
- Hahn, S. F. *J. Polym. Sci., Part A: Polym. Chem.* **1992**, 30, 397.
- Hahn, S. F. *J. Polym. Sci., Part A, Polym. Chem* **1992**, 30, 397.
- Haines, A. H. In *Comprehensive Organic Chemistry*; Barton, H. R., Ollis, W. D., Eds.; Pergamon Press: Oxford, 1979; Vol. 1, p 19.
- Hall, H. K. J.; Padias, A. B. *Acc. Chem Res.* **1990**, 23, 3.



- Hall, H. K. J.; Snow, L. G. In *Ring-Opening Polymerization*; Ivin, K. J., Saegusa, T., Eds.; Elsevier Applied Science Publishers: New York, 1984; Vol. 1, p 83.
- Hansen, P. E. *Prog. Nucl. Magn. Reson. Spectrosc.* **1981**, *14*, 175.
- Harrelson, J. A., Ph.D. Dissertation, Duke University, 1986.
- Harris, L.; Ashdown, A. A.; Armstrong, R. T. *J. Am. Chem. Soc.* **1936**, *75*, 2315.
- Harwood, H. J. *Rubber Chem. Technol.* **1982**, *55*, 769.
- Harwood, H. J.; Russell, D. B.; Verthe, J. J. A.; Zymonas, J. *Makromol. Chem.* **1973**, *163*, 1.
- Harwood, H. J. R., D.B.; Verthe, J. J. A.; Zymonas, J. *Makromol. Chem.* **1973**, *163*, 1.
- Hatada, K. *J. Polym. Sci. Part A: Polym. Chem.* **1999**, *37*, 245.
- Hatada, K.; Kitayama, T.; Ute, K. *Prog. Polym. Sci.* **1988**, *13*, 189.
- Hatada, K.; Ute, K.; Tanaka, K.; Okamoto, Y.; Kitayama, T. *Polym. J.* **1986**, *18*, 1037.
- Hirano, T.; Nakayama, S.; Tsuruta, T. *Makromol. Chem.* **1975**, *176*, 1897.
- Hoz, S.; Speizman, D. *J. Org. Chem.* **1983**, *48*, 2904.
- Huisgen, R. *Acc. Chem. Res.* **1977**, *10*, 117.
- Hunig, S.; Muller, R.; Thier, W. *Angew. Chem. Int. Ed. Eng.* **1965**, *4*, 271.
- Hunig, S.; Muller, R.; Thier, W. *Angew. Chem. Int. Ed. Eng.* **1963**, *2*, 214.
- Hunig, S.; Muller, R.; Thier, W. *Tetrahedron Lett.* **1961**, 353.
- Ibne-Rasa, K. M. *J. Chem. Edu.* **1967**, *44*, 89.
- Illers, K. H.; *Kolloid-Z. Polym.* **1974**, *252*, 1.
- Illers, K. H.; *Kolloid-Z. Polym.* **1973**, *251*, 394.
- Illers, K. H.; *Kolloid-Z. Polym.* **1969**, *231*, 62.

- Illuminati, G.; Mandolini, L. *Acc. Chem. Res.* **1981**, *14*, 95.
- Inoue, Y.; Ohta, Y.; Sakurai, M.; Chujo, R.; Seo, I.; Kishimoto, M. *Polymer* **1994**, *35*, 718.
- Inoue, Y.; Maruyama, Y.; Kawaguchi, K.; Ohta, Y.; Sakurai, M.; Jo, Y. S.; Chujo, R. *Polymer* **1991**, *32*, 2958.
- Inoue, Y.; Maruyama, Y.; Sakurai, M.; Chujo, R. *Polymer* **1990**, *31*, 850.
- Inoue, Y.; Jo, Y. S.; Kashiwazaki, A.; Maruyama, Y.; Chujo, R.; Kishimoto, M.; Seo, I. *Polym. Commun.* **1988**, *29*, 105.
- Inoue, Y.; Kashiwazaki, A.; Maruyama, Y.; Jo, Y. S.; Chujo, R.; Kishimoto, M.; Seo, I. *Polymer* **1988**, *29*, 144.
- Inoue, S.; Aida, T. In *Ring-Opening Polymerization*; Ivin, K. J., Saegusa, T., Eds.; Elsevier Applied Science Publishers: New York, 1984; Vol. 1, pp 185-298.
- Ivin, K. J.; Saegusa, T. In *Ring-Opening Polymerization*; Ivin, K. J., Saegusa, T., Eds.; Elsevier Applied Science Publishers: New York, 1984; Vol. 1, pp 1-3.
- Ivin, K. J. *J. Chem. Soc.* **1959**, 1352.
- Ivin, K. J.; Busfield, W. K. In *Encyclopedia of Polymer Science and Technology*; Wiley: London, 19; Vol. 12, pp 555-605.
- Jessup, J. *J. Chem. Phys.* **1948**, *16*, 661.
- Jo, Y. S.; Maruyama, Y.; Inoue, Y.; Chujo, R.; Tasaka, S.; Miyata, S. *Polym. J.* **1987**, *19*, 769.
- Jones, W. J.; Stoicheff, B. P. *Can. J. Phys.* **1960**, *42*, 2259.
- Jones, R. V.; Moberly, C. W.; Reynolds, W. B. *Ind. Eng. Chem.* **1953**, *45*, 1117.
- Jung, D.; Bothner-By, A. A. *J. Am. Chem. Soc.* **1964**, *86*, 4025.
- Kagumba, L.; Penelle, J. *Polym. Prepr. (Am. Chem. Soc., Div. Polym. Chem.)* **2000**, *41*, 1290.
- Kagumba, L.; Penelle, J. *Polym. Prepr. (Am. Chem. Soc., Div. Polym. Chem.)* **2000**, *41*, 1313.
- Karplus, M. *J. Chem. Phys.* **1956**, *30*, 11.

- Kasatkin, A. N.; Biktimirov, R. K.; Tolstikov, G. A.; Khalilov, L. M. *Zh. Org. Khim. (Engl. Transl.)* **1990**, 26, 1191.
- Katz, T. J.; Lee, J. S.; Acton, N. *Tetrahedron Lett.* **1976**, 47, 4247.
- Kawai, H. In *Japan J. Appl. Phys.*, 1969; Vol. 8, pp 975-976.
- Keller, A.; O'Conner, J. T. *Discuss. Faraday Soc.* **1958**, 25, 114.
- Kennedy, J. P.; Elliott, J. J.; Butler, P. E. *J. Macromol. Sci.* **1968**, A2, 1415.
- Kennedy, J. P.; Minckler, L. S.; Wanless, G.; Thomas, R. M. *J. Polym. Sci.* **1964**, A2, 2093.
- Kennedy, J. P.; Thomas, R. M. *Makromol. Chem.* **1962**, 53, 28.
- Ketley, A. D.; Berlin, A. J.; Fisher, L. P. *J. Polym. Sci. A-1* **1967**, 5, 227.
- Ketley, A. D.; Ehrig, R. S. *J. Polym. Sci., Part A: Polym. Chem.* **1964**, 2, 4461.
- Ketley, A. D. *J. Polym. Sci., Polym. Lett. Ed.* **1963**, 1, 313.
- Kharasch, M. S.; Fineman, M.; Mayo, F. *J. Am. Chem. Soc.* **1939**, 61, 2139.
- Kierstead, R. W.; Linstead, R. P.; Weedon, B. C. L. *J. Chem. Soc.* **1952**, 3616.
- Kim, J.-B. C., I. H. *Tetrahedron* **1997**, 53, 15157-15166.
- Kim, J.-B. *J. Polym. Sci., Polym. Chem.* **1980**, 18,, 3053.
- Kirby, A. J. *Adv. Phys. Org. Chem.* **1980**, 17, 183.
- Kirmse, W. *Top. Curr. Chem.* **1979**, 80, 125.
- Kitayama, T.; Zhang, Y.; Hatada, K. *Polym. J.* **1994**, 26, 868.
- Kitayama, T.; Masuda, E.; Yamaguchi, M.; Nishiura, T.; Hatada, K. *Polym. J.* **1992**, 24, 81.
- Knipe, A. C.; Sterling, C. J. M. *J. Chem. Soc. B* **1968**, 67.
- Kobayashi, S.; Morikawa, K.; Saegusa, T. *Polym. J.* **1979**, 11, 405.
- Kohler, E. P.; Conant, J. B. *J. Am. Chem. Soc.* **1917**, 39, 1404.
- Kolthoff, I. M.; Chantooni, J. K., Jr.; Bhowmik, S. *J. Am. Chem. Soc.* **1968**, 90, 23.

- Kramer, G. M. *J. Am. Chem. Soc.* **1970**, 92, 4344.
- Krapcho, A. *Synthesis* **1982**, 893.
- Kubisa, P. In *Cationic Polymerizations: Mechanisms, Synthesis and Applications*; Matyjaszewski, K., Ed.; Marcel Dekker: New York, 1996.
- Kuivila, H. G.; Cagwood, S. C.; Bayer, W. F.; Langrain, F. L. *J. Am. Chem. Soc.* **1955**, 77, 5175.
- Kukarni, R. K.; Porter, H. S.; Leonard, F. *J. Appl. Polym. Sci.* **1973**, 17, 3509.
- Kushibiki, N.; Irie, M.; Hayashi, K. *J. Polym. Sci., Polym. Chem. Ed.* **1975**, 13, 77.
- LaLonde, R. T.; Ferrara, P. B.; Debboli, A. D. *J. Org. Chem.* **1972**, 37, 1094.
- Lee, J.-Y.; Cho, I. *Bull. Korean Chem. Soc.* **1986**, 7, 210.
- Lemieux, R.-U.; Nagabhushan, T. L.; Paul, B. *Can. J. Chem.* **1972**, 50, 773.
- Levowitz, I. In *Modern Plastics Encyclopedia*, **1998**; Vol. 75, p B3.
- Lishanskii, I. S.; Zak, A. G.; Zhrebetskaya, Y.; Khachaturov, A. S. *Polym. Sci. USSR* **1967**, 49, 2138.
- Lishanskii, I. S.; Zak, A. G.; Fedorova, E. F.; Khachaturov, A. S. *Vysokomol. Soedin* **1965**, 7, 966. Translated into English in *Polym. Sci. USSR*, **1965**, 1967, 1066.
- Lovinger, A. J. In *Developments in Crystalline Polymers-I*; Bassett, D. C., Ed.; Applied Science Publishers: London, 1982, Chapt. 5.
- Machon, J. P.; Nicco, A. *Europ. Polym. J.* **1971**, 7, 353.
- Makino, K.; Ikeyama, Y.; Takeuchi, Y.; Tanaka, Y. *Polymer* **1982**, 23, 287.
- Mango, L. A.; Lenz, R. W. *Makromol. Chem.* **1973**, 163, 13.
- March, J. In *Advanced Organic Chemistry*; Wiley-Interscience: New York, 1992; p 263.
- Maruyama, Y.; Jo, Y. S.; Inoue, Y.; Chujo, R.; Tasaka, S.; Miyata, S. *Polymer* **1987**, 28, 1087.



- Matter, U.; Pascual, C.; Pretsch, E.; Pross, W. S.; Sternhell, S. *Tetrahedron* **1969**, 25, 691.
- Maynes, G. C.; Applequist, D. E. *J. Am. Chem. Soc.* **1973**, 95, 856.
- McGinnis, J.; Katz, T. J.; Hurwitz, S. *J. Am. Chem. Soc.* **1976**, 98, 606.
- McQuillan, F. J. In *Homogeneous Hydrogenation*; John Wiley & Sons, Inc.: NY, 1973.
- Miller, C. E. *J. Chem. Ed.* **1965**, 42, 254.
- Miller, W. T.; U.S. Patent 2, 283, May 27, 1952.
- Miyata, S.; Yokshikawa, M.; Takasa, S.; Ko, M. *Polymer J.* **1980**, 12, 857.
- Miyata, S.; Yoshikawa, M.; Tasaka, S.; Ko, M. *Polym. J.* **1980**, 12, 857.
- Moberly, C. W. In *Enclopedia of Polymer Science and Engineering*; Mark, H., Bikales, N. M., Overberger, C. G., Menges, G., Kroschwitz, J. I., Eds.; Interscience: N.Y, 1967; Vol. 7, p 557.
- Mochel, V. D. *J. Polym. Sci., Part A: Polym. Chem.* **1972**, 10, 1009.
- Mohajer, Y.; Wilkes, G. L.; Wang, I. C.; McGrath, J. E. *Polymer* **1982**, 23, 1523.
- Morton, M.; Fetters, L. J. *J. Polym. Sci., Part A: Polym. Chem.* **1964**, 2, 3311.
- Naegele, W.; Haubenstock, H. *Tetrahedron Lett.* **1965**, 4283.
- Nakagawa, T.; Okawara, M. *J. Polym. Sci., Part A: Polym. Chem.* **1968**, 6, 1795.
- Nakano, T.; Mori, M.; Okamoto, Y. *Macromolecules* **1993**, 26, 867.
- Natta, G; Corradini, P. *Makromol. Chem.* **1955**, 16, 77;
- Natta, G; Corradini, P; Bassi, I. W. *Nuovo Cimento, Suppl. 1*, **1960**, 15, 68.
- Natta, G.; Pasquon, I.; Zambelli, A.; Gatti, G. *J. Polym. Sci.* **1961**, 51, 387.
- Natta, G. P., I.; Zambelli, A.; Gatti, G. *J. Polym. Sci.* **1961**, 51, 387.
- Natta, G.; Danuso, F.; Sianesi, D. *Makromol. Chem.* **1959**, 30, 238.
- Natta, G.; Danuso, F.; Sianesi, D. *Makromol. Chem.* **1958**, 28, 253.

- Natta, G.; Pino, P.; Corradini, P.; Danusso, F.; Mantica, E.; Mazzanti, G.; Moraglio, G. *J. Am. Chem. Soc.* **1955**, *77*, 1708.
- Natta, G. *J. Polym. Sci.* **1955**, *16*, 143.
- Neumann, R.; Sanui, K.; MacKnight, W. J. *Macromolecules* **1975**, *8*, 665.
- Neureiter, N. P. *J. Org. Chem.* **1959**, *24*, 2044.
- Odian, G. In *Encyclopedia of Polymer Science and Engineering*; Mark, H., Bikales, N. M., Overberger, C. G., Menges, G., Kroschwitz, J. I., Eds.; Wiley-Interscience: New York, 1985; Vol. 3, p 274.
- O'Gara, J. E.; Wagener, K. B.; Hahn, S. F. *Makromol. Chem.* **1993**, *14*, 657.
- Olah, G. H. *Top. Curr. Chem.* **1979**, *80*, 19.
- Otsu, T.; Matsumoto, A.; Shiraishi, K.; Amaya, N.; Koinuma, Y. *J. Polym. Sci., Part A: Polym. Chem.* **1992**, *30*, 1559.
- Overberger, C. G.; Halek, G. W. *J. Polym. Sci., Part A: Polym. Chem.* **1970**, *8*, 359.
- Overberger, C. G.; Bochert, A. E.; Katchman, A. *J. Polym. Sci.* **1960**, *44*, 491.
- Overberger, C. G.; Borchert, A. E. *J. Am. Chem. Soc.* **1960**, *82*, 1007, 4896.
- Pasika, W. M. *J. Polym. Sci.* **1965**, *A3*, 4287.
- Pasto, D. J. In *Comprehensive Organic Synthesis*; Twist, B. M., Fleming, I., Eds.; Pergamon: Oxford, 1991; Vol. 8, pp 471- 488.
- Pell, A. S.; Pilcher, G. *Trans. Faraday Soc.* **1965**, *61*, 71.
- Penelle, J. *Advanced Catalysis: New Polymer Syntheses and Modifications, ACS Symposium Series*; American Chemical Society: Washington, 2000.
- Penelle, J.; Xie, T. *Macromolecules* **2000**, *33*, 4667.
- Penelle, J.; Herion, H.; Xie, T.; Gorissen, P. *Macromol. Chem. Phys.* **1998**, *199*, 1329.
- Penelle, J.; Herion, H.; Soree, A.; Gorissen, P. *Polym. Prepr. (Am. Chem. Soc., Div. Polym. Chem.)* **1996**, *37 (1)*, 208.
- Penelle, J.; Clarebout, G.; Balikdjian, I. *Polym. Bull. (Berlin)* **1994**, *32*, 395.

- Pepper, D. C.; Ryan, B. *Makromol. Chem.* **1983**, 184, 383.
- Pepper, D. C. *Polymer J.* **1980**, 12, 629.
- Pepper, D. C. *J. Polym. Sci., Polym. Sym.* **1978**, 62, 65.
- Perry, S.; Hibbert, H. *J. Am. Chem. Soc.* **1940**, 62, 2599.
- Perry, S.; Hibbert, H. *Can. J. Chem.* **1933**, 8, 102.
- Peters, D. *Tetrahedron* **1963**, 19, 1539.
- Pinazzi, C.; Brossas, J.; Clouet, G. *Makromol. Chem.* **1971**, 148, 81.
- Pinazzi, C.; Brosse, J. C.; Pleurdeau, A. *Makromol. Chem.* **1971**, 142, 273.
- Pinazzi, C.; Brossas, J.; Brosse, J. C.; Pleurdeau, A. *Makromol. Chem.* **1971**, 144, 155.
- Pinazzi, C. B., J. C.; Brossas, J.; Pleurdeau, A. *C. R. Acad. Sci. Paris* **1970**, 270, 1650.
- Pinazzi, C.; Brossas, J. *Makromol. Chem.* **1969**, 122, 105; **1971**, 1147, 1915.
- Pinazzi, C.; Brosse, J. C.; Brossas, J.; Pleurdeau, A. *C. R. Acad. Sci. Paris* **1968**, 266, 443.
- Pinazzi, C.; Pleurdeau, A.; Brosse, J. C. *C. R. Acad. Sci. Paris* **1968**, 266, 1032.
- Pines, H.; Huntsman, W. D.; Ipatieff, V. N. *J. Am. Chem. Soc.* **1953**, 75, 2315.
- Plesch, P. H. In *The Chemistry of Cationic Polymerization*; McMillan: New York, 1963; p 233.
- Prak., J. *Chem.* **1999**, 3, 341.
- Price, C. C.; Blair, E. A. *J. Polym. Sci., Part A: Polym. Chem.* **1967**, 5, 171.
- Pritchard, G.; Long, F. A. *J. Am. Chem. Soc.* **1958**, 80, 4162.
- Rachapudy, H.; Smith, G. G.; Raju, V. R.; Graessley, W. W. *J. Polym. Sci., Polym. Phys. Ed.* **1979**, 17, 1211.
- Rahrig, D.; MacKnight, W. J. *Macromolecules* **1979**, 12, 195.
- Raj, D. J. A.; Wadgaonkar, P. P.; Saviram, S. *Macromolecules* **1992**, 25, 2774.

- Ramp, F. L.; DeWitt, E. J.; Trapasso, L. E. *J. Org. Chem* **1962**, 27, 4368.
- Randall, J. C. In *Encyclopedia of Polymer Science and Engineering*; Mark, H., Bikales, N. M., Overberger, C. G., Menges, G., Kroschwitz, J. I., Eds.; Wiley-Interscience: New York, 1985; Vol. 9, p 797.
- Randall, J. C. In *Carbon-13 NMR and Polymer Stereochemical Configuration, ACS Symposium Series*; Pasika, W. M., Ed.: Washington, D.C., 1979; pp 291-318.
- Reding, F. P. *J. Polym. Sci.* **1956**, 547.
- Reetz, M. T.; Hutte, S.; Goddard, R. *J. Am. Chem. Soc.* **1993**, 11, 9339.
- Reetz, M. T.; Knauf, T.; Minet, U.; Bingel, C. *Angew. Chem. Int. Ed. Eng.* **1988**, 27, 1373.
- Richardson, A.; Hope, P. S.; Ward, I. M. *J. Polym. Sci., Polym. Phys. Ed.* **1983**, 21, 2525.
- Rickborn, B.; Jensen, F. R. *J. Org. Chem.* **1962**, 4608.
- Ritchie, C. D. *Pure Appl. Chem.* **1978**, 50, 1281.
- Robello, D. R.; Eldridge, T. D.; Michaels, F. M. *J. Polym. Sci., Part A: Polym. Chem.* **1999**, 37, 2219.
- Roberts, J. R.; Sharts, C. M. In *Organic Reactions*; John Wiley and Sons: New York, 1962; Vol. 12, p 1.
- Rooney, J. M. *Br. Polym. J.* **1981**, 13, 160.
- Rose, J. B. *J. Chem. Soc.* **1956**, 542.
- Rossi, R.; Diversi, P.; Porri, L. *Macromolecules* **1972**, 5, 247.
- Sakurai, M.; Ohta, Y.; Inoue, Y.; Chujo, R. *Polym. Commun.* **1991**, 32, 397.
- Santee, E. R.; Chang, R.; Morton, M. *J. Polym. Sci. Polym. Lett. Ed.* **1973**, 11, 449.
- Samuels, R. J.; Yee, R. Y. *J. Polym. Sci. A2* **1972**, 10, 358.
- Sanui, K.; MacKnight, W. J.; Lenz, R. W. *J. Polym. Sci., Polym. Lett. Ed.* **1973**, 11, 427.



- Sawada, H. In *Thermodynamics of Polymerization*; Sawada, H., Ed.; Marcel Dekker: New York, 1976.
- Schmidt, R. F.; U.S. Patent 2,594,353 (April 29, 1952)
- Schultz, D. N. In *Encyclopedia of Polymer Science and Engineering*; Mark, H., Bikales, N. M., Overberger, C. G., Menges, G., Kroschwitz, J. I., Eds.; Wiley-Interscience: N. Y, 1985; Vol. 7, pp 807-817.
- Schultz, D. N.; Turner, S. R.; Golub, M. A. *Rubber Chem. Technol.* **1982**, *55*, 809.
- Schwarcz, J. A.; Perlin, A. S. *Can. J. Chem.* **1972**, *50*, 3667.
- Searles, S. *J. Am. Chem. Soc.* **1951**, *73*, 4515.
- Semen, J.; Lando, J. B. **1969**, *2*, 570.
- Setzer, W.; Schleyer, P. v. R. *Adv. Organomet. Chem.* **1985**, *24*, 353.
- Shea, K. J.; Skell, P. S. *J. Am. Chem. Soc.* **1973**, *95*, 6728.
- Shibaev, V. P.; Kostromin, S. G.; Plate, N. A.; Ivanov, S. A.; Vetrov, V. Y.; Yakolev, I. A. *Polymer Commun.* **1983**, *24*, 364.
- Shroff, R.; Prasad, A.; Lee, C. J. *J. Polym. Sci., Part B: Polym. Phys.* **1996**, *34*, 2317.
- Sigwalt, P.; Spassky, N. In *Ring-Opening Polymerization*; Ivin, K. J., Saegusa, T., Eds.; Elsevier Applied Science Publishers: New York, 1984; Vol. 2, pp 603-714.
- Silas, R. S.; Yates, J.; Thornton, N. *Anal. Chem.* **1959**, *31*, 529.
- Singh, R. K.; Danishefsky, S. *J. Org. Chem.* **1975**, *40*, 2969.
- Sloan, M. F.; Matlack, A. S.; Breslow, R. *J. Am. Chem. Soc.* **1963**, *85*, 4014.
- Stempel, G. H. In *Polymer Handbook*; Brandrup, J., Immergut, E. H., Eds.; Wiley: New York, 1975; Vol. V-1 - V-5.
- Stevens, M. P. *Polymer Chemistry, An Introduction*; Oxford University Press: New York, 1999.
- Stewart, J. M.; Pagenkopf, G. K. *J. Org. Chem.* **1969**, *34*, 7.

- Stewart, J. M.; Olsen, D. R. *J. Org. Chem.* **1968**, *33*, 4534.
- Stewart, J. M.; Westberg, H. H. *J. Org. Chem.* **1965**, *30*, 1951.
- Stirling, C. J. M. *Tetrahedron* **1985**, *41*, 1613.
- Storey, R. F.; George, S. E. *Proc. Am. Chem. Soc. Div. Polym. Mat. Sci. Eng.* **1988**, *58*, 985.
- Sung Jo, Y.; Inoue, Y.; Chujo, R.; Saito, K.; Miyata, S. *Macromolecules* **1985**, *18*, 1850.
- Swain, G. C.; Scott, C. B. *J. Am. Chem. Soc.* **1953**, *75*, 141.
- Takahashi, T. *J. Polym. Sci., Part A: Polym. Chem.* **1968**, *6*, 3327.
- Takahashi, T. *J. Polym. Sci., Part A: Polym. Chem.* **1968**, *6*, 403.
- Takahashi, T.; Yamashita, I. *J. Polym. Sci.* **1965**, *B3*, 251.
- Takahashi, T.; Yamashita, I.; Miyakawa, T. *Bull. Chem. Soc. Jpn.* **1964**, *37*, 131.
- Tasaka, S.; Inagaki, N.; Okutani, T.; Miyata, S. *Polymer* **1989**, *30*, 1639.
- Tasaka, S. A., K. M.; Yoshikawa, M.; Miyata, S.; Ko, M. *Ferroelectrics* **1984**, *57*, 267.
- Tashiro, K.; Kobajashi, M.; Tadokoro, M.; Furukawa, T. *Macromolecules* **1980**, *13*, 691.
- Tate, D. P.; Bethea, T. W. In *Encyclopedia of Polymer Science and Engineering*; John Wiley & Sons: New York, 1985; Vol. 2, p 537.
- Taylor, G. L.; Davison, S. *J. Polym. Sci., Part B: Polym. Lett.* **1968**, *6*, 699.
- Tipper, C. F. H.; Walker, D. A. *J. Chem. Soc.* **1959**, 1352.
- Tobolsky, A. V.; Rogers, C. E. *J. Polym. Sci.* **1959**, *40*, 73.
- Tonelli, A. E. In *NMR Spectroscopy and Polymer Microstructure: the conformational connection*; VCH: New York, 1989.
- Trost, B. M.; Cossy, J.; Burks, J. *J. Am. Chem. Soc.* **1983**, *105*, 1052.
- Truce, W. E.; Lindy, L. B. *J. Org. Chem.* **1961**, *26*, 1463.

- Tseng, Y.-C.; Hyon, S.-H.; Ikada, Y. *Biomaterials* **1990**, *11*, 73.
- Turner-Jones, A; Cobbold, A. J. *J. Polym. Sci. B* **1968**, *6*, 539;
- U.S. Patent. 2, 283 (May 27, 1952), W.T. Miller (USAEC), U.S. Patent 2, 946, 763 (July ; 26, B. M. I. S., B. W.; (Eu I du Pont de Nemours & Co. Inc.), Br. Pat. 781, 532 ; (Aug. 21, K., C. G.; (Eu I du Pont de Nemours & Co. Inc.), U. S. Pat. 3, 132, 124 ; (May 5, Couture, M. J. Schindler, D. L.; Weiser, R. B. (Eu I du Pont de Nemours & ; Inc.), C. In.
- Ulrich, H. In *Introduction to Industrial Polymers*; Hanser: Munich, 1993; pp 48, 63-64, 180.
- Upton, C. J.; Incremona, J. H. *J. Org. Chem.* **1976**, *41*, 523.
- Van Tamelen, E. E.; Dewey, R. S.; Timmons, R. J. *J. Am. Chem. Soc.* **1961**, *83*, 3729.
- Vijayalakshmi, V.; Rupavani, J. N.; Krishnamurti, N. *J. App. Polym. Sci* **1993**, *49*, 1387.
- Virtanen, P. O.; Korhonen, R. *Acta Chem. Scand.* **1973**, *27*, 2650.
- Vogel, E. *Angew. Chem.* **1960**, *72*, 4.
- Vol'pint, M. E.; Kolomnnikov, I. S. *Russ. Chem. Rev. (English Trans.)* **1969**, *38*, 273.
- Walling, C.; Fredricks, P. S. *J. Am. Chem. Soc.* **1962**, *84*, 3326.
- Walsh, A. D. *Trans. Faraday Soc.* **1949**, *45*, 179.
- Warner, D. T.; Moe, O. A. *J. Am. Chem. Soc.* **1948**, *70*, 3470.
- Weigert, R. *J. Am. Chem. Soc.* **1967**, *89*, 5962.
- Wells, P. R. *Chem.Rev.* **1963**, *63*, 171.
- Wicklatz, J. In *Chemical Reactions of Polymers*; Fetters, E. M., Ed.; Wiley-Interscience: N.Y, 1964; Chapt. 2F.
- Williams, K. K.; Wiley, D. W.; McKusick, B. C. *J. Am. Chem. Soc.* **1962**, *84*, 2210.
- Wilson, A.; Goldhamer, D. *J. Chem. Edu.* **1963**, *40*, 504.

- Witt, D. R.; Hogan, J. P. *J. Polym. Sci., Part A: Polym. Chem.* **1970**, *8*, 2689.
- Wittig, G.; Todt, U.; Nagel, K. *Chem. Ber.* **1950**, *83*, 110.
- Wong, H. N. C.; Hon, M.; Tse, C.; Yip, Y. *Chem. Rev.* **1989**, *89*, 165.
- Woods, J. In *Polymeric Materials Encyclopedia*; Salamone, J. C., Ed.; CRC Press: N.Y, 1996; Vol. 2, p 1632.
- Worsfold, D. V.; Eastham, A. M. *J. Am. Chem. Soc.* **1957**, *79*, 900.
- Xie, T., Ph.D Dissertation, University of Massachusetts, Amherst **2001**.
- Yakubchik, A. I.; Tikhomirov, B. I.; Sulimov, V. S. *Rubber Chem. Technol.* **1962**, *35*, 1063.
- Yakubchik, A. I.; Gromova, G. N. *Rubber Chem. Technol.* **1958**, *31*, 156.
- Yang, X.; Jia, L.; Marks, T. J. *J. Am. Chem. Soc.* **1993**, *115*, 3392.
- Yokota, K.; Hirabayashi, T. *Polym. J.* **1981**, *13*, 813.
- Yokozawa, T.; Wakabayashi, Y.; Kimura, T. *J. Polym. Sci., Part A: Polym. Chem.* **1997**, *35*, 1563.
- Yokozawa, T.; Miyamoto, Y.; Futamura, S. *Makromol. Chem., Rapid Commun.* **1993**, *14*, 245.
- Young, R. J.; Lovell, P. In *Introduction to Polymers*; Chapman & Hall: New York, 1991; p 251.
- Yuki, Y.; Hatada, K. *Adv. Polym. Sci.* **1979**, *31*, 1.
- Zefirov, N. S. K., T. S.; Kozhushkov, S. I.; Surmina, L. S.; Rashchupkina, Z. A. *Zh. Org. Khim. (Engl. Transl.)* **1983**, *19*, 474.





